Synthesis, characterization and pharmaceutical application of selected copolymer nanoparticles

DP Otto

Thesis submitted for the degree Doctor of Philosophy in Pharmaceutics at the Potchefstroom campus of the North-West University

Promoters: Prof HCM Vosloo

Prof MM de Villiers

Co-promoter: Prof W Liebenberg

October 2007

TABLE OF CONTENT

PREFACE

The thesis that is presented here represents a series of manuscripts that were submitted to various journals. It was agreed by the candidate and promoters that the article format would be submitted.

The manuscripts were formatted to chapters that presented a uniform style; however, the reference citation style was preserved to suit the particular journal style. A guideline to the authors regarding the preparation of the manuscript was included before each chapter.

The candidate was responsible for conducting the requisite experimental work and also the preparation of the manuscripts under judicious supervision of the co-authors.

The targeted journals were:

Journal of Liquid Chromatography & Related Technologies

Journal of Applied Polymer Science

Colloid & Polymer Science

Journal of Controlled Release

The candidate was the primary author and also the corresponding author with the exception of the submission to Journal of Liquid Chromatography & Related Technologies. The manuscripts presented in chapter 2 (Journal of Liquid Chromatography & Related Technologies) and 3 (Journal of Applied Polymer Science) were accepted although these were still not printed by the journal yet.

The manuscript chapters were preceded by a literature survey chapter and a conclusion chapter was included after the last manuscript chapter. Appropriate appendices followed.

AIM AND OBJECTIVES

AIM

Dispersions of copolymer nanoparticles are widely utilized in several applications i.e. paints, adhesives and packaging materials. Of late, lots of interest was developed in the application of copolymeric nanoparticles in the production of drug delivery systems.

The dual-purpose aim of this project was to produce a controlled-release drug delivery system assembled from copolymer nanoparticles that could also prevent bacterial biofilm adhesion. To achieve this aim several objectives needed to be attained to ensure the success of the project.

OBJECTIVES

1. A systematic literature survey should be performed to illuminate the relevance of nanoparticulate materials in pharmaceutical science. This survey will also clarify the choice and application of copolymeric materials. Additionally, methods and formulation guidelines for the synthesis of these nanoparticles will be found. Finally, a feasible drug delivery application for nanoparticles will be identified.

2. The literature survey revealed the essential role of gel permeation chromatography (GPC) as a characterization method for polymer-based nanoparticles. Subsequently the value of the technique, i.e. determination of molecular weight, particle size and conformational analysis will be reviewed.

3. Apply an experimental design to investigate microemulsion copolymerization as a method to produce poly(styrene-*co*-methyl methacrylate) and poly(styrene-*co*-ethyl methacrylate) nanoparticles. Subsequent characterization of the particles with gel permeation chromatography (GPC-MALLS) will be performed. Additionally, chemical composition will be determined with attenuated total reflectance Fourier transform infrared spectroscopy (ATR-FTIR) as an alternative to problematic solvent-based NMR.

4. Produce and characterize a series of an antibiotic-loaded, controlled-release drug delivery systems that could also potentially prevent biofilm formation from a selection of P(St-*co*-MMA) and P(St-*co*-EMA) nanoparticles. The selection will be based on nanoparticle molecular weight, size, conformation and chemical composition. The release of the antibiotic, rifampin, from the delivery system will be investigated and accompanied by scanning electron microscopy studies, contact angle measurements and ATR-FTIR analysis.

ABSTRACT

A multidisciplinary literature survey revealed that copolymeric nanoparticles could be applied in various technologies such as the production of paint, adhesives, packaging material and lately especially drug delivery systems. The specialized application and investigation of copolymers in drug delivery resulted in the synthesis of two series of copolymeric materials, i.e. poly(styrene-*co*-methyl methacrylate) (P(St-*co*-MMA)) and poly(styrene-*co*-ethyl methacrylate) (P(St-*co*-EMA)) were synthesized via the technique of o/w microemulsion copolymerization. These copolymers have not as yet been utilized to their full potential in the development of new drug delivery systems. However the corresponding hydrophobic homopolymer poly(styrene) (PS) and the hydrophilic homopolymer poly(methyl methacrylate) (PMMA) are known to be biocompatible. Blending of homopolymers could result in novel applications, however is virtually impossible due to their unfavorable mixing entropies. The immiscibility challenge was overcome by the synthesis of copolymers that combined the properties of the immiscible homopolymers. The synthesized particles were analyzed by gel permeation chromatography combined with multi-angle laser light scattering (GPC-MALLS) and attenuated total reflectance Fourier infrared spectroscopy (ATR-FTIR). These characterizations revealed crucial information to better understand the synthesis process and particle properties i.e. molecular weight, nanoparticle size and chemical composition of the materials. Additionally, GPC-MALLS revealed the copolymer chain conformation. These characterizations ultimately guided the selection of appropriate copolymer nanoparticles to develop a controlled-release drug delivery system. The selected copolymers were dissolved in a pharmaceutically acceptable solvent, tetrahydrofuran (THF) together with a drug, rifampin. Solvent casting of this dispersion resulted in the evaporation of the solvent and assembly of numerous microscale copolymer capsules. The rifampin molecules were captured in these microcapsules through a process of phase separation and coacervation. These microcapsules finally sintered to produce a multi-layer film with an unusual honeycomb structure, bridging yet another size scale hierarchy. Characterization of these delivery systems revealed that both series of copolymer materials produced films capable of controlling drug release and that could also potentially prevent biofilm adhesion.

Keywords: microemulsion copolymerization, nanoparticle, GPC-MALLS, microcapsule film, controlled release

UITTREKSEL

'n Multidisiplinêre literatuuroorsig het getoon dat kopolimeernanopartikels 'n wye reeks toepassings in verskeie industrieë bied byvoorbeeld verf-, verpakkingsmateriaal en gomproduksie en veral die vervaardiging van geneesmiddelafleweringsisteme. Dus is twee reekse kopolimere, nl. poli(stireen-*ko*-metiel metakrilaat) (P(St-*ko*-MMA) en poli(stireen-*ko*-etiel metakrilaat) (P(St-*ko*-EMA) gesintetiseer deur die tegniek van o/w mikroëmulsiekopolimerisasie. Hierdie materiale is verder ontwikkel vir 'n gekontroleerde geneesmiddelvrystellingsisteem. Dié kopolimere is tot op hede nog nie algemeen aangewend vir geneesmiddelafleweringsisteme nie, alhoewel dit bekend is dat die hidrofobe homopolimeer poli(stireen) (PS) en die hidrofiele homopolimeer poli(metiel metakrilaat) (PMMA) bioaanpasbaar is. Vermenging van homopolimere kan unieke materiaaleienskappe oplewer, maar word gekortwiek vanweë die ongunstige polimeervermengingsentropie. Kopolimere kan die eienskappe van die onmengbare homopolimere kombineer in 'n nuwe materiaal en kopolimerisasie is dus aangewend vir hierdie kombinasie. Karakterisering van die kopolimeerpartikels is uitgevoer met behulp van 'n jelpermeasiechromatograaf gekoppel aan 'n veelvoudige hoek laserligverstrooiingsdetektor (GPC-MALLS). Die chemiese samestelling van die kopolimere is vasgestel met behulp van verswakte totale refleksie Fourier-transformasie infrarooispektroskopie (ATR-FTIR). Die analises het kardinale kopolimeereienskappe bv. molekulêre gewig, nanopartikelgrootte en polimeerkettingkonformasie onthul. Die keuse van die kopolimere vir ontwikkeling van die gekontroleerde afleweringsisteem is gebaseer op hierdie eienskappe. Die geskikte kopolimere is gevolglik gedispergeer in die farmaseuties-aanvaarbare oplosmiddel, tetrahidrofuraan (THF) en die geneesmiddel rifampisien is bygevoeg. Dispersies is gevolglik gegiet en oplosmiddel verdamping het gelei tot die ontstaan van mikrokapsules wat tydens die verdampingsproses gevul is met rifampisien vanweë faseskeiding en koaservasie. Aaneenskakeling van die mikrokapsules het 'n multilaagfilm opgelewer met 'n ongewone heuningkoekstrukuur wat uiteindelik gekontroleerde geneesmiddelvrystelling bewerkstellig het. Potensiële toepassings in die voorkoming van biofilmaanhegting kon ook voorgestel word.

Sleutelwoorde: mikroëmulsiekopolimerisasie, nanopartikel, GPC-MALLS, mikrokapsulefilm, gekontroleerde vrystelling

CHAPTER 1

NANOTECHNOLOGY APPLIED IN PHARMACEUTICAL SCIENCE

1.1 INTRODUCTION

Technologies and scientific disciplines, such as the development of drug delivery systems, are all bound to a sigmoidal growth pattern. Therefore, the initial growth of technology is very slow until certain critical events or inputs are incorporated, resulting in rapid growth. However, growth will eventually again decelerate and finally terminate. At this stage, a technology or discipline might seem to be exhausted, even irrelevant. It is therefore, necessitated to continuously integrate input from all peripheries to sustain the development of relevant technologies (Messler, 2004:44). Recently nanotechnology has become such a critical peripheral input that has breathed new life into the development of drug delivery systems.

Nanotechnology is the study, manufacturing and application of materials science at the near-atomic (10^{-9} m) scale in the range 1-100 nm (Roco, 2003:337, Sahoo, & Labhasetwar, 2003:1112) and has found a vast array of applications in numerous fields of natural science with promising effect in understanding biological mechanisms (Roco, 2003:337, biotechnology (Laval, 1995:479) and pharmaceutical applications including specialized drug delivery systems for controlled release including polymeric implants (Moghimi *et al.*, 2006:29, Harabaigu *et al.*, 2006:69).

1.2 NANOTECHNOLOGY AND THE CONVERGENCE WITH BIOLOGY

Nanotechnology has been largely developed in the past two decades. This occurrence has depended to a large extent on the invention of nanostructure fabrication techniques in conjunction with characterisation methods especially to study surfaces (Curtis & Wilkinson, 2001:97).

The extent of nanotechnology could be described as the manipulation of materials at the molecular level in such a mode as to assemble it into objects along several hierarchical length scales i.e. carbon nanotubes as drug-loaded devices (Bellucci *et al.*, 2007:95), nanofilms (Russell *et al.*, 2007:7466), microfilms produced for tablet coating (Nguyen *et al.*, 2006:1) or agglomerates to form nanocomposites in microstructures useful in bone regeneration (Kim, 2007:169).

According to Kulkarni (2007) several biological processes occur at the nanoscale, however traditionally research dealing with these events was not considered nanotechnology since they could not be directly manipulated. The unravelling of DNA and finally the discovery of the polymerase chain reaction (Mullis & Faloona, 1987:335) that produced synthesized DNA fragments added the technological aspect to biology.

Bionanotechnology has been defined as nanotechnology that draws inspiration form biology to guide technological applications. Examples of molecular self-assembly i.e. minerals, pearls, silk, teeth, membranes and many other examples serve as inspiration for the creation of scaffold-based delivery systems as an application of bionanotechnology (Taylor, 2007:1313, Sarikaya *et al.*, 2003:577).

Pharmaceutical industry might be one beneficiary of bionanotechnology if it were able to assimilate the discipline into the innovation or improvement of drug delivery systems i.e. production of biomaterials (Langer & Peppas, 2003:2990), consequently expanding drug markets and biological applications. The incorporation of drugs into tailored delivery devices currently accounts for 13% of the global market. It is projected that this U.S. drug market sector will expand by 9-11% annually to a projected US$82 billion in 2007/2008. Additional advantages conferred by these technologies to pharmaceuticals might be improved product life, performance and acceptability (Orive *et al.*, 2003:659, Sahoo & Labhasetwar, 2003:1112).

1.3 THE SIGNIFICANCE OF PHARMACEUTICAL NANOTECHNOLOGY

The pharmaceutical industry is showing an escalating interest in the development of effective drug delivery systems. It was recognised that the *in vivo* fate of drugs was not determined solely by drug properties. In fact, the carrier systems that were used to deliver the drug also affected the release of drug. In turn, the desired route of administration could influence the choice of delivery system. Therefore, the requirements of a specific treatment should act as a guide to design the delivery system and materials that were chosen (Mehmert & Mäder, 2001:166).

The ultimate objective of these nanosystems is to precisely deliver therapeutic substances to its site of action. Reproducibility of drug delivery at the appropriate concentration is another prerequisite for the success of these dosage forms (Orive *et al.*, 2003:659).

1.3.1 Materials used in pharmaceutical nanotechnology

Several types of materials could be used to produce nanodelivery systems or nanoparticle-based delivery systems. Two broad categories i.e. organic and inorganic materials have been used to manufacture these nanodelivery systems. Combinations of both categories of materials were also found i.e. inorganic calcium hydroxyapatite was used to produce a nanocomposite material with synthetic polymers such as poly(caprolactone) (Kim, 2007:169) or with poly(vinyl alcohol) (Mollazadeh, 2007:165). Combination of hydroxyapatite with chitosan, a polymer derived from a natural source, was also successfully utilized to produce a bone-tissue engineering composite material (Kong *et al.*, 2006:3171).

1.3.2 Focus on biocompatible polymers

The focus will be placed on polymeric materials since these are the most commonly employed biocompatible materials in pharmaceutical industry to produce nanomaterials (Maysinger, 2007:2335). Both natural and synthetic polymers are used and some examples are mentioned below.

Biocompatible polymers are commonly employed in pharmaceutical industry for production of devices for site-specific delivery, excipients for coating and aggregating reagents for nano and larger particles (Godwin *et al.*, 2001:1175). Two discrete groups of biopolymers are distinguished namely hydrogels and lipophilic materials (Drotleff *et al.*, 2004:391).

Hydrogel polymers are hydrophilic, absorb water and therefore are capable of significant swelling. Hydrogels allow for rapid diffusion of nutrients, drugs and oxygen. These polymers can easily adapt to complement the shape of their environment. Poly(ethylene glycol) (PEG) is widely accepted and known for its biocompatibility and conformational adaptability (Coombes *et al.*, 1997:1156).

Naturally occurring polymers are alginates (Thornton *et al.*, 2004:763), chitosans (Rossomachna *et al.*, 2004:31), fibrins employed for hormone release in nerve lesions (Bhang *et al.*, 2007:998) and agarose (Toussaint *et al.*, 2007:1167) used for DNA vaccine delivery. Frequently employed synthetic hydrogels include PEG, poly(acrylic acid) derivatives (PAA) and poly(vinyl alcohol) (PVA). Hydrogels could be injected as relatively non-invasive implantations (Drotleff *et al.*, 2004:391). Yet another popular example of a hydrogel is gelatine and this was used for the controlled release of DNA (Young *et al.*, 2005:256).

Lipophilic, water-insoluble polymers include poly(styrene) (PS) and poly(methyl methacrylate) (PMMA). These polymers are characterised by an inflexible structure as well as preservation of its conformation in the presence of water. Mechanical stability of these devices is usually guaranteed and furthermore, provides suitable environments for cell adhesion and migration (Drotleff *et al.*, 2004:393).

1.4 PRODUCTION OF POLYMERIC NANOPARTICLES OR NANOMATERIALS

Two approaches are followed to produce nanomaterials from polymers. Dispersion of preformed polymers could be employed to produce a nanodispersion of the material in a suitable medium (Thioune *et al.*, 1997:233). Alternatively, polymers could be synthesized by assembly of monomer units by suitable methods that finally produce a nanosized polymer chain (§1.3.2). The combination of synthesis and redispersion is of course also possible and a synthesized polymer could be isolated after the synthesis, purified from unwanted reactants and then redispersed to form the latex that will be utilized in the selected application.

A method that will not be discussed in great detail is the production of nanocomposites. These polymer dispersions can be mixed with a variety of metals, ceramics or oxides to produce a composite material (Schadler *et al.*, 2007:53). Alternatively, these added materials could already be introduced to the polymerization reaction and react with the polymer chains (Khomutov, 2004:79). The unreacted materials are then removed after the reaction has been completed.

1.4.1 Dispersion Methods

1.4.1.1 Polymer emulsification methods

Three types of emulsions, micro- (Danielsson & Bjoern, 1981:391), mini- (El-Aasser *et al.*, 1988:103) and nanoemulsions (Morales *et al.*, 2003), are especially suited to the production of ultradispersed particles. The normal emulsions were described as producing coarsely dispersed micronized droplets in the dispersion medium whereas the micro- and miniemulsions produce droplets in the nanoscale range (Fernandez *et al.*, 2004:53).

The success of emulsification depends to a large extent on the ease of generation of droplets (rupture) during the emulsification step and the degree of coalescence of the formed droplets (Lobo *et al.*, 2002:409). Surfactants are paramount in the droplet generation and long-term stability of droplets after its formation. Rupture of drops results as a consequence of a decrease in interfacial energy and tension due to surfactant interaction with the oil and water phases

(Lobo & Svereika, 2003:498 [22]). Simultaneously, a barrier is presented to coalescence by repulsion of similarly charged adsorbed surfactant layers on adjacent droplets. Steric hindrance induced by surface adsorption might augment repulsion (Ito *et al.*, 2004:172).

The key determinants of the success of the methods are material solubility, polymer concentration and molecular weight, drug to polymer ratio, solvent type, concentration and characteristics of surfactants, temperature, agitation rate, viscosity and volume ratio of dispersed and continuous phases. In some cases sonication and homogenisation should also be employed to optimize product characteristics (Jain, 2000:2478).

Various stability issues exist that may complicate the emulsification processes. Coalescence may occur due to collisions during agitation, resulting in phase separation. Ostwald ripening is a phenomenon of molecular diffusion resulting in degradation of the internal phase. This ripening is the result of droplet size distribution, with smaller droplets more prone to diffusion into other droplets than larger counterparts. This process continues up to the point where a certain minimum of particles exceed a specified size and then continue to grow and assimilate the other internal phase droplets (Antonietti & Landfester, 2002:693).

1.4.1.2 Microemulsions

The solvent evaporation methods all rely to some extent on the production of microemulsions. Microemulsions are translucent systems demonstrating low viscosity. The high proportion of oil and water contained in these systems are stabilised by amphiphilic compounds. In contradiction to conventional emulsification, microemulsions form spontaneously, are thermodynamically stable and exhibit a wide variety of structures. These structures could be globular, bicontinuous, cubic or lamellar (Candau *et al.*, 1999:47). Additionally, large interfacial surface area, optical transparency and nanoscale domain ranges adds to the usefulness of these systems (Candau, 1997:127).

The method is however, restricted to some extent due to the necessity of an excessive quantity of surfactant to produce emulsion. Colloidal instability as well as costly procedures presents additional challenges that preclude frequent utilisation of the technique on a large scale (Antonietti & Landfester, 2002:691).

1.4.1.3 Miniemulsions

Nanoemulsions are also described as miniemulsions and are only kinematically stable; however these emulsions do not exhibit flocculation or coalescence upon long-term storage if prepared appropriately. These systems are described as approaching thermodynamic stability since they could resist Ostwald ripening for prolonged periods of time if components were added that were insoluble in the dispersion phase to counteract osmotic pressure (Laplace pressure) from the dispersed phase. Therefore miniemulsion could be a compromise for microemulsions by requiring less surfactant than microemulsions. However, miniemulsions will eventually undergo gradual Ostwald ripening (Tadros *et al.*, 2004:303).

Miniemulsions are heterophase systems of stabile nanodroplets of one phase dispersed in a continuous phase. These emulsions are produced analogous to microemulsions; however, additional osmotic ingredients are added to the continuous phase. These osmotic compounds are of exceptionally low solubility in the continuous phase i.e. hexadecane, silanes, siloxanes, isocyanates, polyester and fluorinated alkanes (Antonietti & Landfester, 2002:701).

During monomer or solvent evaporation, droplets exert pressure known as the Laplace pressure that results in diffusional degradation of the internal phase to result in Ostwald ripening. Suitable osmotic agents counter this osmotic phenomenon, resulting in high stability of the internal phase. In general, a reduction in the surfactant quantity could be achieved due to the osmotic stabilisers (Taylor & Ottewill, 1994:199, Landfester, 2000:171, Landfester, 2003:225).

The drawback of the employment of miniemulsions was however identified as their dependence on agitation for stability. This could be an industrially unfeasible process requiring high energy inputs if very small droplets were required (Fernandez *et al.*, 2004:54).

1.4.1.3.1 Oil-in water (o/w) emulsification

A generalised summary of this method is explained. A selected polymer is dissolved in organic solvents i.e. dichloromethane, chloroform or ethyl acetate. A candidate substance is then dissolved or dispersed in this polymer solution. This mixture forms the lipophilic phase that is subsequently dispersed into an aqueous solution comprising of surfactant i.e. gelatin, PVA, polysorbate 80 or poloxamer 188. The organic solvent is extracted from the emulsion via evaporation under conditions of elevated temperature, reduced pressure or continuous agitation. The method is best employed for lipophilic drugs i.e. steroids (Soppimath, 2001:2, Jain, 2000:2477).

The method was also adapted to produce water-in-oil-in-water (w/o/w) emulsions. The resultant particles are purified and filtered to produce nanoparticles. The method is best suited to encapsulation of water-soluble therapeutic compounds i.e. peptides, proteins and vaccines (Soppimath, 2001:2, Jain, 2000:2477).

1.4.1.3.2 Spontaneous emulsification / solvent diffusion method

Modification of the solvent evaporation method (section 1.3.1.1.1) introduced the addition of water-miscible solvents i.e. acetone, ethanol and methanol into the oil phase together with water-insoluble solvents i.e. dichloromethane and chloroform. The water-soluble solvents demonstrate spontaneous diffusion into the aqueous phase, creating interfacial turbulence. Turbulence results in the formation of smaller particles or droplets and can be controlled by variation in the concentration of water-soluble solvents (Soppimath, 2001:2).

1.4.1.4 Supercritical fluid technology

The supercritical state is defined by temperature (T) and pressure (p) of a pure component that exceed certain critical magnitudes e.g. $T > T_c$ and $p > p_c$ of the regarded compound. In a pressure-temperature phase diagram the critical point marks the cessation of the vapour-pressure line (Kaiser *et al.*, 2001:907).

In the supercritical region, a substance exists as a single phase with advantageous properties of both liquids and gases. CO_2 is considered as the ideal candidate (Shekunov *et al.*, 1999:1345, Subramaniam *et al.*, 1997:885).

Pharmaceutical compounds and polymers have reported low solubilities in normal phase CO_2. The substrate is dissolved in a good solvent and then added to compressed CO_2. Varying the conditions, supercritical or subcritical CO_2 is produced. The solvent is usually freely soluble in CO_2 (Revechron, 1999:1).

The agitation of the pressurised mixture produces conditions analogues to that of a quasi-emulsion. The CO_2 acts as a poor solvent and diminishes the solvent power of the good solvent. Emulsification or crystallisation is effected as a consequence. Upon depressurisation the CO_2 regains its low density and the gaseous phase is again produced. However, the solvent saturates CO_2 and both evaporate, depositing the particles of the solute in the container (Kaiser *et al.*, 2001:921, Subra & Jestin, 1999:7, Subramaniam, 1997:886).

1.4.1.5 Phase separation (coacervation)

The process entails the addition of a third component to an emulsion, resulting in a decrease in polymer solubility in an organic solvent. After addition of a suitable amount of the component a certain critical point is exceeded, yielding two discrete liquid phases. The polymer is contained in the coacervate phase and the supernatant is depleted in polymer. Thus, dissolved particles are coated by polymer as a result of phase separation. Solidification completes the phase separation method of nanoparticle production (Jain, 2000:2475).

1.4.2 Synthetic Routes

The emulsions that were discussed above could all offer platforms to perform reactions. The dispersed as well as dispersion phase could both contain reactants that can be exploited to synthesize a desired product. In the next sections the employment of emulsion systems will be discussed to produce nanosized polymer latexes. Polymers have been studied widely as platforms for nanomaterials and the development of new or existing polymers could result in additional applications.

The focus will now shift to microemulsion polymerization since this technique was employed in this study to produce the materials that were ultimately utilized in the pharmaceutical application developed in this project.

1.4.2.1 Microemulsion polymerization

1.4.2.1.1 General formulation guidelines

The 1980's saw the concept of polymerisation in microemulsions introduced (Stoffer & Bone, 1980a:393, 1980b:2641) resulting in a number of publications exploring the potential of the process.

The formulation of polymerizable microemulsions is complex. Due to its large interfacial area, microemulsions require higher quantities of surfactant compared to conventional emulsions. This is restrictive to some extent due the fact that high solid content and low surfactant amounts are often required for industrial applications. The ideal formulation would optimize the reactant ratios by consideration of the partial solubility of the oil and lipophilic surfactant alkyl tail as well as the solubility in the aqueous dispersion medium and the polar head group of the surfactant (Holtzscherer & Candau, 1988:411).

It should also be considered that partially water-soluble monomers could act as cosurfactants. Acrylamide illustrated cosurfactant effects that extended the microemulsion domain and therefore resulted in virtual disappearance of the emulsion region in the phase diagram. This could of course be beneficial if a microemulsion was required (Candau *et al.*, 1984:167).

If a high quantity of a hydrophobic monomer i.e. styrene was used, the opposite effect on the phase diagram would be seen with a marked reduction in the microemulsion phase. Styrene is highly hydrophobic with no cosurfactant action and a mismatch between the hydrophilic-lipophilic balance (HLB) with the surfactant (Beerbower & Hill, 1971:223).

The content of the monomer is usually limited to a maximum of 5-10% wt based on the total formulation weight with surfactant concentration in a similar range. Variations in the ratios of monomer to surfactant and surfactant to water produced various dispersion systems including suspensions, emulsions, microemulsions and miniemulsions (Tauer *et al.* 2003:1245).

1.4.2.1.2 Mechanism of microemulsion polymerization

Numerous reasons inspired the development of microemulsion polymerisation technology. These included regulatory limitation on the use of organic solvents, development of the technique to accommodate high polymer content and the advantage of particle dimension regulation (Antonietti & Landfester, 2002:691).

The concept of nanoreactors in an emulsified state was introduced and implied that each droplet becomes the primary locus of polymerisation initiation. Consequently, the continuous phase acts as the source of initiators, side products and heat. Each reactor may function independently from the other, resulting in the production of various nanostructures as controlled by the addition or adjustment of the continuous phase (Antonietti & Landfester, 2002:691).

The monomer molecules in emulsions are distributed in various structures such as large monomer droplets, small micelles and also in the continuous phase. In contradiction, only a single structure, micelles, contain the monomer in the microemulsion systems (Candau, 1997:131).

Emulsion polymerisation involves the propagation of predominantly water-insoluble monomers e.g. styrene. An aqueous phase is frequently employed as the dispersion phase with a suitable surfactant e.g. sodium dodecyl sulphate (Lin *et al.*, 2001:1481).

Nucleation is characterised by capture of radicals by monomer micelles. The propagation is marked by recruitment of additional monomer and surfactant from emulsified droplets. The termination is a consequence of monomer depletion or radical quenching (Lin *et al.*, 2001:1481).

One of the most characteristic features of microemulsion polymerization is that particle nucleation occurs continuously. This clearly opposes the nucleation mechanism as illustrated in conventional emulsion polymerisation as explained by the Smith and Ewart theory. In emulsion polymerization, the nucleation takes place only in the initial stages until a maximum number of particles were formed. These particles then continue growth with no increase in their number and finally terminate due to monomer depletion or radical combination (Smith & Ewart, 1948:592).

Subsequently only two phases exist for polymer chain growth in microemulsion polymerization i.e. continuous nucleation (due to the immense interfacial area, micelles easily recruit free radicals from the dispersion medium) and end of growth as was illustrated for polymerization of styrene (Girard *et al.*, 1999:997).

The comparison of emulsion and microemulsion copolymerization was aptly investigated for polymerization of methyl methacrylate at various concentration of the surfactant. In microemulsion two phases of polymerization could be observed versus three in emulsions (Gan *et al.*, 1993:2799).

Each of the micellar reactors in these microemulsions contains on average only a single polymer chain. In contradiction thousands of chains could coexist in a conventionally polymerized particle. Additionally, this single particle could either be active in free radical form or inactive, therefore the average number of radicals per particle in the entire population approximates 0.5 (or half of particles in a population are active at any given point in time) (Nomura, *et al.*, 1982:2483, Nomura *et al.*, 1978:1043).

The type of initiator could affect the rate of polymerization since the solubility of the initiator in either monomer or dispersion phases could determine how effective initiator radical formation is (Puig *et al*, 1993:114). If a typical water-soluble initiator potassium persulfate decomposes in water, its radicals could easily distribute in the continuous phase. Consequently, micelles could be exposed to a maximum extent to these radicals with high rates of propagation. In the case of a oil-soluble initiator such as 2,2'-azobisisobutyronitrile, the initiators form in the oil phase. The termination rate of these radicals are higher since they autoterminate due to lack of partitioning to the water phase. The initiation of polymerization with oil-soluble initiators is therefore less effective due to lower micellar exposure and the propagation rates are therefore also slower (Feng & Ng, 1990, Gan *et al.*, 1992:1249).

The polymeric particles that are formed in microemulsion polymerization are generally much larger than the original micelles that gave rise to them in the first place. This was attributed to the formation of a solid particle compared to the liquid state of the emulsion. The size of the particles that were obtained was however found to be significantly smaller than those found for conventional emulsions. The increase in the concentration of monomer or decrease in the concentration of the surfactant that was included in the microemulsion gave rise to an increase in particle size (Guo *et al.*, 1989:691, Perez-Luna, 1990:1040). A decrease in the concentration of the initiator generally also resulted in an increase in particle size (Guo *et al.*, 1989:703).

One aspect of note in microemulsion polymerizations was also that the concentration of the micelles is approximately a thousand times higher than the amount of particles that could form in the reaction. This virtually nullifies the probability of a radical to enter a particle, therefore rendering the chance of biradical termination virtually impossible (Figure 1.1) (O'Donnell & Kaler, 2007:1445).

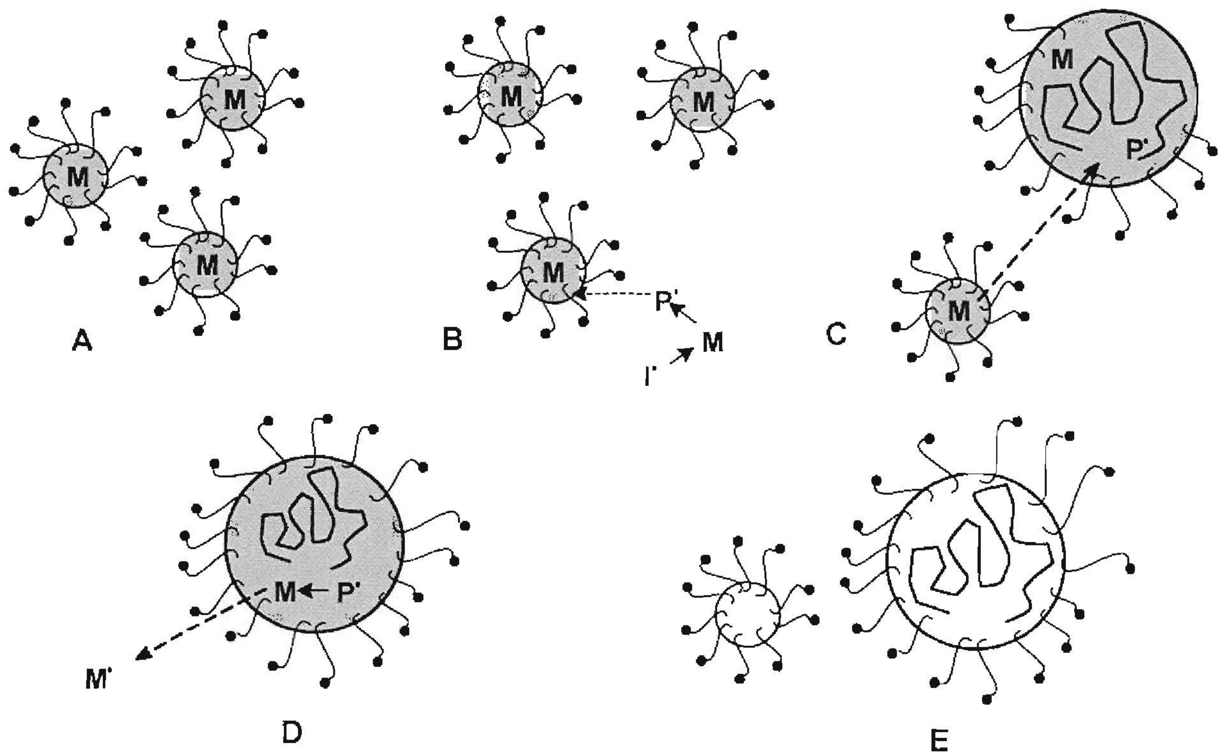

Figure 1.1: Typical oil-in-water microemulsion polymerization initiated by a water-soluble initiator ($I^{\bullet}$). (A) Thermodynamically stable microemulsion of surfactant-stabilized monomer (M) in water. (B). Initiation in the aqueous domain to form a propagating polymer ($P^{\bullet}$) that enters a monomer-swollen micelle upon reaching a critical degree of polymerization. (C). Propagation of a polymer in a surfactant-stabilized particle with monomer diffusing from uninitiated micelles to the locus of polymerization. (D). Transfer of radical activity from a polymer to a monomer and exit of the monomer radical. (E). Final latex of surfactant-stabilized polymer particles and empty micelles (O'Donnell & Kaler, 2007:1446) (Reproduced with permission from Wiley Interscience®).

1.4.2.2 Microemulsion copolymerization

Copolymers and blends have been used to modify the properties of a certain material to such an extent as to combine properties of the corresponding homopolymers (Morais *et al.*, 2006:2349).

A classification of copolymers that are produced today based on monomer composition revealed that 37% were styrene-butadiene copolymers, 30% acrylic or methacrylic based polymers, 28% vinyl acetate-based and 5% allotted for all other products (Tauer, 2003:32).

Copolymers could have numerous advantages regarding their applications. The addition of a certain comonomer into the polymer chain could functionalize the molecule (Marcicinova-Benabdillah *et al.*, 2001:1279, Lou *et al.*, 2001:5806), therefore could augment hydrophilicity and solubility (De Groot *et al*, 2001:1271, Parrish *et al.*, 2002:1983, Leemhuis *et al.*, 2006:3500), modify degradation behavior (Barrera *et al.*, 1995:425, Gerhardt *et al.*, 2006:1735) and modify surface properties. Additionally, these functional groups could facilitate the immobilization of biomolecules on the surface of the polymer particles (Nadeau *et al.*, 2005:11263).

Microemulsion copolymerization involves the same type of free-radical polymerization as for hompolymerizations, however is now complicated by the addition of at least two monomers to the microemulsion. The monomers could partition to different extents to the polymerization locus in the interface. Monomers of comparable water-solubility resulted in copolymers with compositions comparable to that in bulk copolymerizations (Capek & Juranicova, 1996:575). Scheme 1.1 depicts a general reaction scheme that describes the copolymerization of a (meth)acrylate and styrene.

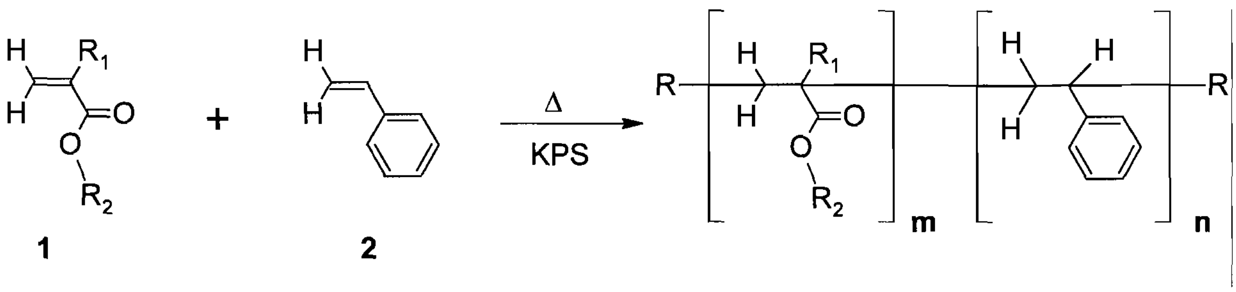

Scheme 1.1: A generic reaction scheme for an acrylate-based monomer (1) and styrene (2) that forms a copolymer chain comprising of *m* and *n* units of the monomers respectively. For the acrylate R_1 = H, for the methacrylate R_1 = CH_3. For (meth)acrylic acid R_2 = H, for the corresponding ester R_2 = alkyl. R represents any carbon chain sections of the polymer.

In the copolymerization of a slightly water-soluble monomer such as styrene and the significantly soluble methyl acrylate, the copolymer content was found to be significantly higher than what was expected. It was concluded that the styrene molecules localized in the micelle core and the methyl acrylate molecules preferred to diffuse into the interfacial corona posed by the surfactant tails. The acrylate was subsequently more exposed to initiator radicals and could polymerize to a higher extent than shielded styrene (Bhawal *et al*, 2003:389, Semchikov *et al.*, 1996:1213).

The role of the polarity of the monomers were also investigated and confirmed that solubility of the monomers was not the only factor to blame for compositional deviation. Two monomer of comparable water-solubility, styrene and butyl acrylate, were copolymerized, however larger fractions of butyl acrylate was found in the copolymer. The higher polarity of butyl acrylate was the driving force for its partitioning to the interfacial polymerization locus whereas the styrene remained in the core of the micellar reactor (Bhawal *et al*, 2003:389).

If comparatively hydrophilic monomers i.e. acrylonitrile were copolymerized with hydrophobic styrene, the hydrophilic monomer significantly decreased the rate of polymerization. As seen from Figure 1.1, the final step in the polymerization reaction transfers the radical from the polymer to a monomer molecule that leaves the micelle as a monomer radical. Therefore if a hydrophilic monomer was employed in a copolymerization, the exiting of the monomer radical would actually be enhanced compared to a more hydrophobic monomer (Pokhriyal & Devi, 2000:333, Capek & Juranicova, 1996:575).

However, in a study performed on the copolymerization of styrene, butadiene and a carboxylic acid monomer, it was seen that the rate of polymerization increased as consequence of the increase in the carboxylic acid monomer. The authors stated that the carboxylic acid monomer could form a substantial number of primary radicals that could propagate in various micelles, subsequently increasing the rate of polymerization. This suggested that radical entry into the micelles and not only radical exit could be important in the propagation of the polymer radicals (Mahdavian & Abdollahi, 2004:3239).

In the emulsion polymerization of methyl methacrylate and methacrylic acid, it was found that the increase in methacrylic acid in the copolymer suppressed the polymerization rate. This implied that the more hydrophilic monomer was polymerized and could not partition to the water phase, engage an initiator radical and re-enter a different micelle to initiate propagation their. The number of active particles decreased as a consequence and decelerated the propagation rate (Kato *et al.*, 1999:127).

In emulsifier-free polymerizations the effect of polarity of the monomers were further illustrated. Styrene was polymerized in water with vinyl acetate or methyl methacrylate. If a polar solvent was added to the aqueous medium, the hydrophilic monomers would partition to some extent and subsequently result in smaller particle sizes. The opposite was also proven for non-polar solvents with particle size increases as result upon addition of ethyl acetate or methyl isobutyrate (Ou *et al.*, 2001:789).

The addition of an alcoholic cosurfactant resulted in several complex effects not yet exhaustively investigated. The alcohol could influence the rate of polymerization and result in a denser packing of micelles, resulting in changes in the polymerization rate (Shi *et al.*, 2005:262, Reddy *et al.*, 2007:3391, Reddy *et al.*, 2002:1503).

It was also illustrated that the inclusion of alcohols as cosurfactant could enlarge the microemulsion region in a phase diagram of formulations containing monomers, water and surfactants. Polar monomers seemed to be effected most and the interaction with alcohol resulted in an increase in the microemulsion region (Donescu *et al.*, 2001:1499).

There were also reports that speculated about the role of alcohols to act as chain transfer agents during the copolymerizations; however, this was not conclusively proven in these studies (Shi *et al.*, 2005:262, Donescu *et al.*, 2001:1503) and only a few examples were found where chain transfer between the monomers in the reaction were observed (Rudin *et al.*, 1979:493, Goldwasser & Rudin, 1982:1993).

In regards to chain transfer agents, these are chemicals that remove the reactivity from the oligomer or polymer radical with subsequent termination of the polymeric radical (De la Fuente & Madruga, 1998:2913, Suzuki *et al.*, 2007:523). Thus, according to Figure 1.1 (D), radical exit from the micelle reactor would be enhanced by the chain transfer agent. Consequently, shorter chains of lower molecular weight resulted if compared to corresponding polymerization systems without a chain transfer agent.

Known alcohol-based chain transfer agents that were investigated included monosaccharides, vinyl or allyl ethers (i.e. allyl alcohol, allyloxyethanol, ethylene glycol vinyl ether and 1,4-butanediol) and halogenated alcohols (i.e. 11-bromoendecanol, chlorodiethoxyethanol and 2-bromoethanol) (Pantiru *et al.*, 2004:506) and dithiobenzoate esters and amides (Takolpuckdee., 2005:66) and various other sulphur-based compounds (Suzuki *et al.*, 2007:523, Fifield & Fitch, 2003:1305).

An early study investigated the polymerization of ethyl acrylate and methyl acrylate in the presence of various solvents. Ethyl acrylate was slightly more prone than methyl acrylate to abstract hydrogen atoms form hydrocarbons and alcohols (chain transfer reaction). It was concluded however that the new solvent-derived radicals were not efficient enough to initiate new polymer chains (Raghuram *et al.*, 1969:2379).

Several copolymers could be synthesized by emulsion-based polymerizations. Table 1.1 summarizes some of the applications of (co)polymeric dispersions.

Table 1.1: Applications of various types of (co)polymer dispersions (De Fusco *et al*, 1997:379).

Application	Polymer latex dispersion/monomer choice	Specific application
Paints	Poly(methyl methacrylate-*co*-butyl acrylate), Poly(vinyl acetate-*co*-butyl acrylate), Poly(vinyl acetate-*co*-ethylene) Poly(styrene-*co*-methyl methacrylate-*co*-butyl acrylate)	Exterior structure coating Interior structure coating High gloss coating
Adhesives	Poly(acrylate) Poly(vinyl acetate) Poly(vinyl acetate-*co*-ethylene) Poly(styrene-*co*-butadiene)	Pressure sensitive applications i.e. tapes and labels Lamination Paper glue Wood glue Packaging material Packaging material Carpet glue
Sealants and caulks	Butyl acrylate Ethyl acrylate Methyl methacrylate Styrene Acrylonitrile	Internal plasticization of polymer chain for enhanced moulding Cohesive strength improvement to prevent peeling and breaking of the sealant in the filled cavity or space
Textile applications	Poly(vinyl acetate) Poly(styrene-*co*-acrylate)s Poly(acrylate)s Poly(styrene-*co*-butadiene) N-methylol acrylamide (prone to crosslinking)	The functional groups i.e. hydroxyl and carboxyl are often crosslinked to produce the material

1.4.2.3 Concluding remarks on microemulsion copolymerization

Clearly, very complex situations could occur in microemulsion copolymerizations and this would serve as motivation to investigate these synthetic routes on a case-by-case basis. Variations in the microemulsion composition could have significant effects on the dispersion properties. Subsequently, if employed for polymerization, various polymeric products could result with different architectures and compositions.

Microemulsion polymerisation could be seen as an improvement on polymer dispersion methods as a technique for the preparation of polymeric nanoparticles. The constitution of microemulsions from reactant ingredients is more convenient than reconstitution of the dispersion system from preformed polymers. However, the applications of polymeric materials in different industries and discipline, complicates their applications in several cases.

One of the drawbacks of microemulsion polymerizations is the fact that a purification step is required to isolate the produced materials. If the particles are intended for use in parenteral dosage forms that circumvent the natural biological barriers, the foreign chemicals in the microemulsions could have fatal effect. Some of the impurities that need to be removed include solvents, surfactants, residual monomers, polymerization initiators and large agglomerates (Limayem *et al.*, 2004:1).

Despite the limitation of the purification process, the microemulsion polymerization method has been used to produce various methacrylate-based polymers and copolymers that could be employed in pharmaceutical applications.

1.5 PHARMACEUTICAL APPLICATIONS OF COPOLYMER NANOPARTICLES

The application of nanotechnology in pharmaceutical science should not rely only on the nanoscale properties of selected materials but also on how they are assembled into a drug delivery system (Xu *et al.*, 2007:579) whether this is on the nano or microscale (Betancourt & Brannon-Peppas, 2006:483).

If parenteral routes were preferred i.e. intravenous injection, stabilized nanoparticles should be used to prevent detrimental uptake and clearance of these particles before any therapeutic effect was seen (Rabinow & Chaubal, 2006:199).

In the case of controlled release applications it might be beneficial to agglomerate nanoparticles to form various barriers to diffusion in order to prevent the immediate release of an active ingredient and prevent exhalation of too fine nanoparticles based on nanosized poly(ethylene glycol) liposomes (Bhavane *et al.*, 93:15) or protein nanoparticle comprised of lysozyme, albumin, and insulin (Bustami *et al.*, 2000:17:1360).

Films could also be used to control drug release since the film matrix could be produced from nanoparticle latexes. If implants were designed to also be a therapeutic drug delivery device, nanocomposite materials could provide the ideal platform for sustained delivery even though the final material exhibits nano-and microstructural aspects (Hwang *et al.*, 2007:589).

1.5.1 Polymer blending

Copolymer nanoparticles were shown to be miscible compared to blending of corresponding homopolymer dispersions. One of the classic examples was described for poly(styrene) and poly(methyl methacrylate) that are immiscible. Upon evaporation of the solvent in which the homopolymers were dispersed, clear separation zones formed that contained only the one homopolymer (Hong & Buns, 1971:1995, Foster & Wool, 1991:1397).

Copolymers could abridge the challenge posed by phase separation by acting as compatibilizers between their corresponding homopolymers (Eastwood & Dadmun, 2002:5069, Pellegrini & Winey, 2000:73, Kulasekere *et al.*, 1996:5493, Morais *et al.*, 2006:2349). This application arose from the fact that the individual copolymer chains already contain a randomized chemical distribution of monomer units, facilitating blending with corresponding chemical sequences in the selected homopolymers.

The effect of phase separation should not be seen as totally unacceptable since nanodomains (blends of poly(styrene) and poly(4-bromostyrene) could form during segregation of polymer blends that could produce different surface topographies. Microdomains were also produced for blends of hyaluronic acid and its sulfated derivative. Cell adhesion could be different if exposed to these surfaces and this can determine or modify the application of a particular blend (Barbucci *et al.*, 2003:721).

1.5.2 Enhancement of drug solubilization

The encapsulation of poorly water-soluble drug candidates could circumvent their failure to reach the market. Therefore, nanodispersion of drugs could be formed that would improve their exposure to the release medium, improving their solubility. Poly(ethylene oxide) copolymers could be used to encapsulate drugs (Attwood *et al.*, 2007:533.) or form micelles containing the drugs (Croy & Kwon, 2006:4669).

Random acrylate-based terpolymers were synthesized by free-radical copolymerization and illustrated the ability to produce micelles that could solubilize poorly water-soluble compounds. The introduction of 2-acry;amido-2-methyl-1-propanesulfonate as comonomer, rendered these polymers sensitive to the ionic strength of the dispersion medium, affecting micellar formation and loading (Szczbialka *et al.*, 2003:699).

1.5.3 Parenteral dosage forms

The parenteral route requires that the nanocarriers should be biodegradable and some poly(alkyl cyanoacrylates) (Duchene & Ponchel, 2003:15) and poly(esters) such as poly(lactide-*co*-lactide) nanoparticles were prepared (Koman *et al.*, 2002:239) for parenteral administration..

Insulin was administered by the subcutaneous route after the insulin was loaded into ethylene oxide-propylene oxide copolymer gels (Pluronic® F-127) as well as poly(lactide-*co*-glycolide) spheres. The route and dosage form proved successful in maintaining insulin and subsequently blood glucose levels in rats (Barrichello *et al.*, 1999:189).

1.5.4 Artificial implants

Several artificial implants have been made and these made extensive use of polymeric materials. Nanocomposite materials could be produced from polymeric materials that incorporated calcium salts to augment biointegration in the event of bone replacements (Sikiric *et al*, 2007:330) or even total joint replacements (Katti, 2004:133). In this regard, nanomodification of microporous surfaces could be promising as seen for titanium surfaces for orthopaedic implants (Yao & Webster, 2006:2682)

A copolymer could also be used in implants to provide the nanotemplate for crystallization of calcium phosphate from aqueous solutions at various pH levels. The resultant polymer/phosphate hybrids could provide novel drug delivery carriers that could be used in biomedical implants (Tjandra *et al.,* 2006:5988).

Poly(styrene-*co*-methyl methacrylate) was employed as a bone cement material and is commercially available as Endurance® that could be loaded with drugs (Cai *et al.*, 2007:3199).

The traditionally used bone cement, poly(methyl methacrylate), still poses challenges that need to be addressed and composite materials consisting of different polymers and excipient additions could circumvent the associated problems (Heo *et al*, 2007:373).

1.5.5 Films

Three steps were identified in the process of film formation. Firstly, solvent evaporation takes place, resulting in packing of the various latex particles. Secondly, these latex particles deform once a critical temperature was reached. The final step results in formation of a homogenous film due to interdiffusion and interpenetration of adjacent polymer chains (Visschers *et al.*, 1997:39, Visschers *et al.*, 2001:49).

Films could be produced from biodegradable polymer latexes i.e. poly(lactide-*co*-glycolide) after this polymer dispersions were produced the emulsification solvent diffusion method. This film could have potential use as a parenteral depot (Schade *et al.*, 1995:209).

As an alternative to degradable depots, non-degradable films could be produced (Figure 1.2) from methacrylate polymer lattices. These films could contain latex particles i.e. methyl methacrylate copolymer that could create channels for diffusion in the film for other soluble materials (Steward *et al.*, 1995:23) or drug molecules such as chlorpheniramine maleate or propranolol hydrochloride that showed controlled release from Eudragit® copolymer films that was laminated again by coating the loaded core with another layer of polymer (Bodmeier & Paeratakul, 1990:32).

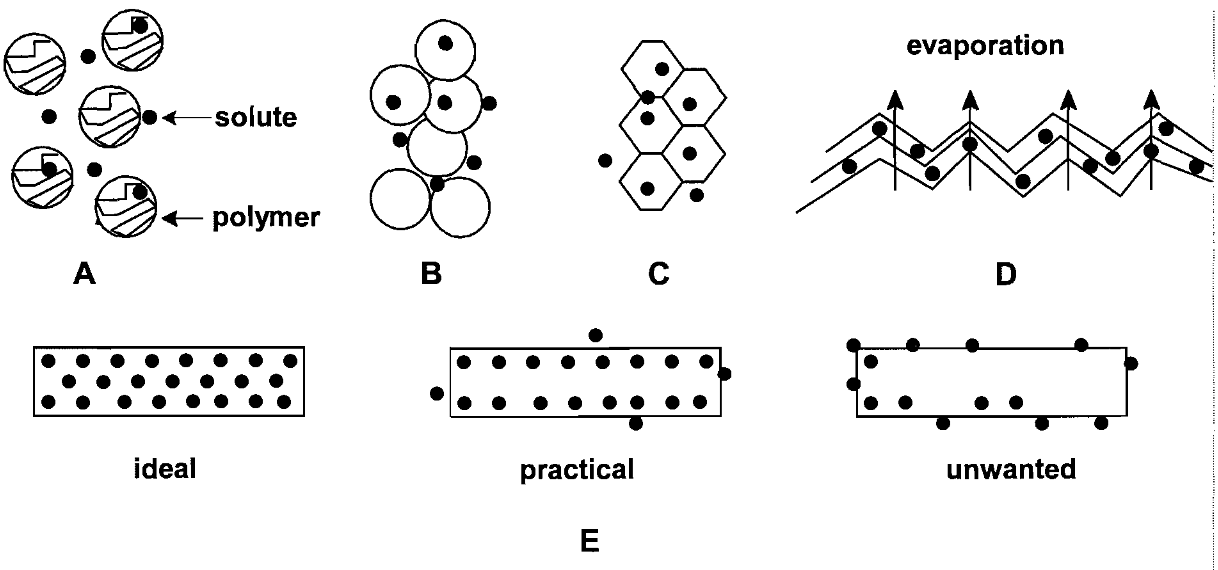

Figure 1.2: (A) a latex dispersion in a solute-containing solvent (B) latex and solute particles pack closer as solvent evaporates (C) latex particles deform and pack even closer (D) interpenetration of latex chains lock solute particles in film layers (E) solvent evaporation transports none (ideal), some (practical) or all (unwanted) solute particles outside the film.

1.5.6 Tables and other oral dosage forms

Even the most prevalent dosage form in the world, tablets, did not escape the revolution brought about by nanotechnology. Commercially available colloidal methacrylate polymer dispersions i.e. Eudragit® and Aquacoat® were utilized as model nanosuspensions. These were incorporated in solid dosage forms including tablets, granules, pellets and films. Several excipients were added to ultimately result in the disintegration of these dosage forms to redisperse the nanoparticles. The authors finally speculated that the nanoparticles could be loaded with drugs before they were compounded into dosage forms (Schmidt & Bodmeier, 1999:115).

A computer-controlled emulsion polymerization was utilized to manufacture montmorillonite nanoparticles that were ultimately employed to coat tablets. The uniformity of the coat thickness was monitored by Raman spectroscopy and occurrence of surface defects was monitored by atomic force spectroscopy (Csontos *et al.*, 2006:884).

1.5.7 Drug-derived monomers for copolymerization

Drug-derived monomers could potentially take copolymerization to a very specialized pharmaceutical application. Poly(hydroxyethyl methacrylate) hydrogels are highly biocompatible and transparent. Additionally, they are resistant to acid and alkaline hydrolysis. Ibuprofen and diclofenac molecules were polymerized to methacrylic monomers using a methacrylic cross-linker to finally produce the drug-methacrylate copolymer. Extended release could be proven for both drugs (Andrade-Vivero *et al.*, 2007:802).

An ibuprofen monomer was synthesized by linking to a methacrylic monomer and insertion of a *p*-aminophenoxy spacer resembled paracetamol. Subsequently, the derived monomer was polymerized to form the poly(drug-*co*-methacrylate). This polymer could be slowly hydrolyzed, releasing both drug and spacer residues. Ultimately both these compound were effective in the reduction of inflammatory responses. The degradation product of the polymer was the soluble salt of poly(methacrylic acid) that could easily be eliminated by the body (Liso *et al.*, 1996:553).

A promising development was found for producing poly(acrylate) nanoparticles prepared by an emulsion polymerization method to incorporate penicillin G. A penicillin acrylamide monomer was synthesized of penicillin G. The penicillin monomer was then copolymerized with styrene and butyl acrylate to produce the random penicillin-stryene-butyl acrylate terpolymer. The polymeric antibiotic retained its activity despite its covalent linkage to the polymer chain. Additionally, it was remarkably resistant to degradation induced by problematic methicillin-resistant strains of *Staphylococcus aureus* (Turos *et al.*, 2007a:53, 2007b:3468).

A generic reaction scheme is given in Scheme 1.2 to demonstrate possible copolymerizations of drug-derived acrylate monomers.

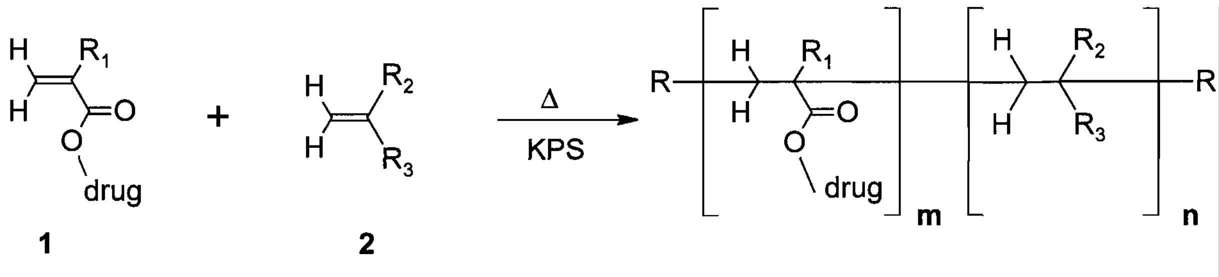

Scheme 1.2: A potential microemulsion copolymerization of a drug-vinyl monomer (1) and a suitable vinyl comonomer (2). R_1, R_2 and R_3 are substituents that could alter polymer properties i.e. -OH, -SH, -COOH, aromatic rings or alkyl chains. R represents any carbon chain sections of the polymer.

1.6 NANOTECHNOLOGY IN CONCLUSION

The onset of nanotechnology made it possible to study and create materials at levels that could not be observed before. Numerous methods exist to produce nanoparticles and a large variety of materials are produces that possess nanoscale characteristics.

The production of nanodevices for biological applications originated from the realization that synthetic nanostructures could be rendered biocompatible with vigilant modification. These applications arise from the unique characteristics that polymers possess to mimic biological systems and also from their surface characteristics.

Two broad categories could be distinguished for the production of polymeric nanoparticles. The first technique follows a dispersion approach where the polymeric material is solubilized in a solvent and then dispersed it in a suitable medium. The source of the polymers is typically commercial and limits the choice of available materials to some extent. However, the commercially available polymers are often characterized and versatile in its applications. The dispersion procedure of the polymer might require the aid of several excipients to stabilize this dispersion, nevertheless, microemulsions and miniemulsions could both be produced.

The second category follows a synthetic route to produce nanoparticles as the final product. A dispersion approach is also followed for this technique, however in this case the dispersion is constituted from various reactants that are required to assemble the final product. Several dispersion systems could be utilized to synthesize polymer nanolatexes and these include emulsions, microemulsions and miniemulsions. These methods produce fairly stable nanoparticles as the end product. This route however offers the advantage to produce new polymers that might not be available commercially.

An even further specialization of material synthesis was also identified for synthesis of drug-derived monomers. These monomers could be copolymerized with available methacrylate and other vinyl monomers. Subsequently drug-methacrylate copolymers could be produced, enhancing the effect of the existing drugs. The activity of the drug could be restored against resistant strains and problematic drug properties i.e. poor water-solubility and chemical instability could be prevented in this way. If the mechanism of microemulsion polymerization is considered (Figure 1.1), a myriad of new challenges could be presented to establish optimal reaction conditions. Nonetheless, the potential for future research resulting from this will be immense.

In pharmaceutical industry, it has always been a prerequisite that material properties should be characterized. If new polymer latexes are therefore produced and an application is sought for them, a combination of the synthesis and reconstitution routes would probably be needed. Both routes could also be customized after characterization of the material to better suit both routes. The optimization of these routes will ultimately depend on the application of the material. It should also be realized that the transition between the nanoscale and microscale hierarchies should be considered to ultimately produce the application.

This was a mere glimpse at the peripheries of various domains of the scientific disciplines that governs the application of nanotechnology. The purpose was to illustrate the necessity of the convergence of different scientific disciplines to achieve the end goal i.e. the development of an application such as a novel drug delivery system. It was shown that microemulsion copolymerization, although a complex process may be utilized to produce novel materials at the nanolevel and depending on the application, such materials can be utilized at the nanoscale or be assimilated to abridge the nanoscopic to microscopic hierarchies.

1.7 REFERENCES

ANDRADE-VIVERO, P., FERNANDEZ-GABRIEL, E., ALVAREZ-LORENZO, C & CONCHEIRO, A. 2007. Improving the loading and release of NSAIDs from pHEMA hydrogels by copolymerization with functionalized monomers. *Journal of pharmaceutical sciences*, 96:802-813.

ANTONIETTI, M. & LANDFESTER, K. 2002. Polyreactions in miniemulsions. *Progress in polymer science*, 27:689-757.

ATTWOOD, D., ZHOU, Z. & BOOTH, C. 2007. Poly(ethylene oxide) based copolymers: solubilisation capacity and gelation. *Expert opinion in drug delivery*, 4:533-546.

BARBUCCI, R., PASQUI, D., WIRSEN,A., AFFROSSMAN, S., CURTIS, A. & TETTA, C. 2003. Micro and nanostructured surfaces. *Journal of materials science: materials in medicine*, 14:721-725.

BARRERA, D.A., ZYLSTRA, E., LANSBURY, P.T. & LANGER, R. 1995. Copolymerization and degradation of poly(lactic acid-*co*-lysine). *Macromolecules*, 28:425-432.

BARRICHELLO, J.M., MORISHITA, M., TAKAYAMA, K. & NAGAI, T. 1999. Absorption of insulin from Pluronic F-127 gels following subcutaneous administration in rats. *International journal of pharmaceutics*, 184:189-198.

BEERBOWER, A. & HILL, M.W. 1971. The cohesive energy ratio of emulsions. A fundamental basis for the HLB basis. (*In* McCutcheon *ed.* Detergents and Emulsifiers Annual. Allured Pub. Co.:NJ 223 p.)

BELLUCCI, S., BERGAMASHI, A., BOTTINI, M., MAGRINI, A. & MUSTELIN, T. 2007. Biomedical platforms based on composite nanomaterials and cellular toxicity. *Journal of physics: conference series*, 61:95-98.

BETANCOURT, T. & BRANNON-PEPPAS, L. 2006. Micro- and nanofabrication methods in nanotechnological medical and pharmaceutical devices. *International journal of nanomedicine*, 1:483-495.

BHANG, S.H., JEON, O., CHOI, C.Y., KWON, Y.H.K. & KIM, B.-S. 2007. Controlled release of nerve growth factor from fibrin gel. *Journal of biomedical materials research, Part A*, 80A:998-1002.

BHAVANE, R., KARATHANASIS, E. & ANNAPRAGADA, A.V. 2003. Agglomerated vesicle technology: a new class of particles for controlled and modulated pulmonary drug delivery. *Journal of controlled release*, 93:15-28.

BHAWAL, S., SHANGVI, S.G. & DEVI, S. 2003. Recalculation of monomer reactivity considering the effect of monomer partitioning in microemulsion. *European polymer journal*, 39:389-396.

BODMEIER, R. & PAERATAKUL, O. 1990. Drug release from laminated polymeric films prepared form aqueous latexes. *Journal of pharmaceutical sciences*, 79:32-36.

BUSTAMI, R.T., CHUN, H.-K., DEHGHANI, F. & FOSTER, N.R. 2000. Generation of micro-particles of proteins for aerosol delivery using high pressure modified carbon dioxide. *Pharmaceutical research*, 17:1360-1366.

CAI, X.-Z., YAN, S.-G., WU, H.-B., HE, R.-G., DAI, X.-S., CHEN, H.X., YAN, R.-J., & ZHAO, X.-H. 2007. Effect of delayed pulse-wave ultrasound on local pharmacokinetics and pharmacodynamics of vancomycin-loaded acrylic bone cement in vivo. *Antimicrobial agents and chemotherapy*, 51:3199-3204.

CANDAU, F. 1997. Microemuslion polymerization. (*In* Asua, J.M. *ed* Polymeric dispersions: principle and applications. Kluwer:Dortrecht. p. 127-140.)

CANDAU, F., LEONG, Y.S., POUYET, G. & CANDAU, S.J. 1984. Inverse microemulsion polymerization of acrylamide: characterization of the water-in-oil emulsions and final microlatexes. *Journal of colloid & interface science*, 101:167-183.

CANDAU, F., PABON, M. & ANQUETIL, J.-Y. 1999. Polymerizable microemulsions: some criteria to achieve an optimal formulation. *Colloids and surfaces A: physicochemical and engineering aspects*, 153:47-59.

CAPEK, I. & JURANICOVA, V. 1996. On kinetics of microemulsion copolymerization of butyl acrylate and acrylonitrile. *Journal of polymer science, part A: polymer chemistry*, 34:575

COOMBES, A.G.A., TASKER, S., LINDBLAD, M., HOLMGREN, HOSTE, K., TONCHEVA, V., SCHACHT, E., DAVIES, M.C., ILLUM, L & DAVIS, S.S. 1997. Biodegradable polymeric microparticles for drug delivery and vaccine formulation: the surface attachment of hydrophilic species using the concept of poly(ethylene glycol) anchoring segments. *Biomaterials*, 18:1153-1161.

CROY, S.R. & KWON, G.S. 2006. Polymeric micelles for drug delivery. *Current pharmaceutical design*, 12:4669-4684.

CSONTOS, I., RONASZEGI, K., SZABO, A., KESZEI, S. & ANNA, P. 2006. Controlled technology for forming a nanostructured polymer coating for solid pharmaceuticals. *Polymers for advanced technologies*, 17:884-888.

CURTIS, A. & WILIKINSON, 2001. Nanotechniques and approaches in biotechnology. *Trends in biotechnology*, 19:97-101.

DANIELSSON, I. & BJOERN, L. 1981. The definition of microemulsion. *Colloids and surfaces*, 3:391.

DE FUSCO, A.J., SEHGAL, K.C. & BASSETT, D.R. 1997. Overview of the use of polymer latexes. (*In* Asua, J.M. *ed* Polymeric dispersions: principle and applications. Kluwer:Dortrecht. p. 379-396.)

DE GROOT, J.H., DILINGHAM, K., DEURING, H., HAITJEMA, H.J., VAN BEIJMA, F.J., HODD, K. & NORRBY, S. 2001. Hydrophilic polymeric acylphosphine oxide photoinitiator/crosslinkers for in vivo blue-light photopolymerization. *Biomacromolecules*, 2:1271-1278.

DE LA FUENTE, J.S. & MADRUGA, E.L. 1998. Determination of chain transfer constant to dodecanethiol in styrene/methyl methacrylate and butyl acrylate/methyl methacrylate copolymerization and effet of chain length on composition and stereochemical configuration of copolymers. *Journal of polymer science, part A: polymer chemistry*, 36:2913-2925.

DONESCU, D., FUSULAN, L., PETCU, C., BORBORODEA, A.-G. & VASILESCU, D.-S. 2001. Copolymerization of vinyl acetate with acrylic monomers in microemulsions. *European polymer journal*, 37:1499.

DROTLEFF, S., LUNGWITZ, U., BREUNIG, M., DENNIS, A., BLUNK, T., TESSMAR, J. & GÖPFERICH, A. 2004. Biomimetic polymers in pharmaceutical and biomedical sciences. *European journal of pharmaceutics and biopharmaceutics*, 58:385-407.

DUCHENE, D. & PONCHEL, G. 2003. Combined poly(alkyl cyanoacrylate)/cyclodextrin nanoparticles. *Journal of inclusion phenomena and macrocyclic chemistry*, 44:15-16.

EASTWOOD, E.A. & DADMUN, M.D. 2002. Mulitblock copolymers in the compatibilization of polystyrene and poly(methyl methacrylate) blends: role of polymer architecture. *Macromolecules*, 35:5069-5077.

EL-AASSER, M.S., LACK, C.D., CRAIG, D., VANDERHOFF, J.W. & FOWKES, F.M. 1988. The miniemulsification process. Different form of spontaneous emulsification. *Colloids and surfaces*, 29:103-118.

FENG, L. & NG, K.Y.S. 1990. In situ kinetic studies of microemulsion polymerization of styrene and methyl methacrylate by Raman spectroscopy. *Macromolecules*, 23:1048-1053.

FERNANDEZ, P., ANDRÉ, V., RIEGER, J. & KÜHNLE, A. 2004. Nano-emulsion formation by emulsion phase inversion. *Colloids and surfaces A: physicochem. eng. aspects*, 251:53-58.

FIFIELD, C.C. & FITCH, R.M. 2003. A unique transurf in styrene emulsion polymerization. *Comptes rendus chimie*, 6:1305-1312.

FOSTER, K.L. & WOOL, R.P. 1991. Strength of polystyrene-poly(methyl methacrylate) interfaces. *Macromolecules*, 24:1397-1403.

GAN, L.M., CHEW, C.N. & LYE, I. 1992. Styrene polymerization in microemulsion in oil-in-water microemulsions: kinetics of polymerization. *Makromolekulare Chemie*, 193:1249-1260.

GAN, L.M., CHEW, C.N., NG, S.G. & LOH, S.E. 1993. Polymerization of methyl methacrylate in ternary systems: emulsions and microemulsion. *Langmuir*, 9:2799-2803.

GERHARDT, W.W., NOGA, D.E., HARDCSTLE, K.H., GARCIA, A.J., COLLARD, D.M. & WECK, M. 2006. Functional lactide monomers: methodology and polymerization. *Biomacromolecules*, 7:1735-1742.

GIRARD, N., TADROS, TH.F. & BAILEY. 1999. Kinetics of polymerisation of styrene-in-water microemulsions. *Colloid and polymer science*, 277:997-1000.

GODWIN, A, BOLINA, K., CLOCHARD, M., DINAND, E., RANKIN, S., SIMIC, S. & BROCCHINI, S. 2001. New strategies for polymer development in pharmaceutical science – a short review. *Journal of pharmacy and pharmacology*, 53:1175-1184.

GOLDWASSER, J.M. & RUDIN, A. 1982. Emulsion copolymerization of styrene and methyl methacrylate. *Journal of polymer science, part A: polymer chemistry*, 20:1993-2006.

GUO, J.S., EL-AASSER, M.S. & VANDERHOFF, J.M. 1989. Microemulsion polymerization of styrene. *Journal of polymer science, polymer chemistry, part A: polymer chemistry*, 27:691-710.

HARABAIGU, V., FUNDUEANU, G., PINTEALA, M., CONSTANTIN, M. & HAMAIDE, T. 2004. Bioapplication oriented polymers. Micro-and nanoparticles for drug delivery systems. *Advances in experimental medicine and biology*, 553(Biomaterials):69-82.

HEO, S.J., PARK, S.A., SHIN, H.J., LEE, Y.J., YOON, T.R., SEO, H.Y., AHN, K.C., KIM, S.E. & SHIN, J.W. 2007. Evaluation of bonding stress for the newly suggested bone cement: comparison with currently used PMMA through animal studies. *Key engineering materials*, 342-343:373-376.

HOLZSCHERER, C. & CANDAU, F. 1988. Application of the cohesive energy ratio concept (CER) to the formation of polymerizable microemulsions. *Colloids and surfaces*, 29:411-423.

HONG, S.D. & BURNS, C.M. 1971. Compatibility of polystyrene and poly(methyl methacrylate) in benzene. Effects of molecular weight and temperature. *Journal of applied polymer science*, 15:1995-2006.

HWANG, J.-S., OH, K.-T., KIM, K.-N. & KIM, K.-M. 2007. The characterization of the nano-micro hybrid structure of titanium surface abd osteoblast response to the surface. *Key engineering materials*, 342-343:589-592.

ITO, F., MAKINO, K., OHSHIMA, H., TERADA, H. & OMI, S. 2004. Salt effects on controlled coagulation in emulsion polymerisation. *Colloids and surfaces A: physicochemical and engineering aspects*, 233:171-179.

JAIN, R.A. 2000. The manufacturing techniques of various drug loaded biodegradable poly(lactide-*co*-lactide) (PLGA) devices. *Biomaterials*, 21:2475-2490.

KAISER, C.S., RÖMPP, H. & SCHMIDT, P.C. 2001. Pharmaceutical applications of supercritical carbon dioxide. *Pharmazie*, 56:907-926.

KATO, S., SATO, K., MAEDA, D. & NOMURA, M. 1999. A kinetic investigation of styrene emulsion polymerisation with surface active polyelectrolytes as the emulsifier. II: effects of molecular weight and composition. *Colloids and surfaces A: physicochemical and engineering aspects*, 153:127-131.

KATTI, K.S. 2004. Biomaterials in total joint replacements. *Colloids and surfaces, B, biointerfaces*, 39:133-142.

KHOMUTOV, G.B. 2004. Interfacially formed organized planar inorganic, polymeric and composite nanostructures. *Advances in colloid and interface science*, 111:79-116.

KIM, H.-W. 2007. Biomedical nanocomposites of hydroxyapatite/polycaprolactone obtained by surfactant mediation. *Journal of biomedical materials reseach, part A*, 83A(1):169-177.

KOMAN, Y.N., GURNY, R. & ALLÉMAN, E. 2002. Preparation and characterization of sterile and freeze-dried sub-200 nm nanoparticles. *International journal of pharmaceutics*, 233:239-252.

KONG, L., GAO, Y., LU, G., GONG, Y., ZHAO, N. & ZHANG, X. 2006. A study on the bioactivity of chitosan/nano-hydroxyapatite composite scaffolds for bone tissue engineering. *European polymer journal*, 42:3171-3179.

KULASEKERE, R., KAISER, H., ANKNER, J.F., RUSSELL, T.P., BROWN, H.R., HAWKER, C.J. & MAYES, A.M. 1996. Homopolymer interfaces reinforced with random copolymers. *Macromolecules*, 29:5493-5496.

KULKARNI, R.J. 2007. Nano-bio-genesis: tracing the rise of nanotechnology and nanobiotechnolgy as 'big science'. *Journal of biomedical discovery and collaboration*, 2:3 doi: 10.1186/1747-5333-2-3.

LANDFESTER, K. 2003. Preparation of of polymer and hybrid colloids by miniemulsion for biomedical applications. *Surface science series*, 115:225-243.

LANDFESTER, K. 2000. Recent developments in miniemulsions – formation and stability mechanisms. *Macromeolecular symposia*, 150:171-178.

LANGER, R. & PEPPAS, N.A. 2003. Advances in biomaterials, drug delivery, and bionanotechnology. *AIChE Journal*, 49:2990-3006.

LAVAL, J.-M., CHOPINEAU, J. & THOMAS, D. 1995. Nanotechnology: R & D challenges and opportunities for application in biotechnology. *Trends in biotechnology*, 13:474-481.

LEEMHUIS, M., NOSTRUM, C.F., KRUIJTZER, J.A.W., ZHONG, Z.Y., TEN BRETELER, M.R., DIJKSTRA, P.J., FEIJEN, J., & HENNINK, W.E. 2006. Functionalized poly(α-hydroxy acid)s via ring-opening polymerization: toward hydrophilic polyesters with pendant hydroxyl groups. *Macromolecules*, 39:3500-3508.

LIMAYEM, I., CHARCOSSET, C. & FESSI, H. 2003. Purification of nanoparticle suspensions by a concentration/diafiltration process. *Separation and purification technology*, 38:1-9.

LIN, S.-H., CHERN, C.-S., HSU, T.-J., HSU, C.-T. & CAPEK, I. 2001. Emulsion polymerisation of styrene: double emulsion effect. *Polymer*, 42:1481-1491.

LISO, P.A., REBUELTA, M., ROMÁN, J.S, GALLARDO, A. & VILLAR, A.M. 1996. Polymeric drugs derived from ibuprofen with improved anti-inflammatory profile. *Journal of biomedical materials research*, 32:553-560.

LOBO, L., SVEREIKA, A. & NAIR, M. 2002. Coalescence during emulsification. 1. Method development. *Journal of colloid and interface science*, 253:409-418.

LOBO, L. & SVEREIKA, A. 2003. Coalescence during emulsification 2. Role of small molecule surfactants. *Journal of colloid and interface science*, 261:498-507.

LOU, X., DETREMBLEUR, C., LECOMTE, P., & JEROME, R. 2001. Living ring-opening (co)polymerizations of 6,7-dihyfro-2(5H)-oxepinone into unsaturated aliphatic polyesters. *Macromolecules*, 34:5806-5811.

MAHDAVIAN, A.-R. & ABDOLLAHI, M. 2004. Investigation into the effect of carboxylic acid monomer on particle nucleation and growth in emulsifier-free emulsion copolymerization of styrene-butadiene-acrylic acid. *Polymer*, 45:3233-3239.

MARCINCINOVA-BENABDILLAH, K., BOUSTTA, M., COUDANE, J. & VERT, M. 2001. Novel degradable polymers combining D-glucoronic acid, a sugar of vegetal origin, with lactic and glycolic acids. *Biomacromolecules*, 2:1279-1284.

MAYSINGER, D. 2007. Nanoparticles and cells: good companions and doomed partnerships. *Organic and biomolecular chemistry*, 5:2335-2342.

MEHNERT, W. & MÄDER, K. 2001. Solid lipid nanoparticles. Production, characterization and applications. *Advanced drug delivery reviews*, 47:165-196.

MESSLER, J.W. 2004. Growth of a new discipline. *Materials today*, 3:44-47.

MOGHIMI, S.M., VEGA, E., GARCIA, M.L., AL-HANABLI, O.A.R. & RUTT, K.J. 2006. Polymeric nanoparticles as drug carriers and controlled release implants. (*In* Nanoparticulates as drug carriers. Torchilin, V.P. *ed.* p. 29-42.)

MOLLZADEH, S., JAVADPOUR, J. & KHAVANDI, A. 2007. Biomimetic synthesis and mechanical properties of hydroxyapatite/poly(vinyl alcohol) nanocomposites. *Advances in applied ceramics*, 106:165-170.

MORAIS, V., ENCINAR, M., PROLONGO, M.G. & RUBIO, R.G. 2006. Dynamical mechanical behaviour of copolymers made of styrene and methyl methacrylate: random, alternate and diblock copolymers. *Polymer*, 2006:2349-2356.

MORALES, D.; GUTIERREZ, J. M.; GARCIA-CELMA, M. J. & SOLANS, Y. C. 2003. A Study of the Relation between Bicontinuous Microemulsions and Oil/Water Nano-emulsion Formation. *Langmuir*, 19:7196-7200.

MULLIS, K.B. & FALOONA, F.A. 1987. Specific synthesis of DNA in vitro via polymerase-catalyzed chain-reaction. *Methods in enzymology*, 155:335-350.

NADEAU, V., LECLAIR, G., SANT, S., RABANEL, J.-R., QUESNEL, R. & HILDGEN, P. 2005. Synthesis of a new versatile functionalized polyesters for biomedical applications. *Polymer*, 46:11263-11272.

NGUYEN, C.A., KONAN-KOUAKOU, Y.N., ALLÉMAN, E., DOELKER, E., QUINTANAR, GUERRERO, D., FESSI, H. & GURNY, R. 2006. Preparation of surfactant-free nanoparticles of methacrylic acid copolymers used for film coating. *AAPS PharmSciTech*, 7(3): Article 63.

NOMURA, M., SASAKI, S., HARADA, M. & EGUCHI, W. 1978. A kinetic study of vinyl acetate polymerization in aqueous media in the absence of emulsifier. *Journal of applied polymer science*, 22:1043-1060.

NOMURA, M., YAMAMOTO, K., HORIE, I., FUJITA, K. & HARADA, M. 1982. Kinetics of emulsion copolymerization. II. Effect of free radical desortption on the rate of emulsion copolymerization of styrene and methyl methacrylate. *Journal of applied polymer science*, 27:2483-2501.

O'DONNELL, J.O. & KALER, E.W. 2007. Microstructure, kinetics, and transport in oil-in water microemulsion polymerizations. *Macromolecular rapid communications*, 28:1445-1454.

ORIVE, G., HERNÁNDEZ, R.M., GASCÓN, A.R., DOMÍNGUEZ-GIL, A. & PEDRAZ, J.L. 2003. Drug delivery in biotechnology: present and future. *Current opinion in biotechnology*, 14:659-664.

OU, J.-L., YANG, J.-K. & CHEN, H. 2001. Styrene/potassium persulfate/water systems: effects of hydrophilic comonomers and solvent additives on the nucleation mechanism and the particle size. *European polymer journal*, 37:789-799.

PANTIRU, M., IOJOIU, C., HAMAIDE, T. & DELOLME, F. 2004. Influence of the chemical structure of transfer agents in the coordinated anionic ring-opening polymerization: application to one-step functional oligomerization of ε-caprolactone. *Polymer international*, 53:506-514.

PARRISH, B., QUANSAH, J.K. & EMRICK, T. 2002. Functional polyesters prepared by Polymerization of α-allyl(valerolactone) and its copolymerization with ε-caprolactone and δ-valerolactone. *Journal of polymer science: part A: polymer chemistry*, 40:1983-1990.

PELLEGRINI, N.N. & WINEY, K.I. 2000. Asymmetric miscibility in random copolymer/homopolymer blends: Monomeric size and polarity. *Macromolecules*, 33:73-79.

PEREZ-LUNA, V.H., PUIG, J.E., CASTANO, V.M., RODRIGUEZ, B.E., MURTHY, A.K. & KALER, E.W. 1990. Styrene polymerization in three-component cationic microemulsions. *Langmuir*, 6:1040-1044.

POKHRIYAL, N.K. & DEVI, S. 2000. Effect of water solubility of monomer on reaction kinetics in oil-water microemulsion copolymerisation. *European polymer journal*, 36:333-343.

PUIG., J.E., PEREZ-LUNA, V.H., PEREZ-GONZALEZ, M., MACIAS, E.R., RODRIGUEZ, B.E. & KALER, E.W. 1993. Comparison of oil-soluble and water-soluble initiation of styrene in three component microemulsion. *Colloid and polymer science*, 271:114-123.

RABINOW, B. & CHAUBAL, M.V. 2006. Injectable nanoparticles for efficient drug delivery. *Drugs and the pharmaceutical sciences*, 159:199-229.

RAGHURAM, P.V.T. & NANDI, U.S. 1969. Polymerization of ethyl acrylate. II. Chain transfer studies. *Journal of polymer science, part A: polymer chemistry*, 7:2379-2385.

REDDY, G.V.R., BABU, Y.P.P. & REDDY, N.S.R. 2002. Microemulsion and conventional emulsion copolymerizations of methyl methacrylate with acrylonitrile. *Journal of applied polymer science*, 85:1503-1510.

REDDY, G.V.R., DEVI, N.G. & PANDA, J. 2007. Microemulsion and conventional emulsion copolymerizations of styrene with methyl methacrylate. *Journal of applied polymer science*, 105:3391-3401.

REVERCHON, E., DELLA PORTA, G. & CIAMBELLI, S.P. 1999. Supercritical antisolvent precipitation of nanoparticles of a zinc oxide precursor. *Powder technology*, 102:127-134.

ROCO, M.C. 2003. Nanotechnology: convergence with modern biology and medicine. *Current opinion in biotechnology*, 14:337-346.

ROSSOMACHA, E., HOEMANN, C.D. & SHIVE, M.S. 2004. Simple methods for staining chitosan in biotechnological applications. *Journal of histotechnology*, 27:31-36.

RUDIN, A; SAMANTA, M.C. & VAN DER HOFF, B.M.E. 1979. Monomer chain-transfer constants from emulsion copolymerization data: styrene and α-methylstyrene. *Journal of polymer science, part A: polymer chemistry*, 17: 493-502.

RUSSELL, L.E., GALYEAN, A.A., NOTTE, S.M. & LEOPOLD, M.C. 2007. Stable aqueous nanoparticle film assemblies with covalent and charged polymer linking networks. *Langmuir*, 23:7466-7471.

SAHOO, S.K. & LABHASETWAR, V. 2003. Nanotech approaches to drug delivery and imaging. *Drug discovery today*, 8:1112-1120.

SARIKAYA, M., TAMERLER, C., JEN, A.K.-Y., SCHULTEN, K., BANEYX, F. 2003. Molecular biomimetics: nanotechnology through biology. *Nature materials*, 2:577-585.

SCHADE, A., NIWA, T., TAKEUCHI, H., HINO, T. & KAWASHIMA, Y. 1995. Aqueous colloidal polymer dispersions of biodegradable DL-lactide/glycolide cpolymer as basis for latex films: a new approach for the development of biodegradable depot systems. *International journal of pharmaceutics*, 117:209-217.

SCHADLER, L.S., BRINSON, L.C. & SAWYER, W.G. 2007. Polymer nanocomposites: a small part of the story. *JOM*, 59:53-60.

SCHMIDT, C. & BODMEIER, R. 1999. Incorporation of polymeric nanoparticles into solid dosage forms. *Journal of controlled release*, 57:115-125.

SEMCHIKOV, Y.D., SMIRNOVA, L.A., KOPYLOVA, N.A. & IZIVOLENSKII, V.V. 1996. The effect of monomer preferential solvation in radical copolymerisation: reactivity ratios and compositional distribution. *European polymer journal*, 32:1213-1219.

SHEKUNOV, B., YU, H. & YORK, P. 1999. Crystalization process in turbulent supercritical flows. *Journal of molecular structure*, 198-199:1345-1351.

SHI, Y., WU, Y., HAO, J. & LI, G. 2005. Kinetics of microemulsion copolymerisation of styrene and acrylonitrile in the presence of cosurfactant. *Colloids and surfaces A: physicochemical and engineering aspects*, 262:191-197.

SIKIRIC, M.D., GERGELY, C., CUISINIER, F. & FUREDI-MILHOFER, H. 2007. Biomimetic organic-inorganic nanocomposite coatings for titanium implants: I. Preparation, physicochemical and mechanical characterization. *Key engineering materials*, 330-332:389-392.

SMITH, W.V. & EWART, R.H. 1948. Kinetics of emulsion polymerization. *Journal of chemical physics*, 16:592-599.

SOPPIMATH, K.S., AMINABHAVI, T.M., KULKARNI, A.R. & RUDZINSKI, W.E. 2001. Biodegradable polymeric nanoparticles as drug delivery devices. *Journal of controlled release*, 70:1-20.

STEWARD, P.A., HEARN, J. & WILKINSON, M.C. 1995. Studies on permeation through polymer latex films. III. Modification using soluble polymeric additives. *Polymer international*, 38:23-32.

STOFFER, J.O. & BONE, T. 1980a. Polymerization in water-in-oil microemulsion systems. I. *Journal of polymer science, part A: polymer chemistry*, 18:2641-2648.

STOFFER, J.O. & BONE, T. 1980b. Polymerization on water-in-oil microemulsion systems. II. SEM investigation of structure. *Journal of dispersion science and technology*, 1:393-412.

SUBRA, P. & JESTIN, P. 1999. Powders elaboration in supercritical media: comparison with conventional routes. *Powder technology*, 103:2-9.

SUBRAMANIAM, B., RAJEWSKI, R.A. & SNAVELY, K. 1997. Pharmaceutical processing with supercritical carbon dioxide. *Journal of pharmaceutical sciences*, 86:885-890.

SUZUKI, S., KIKUCHI, K., SUZUKI, A., OKAYA, T. & NOMURA, M. 2007. Effect of chain transfer agents on the kinetics and mechanism of particle nucleation in the emulsion polymerization of vinyl pivalate. *Colloid and polymer science*, 285:523-534.

SZCZUBIALKA, K., JANKOWSKA, M. & NOWAKOWSKA, M. 2003. "Smart" polymeric nanosphers as new materials form possible biomedical applications. *Journal of materials science, materials in medicine*, 14:699-703.

TADROS, T., IZQUIERDO, P. & SOLANS, E.C. 2004. Formation and stability of nano-emulsions. *Advances in colloid and interface science*, 108-109:303-318.

TAKOLPUCKDEE, P. 2005. Chain transfer agents for RAFT polymerization: molecules to design functionalized polymers. *Australian journal of chemistry*, 58:66.

TAUER, K. 2003. The role of emulsifiers in the kinetics and mechanism of emulsion polymerization. (*In* Karsa, D.R. *ed.* Surfactants in polymers, coatings, inks, and adhesives. Blackwell Publishing Ltd.:Edinburgh. p. 32-70.)

TAUER, K., RAMÍREZ, A.G. & LÓPEZ, R.G. 2003. Effect of the surfactant concentration on the kinetics of oil in water microemulsion polymerization: a case study with butyl acrylate. *Comptes rendus chimie*, 6:1245-1266.

TAYLOR, P.M. 2007. Biological matrices and bionanotechnology. *Philosophical transactions of the Royal Society B*, 362:1313-1320.

TAYLOR, P. & OTTEWILL, R.H. 1994. Ostwald ripening in o/w miniemulsions formed by the dilution of o/w microemulsions. *Progress in colloid & polymer science*, 97:199-203.

THIOUNE, O., FESSI, H., DEVISSAGUET, J.P. & PUISIEUX, F. 1997. Preparation of pseudolatex by nanoprecipitation: influence of the solvent nature on intrinsic viscosity and interaction constant. *International journal of pharmaceutics*, 146:233-238.

THORNTON, A.J., ALSBERG, E., HILL, H.E. & MOONEY, D.J. 2004. Shape retaining injectable hydrogels for minimally invasive bulking. *Journal of urology*, 172:763-768.

TJANDRA, W., RAVI, P., YAO, J. & TAM, K.C. 2006. Synthesis of hollow spherical calcium phosphate nanoparticles using polymeric nanotemplates. *Nanotechnology*, 17:5988-5994.

TOUSSAINT, J.F., DUBOIS, A., DISPAS, M., PAQUET, D., LETELLIER, C. & KERKHOFS, P. 2007. Devlivery of DNA vaccines by agarose hydrogel implants facilitates genetic immunization. *Vaccine*, 25:1167-1174.

TUROS, E., REDDY, G.S.K., GREENHALGH, K., RAMARUJA, P., ABEYLATH, S.C., JANG, S., DICKEY, S. & LIM, D.V. 2007b. Penicillin-bond polyacrylate nanoparticles: restoring the activity of β-lactam antibiotics against MRSA. *Bioorganic & medicinal chemistry letters*, 17:3468-3472.

VISSCHERS, M., LAVEN, J. & GERMAN, A.L. 1997. Current understanding of the deformation of latex particles during film formation. *Progress in organic coatings*, 30:39-49.

VISSCHERS, M., LAVEN, J. & VAN DER LINDE, R. 2001. Film formation from latex dispersions. *Journal of coatings technology*, 73:49-55.

XU, T., ZHANG, N., NICHOLS, H.L., SHI, D. & WEN, X. 2007. Modification of nanostructured materials for biomedical applications. *Materials science and engineering C*, 27:579-594.

YAO, C. & WEBSTER, T.J. 2006. Anodization: a promising nano-modification technique of titanium implants for orthopedic applications. *Journal of nanoscience and nanotechnology*, 6:26822-2692.

YOUNG, S., WONG, M., TABATA, Y. & MIKOS, A.G. 2005. Gelatin as a delivery vehicle for the controlled release of bioactive molecules. *Journal of controlled release*, 109:256-274.

CHAPTER 2 WAS SUBMITTED TO

JOURNAL OF LIQUID CHROMATOGRPAHY & RELATED TECHNOLOGIES

2. INSTRUCTIONS FOR AUTHORS

*****Note to Authors:** please make sure your contact address information is clearly visible on the **outside** of all packages you are sending to Editors.***

Aims and Scope

Journal of Liquid Chromatography & Related Technologies® publishes an outstanding selection of critical, peer-reviewed papers dealing with analytical, preparative and process-scale liquid chromatography of all types and related technologies such as TLC; capillary electrophoresis; supercritical fluid extraction and chromatography; membrane separation technology; field-flow techniques; and others. As new separation techniques are introduced, they will also be included in the journal. On a regular basis, special topical issues are devoted to specific technologies and applications. Book reviews, software reviews and a calendar of meetings, symposia and expositions are also included.

Submission of Manuscripts

Please submit three copies of your manuscripts to the Editor-In-Chief: Dr. Jack Cazes, P. O. Box 1149 Lady Lake, FL 32158-1149, USA; E-Mail: jackcazes@embarqmail.com.

Authors are strongly encouraged to submit manuscripts on disk (3.5 in. or CD-ROM). The disk should be prepared using MS Word or WordPerfect and should be clearly labeled with the authors' names, file name, and software program. Each manuscript must be accompanied by a statement that it has not been published elsewhere and that it has not been submitted simultaneously for publication elsewhere. Authors are responsible for obtaining permission to reproduce copyrighted material from other sources and are required to sign an agreement for the transfer of copyright to the publisher. All accepted manuscripts, artwork, and photographs become the property of the publisher.

All parts of the manuscript should be typewritten, double-spaced, with margins of at least one inch on all sides. Number manuscript pages consecutively throughout the paper. Authors should also supply a shortened version of the title suitable for the running head, not exceeding 50 character spaces. Each article should be summarized in an abstract of not more than 100 words. Avoid abbreviations, diagrams, and reference to the text. Six keywords should be provided.

References

Please cite references in the text by number only enclosed in parentheses. At the end of the article, list the references in the order they appear in the text. Footnotes should be included in the list of references. Examples:

Journal: Brown, P.R.; Lundie-Jenkins, G. Non-target Mortalities during Aerial Strychnine Baiting of House Mice. Wildl. Res. 1999, 26 (1), 1-15.
Book: New, T.R. *Insects as Predators*; New South Wales Univ. Press: Kensington, Australia, 1991; 178 pp.
Work presented at Meetings and Conferences: Garrone, E.; Ugliengo, O. In *Structure and Reactivity of Surfaces*, Proceedings of the European Conference, Trieste, Italy, Sept 13-20, 1988; Zecchina, A., Costa, G., Morterra, C., Eds.; Elsevier: Amsterdam, 1988.

Illustrations

Illustrations submitted (line drawings, halftones, photos, photomicrographs, etc.) should be clean originals or digital files. Digital files are recommended for highest quality reproduction and should follow these guidelines:

- 300 dpi or higher
- Sized to fit on journal page
- EPS, TIFF, or PSD format only
- Submitted as separate files, not embedded in text files

Color illustrations will be considered for publication; however, the author will be required to bear the full cost involved in their printing and publication. The charge for the first page with color is $900.00. The next three pages with color are $450.00 each. A custom quote will be provided for color art totaling more than 4 journal pages. Good-quality color prints should be provided in their final size. The publisher has the right to refuse publication of color prints deemed unacceptable.

Tables and Figures

Tables and figures (illustrations) should not be embedded in the text, but should be included as separate sheets or files. A short descriptive title should appear above each table with a clear legend and any footnotes suitably identified below. All units must be included. Figures should be completely labeled, taking into account necessary size reduction. Captions should be typed, double-spaced, on a separate sheet. All original figures should be clearly marked in pencil on the reverse side with the number, author's name, and top edge indicated.

Proofs

Page proofs are sent to the designated author using Taylor & Francis' EProof system. They must be carefully checked and returned within 48 hours of receipt.

Offprints/Reprints

Each corresponding author will receive a PDF file of the the article via email. This file is for personal use only and may not be copied and disseminated in any form without prior written permission from Taylor and Francis Group, LLC.

REMARK

The manuscript was formatted for uniformity of the thesis; however the reference citation style was preserved. Permissions for figures appear in the appendix.

CHAPTER 2

THE APPLICATION OF SIZE EXCLUSION CHROMATOGRAPHY IN THE DEVELOPMENT AND CHARACTERIZATION OF NANOPARTICULATE DRUG DELIVERY SYSTEMS

Daniel P. Otto[+,†], Hermanus C.M. Vosloo[‡] and Melgardt M. de Villiers[+,*]

[+]Pharmaceutical Sciences Division, School of Pharmacy, University of Wisconsin-Madison, 777 Highland Avenue, Madison, WI 53705, USA. [‡]School of Chemistry, Private Bag X6001, North-West University, Potchefstroom, 2520, South Africa. [†]Research Institute for Industrial Pharmacy, Private Bag X6001, North-West University, Potchefstroom, 2520, South Africa.

[*]Corresponding author. E-mail: mmdevilliers@pharmacy.wisc.edu. Telephone: 1-608-890-0732. Pharmaceutical Sciences Division, School of Pharmacy, University of Wisconsin-Madison, 777 Highland Avenue, Madison, WI 53705, USA.

Abstract

The successful production of effective nanoparticulate drug delivery systems depends on maintaining the characteristics of the starting materials and the final formulation. Since compendial standards for traditional drug delivery systems do not always apply to nanosystems, analytical procedures for nanosized delivery systems must be established. This will ensure the quality of such products as they reach the marketplace. Size exclusion chromatography provides a method to continuously monitor all the development stages of nanoparticulate drug delivery systems thereby ensuring the quality of the starting materials used and the final product. The primary properties that can be monitored with this technique include particle size and molecular weight. Information about these properties not only serves as quality control measures, but can be used to monitor formulations for potential degradation products or impurities. Recent advances in size exclusion chromatography such as the introduction of rapid analysis size exclusion columns and new chromatographs will make this technique even more applicable for nanosystem characterization. This implies that size exclusion chromatography might become an essential, economically feasible and necessary analytical tool for ensuring the quality of nanoparticulate drug delivery systems.

Key Words: Size exclusion chromatography, nanoparticulate, drug delivery, quality control

Running head: SEC characterization of nanoparticulate drug delivery systems

2.1 INTRODUCTION

Size exclusion chromatography (SEC) is a separation technique by which analytes are retained in a suitable polymeric packing material based solely on particle permeation into and out of the packing material[1]. This is the primary property that distinguishes SEC from other chromatographic techniques that are based on polarity and chemical interaction between the analyte and packing material. The packing material exposes a variety of pore sizes to the eluted species and ideally separation is imparted by molecular sieving of different particles in the sample. Particles that are larger than the pores are excluded from the pores and are not retained in the packing material, whilst very small particles are significantly retained in the pores and elute at a later stage. Particles with intermediate size ranges are separated through a combination of these sieving mechanisms and therefore correspond to intermediate retention times[1,2].

The applications of SEC are manifold if coupled to appropriate detectors e.g. light scattering photometers, viscometers, UV detectors, refractive index detectors, fluorescence detectors, NMR, FTIR, MS, scintillation counters and various combinations of these to determine the molecular weight (ranging a few thousand to millions of $g.mol^{-1}$), particle size (up to a few hundred nanometers), polymer chain conformation, chain composition, particle association behavior, purity and stability of polymeric systems to name but a few[3]. These properties are all vital in the development of nanoparticulate drug delivery systems.

Nanotechnology is concerned with technological manipulation of material properties at a length scale between 1-100 nm[4]. As a restriction, nanoparticulate drug delivery systems should therefore also assume size aspects in this range; however, this is not always realistic, practical and might be adjusted to fit a specific application[5]. In the day and age of nanotechnological advances, various applications have been realized in the biomedical field by nanoparticulate drug delivery systems including dendrimers[6], core-shell nanoparticles[7], polymeric nanocapsules[8] and polymeric micelles[9]. The application of nanoparticulate drug delivery systems arises from their numerous advantages over their larger-sized counterparts i.e. crossing of biological barriers[10], enhancement of solubility properties of drugs[11], presentation of a biocompatible or targeted topography on their surfaces that could be recognized by cells and circumvention of the abrasive nature of certain ceramic materials at a larger size scale[12].

A wide selection of nanoparticles for drug delivery is manufactured from polymeric materials. SEC can be used to monitor at least three important characteristics of these polymers used to manufacture these delivery systems namely the quality of the materials employed, the quality of the derived nanoparticles and stability of the delivery system. Quality of the employed starting material could be investigated with SEC analyses of molecular weight and particle size if suitable detection methods i.e. light scattering is applied[13, 14].

The reason for developing quality control methods involving SEC, recalls the properties of materials at the nanoscopic level. These particles have a significantly larger surface to volume ratio compared their macroscopic counterparts and therefore their behavior is fundamentally different[15]. By applying SEC formulators can ensure that the required quality or sufficient degree of nanoscopic properties are retained for the macromolecular excipients and delivery systems by continuous evaluation of particle size and molecular weight characteristics, delivery system size characteristics and finally time-dependent size stability of the product.

2.2 ROLE OF SEC IN ENSURING DESIRED MACROMOLECULAR EXCIPIENT PROPERTIES

The properties of starting material could markedly influence the performance of the formulated nanoparticulate delivery systems. For this reason the FDA requires that all excipients that are formulated in pharmaceutical industry have to comply with strict standards before it could be considered for use. These restrictions ensure that product properties can be correlated to the starting material properties in the situations where a product batch proved contaminated or defective.

2.2.1 Batch Conformity

A primary example for the need of restrictions on the use of cellulose powders was illustrated by SEC of commercially available cellulose powders[16]. Hemicellulose can be found in cellulose powders as a byproduct of the pulping and alkaline treatment of source materials to produce microcrystalline cellulose. Hemicellulose could influence the technological properties (since it is a swelling agent) of the excipient and according to various monographs microcrystalline cellulose should contain 97-102% of cellulose. The study concluded that only two batches out of twenty two cellulose products complied with this restriction.

Careful optimization of the sampling conditions could decrease analysis time and solvent usage in industrial applications of SEC when used as a quality control measure. This was illustrated for a purification procedure for insulin products[17]. Instead of singe batch conformity evaluations, a moving bed system could be employed by which four sampling ports were used to sample four insulin batches at selected intervals. Therefore these batches of insulin could be evaluated by the same SEC after optimization of the sampling interval and injection gap periods to prevent mixing of different samples.

2.2.2 Selection of Polymeric Excipient

The quality of polymeric pharmaceutical excipients is routinely examined with SEC techniques. Especially to select polymers that could be applied to control the residence time and pharmacokinetics of drugs formulated in a specific polymeric nanodelivery system. Generally, macromolecules with weights lower than 50 kDa and sizes below 6 nm tend to filtered by the kidneys whilst those exceeding 50 kDa could be affected by the liver by showing significant accumulation. Positively charged macromolecules tend to associate with negatively charged hepatic cell surfaces and the negatively charged polymeric carrier tend to escape this interaction; however they are absorbed by sinusoidal liver cells.[18]

Therefore the appropriate molecular weight of the polymer should be maintained in order to control the pharmacokinetics of the active ingredient or to suit the particular application as found for the multi-application excipient, pectin, for which a wide size and weight distributions were found by SEC for different commercially available products. These pectin products all show differences in their swelling and mucoadhesive properties that were in some way related to their molecular weight. These properties significantly affected the residence times of drugs in the body as well as targeted tissue accumulation. Thorough weight characterization is therefore required before a pectin formulation is manufactured to suit the applications of this polymer in the formulation of cytotoxic drugs, mucoadhesive ophthalmic delivery systems and prevention of pathogens to human cells.[19]

The size exclusion process is often time-consuming, however, application of flow injection analysis by SEC made this analyses a feasible, time effective process as was demonstrated for poly(lactide-*co*-glycolide) polymerization and swelling characteristics. Consequently this process ensures that a continuous analysis of the polymer could be performed to ensure that the dosage form properties will be consistent.[13]

The quality of starting materials that are used is important since they should impart the desired properties to the delivery system such as nanosize or release control. These materials must be manipulated through some manufacturing technique to produce these nanocarriers for it to retain its properties. For example, the molecular weight of the starting material could markedly affect the functionality and drug release of the derived delivery vehicle of implant device manufactured from poly(dimethyl siloxane)[20] and SEC could be employed to monitor the molecular weight of the starting polymer as well as determine the purity of the material.

2.2.3 Quantification of Polymers in Pharmaceuticals

Quantification of functional excipients including the poloxamers 188 and 407 was aptly illustrated by employment of SEC. These excipients act as emulsifiers, surfactants, solubilizing agents, dispersing agents as well as in vivo absorbance enhancers and their quantification in pharmaceutical products could again influence the product performance significantly. A limited number of analytical techniques were described to evaluate the content of poloxamers and some colorimetric methods[21,22,23,24] have been documented, however, application of these methods to solid dosage forms pharmaceutical proved inferior to a size exclusion method developed (Figures 2.1-2.3)[25] in the presence of various other pharmaceutical excipients of which none showed significant interference in the analysis. These results show the linearity, specificity and sensitivity of the SEC to distinguish between structurally similar molecules.

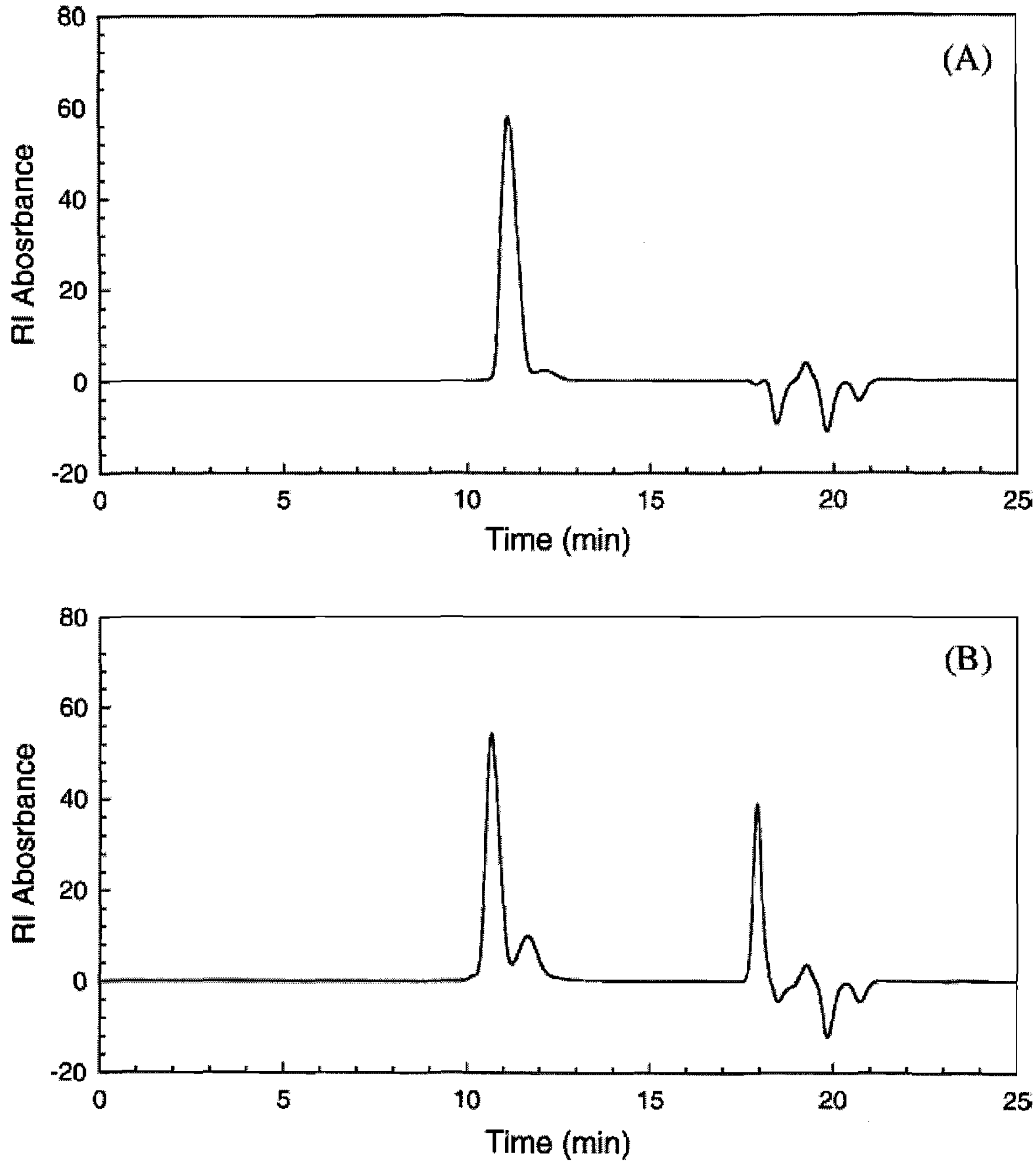

Figure 2.1: Size exclusion chromatograms of (A) poloxamer 188 and (B) poloxamer 407. Experimental conditions: stationary phase, two serially connected PLGel 3 μm mixed E columns (300 × 7.5 mm each); mobile phase, tetrahydrofuran; flow rate 1 mL/min; detection RI; temperature setting for the column and detector 35 °C; solute concentration 2.0 mg/mL.[25] (Permission from Elsevier)

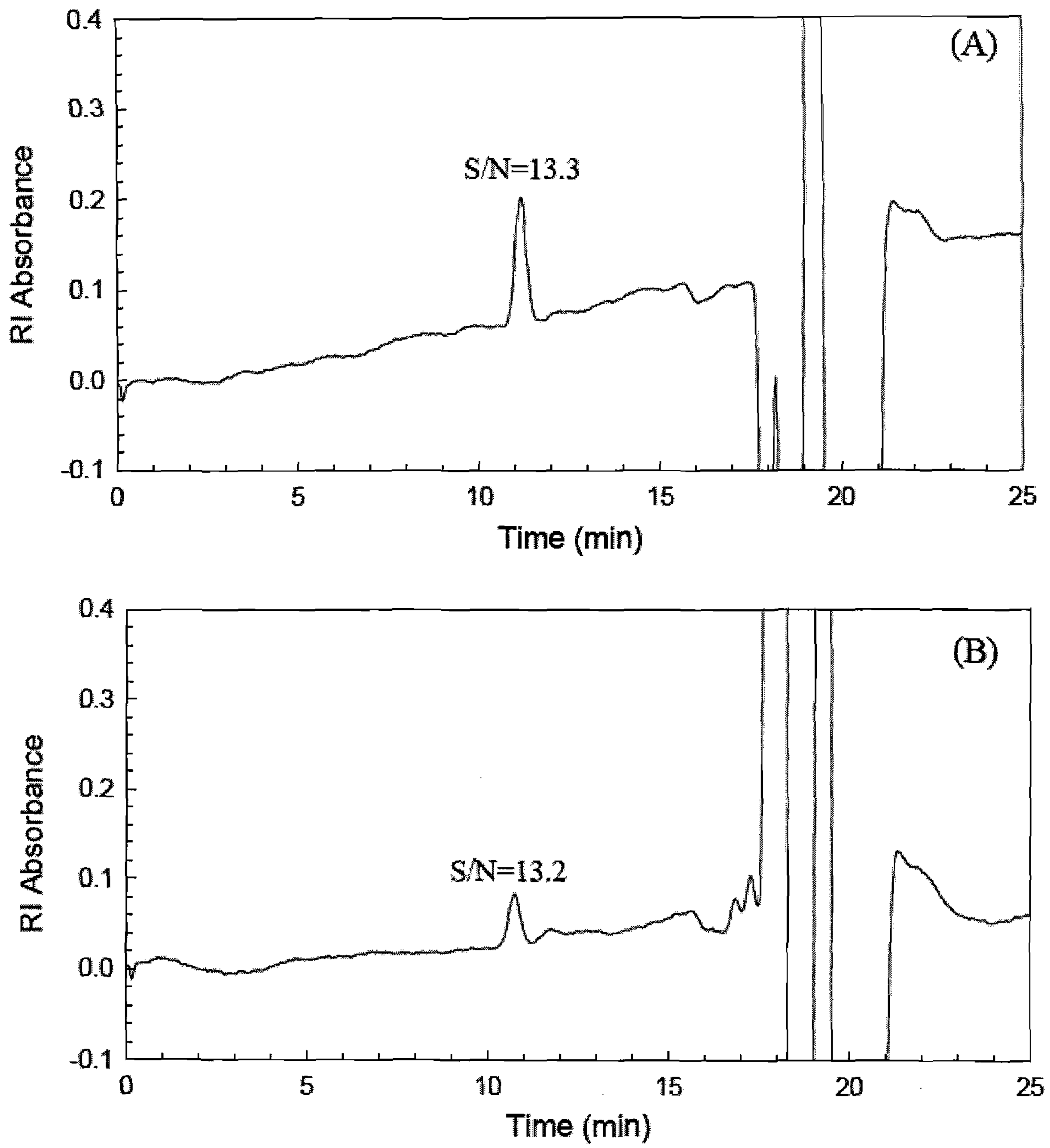

Figure 2.2: Size exclusion chromatograms of (A) poloxamer 188 and (B) poloxamer 407 at the limit of quantitation. Experimental conditions are the same as described before; solute concentration 0.005 mg/mL.[25] (Permission from Elsevier)

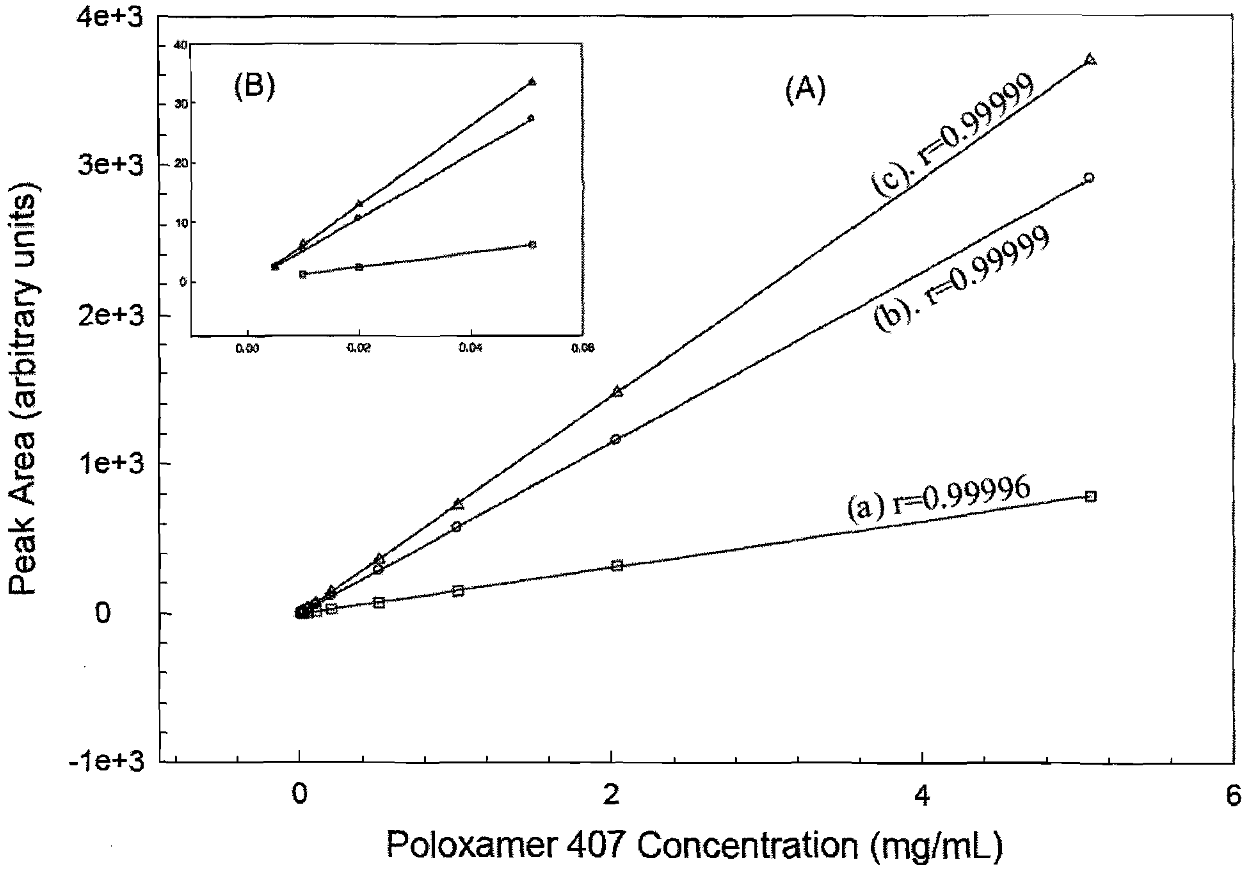

Figure 2.3: (Plot A) Calibration curve for poloxamer 407 with the concentration from 0.005 to 5 mg/mL. Symbol (□) and line (a): peak area for 11.69 min peak (diblock impurity peak) only; symbol (○) and line (b): peak area for the 10.71 min peak (poloxamer 407 peak) only; symbol (Δ) and line (c) sum of peak areas at 10.71 min and 11.68 min. (Plot B) Zoom in plot at the lower concentrations.[25] (Permission from Elsevier)

2.2.4 Dosage Form Optimization

A striking example of the application of SEC for evaluation of chitosan nanoparticles was found[26]. In this study the effects of polymer weight and polymer salt form of chitosan on the particle size, drug encapsulation efficiency and release properties of bovine serum albumin was determined. It could be seen from this study that the relationships between molecular weight, particle size, drug encapsulation and finally the release were not that obvious and that a particular chitosan had to be chosen following after physicochemical characterization and evaluation of in vivo performance[26]. This clearly demonstrated the need for thorough polymer molecular weight characterization prior to formulation of the nanoparticles.

In a study concerning the production of gelatin nanoparticles, the production method was optimized by thorough characterization of the gelatin molecular weight as determined by SEC.

It was illustrated that the size distribution of the produced particles varied with the molecular weight, temperature, ethanol concentration and pH, resulting in significant agglomeration and polydispersity in the particle size if these manufacturing conditions were not controlled. With SEC the researchers could monitor the particle sizes and weight simultaneously and could be exploited to optimize the manufacturing conditions for these gelatin particles and preclude the solvation and swelling effects that were previously observed for agglomerates of gelatin nanoparticulates.[27]

The example of gelatin nanoparticles[27] reported that the gelatin particle could agglomerate under certain reaction conditions and a study on paclitaxel-loaded polybutylcyanoacrylate nanoparticulate drug delivery systems[28] showed that a decrease in particle size resulted in an increase in the zeta potential that disfavored agglomeration. Both these studies illustrated that SEC could clarify and develop these excipients to avoid agglomeration of particles that could potentially result in adverse effects in the body i.e. trombi in the vasculature. Indeed aggregation of nanoparticulates was identified as one of the challenges of designing successful nanoparticulate pharmaceutical systems and upon agglomeration; the desired pharmaceutical properties could be lost during manufacturing stages and as mentioned result in adverse affects in the body[5].

2.2.5 Monitoring Synthesis

In addition to the gelatin and chitosan example characterization by SEC a polymer was synthesized by employment of an enzyme and also analyzed by SEC. The copolymer consisted of adipic acid and glycerol and was characterized through various techniques and gel permeation chromatography to monitor the molecular weight of the material and optimize the copolymerization conditions of temperature and enzyme concentration that was also time-dependent. In addition, dexamethasone phosphate loading capacity of these nanoparticles were correlated to copolymer weight and size.[29]

Yet another polymer was synthesized and characterized with SEC to be evaluated for its utilization as a drug nanocarrier. An amphiphilic graft copolymer was synthesized by grafting of poly-L-aspartic acid to 1,3-trimethylene carbonate. Analysis by multi-angle light scattering coupled to size exclusion chromatography revealed that the copolymer assumed a brush-like structure with branching that confirmed the grafting reaction and in addition, the conformation analysis of these polymers revealed that micelles were formed in water. The structure and composition of the polymers resulted in a complex, sustained release pattern of two drugs i.e.

prednisone acetate and tegafur from formulated nanoparticles with no detected degradation over a release period of four days.[30]

2.2.6 Purification

Purification and incorporation of certain materials into a specified formulation could ultimately determine its performance. The two properties are interrelated and could arise from synthesis reaction or nanoparticle loading procedures. A few examples are discussed to illustrate this point. SEC was also successfully employed to characterize and purify a novel block copolymer consisting of a poly(lactic acid) derivative and poly(ethylene glycol). The polymer weight was first characterized by a typical characterization chromatographic analysis, followed by a preparative size exclusion procedure to purify and fraction the polymer into the desired weight range. The fractions were then employed to prepare nanoparticles that were loaded with a molecular probe to monitor uptake when passively targeted to solid cancer tumors.[31]

2.2.7 New Developments

A new development was recently realized in the form of size exclusion reaction chromatography and arose from the need to reprocess and analyze materials after synthesis was completed. A size exclusion column could be utilized as the reactor in which a reaction could be performed to graft poly(ethylene glycol) to the proteins α-lactalbumin and β-lactoglobulin. In principle a reaction zone was created in the packing material that retained some reactants. As the reaction took place a more voluminous product formed and this product was excluded from the pores and eluted from the column. In addition this purified the product by retention of reactants in the packing material. The method determined the ideal reactant injection conditions to ensure overlap in the column for the specified reaction time (Figure 2.4 shows the reaction results for the α-lactalbumin PEGylation). As conclusion, control of the introduction of reactants into the column and additional packing length could optimize the production of a mono-PEGylated protein of predictable properties that was purified and separated from its reactants and undesired higher PEGylated species.[32].

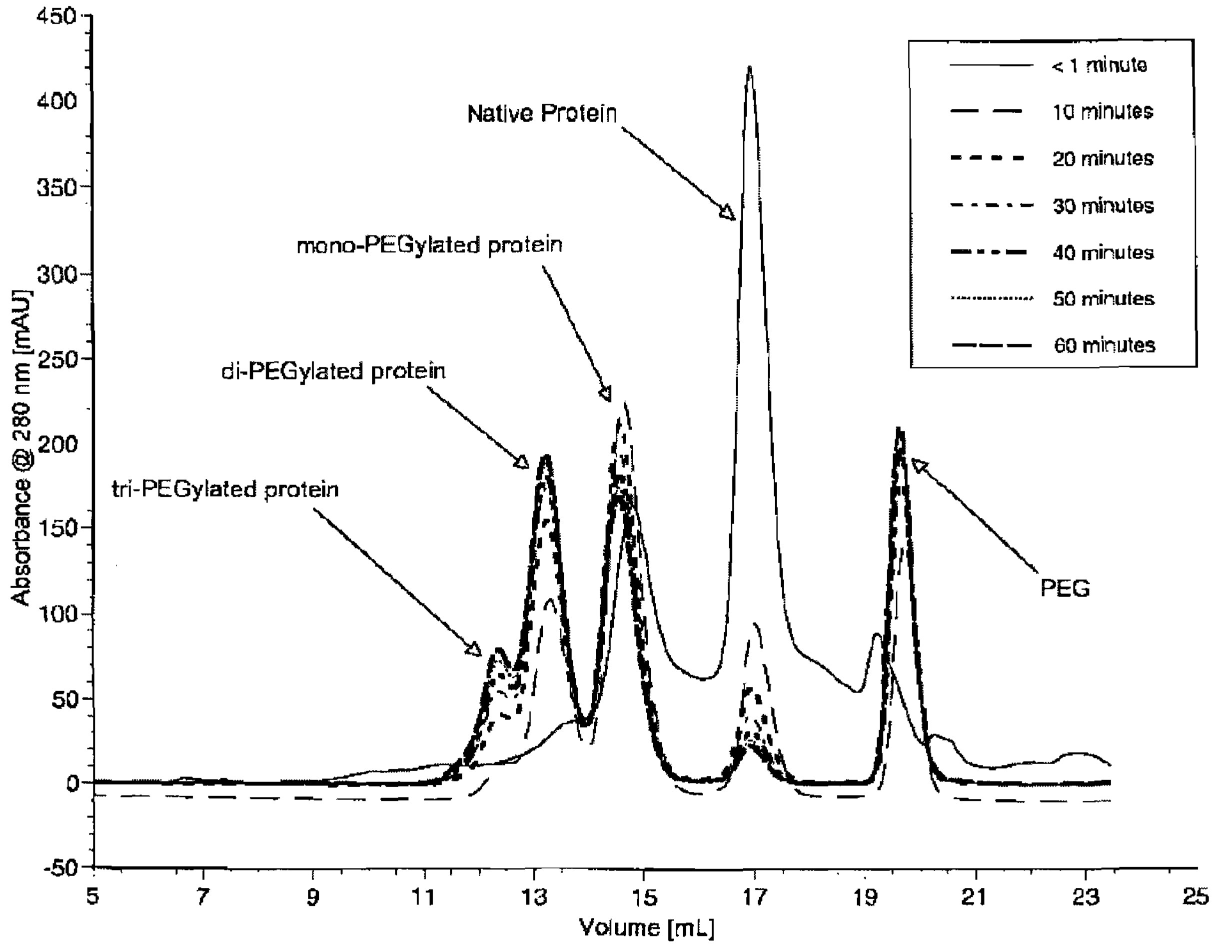

Figure 2.4: The effect of reaction time on the apparent molecular weight of α-lactalbumin for batch PEGylation.[32] (Permission from Wiley Interscience®)

A screening procedure for drug discovery compounds have also been realized based on a preparative or purification method based on size exclusion. A mixture of small molecule ligands such as actinonin were introduced to a macromolecular target i.e. peptide deformylase and incubated and then followed by size-exclusion separation. Compound which showed no affinity for the protein were retained in the column whilst the larger reaction products were eluted. The retained products were then analyzed and excluded as potential drug candidates since they did not interact with the target protein. The analyses of these unbound ligands were also considerably easier compared to analyses of the protein-ligand products.[33]

2.2.8 Drug-Polymer Interaction in the Dosage Form

SEC coupled to light scattering and viscometry detectors could also illuminate the effects of the assimilation of a drug into polymer chains. A water-soluble conjugate of paclitaxel and poly[*N*-(2-hydroxypropyl)methacrylamide)] (PNU) was studied and compared to unconjugated samples of poly[*N*-(2-hydroxypropyl)methacrylamide)] (PHPMA). Comparison of the polymeric carrier and the drug-polymer conjugate revealed that the conformation of the polymer chains was markedly affected even though the total concentration of drug was approximately 1% of the total conjugate. However, it was also concluded that the drug moieties in the chain did not demonstrate any significant intramolecular force interactions[33]. Figure 2.5 shows the conformation plots which were derived from light scattering analysis. The figure plots root mean square radius of gyration versus molar mass.

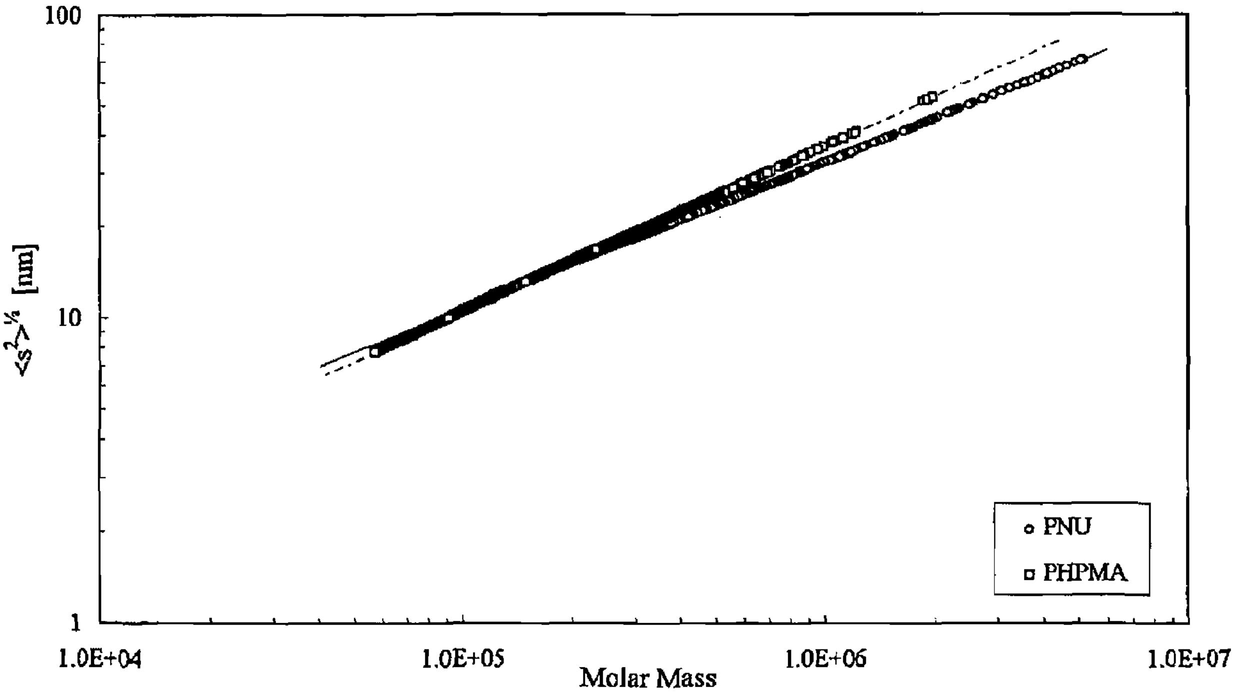

Figure 2.5: Comparison of the $<s^2>^{1/2} = f(M)$ power laws for PHPMA and PNU constructed by gathering the data of seven higher molar mass PNU fractions.[34] (Permission from ACS)

Application of the PHPMA polymer to another antitumor drug, camptothecin[35], again illustrated exhaustive characterization of both raw materials and the conjugated polymeric delivery systems. Narrow molar mass distribution (MMD) PHPMA polymer carrier samples were obtained and compared with a synthesized laboratory batch. The difference in retention times as well as weight polydispersity was determined by size exclusion chromatography for the different batches and is shown in Figure 2.6.

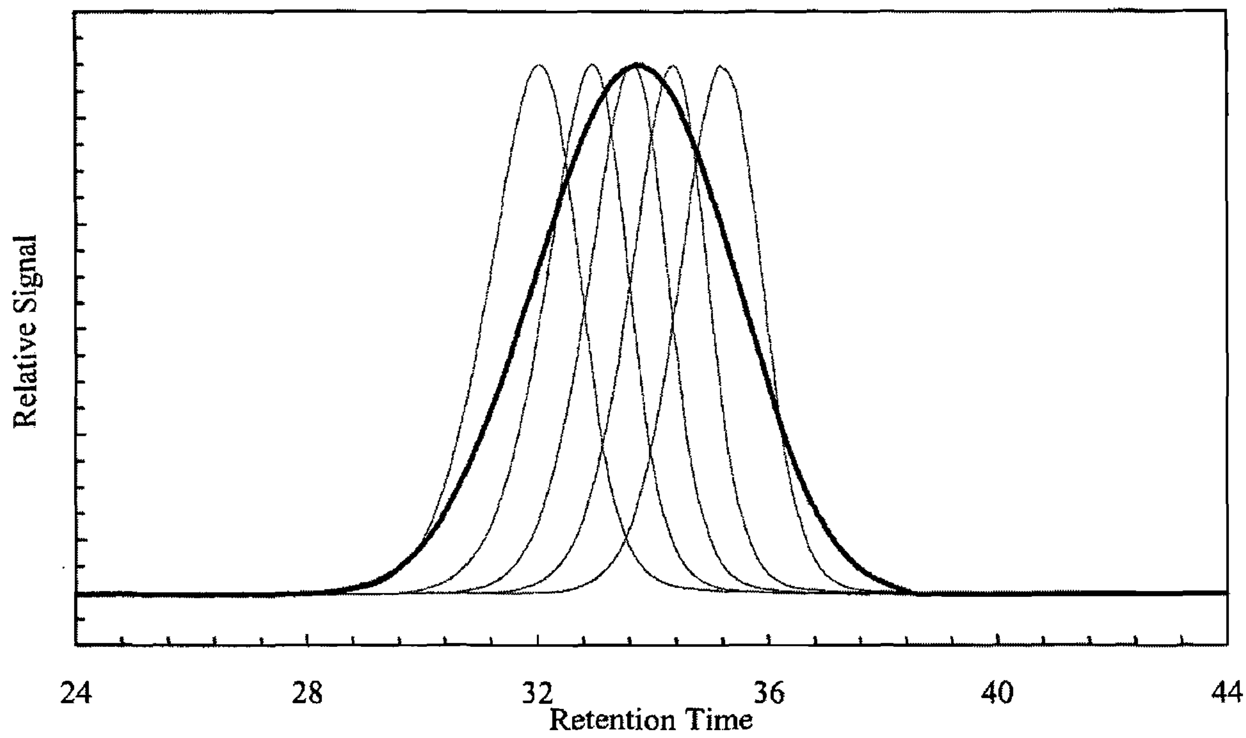

Figure 2.6: Comparison of the refractometer signals of five narrow MMD fractions (5-9) and of a broad MMD PHPMACPT sample (lot 5, boldface line).[35] (Permission from ACS.)

A succession of measurements followed the evaluation of molar mass for these PHPMA samples in order to determine the conformation of the polymer conjugates through off-line viscometry of 11 separate narrow standards and subsequently evaluating the suitability of the on-line method to determine the same parameters. Figures 2.7 and 2.8 shows the results off-line and on-line methods and generally showed excellent agreement and the on-line method showed the suitability of deriving the plots from a broad standard.

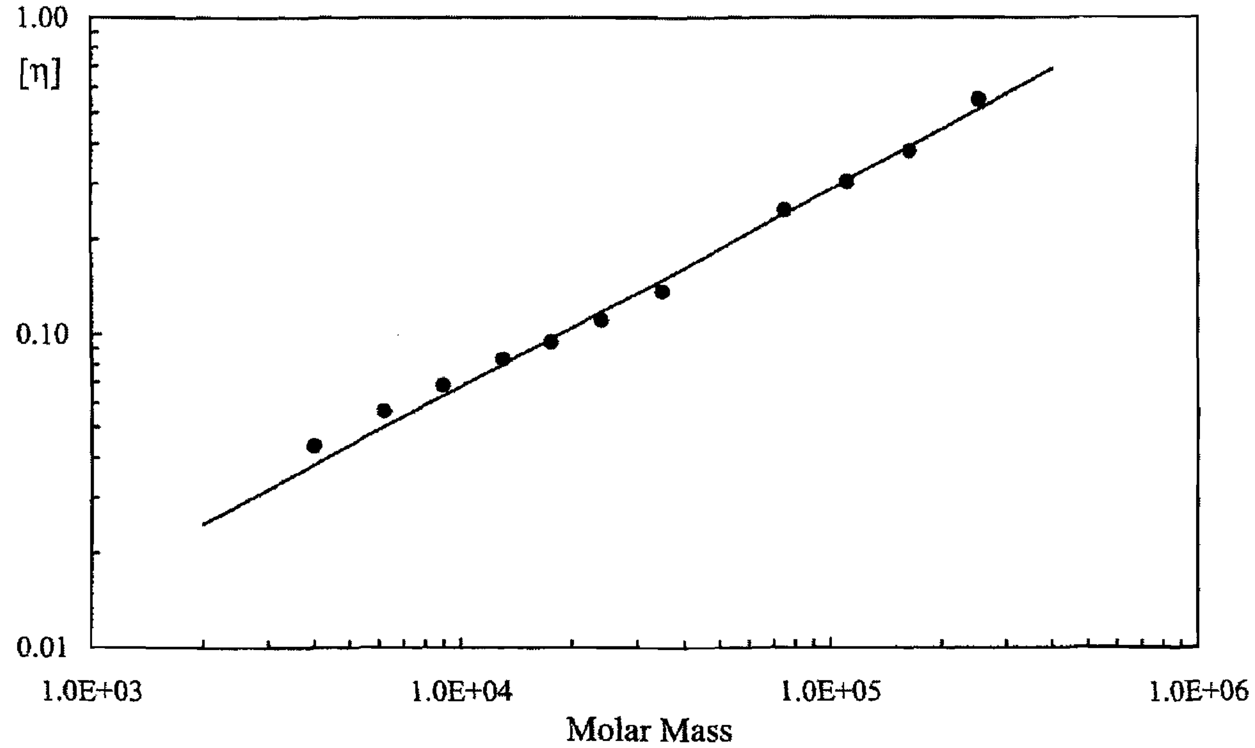

Figure 2.7: MHS plot for the PHPMA-CPT conjugate from 11narrow MMD fractions.[35] (Permission from ACS)

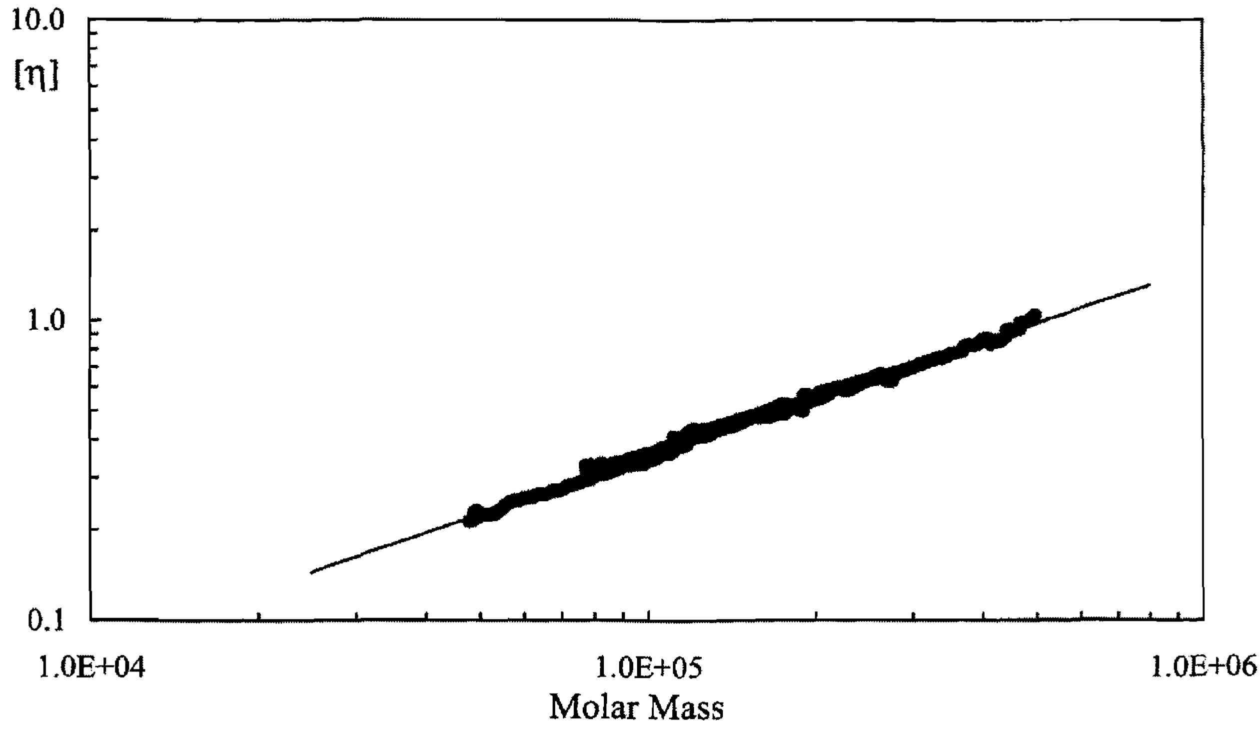

Figure 2.8: MHS plot for the PHPMA-CPT conjugates from online MALS and SCV data.[35] (Permission from ACS)

Due to instrumental limitations, the MALS wavelength of 632.8 nm proved unsuitable for measurement of radius of gyration, $<s^2>^{1/2}$ for small fractions; however, the high molar weight fractions could be used to extrapolate the conformation. Figure 2.9 shows the extrapolation of the conformational data for four higher molar mass fractions of the conjugates. Finally, it was concluded that the laboratory batch of the PHPMA-drug conjugate would be suitable for clinical use since its characteristics complied with the clinically evaluated narrow standards also evaluated in the study.

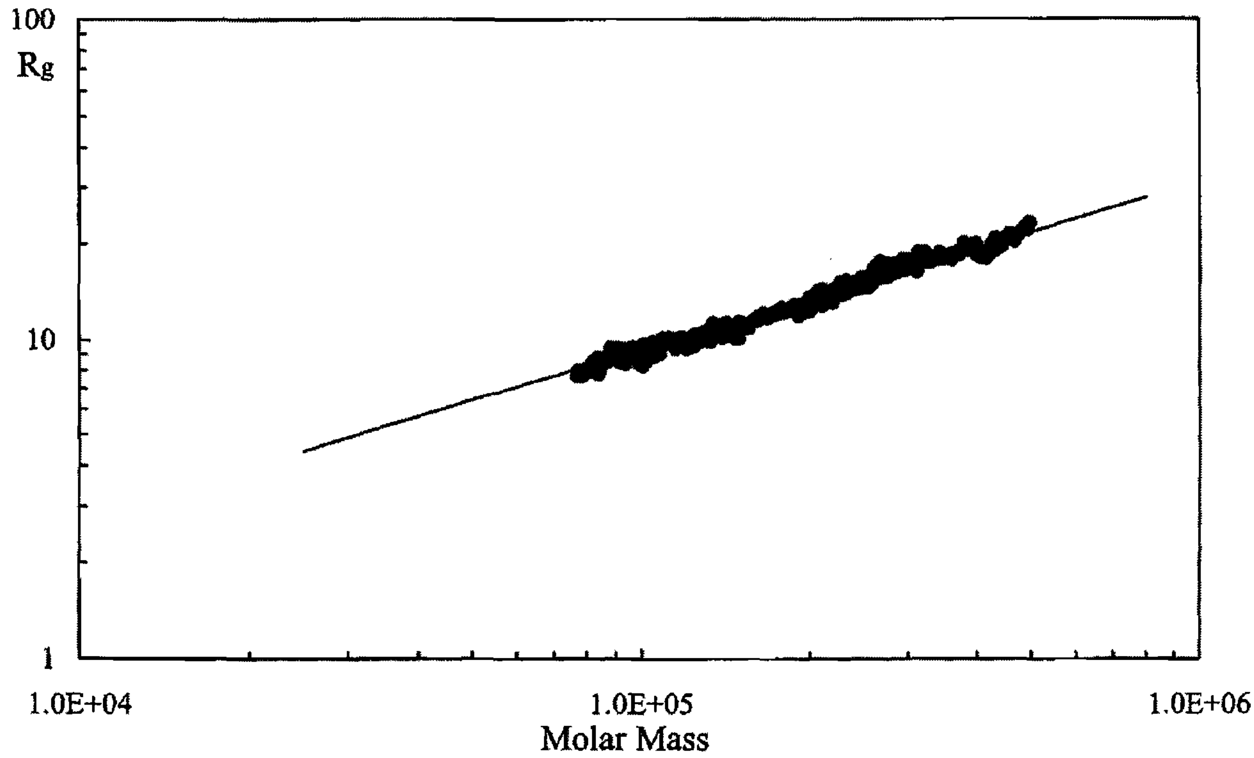

Figure 2.9: $R_g = f(M)$ power law for the PHPMA-CPT conjugate from on-line MALS data.[35] (Permission from ACS)

These examples are but a small selection of studies pertaining to biological applications and the role that SEC has to play in the quality control of the materials and conjugates used in the production of nanoparticulate delivery systems. It was apparent that the reports here indicated a link between material properties and the final application of the material.

Clearly, SEC can be employed to monitor or control the synthesis of new materials and conjugates from which nanoparticles could be prepared and should prove more vital in the future since novel polymeric materials are currently being developed.

2.3 CHARACTERIZATION OF NANOPARTICULATE DRUG DELIVERY SYSTEMS

SEC has also found application in the characterization of nanoparticulate delivery system performance as well as in quality control aspects of these formulations.

2.3.1 Liposomes

Although, liposomes have often been described as micro sized amphiphilic vesicles consisting of lipid bilayers, numerous nanosized variations have been produced over the years. An outline of the applications of SEC in the development and characterization of liposomes is illustrated in Figure 2.10.

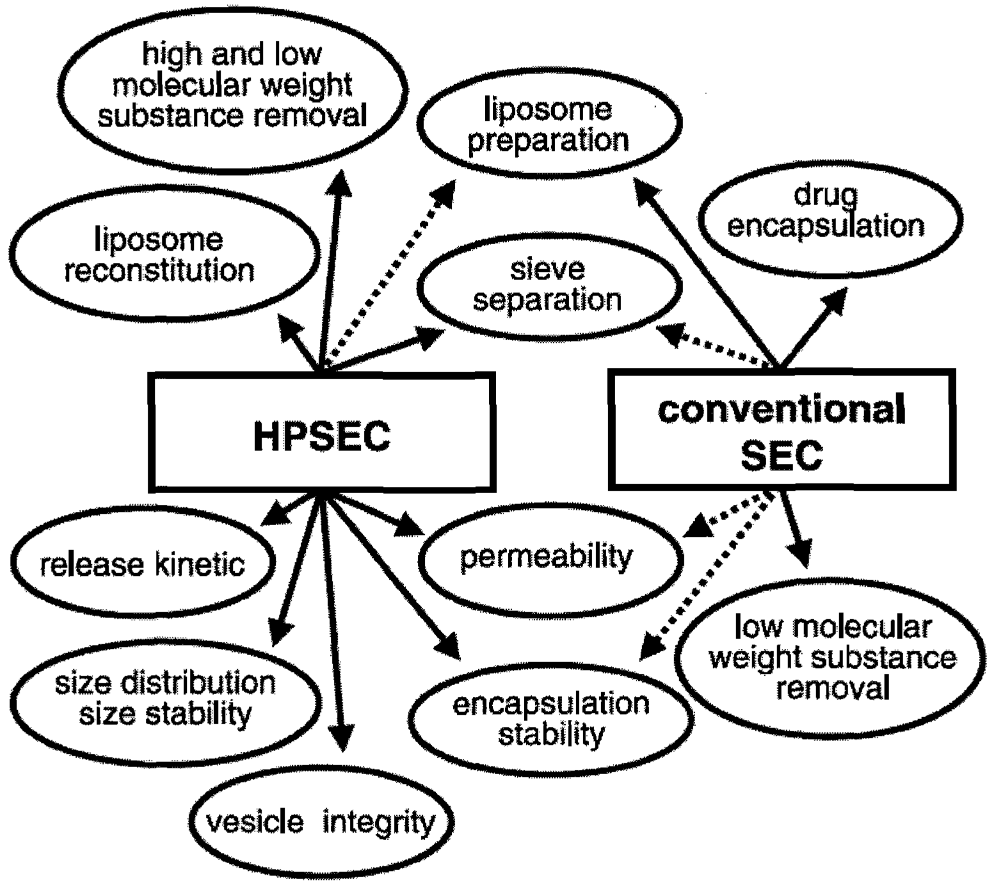

Figure 2.10: Application fields of HPSEC and conventional SEC in liposome technology from preparative uses to analytical ones. According to the purpose of analysis, the full arrows indicate the best potentialities of HPSEC and SEC, while dashed arrows show possible but less efficient routes.[36] (Permission from Elsevier)

The differences between conventional and high performance SEC were illustrated by their specific application in liposome delivery systems. The conventional method refers to employment of the size exclusion technique with SEC columns with specific size range restrictions. The conventional techniques served best a preparative and purification technique and in addition could be employed for drug loading. The high performance technique incorporates a full HPLC system coupled to columns with packing materials with a wider pore size range for a relatively fast analysis compared to conventional SEC . The use of this system enables accurate size distribution, stability and reconstitution characterization and additionally realizes time-resolved studies of release kinetics, permeability and encapsulation stability.[36]

As an example of size distribution and stability studies of liposomes was reported employing size exclusion chromatography[37]. The study exploited various detection methods including light scattering, refractive index, fluorescence and radioactivity and only the application of the light scattering technique would be highlighted here since it could be utilized for studying aggregation of the liposomes and its time-dependent evolution as demonstrated in Figure 2.11.

Again, liposomes served only as an example and the technique could be applied to other nanoparticulate systems to illustrate their aggregation behavior to serve as a quality control measure of any prepared nanoparticulate system.

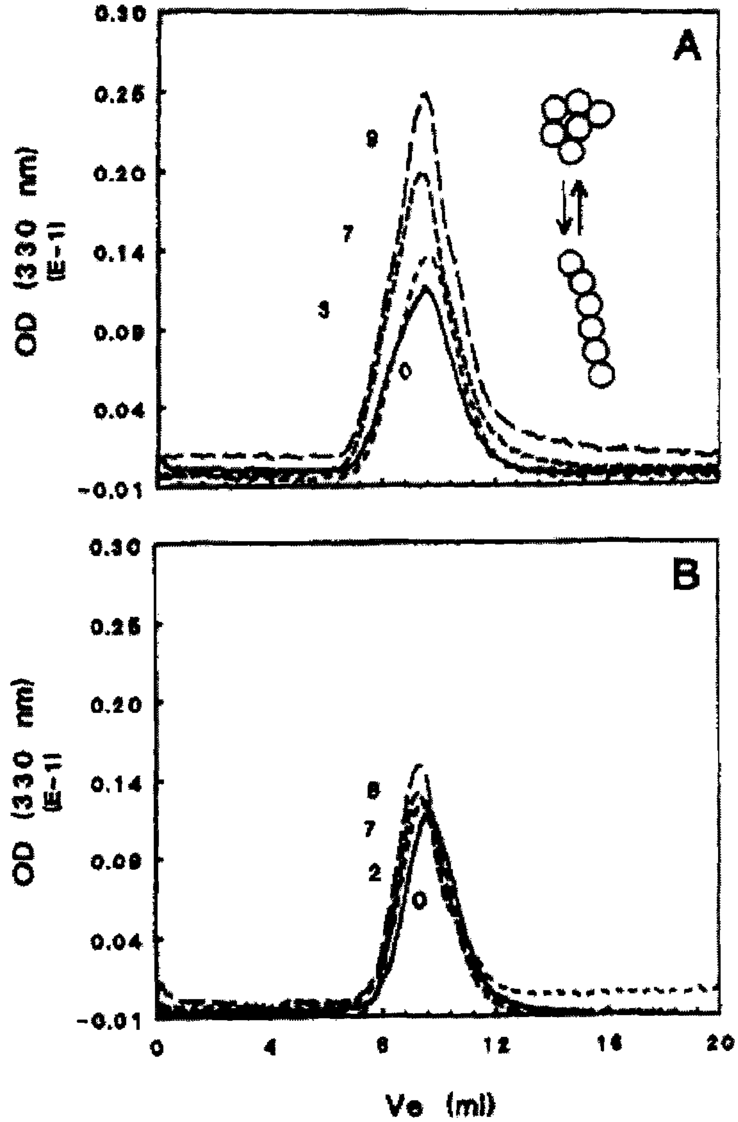

Figure 2.11: Study of vesicle size stability. Coupling light scattering to HPLC-GEC allows a distinction between aggregation and fusion processes to be made. Gel exclusion chromatograms were recorded by turbidity at 330 nm, of pure EPC SUV (A) and mixed EPC/EPA (91/9 mol ratio) SUV (B); (A) after 0, 3, 7 and 9 days; (B) after 0, 2, 7 and 8 days at 25°C (sample loading, 50 p,l; eluant flow rate, 1 ml/min). The eluant was the buffer (aqueous 145 mM NaCI, 10 mM HEPES, pH 7.4) used for vesicle preparation and calibration curve determination.[37] (Permission from Elsevier)

2.3.2 Stimuli-Responsive Nanoparticulate systems

Development of stimuli-responsive polymeric nanoparticles is a recent development in membrane science. An example was found where a membrane was fabricated from poly(*N*-isopropylacrylamide) that was grafted onto an ion-track pore wall in another polymer support, poly(ethylene terephtalate). By exposing the membrane to various temperature levels, the pores on the membrane opened or closed in accordance to swelling of the polymer membrane pores and allowed conductivity measures of selected ions and quantitation poly(ethylene glycol) molecules. The poly(ethylene glycol) served as a marker to determine if the membrane would allow organic molecule permeation in addition to ion diffusion and SEC was crucial to determine the range of poly(ethylene glycol) that was allowed to permeate. The method established that organic molecules larger than 2 nm could not transverse.[38]

The example above could illustrate a very significant application in evaluating the efficiency of membranes to selectively allow permeation of certain substances from the interior of a delivery system and thermoresponsive (and other stimuli) nanoparticles for drug delivery would seem a very promising delivery tool. The employment of SEC could further develop future membranes that could demonstrate different permeation properties and could serve as a control measure in industry to ensure that the manufacture delivery systems comply with a certain standard that was set for the delivery system.

2.3.3 Physical stability

The production of drug-loaded nanoparticles is not without problems and often these particles tend to agglomerate or flocculate as found for nanosuspensions. Polymers have often been used to prevent this flocculation phenomenon by adhering these molecules to the surface of the nanoparticle. The effect of the polymer charge has been demonstrated to repel adjacent particles that were also covered with charged polymer particles. Hydroxypropylcellulose was previously used to stabilize a classified drug nanosuspension. Evaporative light scattering was combined with SEC to determine surface coverage of the nanosuspension to aid and optimize the development of the formulation employed by the pharmaceutical company. The bound and unbound fractions of the polymer could be determined by a validated method to ensure future quality control of the formulation procedure[39] as shown in Figure 2.12.

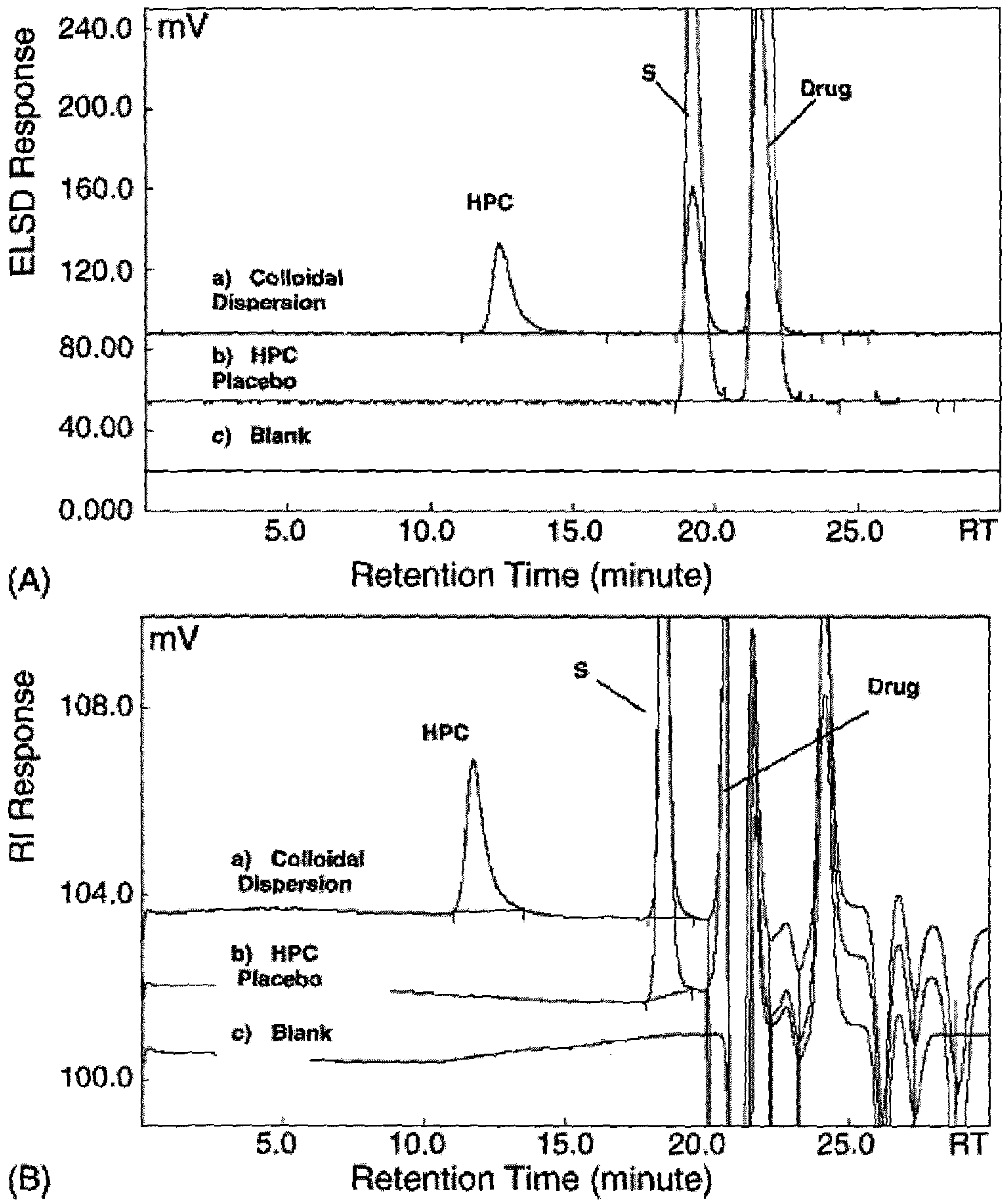

Figure 2.12: ELS (panel A) and RI (panel B) chromatograms showing separation of HPC from the other components of the colloidal dispersion: dispersing agent S and the drug.[39] (Permission from Elsevier)

2.3.4 Biodegradation

The synthesis of biodegradable polymeric nanoparticles based on poly(ε-caprolactone) grafted to dextran chains have been described using SEC as characterization method. Dextran grafting of the nanoparticle surface prevents uptake by macropghages, prolonging blood circulation.

Additionally, polysaccharides could be used for target-specific drug delivery because of recognition by surface proteins. A potential advantageous effect was also realized in that the total content of dextran significantly influenced the adsorption to bovine serum albumin (a common blood serum carrier protein) with a maximum nanoparticle adsorption seen at 33% dextran content. Different weight dextrans also influenced bovine serum album adsorption with a 40 000 $g.mol^{-1}$ dextran showing 2-4 fold higher adsorption compared to its 5000 $g.mol^{-1}$ counterpart. The pharmacokinetics of the dextran-grafted poly(ε-caprolactone) could therefore be adjusted and SEC provided essential information to modify these properties.[40]

2.3.5 Target-Specific Delivery

Site-specific delivery of nanoparticles has been identified as a very attractive advantage in the employment of the technology. Coating of these particle with biodegradable and biocompatible poly(lactic acid)-fetuin could circumvent problematic uptake of these particles by macrophages, a problem that is compounded by particle size aspects as well as surface characteristics[41]. The successful employment of nanoparticles therefore necessitates meticulous characterization of particle size distribution to establish the in vivo correlation to their effects. Fetuin-coated poly(lactic acid) particles were prepared in a size range of 50-200 nm. The poly(lactic acid) was radiolabeled with ^{14}C and fetuin with ^{125}I to determine the concentration of the particles in each fraction that was collected from the size exclusion chromatograph. These samples were analysed with photon correlation spectroscopy and the results and finally revealed the amount of fetuin bond to the nanoparticles as a function of particle diameter Figure 2.13.[42]

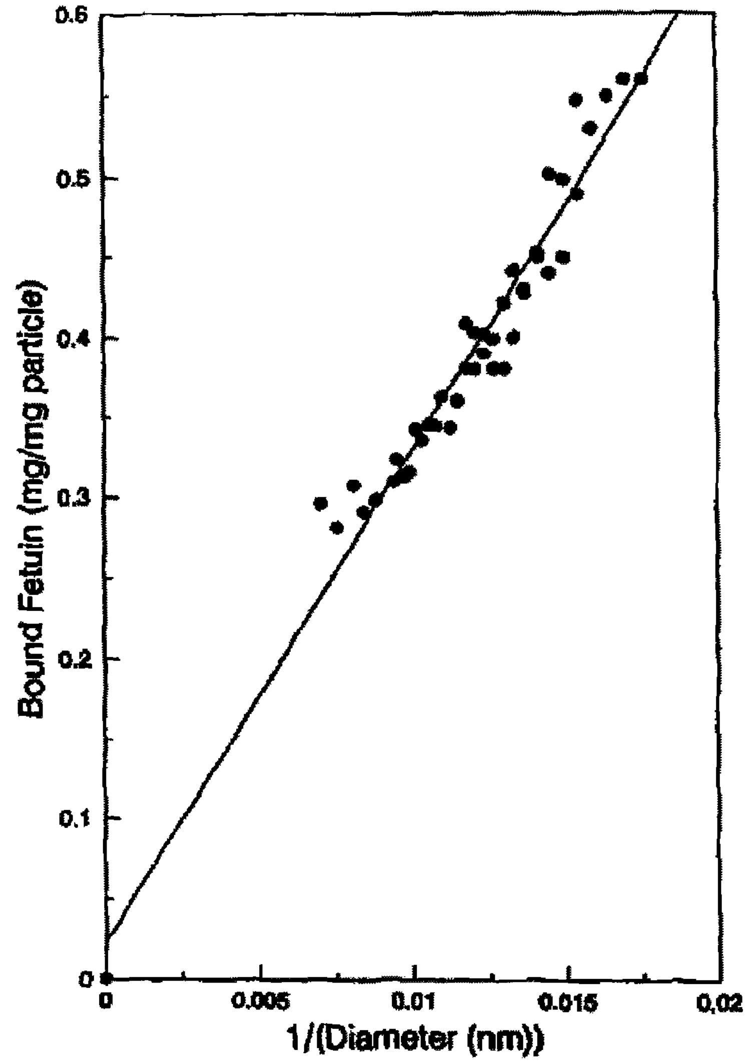

Figure 2.13: Amount of bound protein per unit mass of the polymer as a function of the inverse diameter.[42] (Permission from Elsevier.)

2.3.6 Substrate-Nanoparticle Interaction

This method could illustrate a useful tool to analyze particle size and the relationship of substrate binding as function of nanoparticle size. It could be suggested that future studies could exploit similar techniques in order to establish the optimum particle size to bind or incorporate a specific active ingredient at a selected dose. Additionally, the method could also be employed to estimate or assay a specific product to determine both particle size and drug loading whether the drug is a protein or polymeric material.

2.3.7 Protein Delivery

Dwelling on the topic of proteins and their ever-increasing role in pharmaceutical application we discuss yet another protein-related study. Nanoparticles were prepared by polymerization of human serum albumin and an antibody, IgG1 to result in polymeric colloidal carrier matrix. This nanoparticle-antibody polymerization was optimized by optimization of the degree of thiolation of IgG1 which was responsible for the cross-linking polymerization with the human serum albumin particle[43]. SEC was used to optimize the modification of the antibody by thiolization of the antibody surface. The thiolation results obtained with SEC are shown in Figure 2.14.

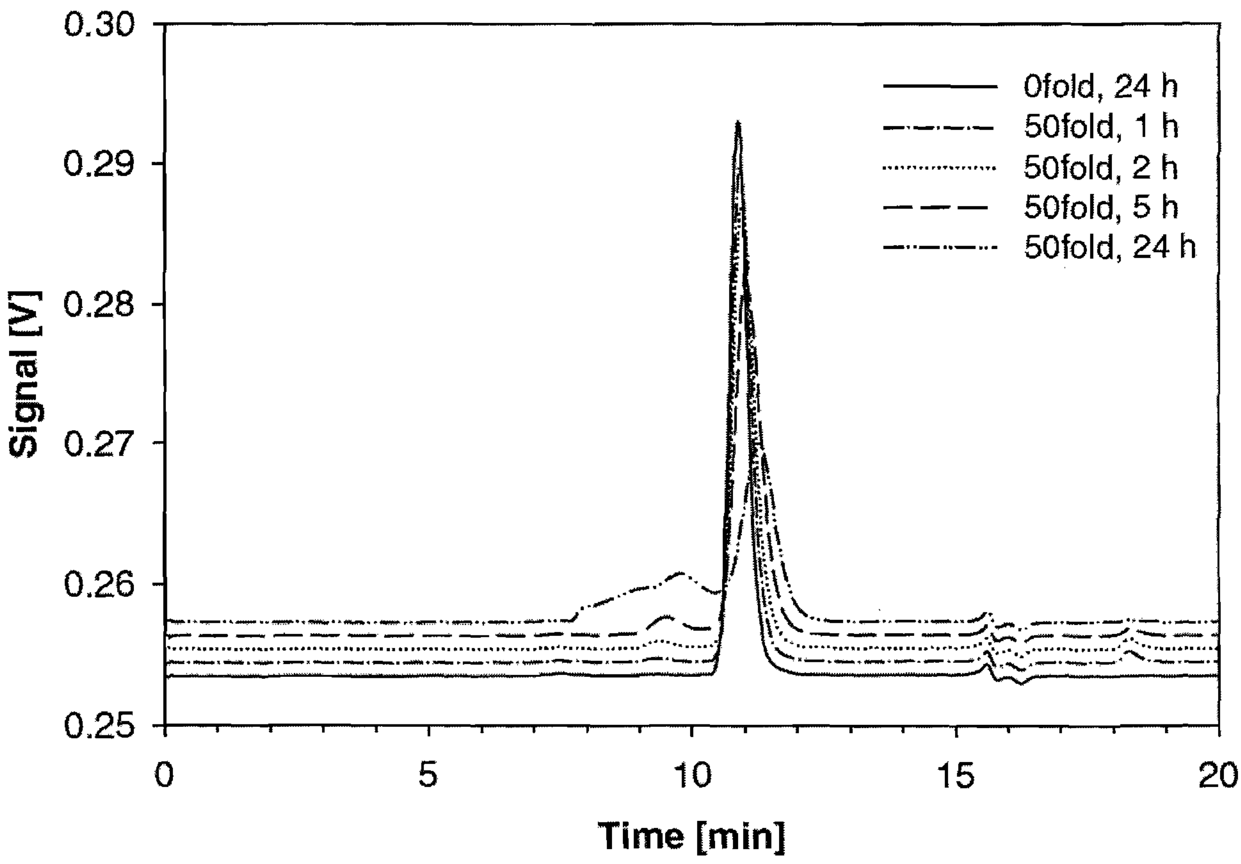

Figure 2.14: Thiolation of trastuzumab with 50-fold molar excess of 2-iminothiolane. The antibody was analyzed by SEC after 1, 2, 5 and 24 h of reaction time. Tastuzumab was detected at a retention time of about 11 min whereas higher conjugates were detected at shorter times.[43] (Permission from Elsevier)

The results suggested that a 2 hour period was sufficient for production of thiolated particles in a 50-fold excess without significant dimerization of the antibody. These particles were then compared to several controls and it could be demonstrated that the particles prepared from thiolated IgG1 showed higher biological efficiency than those prepared without thiolation or those coated by PEG. This study showed a full design of a nanoparticulate system and evaluated its biological activity and stability. SEC proved vital for optimization of the system and linking its performance to basic material properties.

The coating of poly(lactic acid) nanoparticles ranging 90-250 nm with human serum albumin was also determined by employing a SEC analysis with a turbidity detection method based on Mie's law that could easily indicate linearity of turbidity as function of the square of the mean population diameter[44]. This analysis provided proof that the albumin coated the nanoparticles and did not get incorporated into the polymer matrix. Furthermore, proving that the particles were coated could be related to their increased residence time in the body compared to uncoated particles.

2.3.8 Biodistribution

Nanoparticles were also developed from synthetic monomer polymerization to reach the target size below 50 nm in order to ensure the extravasation of nanoparticles from the blood vessels to a selected target. Isohexylcyanoacrylate and isobutylcyanoacrylate particles were prepared and loaded with the drugs ampicillin and dexamethasone[45]. The effects of pH showed that more acidic conditions resulted in larger particles, whilst addition of MeOH or acetone resulted in a decrease in particle size. The SEC analysis of polymer chain weight indicated that the weight was virtually unchanged after loading, indicating that the drug was mechanically trapped in the particle matrix and did not react with the monomer units. Large amount of the drug was released despite this entrapment and confirmed that esterases could result in bioerosion of the polymer matrix. In addition, the particle size demonstrated that these particles would deliver drugs by crossing the blood vessel walls.

Some useful applications of SEC in the performance of nanoparticulate drug delivery systems were demonstrated by appropriate detection methods coupled to SEC. The development of these systems was often described as an extension of the development of a selected starting material or characterization thereof. Some instances could clearly illustrate a link and it should perhaps be suggested that all nanoparticulate systems that are developed should follow a route of investigation at the starting material level and then continued at the application level to optimize the product performance.

2.4 STABILITY ISSUES MONITORED WITH SEC

2.4.1 Aggregation and Complexation

SEC techniques could be combined with appropriate detection methods i.e. light scattering, UV detection and refractive index measurements to study aggregation behavior and complexation[46] in addition to chemical instability and subsequent biodegradation and biodistribution of a polymeric drug carrier could affect the drug delivery system adversely. It was previously proven that polystyrene nanoparticles ranging 50 nm – 3 µm showed a particle size-dependent distribution in mice[47] with particles exceeding 300 nm not entering the blood circulation as was also evident from polyalkylcyanoacrylate nanocapsules studies following X-ray analysis[48].

Concerning the polystyrene nanoparticles, the 50 nm fraction was absorbed to the highest extent (34% of dose), whilst 100 nm particles ranked second (26% of dose). Particles larger than 100 nm did not reach the bone marrow whereas up to 7% accumulation of the 50 nm doses were observed in organs. SEC was employed to determine the particle absorptions and this study provided very significant information for the development of future nanoparticulates and should be considered in the design of these delivery systems and also the stability of these delivery systems. It could be required by a certain application that a localized effect is desired or that it the polymeric material should not accumulate in the body as consequence of degradation of the original polymeric delivery system to smaller particles.

2.4.2 Physiological Stability

A stability study was performed on poly(lactic acid) particles coated with albumin or poly(vinyl alcohol) to determine the effect of the polymer coating on particle degradation in simulated gastric fluid containing pepsin and simulated intestinal fluid containing pancreatin[49]. No degradation was illustrated for both coatings in pepsin-containing fluid; however pancreatin-enriched medium degraded the albumin coating significantly. Despite the degradation no particle accumulated since the poly(lactic acid) was readily metabolized to lactate. The size exclusion chromatograms are shown in Figure 2.15 to illustrate the effect of digestive fluid on polymer degradation and subsequently on polymer weight as time-dependent function.

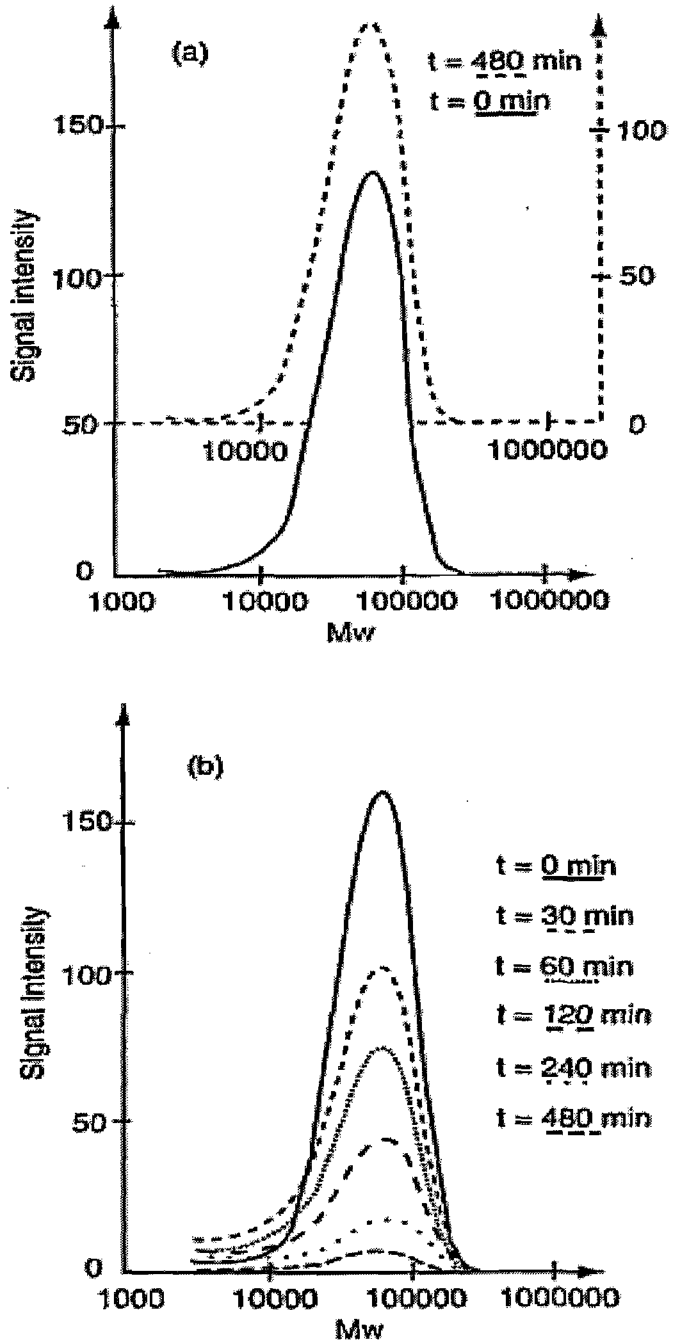

Figure 2.15: Size exclusion chromatogram of albumin coated PLA_{50} nanoparticles after 0 and 480 min in incubation of simulated gastric fluid (a) and simulated intestinal fluid (b) (USP XXII).[49] (Permission from Editions De Sante)

SEC was also used to study the incorporation of cyclosporine A loaded into poly(lactic acid) particles that were coated with poly(ethylene glycol)[50]. Cyclosporine A could be considered as one of the model drugs that pose all the problems encountered in pharmaceutical science. It is a poorly water-soluble, biodegradable peptide and has showed poor bioavailability in several studies[51,52]. Nanoparticles were developed that contained this troublesome drug and evaluated by SEC to characterize particle weight and stability of the particles.

The study[50] showed that poly(ethylene glycol) was an effective control measure to control release of the drug compared to uncoated poly(lactic acid) loaded particles. Stability analysis showed that the ester linkage between the PEG and poly(lactic acid) did not degrade significantly even over prolonged periods of time. In addition it could be illustrated that the surface loading of cyclosporine into the PEG layer of nanoparticles was also higher than that of microparticles, again emphasizing the difference in the surface-volume ratio encountered between nano-and microparticulates. The entrapped cyclosporine then diffused through the PEG layer with controlled release. This study is one of the ultimate examples of nanotechnology applied in pharmaceutical science and the application of SEC chromatography to evaluate the delivery system from the top down.

2.4.3 Product Storage

A study performed on human serum albumin indicated the adverse effects of temperature on the protein stability in pharmaceutical preparations. The size exclusion analysis of the preparation indicated that protein concentration decreased significantly at 55 and 70°C. A dimer was also seemed to form with a weight double that of the original protein. Monomeric species could also be observed and higher aggregates were found in the different formulations. No specific pattern or kinetics could be established; however, it was concluded that the formulation variables significantly influenced stability at various temperatures and storage times.

Some examples have been discussed to illustrate the application of SEC in establishing the integrity of nanoparticulate delivery systems after manufacture, however, time-dependent stability aspects could also be identified including agglomeration and biodegradation behavior.

2.5 CONCLUSION

Pharmaceutical standards have been documented in compendial format for various medicinal products. Specifications are set for starting materials and excipients as well as the active ingredients. However, some excipients or products require characterization beyond compendial standards and for some instances techniques that are not commonly used, i.e. SEC, capillary electrophoresis and supercritical fluid chromatogrpahy[53]. Recently, some challenges that have been identified in pharmaceutical industry regarding chromatography and these include suitable evaluation procedures for nanosized drug delivery systems.

The studies that were discussed in this review illustrated that nanoparticulate drug delivery systems already employ SEC in the developmental, characterization and stability evaluation phases of these products. Many of these products were shown to be polymeric in nature and included several proteins and the development of even more of these products seems very probable. In addition, some problematic as well as characteristic aspects in the development of these nanodelivery systems can already be identified by SEC when analyzing the starting materials. It would seem that both starting material characterization in conjunction with delivery system evaluation by SEC can greatly increase the success of nanoparticulate drug delivery systems. The implementation of SEC as a quality control procedure for nanosized delivery systems in constantly enhanced by improvement in SEC such as columns[54] which can be used under more extreme conditions such as high flow rates. Shortening analysis times has developed to a point where we can now employ superspeed SEC[55].

Finally, we would like to suggest that improved standards for SEC might need to be developed to accommodate nanoparticulate drug delivery systems since it is their specific size-related properties that distinguish them from other medicinal products.

2.6 REFERENCES

(1) Wehr, Tim; Rodriguez-Diaz, Roberto. Use of Size Exclusion Chromatography in Biopharmaceutical Development. Wehr, T.; Rodriguez-Diaz, R. *In* Analytical Techniques for Biopharmaceutical Development, Rodriguez-Diaz, R.; Wehr, T.; Tuck, S ., Eds. **2005**, 95-112. Marcel Dekker: New York, 2005.

(2) The United States Pharmacopeia XXIX. United States Pharmacopeial Convention Inc., Rockville, MD. 2006.

(3) Barth, H.; Boyes, B.E.; Jackson, C. Size Exclusion Chromatography and Related Separation Techniques. Anal. Chem. **1998**, *70*(12), 251R-278R.

(4) National Nanotechnology Initiative. What is Nanotechnology? <http://www.nano.gov/html/facts/whatIsNano.html>. Accessed: 01.08.2007.

(5) Shah, P. Use of Nanotechnologies for Drug Delivery. MRS Bull. **2006**, *31*(11), 894-899.

(6) Yang, Hu; Kao, Weiyuan John. Dendrimers for Pharmaceutical and Biomedical applications. J. Biomater. Sci., Polym. Ed. **2006**, *17*(1-2), 3-19.

(7) Chan, Y.; Bulmus, V.; Zareie, M.H.; Byrne, F.L.; Barner, L.; Kavallaris, M. Acid-Cleavable Polymeric Core-Shell Particles for Delivery of Hydrophobic Drugs. J. Controlled Release. **2006**, *115*(2), 197-207.

(8) Sukhorukov, G.B.; Rogach, A.L.; Zebli, Bernd; Liedl, T.; Skirtach, A.G.; Koehler, K.; Antipov, A.A.; Gaponik, N.; Susha, A.S.; Winterhalter, M.; Parak, W.J. Nanoengineered Polymer Capsules: Tools for Detection, Controlled Delivery, and Site-Specific Manipulation. Small. **2005**, *1*(2), 194-200.

(9) Osada, K.; Kataoka, K. Drug and Gene Delivery Based on Supramolecular Assembly of PEG-Polypeptide Hybrid Block Copolymers. Adv. Polym. Sci. **2006**, 202 (Peptide Hybrid Polymers), 113-153.

(10) Jose Alonso, Maria. Nanomedicines for Overcoming Biological Barriers. Biomed. Pharmacother. **2004**, *58*(3), 168-172.

(11) Shekunov, B.Y.; Chattopadhyay, P.; Seitzinger, J.; Huff, R. Nanoparticles of Poorly Water-Soluble Drugs Prepared by Supercritical Fluid Extraction of Emulsions. Pharm. Res. **2006**, *23*(1), 196-204.

(12) Hasirci, V.; Vrana, E.; Zorlutuna, P.; Ndreu, A.; Yilgor, P.; Basmanav, F.B.; Aydin, E. Nanobiomaterials: A Review of the Existing Science and Technology, and New Approaches. J. Biomater. Sci. Polym. Ed. **2006**, *17*(11), 1241-1268.

(13) Meehan, E. Flow Injection Analysis of Polymeric Excipients Used in Pharmaceutical Formulations. Int. J. Polym. Anal. Charact. **2006**, *11*(1), 35-45.

(14) Wyatt, P.J. Light Scattering and the Absolute Characterization of Macromolecules. Anal. Chim. Acta. **1993**, *272*(1), 1-40.

(15) Roduner, E. Size Matters: Why Nanomaterials are Different. Chem. Soc. Rev. **2006**, *35*(7), 583-592.

(16) Baehr, M.; Führer, C.; Puls, J. Molecular Weight Distribution, Hemicellulose Content and Batch Conformity of Pharmaceutical Cellulose Powders. Eur. J. Pharm. Biopharm. **1991**, *37*(3), 136-141.

(17) Mun, S.; Xie, Y.; Wang, N.-H., L. Strategies to Control Batch Integrity in Size-Exclusion Simulated Moving Bed Chromatography. Ind. Eng. Chem Res. **2005**, *44*(9), 3268-3283.

(18) Takakura, Y.; Mahato, R.I.; Vishikawa, M.; Hashida, M. Control of Pharmacokinetic Profiles of Drug-Macromolecule Conjugates. Adv. Drug Delivery Rev. **1996**, *19*(3), 377-399.

(19) White, G.W.; Katone, T.; Zodda, J.P. The Use of High-Performance Size Exclusion Chromatography (HPSEC) as a Molecular Weight Screening Technique for

Polygalactouronic Acid for Use in Pharmaceutical Applications. J. Pharm. Biomed. Anal. **1999,** *20*(6), 905-912.

(20) Liu, X.M.; Maziarz, E.P., Heiler, D.J. Characterization of Implant Device Materials Using Size-Exclusion Chromatography with Mass Spectrometry and with Triple Detection. J. Chromatogr., A. **2004,** *1034*(1-2), 125-131.

(21) Gref, R.A.; Setzkom, E.A.; Leslie, W.D. A Colorimetric Method for the Determination of Parts/Million of Nonionic Surfactants. J. Am. Oil Chem. Soc. **1965,** *42*(3), 151-164.

(22) Tercyak, A.M.; Felker, T.E. Colorimetric Assay for Pluronic F-68 as Measured in Ioslated Rat Liver Perfusion Systems. Anal. Biochem. **1990,** *187*(1), 54-55.

(23) Li, C.; Palmer, W.K., Johnston, T.P. Disposition of Poloxamer 407 in Rats Following a Single Intraperitoneal Injection Assessed Using A Simplified Colorimetric Assay. J. Pharm. Biomed. Anal. **1996,** *14*(5), 659-665.

(24) Ghebeh, H.; Handa-Corrigan, A.; Butler, M. Development of an Assay for the Measurement of the Surfactant Pluronic F-68 in Mammalian Cell Culture Medium. **1998,** *262*(1), 39-44.

(25) Mao, Y.; Thompson, M.J.; Wang, Q.; Tsai, E.W. Quantitiation of Polxamers in Pharmaceutical Formulations Using Size Exclusion Chromatogrpahy and Colorimetric Methods. J. Pharm. Biomed. Anal. **2004,** *35*(5), 1127-1142.

(26) Luangtana-Anan, M.; Opanasopit, P.; Ngawhirunpat, T.; Nunthanid, J.; Sriamornsak, P.; Limmatvapirat, S.; Lim, L. Y. Effect of Chitosan Salts and Molecular Weight on a Nanoparticulate Carrier for Therapeutic Protein. Pharm. Dev. Technol. **2005,** *10*(2), 189-196.

(27) Farrugia, C.A.; Groves, M.J. Gelatin Behavior in Dilute Aqueous Solution: Designing a Nanoparticulate Fomulation. J. Pharm. Pharmacol. **1999,** *51*(6), 643-649.

(28) Mitra, A.; Lin, S. Effect of Surfactant on Fabrication and Characterization of Paclitaxel-loaded Polybutylcyanoacrylate Nanoparticulate Delivery Systems. J. Pharm. Pharmacol. **2003**, *55*(7), 895-902.

(29) Kallinteri, P.; Higgins, S.; Hutcheon, A.C.; St. Pourcain, C.B.; Garnett, M.C. Novel Functionalized Biodegradable Polymers for Nanoparticle Drug Delivery Systems. Biomacromolecules, **2005**, *6*(4), 1885-1894.

(30) Peng, T.; Su, J.; Cheng, S.-X.; Zhou, R.-X. Poly-α,β-(N-(2-hydroxyethyl)-L-aspartamide)-*g*-poly(1,3-trimethylene carbonate) Amphiphilic Graft Co-Polymer as a Potential Drug Carrier. J. Biomater. Sci. Polym. Ed. **2006**, *17*(8), 941-951.

(31) Sasatsu, M.; Onishi, H.; Machida, Y. Preparation of a PLA-PEG Block Copolymer Using a PLA Derivative with a Formyl Terminal Group and Its Application to Nanoparticulate Formulation. Int. J. Pharm. **2005**, *294*(1-2), 233-245.

(32) Fee, C.J. Size-Exclusion Reaction Chromatography (SERC): A New Technique for Protein PEGylation. Biotechnol. Bioeng. **2003**, *82*(2), 200-206.

(33) Wabnitz, P.A.; Loo, J.A. Drug Screening of Pharmaceutical Drug Discovery Compounds by Micro-size Exclusion Chromatography. Rapid Commun. Mass Spectrom. **2002**, *16*(2), 85-91.

(34) Mendichi, R.; Rizzo, V.Gigli, M.; Giacometti Schieroni, A. Dilute Properties of a Polymeric Antitumor Drug Carrier by Size-Exclusion Chromatography, Viscometry and Light Scattering. J. Appl. Polym Sci. **1998**, *70*(2), 329-338.

(35) Mendichi, R.; Rizzo, V.Gigli, M.; Giacometti Schieroni, A. Fractionation and Characterization of a Conjugate Between a Polymeric Drug-Carrier and the Antitumor Drug Camptothecin. Bioconjugate Chem, **2002**, *13*(6), 1253-1258.

(36) Gabrielle-Madelmont, C.; Lesieur, S.; Ollivon, M. Characterization of Loaded Liposomes by Size Exclusion Chromatography. J. Biochem. Biophys. Methods. **2003**, *56*(1-3), 189-217.

(37) Lesieur, S.; Gabrielle-Madelmont,C.; Paternostre, M.; Ollivon, M. Study of Size Distribution and Stability of Liposomes by High Performance Gel Exclusion Chromatography. Chem. Phys. Lipids. **1993**, *64*(1-3), 57-82.

(38) Reber, N.; Spohr, R.; Wolf, A.; Omichi, H.; Tamada, M.; Yoshida, M. Closure Characteristics of a Thermally Responsive Single Ion-Track Pore Determined By Size Exclusion Method. J. Membr. Sci. **1998**, *140*(2), 275-281.

(39) Zhu, L.; Seburg, R.A.; Tsai, E.W. Determination of Surface-Bound Hydroxypropylcellulose (HPC) on Drug Particles in Colloidal Dispersions Using Size Exclusion Chromatography: A Comparison of ELS and RI Detection. J. Pharm. Biomed. Anal. **2006**, *40*(5), 1089-1096.

(40) Lemarchand, C.; Gref, R.; Lesieur, S.; Hommel, H.; Vacher, B.; Besheer, A.; Maeder, K.; Couvreur, P. Physico-chemical Characterization of Polysaccharide-Coated Nanoparticles. J. Controlled Release. **2005**, *108*(1), 97-111.

(41) Juliano, R.L. Factors Affecting the Clearance Kinetics and Tissue Distribution of Liposomes, Microspheres and Emulsion. Adv. Drug Delivery Rev. **1988**, *2*(1), 31-54.

(42) Huve, P.; Verrecchia, T.; Bazile, D.; Couvreur, P. Simultaneous Use of Size-Exclusion Chromatography and Photon Correlation Spectroscopy for The Characterization of Poly(Lactic Acid) Nanoparticles. J. Chromatogr., A. **1994**, *675*(1-2), 129-139.

(43) Steinhauser, I.; Spänkuch B.; Strebhardt, K.; Langer, K. Trastuzumab-Modified Nanoparticles: Optimisation of Preparation and Uptake in Cancer Cells. Biomaterials. **2006**, *27*(28), 4975-4983.

(44) Bazille, D.V.; Ropert, C.; Huve, P.; Verrecchia, T.; Marland, M.; Frydman, M.; Veillard, M.; Spenleuhauer, G. Body Distribution of Fully Biodegradable [^{14}C]-Poly(D,L-Lactic Acid) Nanoparticles Coated with Albumin After Parenteral Administration to Rats. Biomaterials. **1992**, *13*(15), 1093-1102.

(45) Seijo, B.; Fattal, E.; Roblot-Treupel, L.; Couvreur, P. Design of Nanoparticles of Less Than 50 nm Diameter: Preparation, Characterization and Drug Loading. Int. J. Pharm. **1990**, *62*(1), 1-7.

(46) Nguyen, L.T.; Wienceck, J.M.; Kirsch, L.E. Characterization Methods for the Physical Stability of Biopharmaceuticals. PDA J Pharm. Sci. Technol. **2003**, *57*(6), 429-445.

(47) Jani, P.; Halbert; G.W.; Langridge, J.; Florence, A.T. Nanoparticles Uptake by Rat Gastrointestinal Mucosa: Quantitation and Particle Size Dependency. J. Pharm. Pharmacol. **1990**, *42*(12), 821-826.

(48) Aprahamian, M.; Michel, C.; Humbert, W.; Devissaguet, J.-P.; Damge, C. Transmucosal Passage of Polyalkylcyanoacrylate Nanocapsules as a New Drug Carrier in the Small Intestine. Biol. Cell. **1987**, *61*(1-2), 69-76.

(49) Landry, F.B.; Bazille, D.V.; Spenlehauer, G.; Veillard, M.; Kreuter, J. Influence of Coating Agents on the Degradation of Poly(D,L,-Lactic Acid) Nanoparticles in Model Digestive Fluids (USP XXII). S.T.P. Pharm. Sci. **1996**, *6*(3), 195-202.

(50) Gref, R.; Quellec, P.; Sanchez, A.; Calvo, P.; Dellacherie, E.; Alonso, M.J. Development and Characterization of CyA-Loaded Poly(Lactic Acid)-Poly(Ethylene Glycol)PEG Micro- and Nanoparticles. Comparison With Conventional PLA Particulate Carriers. Eur. J. Pharm. Biopharm. **2001**, *51*(2), 111-118.

(51) Ismailos, G.; Reppas, C.; Dressman, J.B.; Macheras, P.; Unusual Solubility Behavior of Cyclosporin A in Aqueous Media. J. Pharm. Pharmacol. **1991**, *43*(4), 287-289.

(52) Taylor, N.E.; Mark, A.E.; Vallat, P.; Brunne, R.M.; Testa, B.; Van Gunteren, W.F. Solvent Dependent Conformation and Hydrogen Bonding Capacity of Cyclosporin A: Evidence from Partition Coefficinet and Molecular Dynamics Simulations. J. Med. Chem. **1993**, *36*(24), 3757-3764.

(53) Sautel, M.; Kristulović, A.M. Pharmaceutical Analysis beyond Compendial Requirements. J. Sep. Sci. **2005**, *28*(13), 1529-1538.

(54) Romero, I.G.; Pasch, H. High-Throughput Screening of the Chemical Composition Distribution of Random Styrene-Butyl Acrylate Copolymers. e-Polymers. **2005,** *042*(1), 1-13.

(55) Renn, C.N.; Synovec, R.E. Improved Detection in Superspeed Size-Exclusion Chromatography by Reducing On-Column Dilution and Detector Noise. Anal. Chem. **1988,** *60*(17), 1829-1832.

CHAPTER 3 WAS SUBMITTED TO

JOURNAL OF APPLIED POLYMER SCIENCE

3. FOR AUTHORS

For additional tools visit Author Resources - an enhanced suite of online tools for Wiley InterScience journal authors, featuring Article Tracking, E-mail Publication Alerts and Customized Research Tools.

- Copyright Transfer Agreement
- Permission Request Form
- The National Institutes of Health Public Access Initiative

Instructions to Authors

Polymer Keyword Catalog

Wiley's Journal Styles and EndNote

1. In order to speed the editorial evaluation process and reduce times from submission to publication, the Journal of Applied Polymer Science is now pleased to offer web-based submission and peer review. To submit your manuscript online, please:
* Point your browser to http://mc.manuscriptcentral.com/app.
* To login, enter your User ID and Password into the boxes provided, then click "Log In." If you are unsure about whether or not you have an account, or have forgotten your password, enter your e-mail address into the "Password Help" section to the right of the screen. If you do not have an account, click on the "Create Account" Link at the top right of the screen. Subsequently, to monitor the progress of your manuscript throughout the review process, just login periodically and check your Author Center.
* Let the system guide you through the 7-step submission process. Please be sure to pay special attention to instructions given at the top of each page.
* **Please note: This journal does not accept Microsoft Word 2007 documents at this time. Please use Word's "Save As" option to save your document to an older (.doc) file type. You will be restricted to uploading the following file types for your text: .rtf, .doc, and for your figures, you will be restricted to file types .tif and .eps. OTHER FILE TYPES ARE NOT SUITABLE FOR PRODUCTION PURPOSES.** The Journal requires separate files for your text, tables, and graphical material. If you submit non-conforming material, this may slow review and publication.

* All submissions are kept strictly confidential. Online help is available to you at all times during the process at support@scholarone.com. You are also able to exit and re-enter the process at any stage before finally "submitting" your work.

2. If authors are unable to submit online, please submit hard copy in triplicate to ONE of the Journal Editors: Dr. E. Baer, Dept. of Macromolecular Science, Case Western Reserve University, Cleveland, OH 44106; Dr. Anne Hiltner, Case Western Reserve University, Cleveland, OH 44106; Dr. Edmund Elce, Promerus LLC, 9921 Brecksville Road, Brecksville, OH 44141; Dr. B.W. Pengilly, 430 Delaware Avenue, Akron, OH 44303-1236; Dr. W. G. Perkins, 304 Silver Meadow Drive, Wadsworth, OH 44281; Dr. D. A. Schiraldi, Case Western Reserve University, Cleveland, OH 44106; Dr. Mark A. Schubert, Energizer Battery Company, 25225 Detroit Road, Westlake, OH 44145. Reviewers: Authors are encouraged to suggest potential reviewers for the journal. Correspondence: All other correspondence should be addressed to the Publisher, c/o John Wiley & Sons, Inc., 111 River Street, Hoboken, New Jersey 07030-5774.

3. The Editors desire to receive manuscripts based on original research in any phase of the chemistry or physics of large molecules which have a practical applicability, including analysis and characterization of polymers. It is the preference of the Editors that papers be published in the English language. The author is responsible for the technical aspect of the manuscript, which could be obscured by faulty English. **Note:** Manuscripts that are returned by authors six months after the request for revision from the Editor will be considered as new submissions.

4. Manuscripts should be submitted in triplicate (one original, two copies) and double-spacedghout2.54 cm (1 in.).

5. Authors should supply up to five (5) keywords or phrases which best characterize the manuscript. To facilitate online searching, the editors of the Wiley polymer journals have complied a common keyword catalog, available in the first issue of every year and at http://www.interscience.wiley.com/jpages/0021-8995/keyword.pdf. At least three of the maximum of five keywords assigned to an article must come from this list.

6. A short synopsis (maximum length 200 words) of the main contributions in the paper is required. This synopsis should be carefully prepared, for it is automatically the source of most abstracts. A short summary of the whole paper, not the conclusions alone, should form the synopsis.

7. The paper should be reasonably subdivided into sections and, if necessary, subsections. Please refer to any issue of this journal for examples.

8. Authors are cautioned to type--wherever possible--all mathematical and chemical symbols, equations, and formulas. If these must be hand-written, please write clearly and leave ample space above and below for printer's marks; please use only ink. All Greek or unusual symbols should be identified in the margin the first time they are used. Please distinguish in the margins of the manuscript between capital and small letters of the alphabet wherever confusion may arise (e.g., k, K, κ). Please underline with a wavy line all vector quantities. Use fractional exponents to avoid root signs.

The nomenclature sponsored by the International Union of Pure and Applied Chemistry is requested for chemical compounds. Chemical bonds should be correctly placed, and double bonds clearly indicated. Valence is to be indicated by superscript plus and minus signs. The use of SI units is preferred.

9. References.

Wiley's Journal Styles Are Now in EndNote
EndNote is a software product that we recommend to our journal authors to help simplify and streamline the research process. Using EndNote's bibliographic management tools, you can search bibliographic databases, build and organize your reference collection, and then instantly output your bibliography in any Wiley journal style.
Download Reference Style for this Journal: If you already use EndNote, you can download the reference style for this journal.
How to Order: To learn more about EndNote, or to purchase your own copy, click here.
Technical Support: If you need assistance using EndNote, contact endnote@isiresearchsoft.com, or visit www.endnote.com/support.

The references should be numbered consecutively in the order of their appearance and should be complete, including authors' initials and--for unpublished lectures or symposia--the title of the paper, the date, and the name of the sponsoring society. Please compile references on a separate sheet at the end of the manuscript. Abbreviations of journal titles should conform to the practices of Chemical Abstracts.

Examples:

1. Olabisi, O.; Robeson, L. M.; Shaw, M. T. Polymer-Polymer Miscibility; Academic Press: New York, 1979.

2. Guilbault, G. G.; Chen, R. F.; Govindjee; Papageorgiou, G.; Rabinowitch, E.; Wehry, E. L. In Practical Fluorescence, Guilbault, G. G., Ed.; Marcel Dekker: New York, 1973, Chap. 1.

3. Hegazy, E. A.; Dessouki, A. M.; El-Assy, N. B.; El-Sawy, N. M.; El-Ghaffar, M. A. A. J Appl Polym Sci 1992, 30, 1969.

10. Please supply numbers and titles for all tables. All table columns should have an explanatory heading.

11. Please submit copies (not originals) of all figures for the peer review process. Upon acceptance, all original figures must be submitted in a form suitable for reproduction.Authors are encouraged to submit digital art. Hard copies of all artwork must accompany the digital files. Please provide digital files on 3 1/2" diskette, 100-mb or 200-mb Iomega Zip disk, or CD-ROM. Scaling, cropping, and rotating should be performed in the originating application. We recommend Adobe Photoshop for generating pixel-based graphics and either Adobe Illustrator or Macromedia's Freehand for generating vector-based graphics. Black and white (B/W) line art is either pixel based (typically generated by scanning the image) or vector based (generated using a drawing program such as Freehand or Illustrator). Pixel-based artwork should be supplied in TIFF format and at a resolution of not less than 1,000 dots per square inch (dpi). Vector-based artwork should be supplied as EPS files. B/W halftones should be supplied in TIFF format. The halftone should be provided at the proper resolution. The finished resolution should be at least 300 dpi. Color artwork should be provided as an EPS or TIFF file. Files should be converted from RGB to CMYK. The finished resolution should be at least 300 dpi.Note that these file formats are not acceptable for printing: JPG, GIF, ONG, PCX, PNG, XBM, Word, and Excel. We recommend creating your graphics in Photoshop, Illustrator, or Freehand and importing them into your page applications as TIFFs with all fonts included. Do not scan figures as JPEGs and convert to TIFFs. If in doubt about the preparation of illustrations suitable for reproduction, please consult one of the Production Editors (contact information appears at the end of these instructions). Poor quality artwork will lead to delay in publication.

Color illustrations. All color figures will be reproduced in full color in the online edition of the journal at no cost to authors. Authors are requested to pay the cost of reproducing color figures in print. Authors are encouraged to submit color illustrations that highlight the text and convey essential scientific information. For best reproduction, bright, clear colors should be used. Dark colors against a dark background do not reproduce well; please place your color images against a white background wherever possible. Please contact Glenn Beck at 201-748-8659/APPJournal@wiley.com for further information.

To ensure that your digital graphics are suitable for print purposes, please go to Rapid Inspector™ at http://rapidinspector.cadmus.com/zwi/index.jsp. This free, stand-alone software application will help you to inspect and verify illustrations right on your computer.

12. Please supply legends for all figures and compile these on a separate sheet.

13. Electronic Proofing In order to expedite the publication and on-line posting of articles in Wiley InterScience, the Journal of Applied Polymer Science now offers electronic proofing. Corresponding authors with e-mail addresses will be sent page proofs (and paperwork, such as reprint order forms) in pdf format via e-mail. Please follow the instructions in the e-mail; contact names and numbers are given for questions, problems, or if an author wishes to receive a paper proof. A fax cover form with the Production Editor's information is also provided for authors to fax their corrections.

14. Reprints can be ordered and purchased by filling out the form attached to the proof. This journal does not carry a page charge for contribution.

15. Copyright: No article can be published unless accompanied by a signed publication agreement, which serves as a transfer of copyright from author to publisher. A publication agreement may be obtained from the editor or the publisher. A copy of the publication agreement appears in most issues of the journal. Only original papers will be accepted and copyright in published papers will be vested in the publisher. It is the author's responsibility to obtain written permission to reproduce material that has appeared in another publication. A copy of that agreement, executed and signed by the author, is now required with each manuscript submission. A manuscript cannot be accepted for publication without the signed agreement. (If the article is a "work made for hire," the agreement must be signed by the employer.)

REMARK:

The manuscript was formatted for uniformity of the thesis; however, the reference citation style was preserved.

CHAPTER 3

EFFECTS OF THE COSURFACTANT 1-BUTANOL AND FEED COMPOSITION ON NANOPARTICLE PROPERTIES PRODUCED BY MICROEMULSION COPOLYMERIZATION OF STYRENE AND METHYL METHACRYLATE

Daniel P. Otto[1, 3], Hermanus C.M. Vosloo[2], Wilna Liebenberg[3] and Melgardt M. de Villiers[1]

1 School of Pharmacy, University of Wisconsin – Madison, WI 53705, USA.

2 School of Chemistry, North-West University, Potchefstroom, 2520, South Africa

3 Unit for Drug Research, Faculty of Health Sciences, North-West University, Potchefstroom, 2520, South Africa

Corresponding author: Daniel P. Otto, School of Pharmacy, University of Wisconsin – Madison, WI 53705, USA. E-mail: dotto@wisc.edu Telephone: 1-608-262-9351.

Abstract

The concentration of the cosurfactant 1-butanol determined the polymer weight and size for a series of poly(styrene-*co*-methyl methacrylate)s (P(St-*co*-MMA)) synthesized by the free-radical o/w microemulsion technique. A factorial design established the levels of the experimental conditions for the polymerization i.e. concentration of the surfactant, sodium dodecyl sulfate (SDS); concentration of the cosurfactant, 1-butanol (BuOH); temperature and ratio of the styrene (St) to methyl methacrylate (MMA). An increase in the weight average molecular weight (□ $_w$) and number average molecular weight (□ $_n$) was observed in the P(St-*co*-MMA) series with an increase in BuOH concentration from 1–5% wt. These effects could arise from the micellar aggregation induced by interfacial BuOH. The unique micellar conditions could be exploited to synthesize copolymers of varying molecular weight and size. Additionally, the composition of the copolymers was virtually templates of the feed composition.

Keywords: Microemulsion copolymerization, cosurfactant, GPC-MALLS, ATR-FTIR

3.1 INTRODUCTION

Microemulsions have been studied extensively over the years and provided a unique polymerization technique in the 1980's for the production of homopolymers.[1,2] Subsequently, the method was applied to fabricate copolymers in the following decade and since then various reports have been published that illustrated the synthesis of high molecular weight polymers showing high monomer conversion levels.[3-6] Since microemulsions are thermodynamically stable and require virtually no agitation to disperse the oil, water and surfactant pseudophases, it provides an important advantage over the traditional or coarse emulsions that are only kinematically stable upon significant agitation.[7]

The addition of short-chain alcohols such as 1-butanol, 1-pentanol and 1-hexanol provides additional stability of the microemulsions and these are often added as cosurfactants into polymerization mixtures. These cosurfactants act on the micellar surface where they can displace surfactant molecules from the micellar surface, resulting in a decrease in the CMC.[13-15] Factors that influence the effect and localization of alcohol cosurfactants are alcohol chain length,[16,17] chain branching, number of functional hydroxyl groups[18-20] and aromaticity.[21] For example, hydrophilic alcohols partitioned to the bulk dispersion phase whereas long-chain, lipophilic alcohols partitioned to the lipophilic micellar core resulting in larger micellar cores. Therefore, the ideal alcohol cosurfactant would reside in the interface with no significant partitioning to the continuous or dispersed pseudophases.

Since n-butanol, pentanol and even hexanol reside at the interface, they would be the cosurfactants of choice.[6,8-10,22,23] However, the inclusion of these short chain alcohols as cosurfactants into microemulsion copolymerization systems can result in seemingly inexplicable changes in molecular weight as a consequence of the variation of the cosurfactant concentration. Although not clearly understood, some explanations for these observations included the macroradical chain transfer to the cosurfactant and film formation around the surface of the micelle that shield polymer radicals.[24-26]

In this study a series of P(St-*co*-MMA) was synthesized under various concentrations of n-butanol, surfactant, temperature and monomer mixture composition. The aim was to investigate the effects of the experimental factors on the molecular weight, copolymer particle size, and chemical composition of the copolymer. The cosurfactant concentration prevailed as the primary determinant of molecular weight and size, whilst the monomer feed ratio significantly affected chemical composition of the copolymers.

3.2 EXPERIMENTAL SECTION

3.2.1 Materials

Methyl methacrylate (MMA) was donated by Degussa (Düsseldorf, Germany) and styrene (St) was purchased from Merck (Modderfontein, South Africa). The MMA and St were purified prior to polymerization by adsorption of the inhibitors onto dried neutral alumina-packed glass columns. A slightly yellow band was noted for St at the top of the alumina column. 1-Butanol (BuOH, >99%) was purchased from Merck and incorporated as cosurfactant. Ultra pure sodium dodecyl sulfate (SDS, >99%) and hydroquinone (HQ) were obtained from Sigma-Aldrich (Kempton Park, South Africa). Potassium persulfate (KPS) was purchased from Sigma-Aldrich and employed as reaction initiator and double-deionized water was utilized as the aqueous continuous phase.

3.2.2 Synthesis procedure and latex treatment

A report by Tauer *et al.*[27] was used as a guide to determine the compositions of the microemulsion by variation of the concentration of monomer, surfactant and dispersion media. A 500 mL three-necked flask was charged with the requisite quantities of the reagents according to a fractional 3-level-4-factor factorial design, to comprise a final mixture weight of 100 g (Table 3.1).

Table 3.1: The factorial design that was employed to determine mixture composition and reaction conditions. Experiments were conducted for one level for each factor.

	Concentration (% wt)		
Factor	Low	Intermediate	High
SDS	2	4	8
BuOH	1	3	5
%St*	60	70	80
Temperature (°C)	60	70	80

*%St in monomer mixture with a total weight of 6 g monomer mixture. This ratio was converted to %mole fraction of St (f_{St}) in the text and graphs.

The continuous phase consisted of water (to 100 g) and 500 mg KPS (all experiments) and the requisite quantities of SDS and BuOH. These were added to a three-necked flask equipped with a condenser and thermometer and was maintained at the desired reaction temperature (60, 70 or 80 ± 1 °C) to decompose KPS to produce initiator radicals. The dissociation of the initiator KPS necessitated a temperature of at least 60 °C and this was therefore selected as the minimum reaction temperature.

The reaction proceeds with KPS providing the initiator radicals to form primary monomer radicals that propagate the polymer chains. The mixture was magnetically stirred at 500 r.p.m. while continuously purged with filtered nitrogen. After 15 min of nitrogen purging at the specified reaction temperature, 6 g of degassed, vortex-mixed monomer reagents (in the desired ratio) were added to the dispersion medium through a syringe fitted with a 0.22 μm Cameo™ Teflon® filter (Sigma-Aldrich). After monomer addition, colloidal particle growth was observed from the slightly blue, translucent microemulsions. Figure 3.1 renders a graphical depiction of the reaction environment in the three-neck flask. A reaction time of 120 min was employed for all experiments and after this period, the reaction was quenched with an excess of HQ. The design and procedures were performed in duplicate to render 54 (2 sets of 27) experiments.

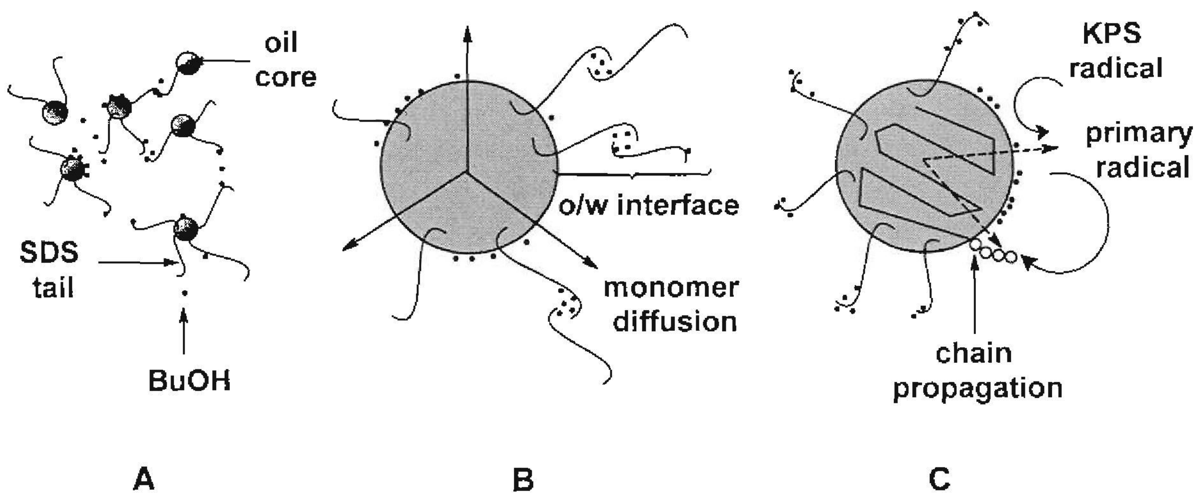

Figure 3.1: Representation of the micellar reaction environment in the three-necked flask. (A) Micelles are formed and BuOH displaces SDS from surface or results in micellar aggregation. (B) Monomer diffuses from the micelle core to the o/w interface. (C) Initiator radicals engage monomer molecules in the interface to form primary radicals that initiate chain propagation by recruitment of additional monomer molecules. (Components are not drawn to scale).

The polymer latex was collected in 50 cm^3 centrifuge tubes in an excess of methanol and allowed to cool to room temperature. The fractions were then centrifuged at 3 500 r.p.m. for 10 min, redispersed and washed in fresh aliquots of methanol. The centrifugation and washing cycle was repeated until the latex could no longer be redispersed. Subsequently, the latex was dried in a fume hood and then pulverized to a fine, white powder. Furthermore, these powders were dried under a vacuum of 13 mbar for 24 h at a regulated temperature of 40 °C (well below T_g of the copolymers ~90-100°C). Finally, the dried polymer samples were stored in opaque, air tight containers.

3.2.3 GPC-MALLS

A DAWN® DSP photometer (Wyatt Corp., Santa Barbara, California) was employed for absolute weight measurements utilizing a size exclusion chromatography setup. The multi-angle laser light scattering (MALLS) detector consisted of a 5 mW He-Ne laser that illuminated samples at a wave- length of 632.8 nm. The MALLS detector was carefully calibrated with filtered HPLC grade toluene (BDH, Merck) and then normalized with an isotropic scattering poly(styrene) (PS) standard (M_w 30 000 $g.mol^{-1}$, polydispersity < 1.05, Pressure Chemical Company, Pittsburgh, PA, USA). The MALLS was connected to a refractive index (RI) detector (Agilent® 1100 series) to determine concentration of the eluting species. On-line determination of the specific refractive index (dn/dc) was performed as reported elsewhere[28-30] by addition of a small, accurately known quantity of a low weight PS standard ($\bar{M}_w$ 2 550 $g.mol^{-1}$, $\bar{M}_w/\bar{M}_n < 1.05$, Pressure Chemical Co.) to the polymer sample.

Samples were prepared at a concentration of 3 $mg.mL^{-1}$ by sonication of the appropriate quantities of polymer and dn/dc standard in HPLC-grade THF for 10 min. Sample solutions were filtered utilizing Millipore® 0.45 μm (Microsep (Pty) Ltd, Sandton, South Africa) filters that were chemically resistant to THF. All samples were prepared and injected in duplicate.

An HPLC (Agilent® 1100) injected100 μL polymer samples (3 mg/mL) prepared in THF into the GPC columns coupled in series. The columns (purchased from Separations Scientific CC, Honeydew, South Africa) comprised of a PLGel® mixed bed type C™ (7.6 × 300 mm, exclusion range 300 – 2 000 000 $g.mol^{-1}$, particle size of 5 μm) and a Phenogel™ (Phenomenex®, 7.8 × 300 mm, exclusion range > 5 000 $g.mol^{-1}$, particle size of 5 μm). HPLC grade THF (BDH) was employed as elution liquid at a regulated flow rate of 1 $mL.min^{-1}$ whilst maintaining the system temperature at 30 °C.

ASTRA™ for Windows® version 4.73.04 (Wyatt Corp.) was utilized to record, overlay and analyze the MALLS and RI detector signals. The software calculated the number average molecular weight (□ n), the weight average molecular weight (□ w), the radius of gyration ($<s^2>^{1/2}$) and the conformation of the copolymer in the theta (θ) solvent, THF. The computations were made according to the Zimm formalism employing all scattering angles from 17-155°.

The molecular weight of each slice was calculated according to the Zimm-Stockmayer equation[31-33] from which the averages M_n and M_w were ultimately derived from Equation (3.1):

$$\frac{R_\Theta}{Kc} = MP(\Theta) - 2A_2cM^2P^2(\Theta) + \ldots \tag{3.1}$$

where M is the molecular weight of a slice of the sample chromatogram, R_Θ is the excess Rayleigh ratio at the scattering angle Θ. Additionally, the wavelength and scattering angle-dependent particle scattering factor is represented by $P(\Theta)$. Furthermore, the concentration of the particles is denoted as c (determined with the refractive index detector) and A_2 is the second virial coefficient (osmotic pressure to light scattering) which becomes negligible at low concentrations as employed here). The constant K was derived by the software from Equation (3.2):

$$K = \frac{4\pi^2 n_0^2}{\lambda_0^4 N_A}\left(\frac{dn}{dc}\right)^2 \tag{3.2}$$

where the refractive index of the solvent in vacuum is n_0 at the incident wavelength of the vertically polarized laser radiation, λ_0, the Avogadro number is N_A and the specific refractive increment of the polymer is *dn/dc*.

Conformational analysis was performed by evaluation of the linear segment of the data if plotted as a double-logarithmic plot and fitted to a power law regression according to Equation (3.3)[34,35]:

$$\left\langle s^2 \right\rangle^{1/2} \propto M_w^q \tag{3.3}$$

where the z-average root mean square $<s^2>^{1/2}$ radius to was related weight average molecular weight M_w.

The exponent q is derived from the slope by fitting a power law regression on the linear segment of the double-logarithmic plot, revealing the chain conformation of the polymers. For the theoretical condition of $q = 1/3$ a spherical, compact conformation of the chain is demonstrated. Under ideal condition where $q = 1/2$, the θ condition prevails, indicating that a cluster of chains has been separated by solvent, however limited chain expansion is evidenced and a more compact conformation is still present. A chain that revealed $0.5 \leq q < 0.6$ indicates that a random coil conformation is assumed and the solvent resulted in some degree of swelling of the species. Values of $q > 3/5$ indicate that the chain assumed a rigid, rod-like conformation possibly with a constant diameter.

Calculation of reliable conformation exponents necessitated eliminating size values and their corresponding weights with a correction factor according to Equation (3.4):

$$\left\langle s^2 \right\rangle_{\text{lim}}^{1/2} = \frac{I_s}{20n} \tag{3.4}$$

where I_s is representative of the source wavelength. The limit at which a reliable radius of gyration could be determined *in vacuo* is set at $1/20^{\text{th}}$ of the I_s. Below this limit, intensity of Rayleigh scattering declines as Debye scattering prevails at this limit.[36,37] Additionally, scattering becomes isotropic below 10 nm and therefore, angle-independent. However, in reality the refractive index of the solvent, n, lowers the limit. The limit for reliable $<s^2>^{1/2}$ in these calculations was therefore determined at approximately 20 nm. In addition, adjustment of the start and endpoints of the light scattering peak made data evaluation possible in the section of low dispersity as well as excluded the minimum radius limit and uncertainties at the high end of the log-log plot of $<s^2>^{1/2}$ versus M_w.

3.2.4 ATR-FTIR

Attenuated total reflectance Fourier transform infrared spectroscopy (ATR-FTIR) is a popular method for quantitative analysis of copolymer composition.[38-41] The (ATR) procedures were performed in the mid-IR region and spectra were recorded in the region 4000-650 cm^{-1}. A Bruker Equinox™ 55 (Bruker, Ettlingen, Germany) IR spectrometer was employed for all data collections. The spectrometer utilized a He-Ne laser operated at 632.8 nm and was equipped with a micro ATR sampling accessory containing a ZnSe crystal. Spectra were recorded by co-addition of 32 scans with a spectral resolution of 4 cm^{-1}. Bruker Opus™ 5.1 software was employed to collect and process the ATR spectra. Baseline correction was performed on all spectra. The spectrometer was operated under continuous N_2 purge.

Low weight homopolymers of low polydispersity were selected to prepare homopolymer blends varying in composition. Suitable quantities of poly(methyl methacrylate) (PMMA) and PS were dissolved in THF and then precipitated. The polymer blends were vacuum-dried for at least 12 hours. Subsequently, the precipitates were ground to produce fine powders. These standards were analyzed directly on the ATR crystal and four spectra were collected per standard. Calibration curves were constructed by plotting the absorbance ratio of two peaks, which could be assigned unambiguously to either the St monomer (~699 cm^{-1} for the out of plane bending of the phenyl ring) and for the methacrylate monomer (saturated alkyl ester carbonyl stretch at ~1729 cm^{-1}), versus the mole fraction ratio (f_{St}) of the two homopolymers employed in each set.

Subsequently, four spectra of the experimental samples were acquired by recording two spectra of a copolymer sample followed by analysis of a duplicate sample of the same specimen.

3.2.5 Calculations and Statistics

STATISTICA 7.1 (Statsoft Inc., Tulsa, OK, USA) was used to evaluate data for possible linear (denoted by 'L') or non-linear (denoted by 'Q') single factor effects as well as for two-way linear by linear interactions between the experimental factors and to determine the significance of factor influences by Pareto density analysis.

The Pareto principle states that in a population of factors that contribute to a common effect, only a few of these factors would contribute significantly to the observed effect.[42] In this study the population of factors were SDS, BuOH, temperature and monomer feed ratio; the two-way linear interactions between these variables and the characteristics of the single factor contributions i.e. linear or quadratic. The analytical results obtained through GPC-MALLS and ATR-FTIR were substituted into the factorial design and analyzed by the statistical software. The Pareto analysis was performed to determine which factor(s) dominated the measured response i.e. $\square_n$. Based on this analysis, explanations for the observations were sought and illustrated through surface plots.

The standard Pareto density function is described by Equation (3.5):

$$f(x) = \frac{c}{x^{c+1}} \quad ,1 \leq x, c > 1 \tag{3.5}$$

where the shape parameter of the population density distribution (spread of contributions of experimental factors to the effect) is c and the factor(s) that contributed to the measurement density is x. The value of $f(x)$ should exceed a specified value at a specified confidence interval should the factor prove significant. In this study we used the absolute values of the Pareto coefficients and these should exceed 2.023 as the minimum for significance at the 95% confidence interval. Figure 3.2 renders the influence of three different shape factors and a hypothetical density of $f(x)$.

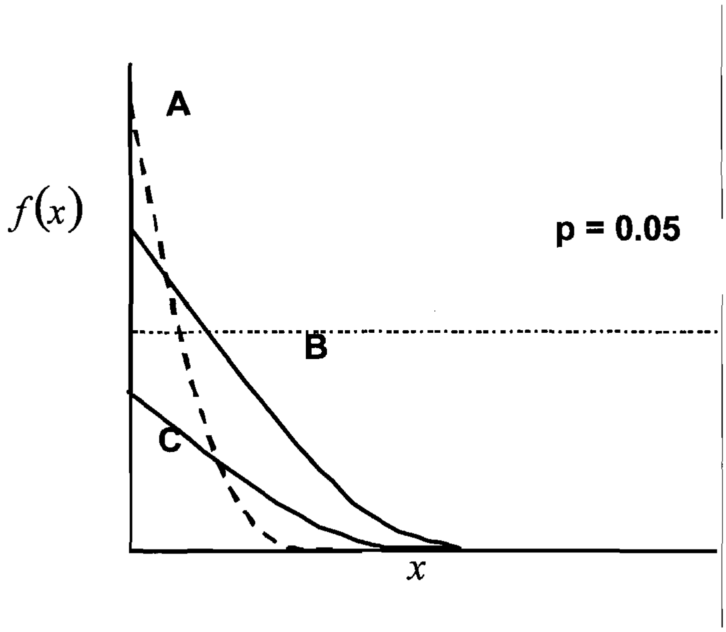

Figure 3.2: Pareto graphs of (A) Low c, narrow density of distribution with a few factors exceeding $p = 0.05$; high Pareto coefficients. (B) Intermediate c, low density with a number of factors proving significant; intermediate Pareto coefficients. The higher c becomes, the broader the density distribution and the less significant the factors, x become until none prove significant as in curve (C) (Equation 5).

3.3 RESULTS AND DISCUSSION

3.3.1 Synthesis, characterization, and processing of raw data

All the reactions produced polymeric materials under the conditions shown in Table 3.1. Subsequently, 54 products were produced and their molecular weights and radii of gyration were characterized with GPC-MALLS. Compositional content of St and MMA was determined by ATR-FTIR analysis. Duplicate samples were analyzed on different days (due to the extensive analysis period required) and these results did not vary significantly, indicating that polymers remained stable. Figure 3.3 illustrates an example of the weight distributions as a function of elution volume.

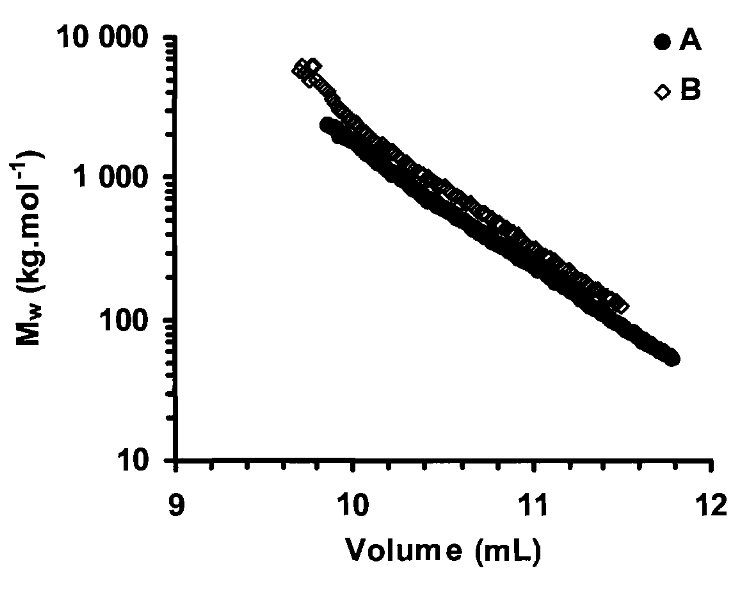

Figure 3.3: The □ $_w$ distribution of two synthesized polymer samples (A) 2% SDS, 1% BuOH, f_{St} of 69.2%, 80 °C and (B) 8% SDS, 3% BuOH, f_{St} 69.2%, 80 °C. The dn/dc standard could not be observed, confirming that it did not interfere with the sample analysis and weight distribution. Each point was calculated from light scattering data (Equation 3.1).

The weight distribution was obtained by converting each data point of the chromatogram and corresponding light scattering data to □ $_w$ (Equation 3.1) and plotting log □ $_w$ vs. elution volume. Note that the elution volume agreed with the chromatograms and that no secondary peaks or weight distributions were observed for the dn/dc standard. As an example of the results an excerpt of the results obtained by GPC-MALLS is listed in Table 3.2 and shows only results of experiments performed with 2% SDS (data for 4% and 8% SDS classifications or for any other factor classifications are not shown, however were automatically compiled and considered by the statistical software). These results (Table 3.2 and the remainder of categorizations) were then substituted into the factorial design.

Table 3.2: Excerpt of the results for P(St-*co*-MMA) as categorized by 2% SDS.*

Reaction conditions					Results				
%BuOH	°C	f_{St} (%)	%St	%MMA	□$_n$	□$_w$	□$_w$/□$_n$	$<s^2>^{1/2}$(nm)	q
	60	59.0	56±10	44±10	214.9±17	362.3±29	1.74±0.2	26.5±0.2	0.449±0.03
1	70	79.4	57±2.2	43±2.2	164.1±3.0	322.5±27	1.98±0.2	27.9±2.2	0.484±0.03
	80	69.2	61±2.5	39±2.5	160.3±17	274.4±49	1.79±0.4	23.2±0.4	0.460±0.04
	60	79.4	72±7.6	28±7.6	294.3±10	493.4±14	1.70±0.1	35.7±0.2	0.465±0.01
3	70	69.2	58±5.2	42±5.2	133.7±13	236.9±31	1.72±0.3	21.6±2.4	0.465±0.01
	80	59.0	53±1.4	47±1.4	300.7±38	499.6±49	1.60±0.3	32.9±2.1	0.497±0.01
	60	69.2	65±8.1	35±8.1	343.0±27	594.9±42	1.79±0.2	39.3±1.6	0.504±0.04
5	70	59.0	49±1.4	51±1.4	262.8±23	394.2±7.0	1.50±0.2	30.9±1.9	0.503±0.00
	80	79.4	73±9.2	27±9.2	452.4±26	733.1±30	1.66±0.1	46.5±3.3	0.463±0.02

*All molecular weight values reported in kg.mol^{-1}

Although the Pareto method had its origins in economical science,[43] it has been applied in various recent polymer studies to determine the contribution of experimental factors to a common effect and to optimize experimental parameters for polymerization reactions.[44-46] As an example, the Pareto graph of standardized factor effects on □ $_n$ for P(St-*co*-MMA) is shown in Figure 3.4. Closer inspection of the Pareto analysis indicated that a positive, linear effect was observed for M_n measurements attributed to an increase in BuOH concentration as denoted by 'L' and a positive value of the Pareto coefficient of 5.256 (Figure 3.4). In contrast, the effect of temperature proved to be significantly quadratic as denoted by 'Q' and a minimum turning point was revealed by the negative sign preceding the coefficient of 2.736 (Figure 3.4).

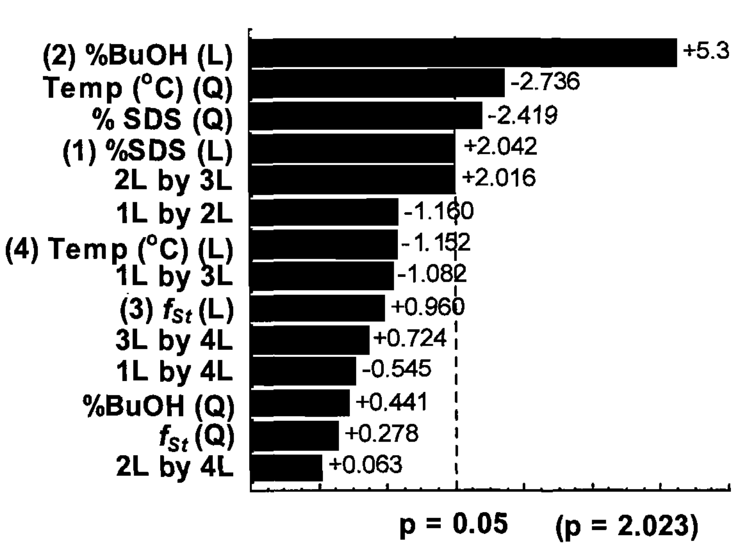

Figure 3.4: Pareto graph of standardized factor effects on □ $_n$ for P(St-*co*-MMA). Linear effects are denoted with the capital 'L' and the non-linear (or quadratic) effects by capital 'Q'. Any interaction is indicated by the term, 'by'. The number that preceded a given factor was generated from the number of the column in which data was entered in the spreadsheet and should not be mistaken for the ranking of the effect.

The Pareto coefficients calculated in this experimental design needed to exceed a minimum value of 2.023 to prove significant at a 95% confidence interval (Figure 3.4). Additionally, a positive or negative sign preceded the coefficient and indicated an increase or decrease in the measured responses and in the case of non-linearity a maximum or minimum turning point in the curvature. The Pareto coefficients were determined for all factors and listed in Table 3.3.

Table 3.3: Pareto coefficients of the full population of P(St-*co*-MMA). For explanations of the abbreviations used see experimental section.

	P(St-*co*-MMA)					
Factor/Interaction†	□$_n$	□$_w$	□$_w$/□$_n$	$<s^2>^{1/2}$	q	%St
(1) SDS (L)	+2.042*	+2.096*	+2.326*	+0.784	-0.530	+0.535
SDS (Q)	-2.418*	-2.257*	+1.825	-0.457	-1.156	+1.077
(2) BuOH (L)	+5.256*	+5.086*	-2.892*	+5.249*	+1.317	+1.025
BuOH (Q)	+0.441	+0.082	-1.874	+0.340	+1.785	+0.043
(3) f_{St} (L)	+0.960	+0.743	-0.661	+0.660	-0.232	+9.088*
f_{St} (Q)	+0.278	+0.354	-0.465	-0.048	+0.531	-0.682
(4) Temperature (L)	-1.152	-1.281	+0.325	-1.631	-1.295	-0.336
Temperature (Q)	-2.736*	-2.369*	+2.182*	-3.005*	+0.840	-1.160
1L by 2L	-1.160	-1.020	+0.526	-0.794	-1.447	-1.346
1L by 3L	-1.081	-1.571	-1.873	-2.446*	+0.820	+1.062
1L by 4L	-0.545	-0.385	+0.437	-0.935	-0.942	+1.161
2L by 3L	+2.016	+1.731	-1.767	+1.027	-1.194	+1.987
2L by 4L	+0.063	+0.148	+0.133	+0.553	+0.381	+0.378
3L by 4L	+0.724	+0.433	-1.991	+0.643	-0.324	+0.556

*Effects are significant ($p < 0.05$) if the Pareto coefficient exceeds an absolute value of 2.023.

†Effects of the factors/interactions not noted according to rank.

Figures 3.5A and B illustrated the effects of BuOH (L) and temperature (Q) respectively and were constructed from the data in Table 2. By addition (automatic function of the statistical software) of the remaining classifications i.e. 4% and 8% SDS (or any other set of classifications) to these graphs, surface plots resulted and several of these were discussed in the text here.

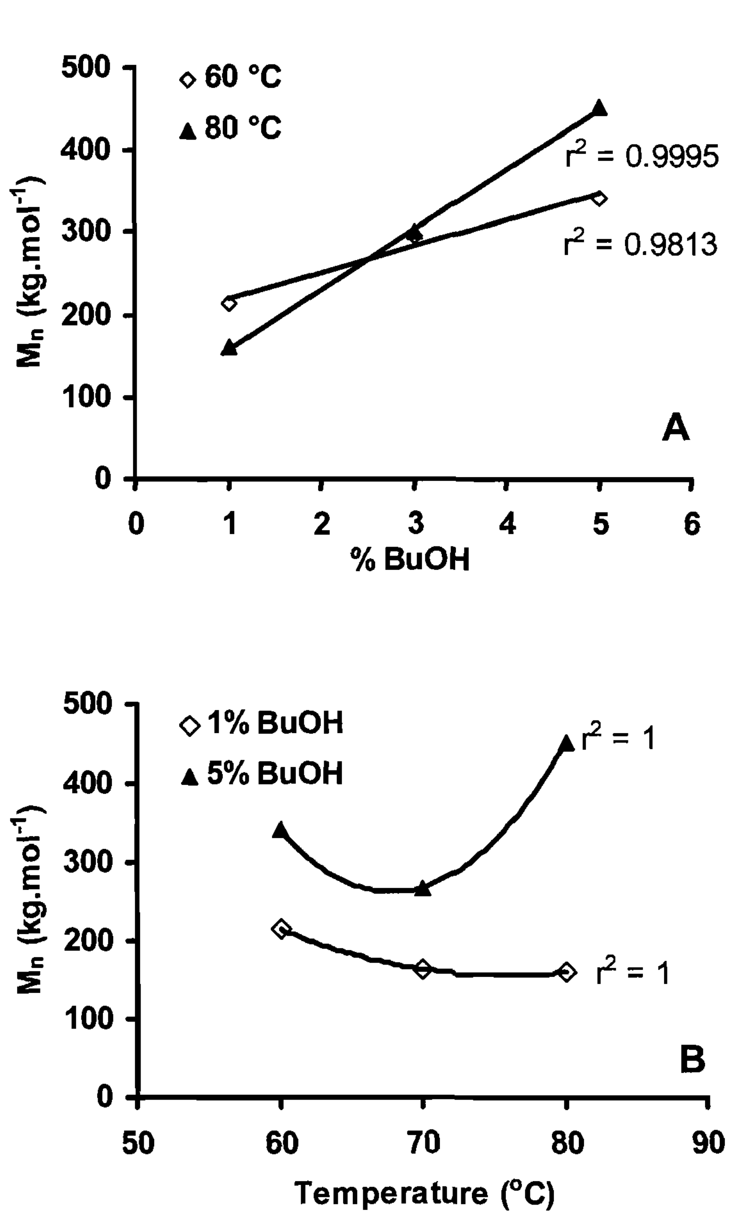

Figure 3.5: Illustration of (A) the linear effect of BuOH and (B) the quadratic effect of temperature (°C) on the response measured for □ $_n$ by fitting a second degree polynomial curve (linear fitting showed $r^2 \sim 0.80$ for 1% BuOH). For both A and B a sample of the data was taken and categorized by 2% sodium dodecyl sulfate (Table 3.2) to construct the graphs.

3.3.2 Compositional analysis

ATR-FTIR analysis revealed two spectral regions of interest for the analysis of the copolymers. The out-of-plane ring deformation of the phenyl ring of the St monomer was clearly observed at ~699 cm^{-1} and the stretching of the saturated ester carbonyl group of the methacrylate monomer at ~1729 cm^{-1} (Figure 3.6).

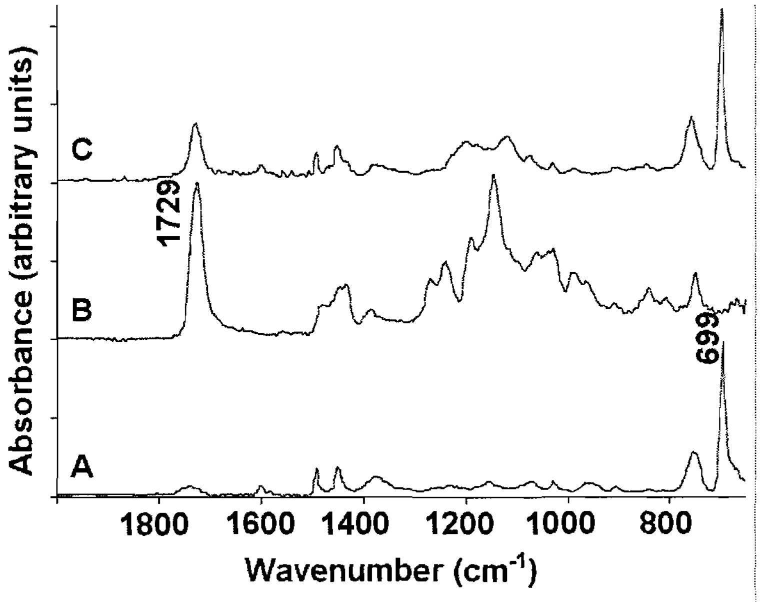

Figure 3.6: Expanded ATR-FTIR spectra of A) PS (phenyl ring out of plane bending at 699 cm^{-1}) B) PMMA (saturated ester carbonyl stretching at 1729 cm^{-1}) and C) P(St-*co*-MMA) comprised of 56% styrene and 44% MMA.

Several spectra were recorded and calibration curves constructed. The St/MMA standards showed strong linearity with $r^2 > 0.99$ for calibration curves with compositions in the range of the monomer content of the synthesized copolymers. On average, the copolymers contained approximately 8% less St than was included in the feed (Table 3.1 and Figure 3.7).

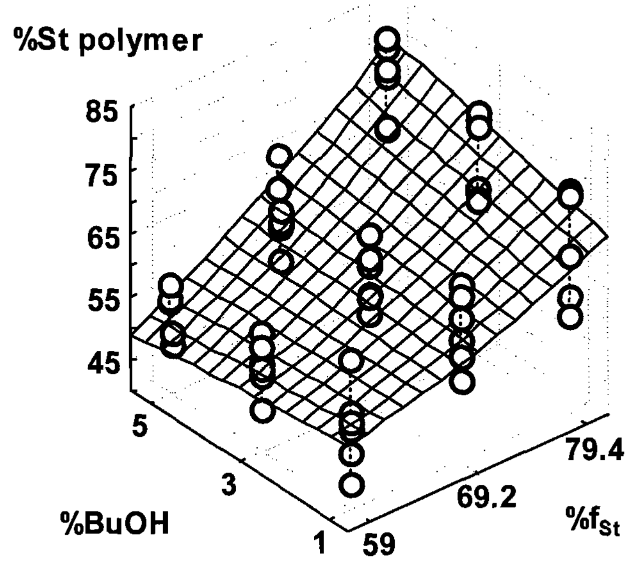

Figure 3.7: Effects of f_{St} and %BuOH on %St in P(St-*co*-MMA).

The mixtures containing 59% styrene in the feed produced copolymers containing 53% styrene as a series average. The 69% feed mixtures yielded copolymers containing 61% St and the maximum feed of 79% resulting in copolymers containing 71% (with the series showing r^2 = 0.9944). This slight compositional drift arose from the slightly higher reactivity ratio of the MMA compared to the St monomer[47], favoring MMA incorporation marginally. The partitioning of the hydrophilic MMA also favored increased MMA content in the copolymers since it could encounter more KPS radicals in the interface. However, the feed served as an approximate template for the composition of the copolymer.

3.3.3 Molecular weight of P(St-*co*-MMA)

$\square_n$ relates to the number of particles that were encountered in the eluted samples, therefore also indicates proportionality to the number of micellar reactors that were involved in particle evolution. It was apparent from Pareto analysis (Figure 3.4, Table 3.3) that the effect of BuOH dominated the measured response for $\square_n$. A positive, linear effect was observed for BuOH (Figure 3.8A) on $\square_n$ as was made apparent by the Pareto coefficient (L, +5.526) and significantly overshadowed the non-linear effects of temperature (Q, -2.736) and SDS (Q, +2.419) (Figure 3.8B, Table 3.3). A linear increase in $\square_n$ (102.0 – 470.7 kg.mol^{-1}, calculated as the averages of all 18 values obtained at a specified concentration of BuOH) was observed as a consequence of a linear increase in the cosurfactant concentration (1-5%). Temperature resulted in a non-linear continuance with minimum turning points as seen from the negative sign before the coefficient (Figure 3.8, Table 3.3). Additionally, the surfactant (SDS) had a predominantly non-linear effect with a minimum turning point if compared to its linear effect (Figure 3.4). Pareto coefficients of SDS (Q, -2.419 and L +2.042) were of comparable magnitude and closely related in magnitude (Table 3.3).

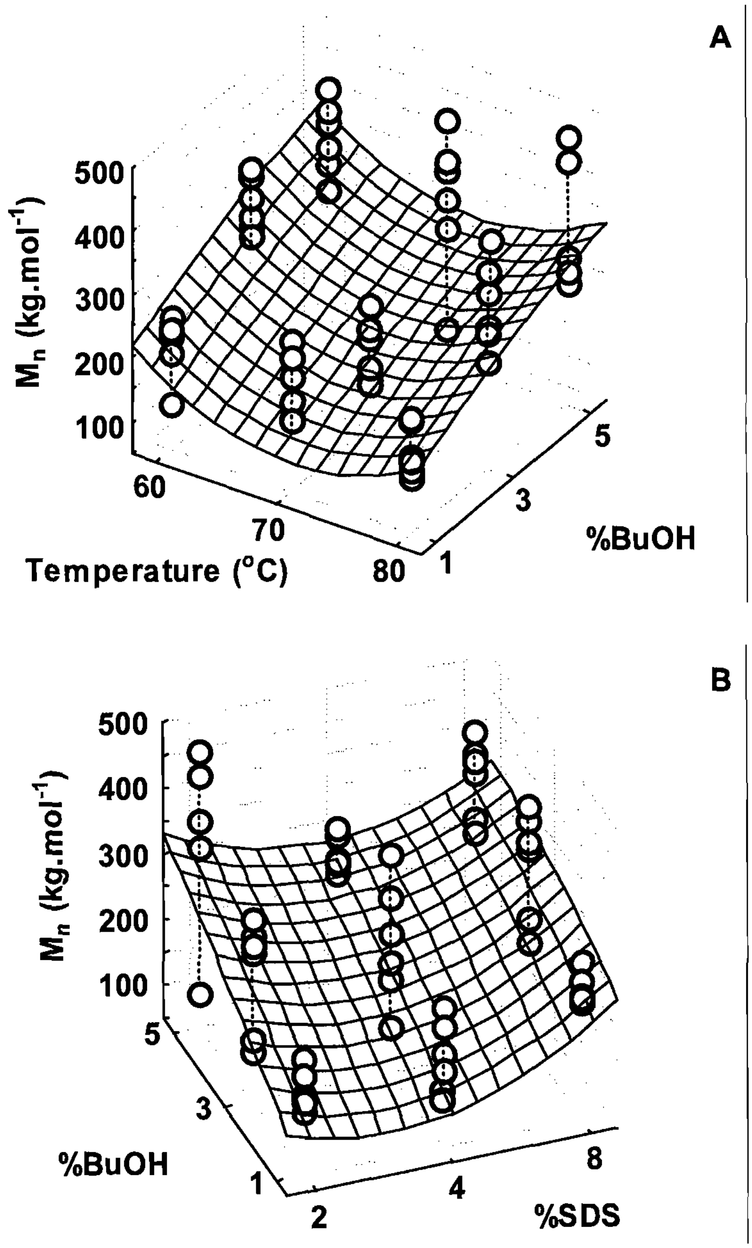

Figure 3.8: Surface plot of the effects of (A) temperature and cosurfactant (B) surfactant on □ $_n$ for P(St-*co*-MMA).

While interpreting the surface plots it should be borne in mind that since no significant interactions were noted in the Pareto analysis, the surface plots should be seen to illustrate the effect of a single factor in isolation from the other plotted variable.

Clearly a larger number of particles was present at 1% BuOH ($\square_n$ of 102.0 $kg.mol^{-1}$ indicated a large number of particles) compared to 5% ($\square_n$ of 470 $kg.mol^{-1}$ demonstrated that the particle number was smaller).

BuOH is a cosurfactant that preferentially resides in the interface at the micellar surface therefore might affect the number of active micellar reactors.[48] The microemulsion essentially consists of three liquid pseudophases, i.e. oil, water and a third pseudophase that is introduced by addition of the alcohol. This alcohol pseudophase could self-associate and since it is located preferentially in the interface, it would also associate the micelles into a denser structure. In fact based on its HLB value of 7.0, BuOH was shown to reside in the interface of Triton X-114 micelles.[49]

The linear increase in $\square_n$ suggested that a cluster of micelles formed with some of the micellar cores in the cluster interior and some exposed to the bulk continuous phase.[50-53] Thus a larger reactor with a higher local monomer concentration available for polymerization in the interface at the 5% BuOH compared to 1%. Additionally, the micelles would act in a cooperative fashion and that monomer molecules in the cluster core had to diffuse through adjacent micellar cores to the exposed reaction interface for chain propagation.

The effect of temperature was perplexing since it demonstrated a non-linear effect that was significantly less dominant than the effect of BuOH (Figure 3.8A, Table 3.3). At the lowest temperature, 60 °C the micelles would have the lowest kinetic energy and therefore might cluster together or at least be found in closer proximity to each other. At 70 °C, an optimal level of kinetic energy is reached and micelles exist in a comparatively unassociated state. However, at 80 °C a maximum response for $\square_n$ was again observed.

Two explanations could elucidate the phenomenon. The kinetic energy of the micelles might be high enough to lead to a significant number of collisions between reactors thereby clustering the cores together. In addition, it has been demonstrated for non-ionic amphiphiles with polar moieties that temperature affected their lipophilicity.[9,54,55] The polar groups of these amphiphiles engaged water molecules through hydrogen bonding that are abolished at high temperatures, dehydrating the amphiphiles to render them more lipophilic. Ultimately, self-association of this relatively lipophilic phase prevailed to a larger extent. Since BuOH also engaged water molecules it would also behave as a true amphiphile at high temperatures due to dehydration. Subsequently, self-association of BuOH would be induced, resulting in the increase in $\square_{n}$.

The non-linear response of SDS was apparent from the Pareto analysis with the SDS (Q) coefficient assuming a value of -2.419 (Table 3.3). Globally, a parabolic continuance was observed and a minimum was demonstrated at the 4% surfactant concentration (Figure 3.8B). The averages of the three groups of minima at 4% SDS were calculated to be 184.7, 247.1 and 271.4 $kg.mol^{-1}$.

The minimum for $\square_{n}$ indicated that 4% surfactant produced the largest quantity of observed particles. Furthermore it implied that the highest number of micellar reactors that were unassociated formed at 4%. At 2% the quantity of surfactant might not be sufficient to produce micelles that would be as small as would be seen at 4%. Since the emulsions were all slightly blue during the reaction process, it could still be assumed that microemulsions were stable, however that the micelles might be slightly larger at 2% (series average $\square_{n}$ of 259.1 $kg.mol^{-1}$) compared to 4% ($\square_{n}$ of 234.6 $kg.mol^{-1}$). At 8% ($\square_{n}$ of 305.5 $kg.mol^{-1}$) micelles might again cluster together since the surfactant tails could associate to some extent and produce micellar aggregates.

The difference between maxima and minima (Figure 3.8B) were marginal, resulting in a low Pareto coefficient value. At 8% SDS, the cooperative nature of the micellar cores could be suggested to result in a cluster reactor rather than in unassociated micellar reactors as seen at 4% SDS. Even if the individual micelles are of similar size as that at 4%, their true size might be obscured by the clustering effect.

$\square_{w}$ is a true measurement of the amount of monomer assembly in a polymer chain. As shown in Table 3.3, the concentration of BuOH significantly influenced the measured responses in a positively, linear fashion (Pareto coefficient L, +5.086). SDS (Q, -2.257) and temperature (Q, -2.236) also showed significant effects although inferior to that of BuOH.

The linear effect of cosurfactant on polymer molecular weight is again observed from the linear perspective of the BuOH and the non-linear SDS effect (Figure 9A). The non-linear effect of temperature on molecular weight is also shown in Figure 9B. The continuances of $\square_{w}$ reflected that of $\square_{n}$ suggested a link between the number of reactors found in the microemulsion and the number of units assembled in a chain as evidenced from M_w.

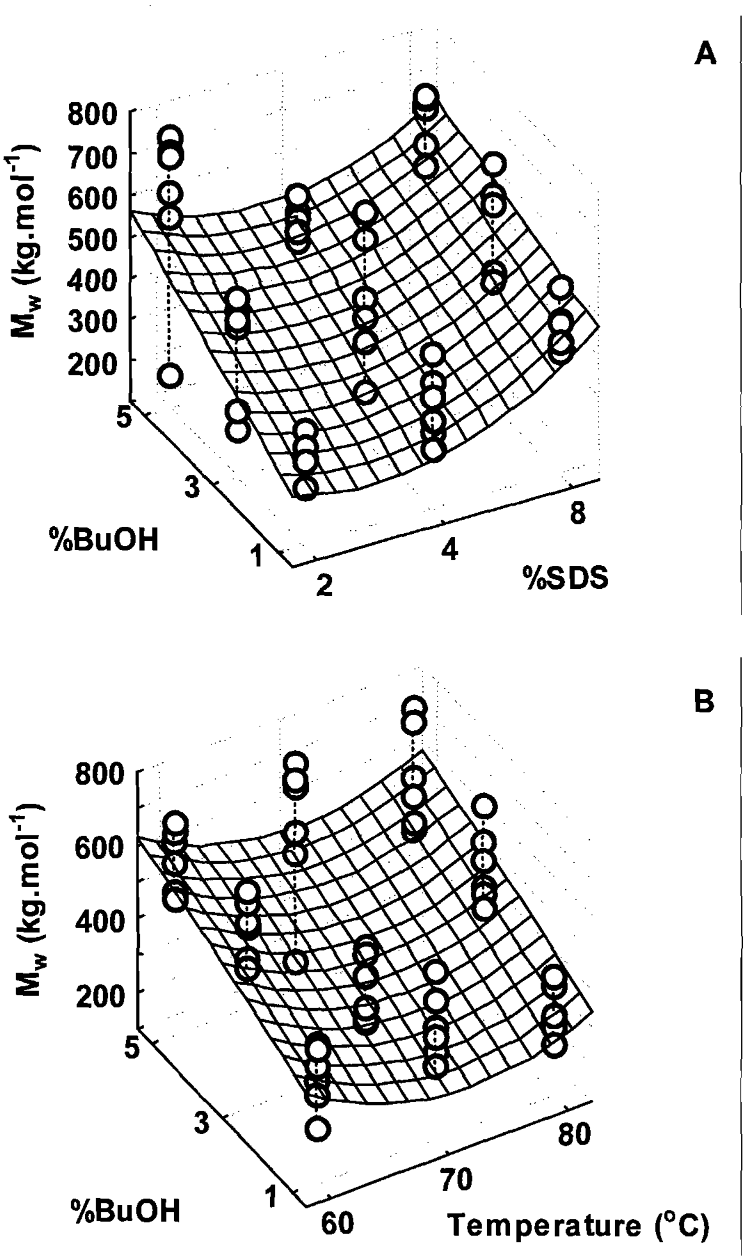

Figure 3.9: Surface plot of the effects of BuOH and temperature on □ $_w$ for P(St-*co*-MMA).

Considering the molecular weight of St and MMA (~100 g.mol^{-1}) and that the various polymers contained between 2 000 and 7 500 monomer units based on □ $_w$, it can be suggested that a link existed between the local concentration of the monomers and the polymer weight, again indicating the suggested micellar coagulation phenomenon. If the micelles were associated to a lesser extent at 1% BuOH it would explain why a lower number of monomers were polymerized (series average □ $_w$ of 375.9 kg.mol^{-1}). Subsequently more pronounced agglomeration was seen as the BuOH increased to 3% (series average $\square_w$ of 472.3 kg.mol^{-1}) and finally achieved a maximum at 5% (series average $\square_w$ of 563.4 kg.mol^{-1}), demonstrating a series regression coefficient of $r^2 = 0.9997$.

Judged by the Pareto analyses (Table 3.3), SDS also had a significant effect on monomer assembly as seen from the values of $\square_w$ (Figure 3.9A). The trends observed for SDS could also be explained by the clustering argument at different surfactant concentrations with $\square_w$ values complimentary to that of $\square_n$. The higher values of $\square_w$ (compared to their corresponding $\square_n$) illustrated that monomer assembly was not equal in all the reactors. The minimum at 2% SDS (series average $\square_w$ of 441.0 kg.mol^{-1}) corresponded to the minimum found for M_n. The minimum $\square_w$ was also found at 4% SDS and attained a series average value of 422.5 kg.mol^{-1} and finally the maximum $\square_w$ was found at 8% SDS with a series average 548.1 kg.mol^{-1}.

Temperature illustrated its effect on $\square_w$ (as with $\square_n$) on particle aggregation with aggregation more prevalent at 60 °C and collisions more prevalent at 80 °C. Consequently, two series of maxima were observed and depending on the desired weight the temperature could be adjusted to render particles between 200 and 750 kg.mol^{-1} (Figure 9B). The minima was again observed at 70 °C and correlated to the fact that the highest number of unassociated reactors were found at this temperature. Note that the effect of BuOH predominated the outcome of final particle properties (Table 3.3).

It was observed that the values of $\square_w$ were approximately 100-200 kg.mol^{-1} higher than their corresponding $\square_n$ values, resulting in differences in polydispersity, $\square_w/\square_n$. The probability of factors having significant effects on the polydispersity was again illustrated with Pareto probability density (Table 3.3).

The polydispersity was fairly broad, exhibiting a range of 1.5 – 2.1. This reflected the nature of the reaction in the aspect of reactor heterogeneity. Clearly, a vast number of radical species were formed in the micellar environment, each of which resulted in different polymer weight characteristics. However, these values are typical for studies of this type of addition polymerization.[24-26] The linear effect of BuOH was again apparent, however demonstrated a negative sign to the coefficient (L, -2.892) suggesting that polydispersity was decreased slightly upon an increase in BuOH concentration. The effects of temperature (Q, +2.182) and SDS (+2.326) were also observed to be significant and these showed positive effects (therefore increasing polydispersity) as noted from the signs preceding the magnitude coefficients (Table

3.3). Although the three factors proved significant, they all approached the minimum Pareto significance coefficient of 2.023.

Based on these findings it would seem advantageous to incorporate a high concentration of cosurfactant to improve the polydispersity to a minimum. This could arise from the fact that fewer reactors were formed in the microemulsion at 5% cosurfactant compared to the 1% (therefore a relatively high $\square_n$ at 5% compared to 1%). The decrease in reactor number could therefore decrease the probability of encountering a high degree of reactor uniqueness. In contrast, the higher the number of reactors, the higher the probability of finding unique micellar reactors that would produce higher polydispersity. Since the number average weight was lower at 1% BuOH than 5% (Figure 3.8) it indicated an increase in the probability of finding a higher reactor count with a resulting higher probability of uniqueness at 1% BuOH.

3.3.4 Radius of gyration of P(St-*co*-MMA)

One measure of polymer particle size is the radius of gyration, $\langle s^2\rangle^{1/2}$.[56,57] As stated earlier the alcohol pseudophase employed as cosurfactant here, could self-associate and since it is located preferentially in the interface, would also associate the micelles into closer proximity to form clusters. From this perspective, the local concentration of monomer at the interface would be relatively higher at 5% BuOH compared to 1%. Consequently, the probability of particle propagation would be higher with longer chains forming during the polymerization. The clustering effect could also decrease the surface area available for termination reactions (in competition with propagation reactions). Therefore, an increase in BuOH concentration resulted in a linear increase in $\langle s^2\rangle^{1/2}$ from approximately 20 to 45 nm (L, +5.249, $r^2 = 0.9958$).

Clearly, all the reactions resulted in the production of nanoparticles according to the definition of nanoparticles, i.e. particles with at least one length dimension between 0.1 -100 nm.[58] The average $\langle s^2\rangle^{1/2}$ of the 1% BuOH category was ~26 nm, the 3% category averaged ~32 nm and the 5% BuOH produced an average of 37 nm (Figure 3.10).

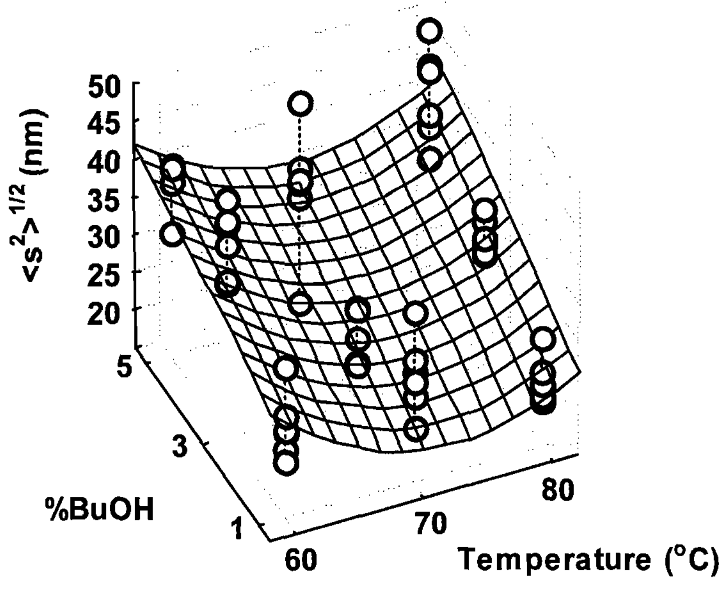

Figure 3.10: Effect of BuOH and temperature on the radius of gyration of P(St-*co*-MMA).

The effect of temperature on the particle size was less dominant, however still significant compared to the effect of the cosurfactant. As seen for changes in □ $_{n}$, temperature exerted a quadratic effect (Q, -3.005), implicating more complex mechanisms of action involved in its effects as stated earlier. At the lowest temperature, the micelles would have the lowest kinetic energy and therefore might cluster together or at least be found in closer proximity (series average $<s^2>^{1/2}$ of ~35 nm). At 70 °C, an optimal level of kinetic energy is reached and micelles exist in a comparatively unassociated state and therefore resulted in the lowest average for $<s^2>^{1/2}$ of ~28 nm. Since radical termination could also prevail at this temperature, particle growth could be curbed to a maximum at 70 °C. At 80 °C a second maximum response for $<s^2>^{1/2}$ was again observed with a series average of ~32 nm, due to an increase in reactor collision.

There was a significant linear by linear interaction between SDS concentration and monomer ratio (L by L, -2.446) since a simultaneous linear by linear increase or decrease in both SDS concentration and feed ratio resulted in a decrease in radius of gyration (Table 3.3). If seen from a concentration of 2% surfactant, the increase in mole fraction ratio (e.g. an increase in styrene mole fraction) resulted in an increase in the particle size. If seen from 4% surfactant, virtually no change in the response was seen with an increase in feed ratio. Therefore, the results for 8% SDS clearly contradicted the observations at 2%, having illustrated a relative decrease in radius of gyration as a function of an increase in mole fraction ratio (f_{St})) (Figure 3.11)

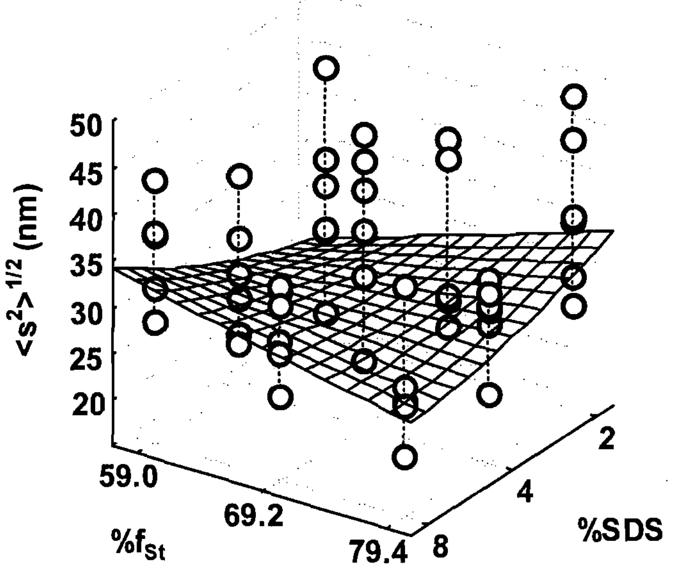

Figure 3.11: Effect of f_{St} and SDS on the radius of gyration of P(St-*co*-MMA).

One explanation for the interaction phenomenon could be that an increase f_{St} resulted in an increase in the styrene content of the copolymers. Conversely, the MMA content decreased and its amphiphilic effect might be less prominent when compared to higher MMA interfacial abundance. It would seem that the higher contribution of MMA to surface tension reduction would result in smaller particles, since micelles could be stabilized at a relatively low concentration of SDS. It would support, from this perspective, that surfactant aggregation would probably be minimized, preventing micellar agglomeration. The function of interfacial MMA as cosurfactant (although significantly eclipsed by the cosurfactant function of 1-butanol) is therefore plausible.

Figure 3.12 shows the distribution of particle sizes as classified by cosurfactant concentration. Reasonable separation of distinct particle size and distribution could be obtained by changing the cosurfactant concentration from 1% to 5% with 3% producing some overlap between both categories.

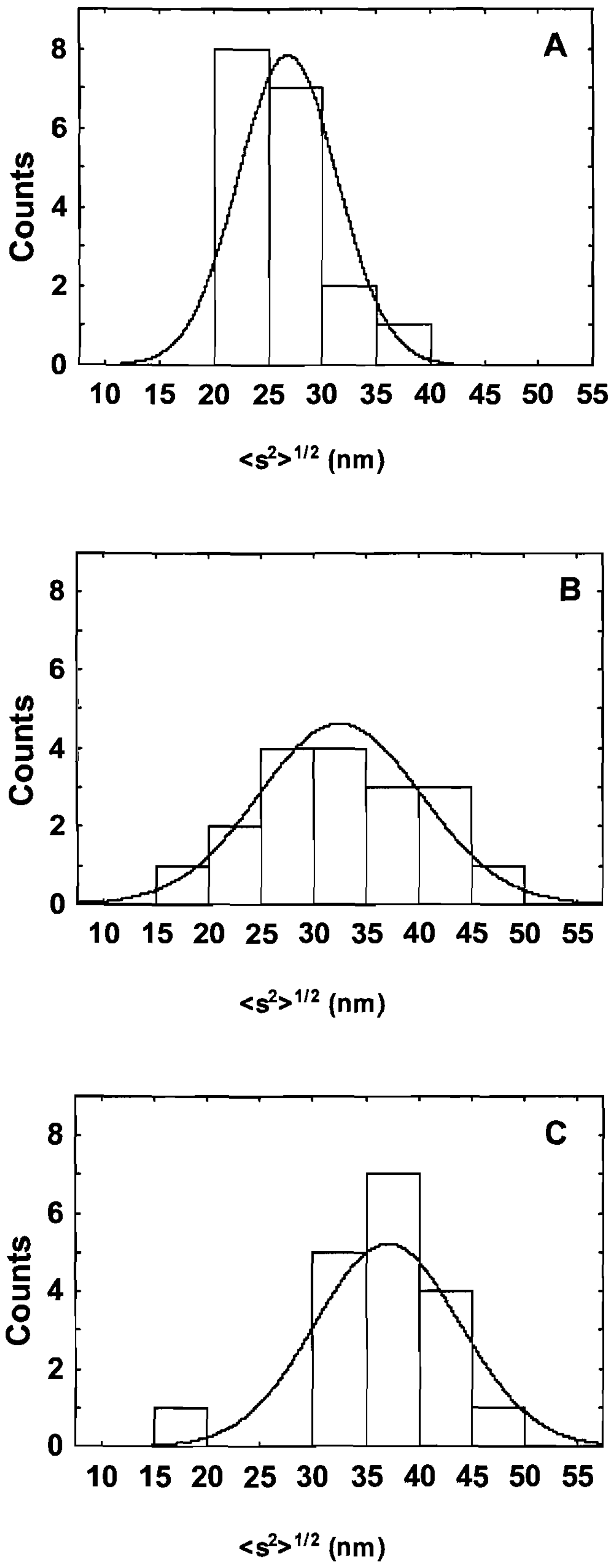

Figure 3.12: Radii of gyration of all samples categorized according to BuOH (A) 1% (average of 26 nm) (B) 3% (average of 32 nm) and (C) 5% (average of 37 nm).

3.3.5 Conformational analysis

Conformational analysis was also performed to study the bulk chain conformation of the copolymers. The conformation of polymer chains is the result of intra- and intermolecular force interactions between polymer-polymer and solvent-polymer associations. Solubility in the solvent could have a significant influence on polymer conformation with different solvent inducing compact through extended conformations of the polymers.[59,60] The copolymer weights (Table 2) varied between 200-750 $kg.mol^{-1}$ for P(St-*co*-MMA) measured in THF. Since these polymers all approached the maximum solubility in THF, they could not show significant extension.

The data in Table 3.2 show that q was very close to 0.5 indicating that the majority of the polymers (data not shown) demonstrated a random coil conformation at or just below the theta condition. This means that the solvent has separated a cluster of chains, however limited expansion of the chains occurred and a more compact conformation was still present. Pareto analysis of copolymer conformation did not reveal statistically significant effects (Table 3), however could still rank the factors and magnitude of the effects. Again, it was clear that the cosurfactant prevailed to be the most dominant factor. These observations could probably be related to the effect that the interfacial cosurfactant had the most profound impact on the polymer size and weight properties during the synthesis. Consequently, the effect on conformation should also be related to the effect of cosurfactant.

3.4 CONCLUSION

The dominating effect of the cosurfactant, 1-butanol, clearly prevailed in the microemulsion copolymerization of styrene and methyl methacrylate. The linear increases observed for molecular weight and particle size with an increasing concentration of BuOH could be exploited for the successful production of a series of nanoparticles, whilst the composition was virtually unaffected by the cosurfactant. It is suggested that the preferential location of the cosurfactant at the oil/water interface resulted in a clustering effect that affected the reactor number and size and subsequently the molecular weight and radius of gyration of the nanoparticles. Factors including temperature and surfactant modulated the clustering effect, however were shown to be inferior based on Pareto analysis. Additionally, as observed from compositional analysis, the feed ratio of the monomers dominated the polymer composition and served as an approximate template for the polymer composition.

3.5 REFERENCES

1. Stoffer, J.O.; Bone, T. J Dispersion Sci Technol 1980, 1, 393.

2. Stoffer, J. O.; Bone, T. J Polym Sci, Part A: Polym Chem 1980, 18, 2641.

3. Puig, J.E.; Corona-Galvan, S.; Maldonado, A.; Schulz, P.C.; Rodriguez, B.E.; Kaler, E.W. J Colloid Interface Sci 1990, 137, 308.

4. Candau, F. Macromol Symp 1995, 92, 169.

5. Puig, J.E.; Mendizabal, E.; Rodriguez, B.E.; Rabelero, V.; Velazquez, R.; Castano, V. Int J Polym Mater 1995, 30, 167.

6. Capek, I.; Juranicova, V. J Polym Sci Part A: Polym Chem 1996, 34, 575.

7. Danielsson, I.; Lindman, B. Colloids Surf 1981, 3, 391.

8. Ganesh, T.; Balamurugan, D.; Sabesan, R.; Krishnan, S. J Mol Lip 2006, 123, 80.

9. Lobo, L.; Svereika, A. J Colloid Interface Sci 2003, 261, 498.

10. Rubio, D.A.R.; Zanette, D.; Nome, F.; Bunton, C.A. Langmuir 1994, 10, 1151.

11. Binks, B.P.; Espert, A.; Fletcher, P.D.I.; Soubiran, L. Colloids Surf., A 2003, 212, 135.

12. Costa, M.F.C.; Froehner, S.J.; Ruzza, Â, A.; Santos, S.F.; Zanette, D. Quím. Nova 1998, 21, 272.

13. Blokhus,A.M.; Høiland, H.; Gjerde, M.I.; Ersland, E.K. J Colloid Interface Sci 1996, 179, 625.

14. Førland, G.M.; Rahman, T.; Høiland, H.; Børve, K.J. J Colloid Interface Sci 1996, 182, 348.

15. Maidment, L.J.; Chen, V.; Warr, G.G. Colloids Surf., A 1997, 129-130, 311.

16. John, A.C.; Rakshit, A.K. Colloids Surf., A 1995, 95, 201.

17. Khadir, A.; Roux-Desgranges, G.; Roux, A.H. Thermochim Acta 1997, 292, 59.

18. Abuin, E., Lissi, E.; Olivares, K. J Colloid Interface Sci 2004, 276, 208.

19. Pokhriyal, N. K.; Devi, S. Eur Polym J 2000, 36, 333.

20. Alany, R.G.; Rades, T.; Agatonovic-Kustrin, S.; Davies, N.M.; Tucker, I.G. Int J Pharm 2000, 196, 141.

21. Sarma, S.; Bora, M.; Dutta, R.K. Colloids Surf., A 2005, 256, 105.

22. Tomšic, M.; Bešter-Rogač, M.; Jamnik, A.; Kunz, W.; Touraud, D.; Bergmann, A.; Glatter, O. J Colloid Interface Sci 2006, 294, 194.

23. Attwood, D.; Terreros, A.; Lopez-Cabarcos, E.; Galera-Gomez, P.A. J Colloid Interface Sci 2000, 225, 25.

24. Gómez-Cisneros, M.; Treviño, M.E.; Peralta, R.D.; Rabelero, M.; Mendizábal, E.; Puig, J.E.; Cesteros, C.; López, R.G. Polymer, 2005, 46, 2900.

25. Shi, Y.; Wu, Y.; Hao, J.; Li, G. Colloids Surf., A 2005, 262, 191.

26. Puig, J.E.; Mendizábal, E.; Delgado, S.; Arellano, J.; López-Serrano, F. C R Chim 2003, 6, 1267.

27. Tauer, K.; Ramírez, A.G.; López, R.G. C R Chim 2003, 6, 1245.

28. Hofe, T.; Koenigsmann, H. GIT Labor-Fachzeitschrift 2003, 47, 380.

29. Kendrick, B.S.; Kerwin, B.A.; Chang, B.S.; Philo, J.S. Anal Biochem 2001, 299, 136.

30. Mhatre, R.; Krull, I.S. Anal Chem 1993, 65, 283.

31. Zimm, B.H. J Chem Phys 1948, 16, 1093.

32. Zimm, B.H.; Stockmayer, W.H. J Chem Phys 1949, 17, 1301.

33. Wyatt, P.J. Anal Chim Acta 1993, 272, 1.

34. Liu, Y.; Bo, S.; Zhu, Y.; Zhang, W. Polymer 2003, 44, 7209.

35. De Gennes, P.G. Scaling Concepts in Polymer Physics, Cornell Univ. Press, 1979

36. Jovin, T.M.; Morris, S.J.; Striker, G.; Schultens, H.A.; Digweed, M.; Arndt-Jovin, D.J. J Histochem Cytochem 1976, 24, 269.

37. Clasen, C.; Kulicke, W.-M. Prog Polym Sci 2001, 26, 1839.

38. Masson, J.-F.; Pelletier, L.; Collins, P. J Appl Polym Sci 2001, 79, 1034.

39. Prasad, A. Polym Eng Sci 1998, 38, 1716.

40. Qin, D. Appl Spectrosc 2001, 55, 871.

41. Karami, A.; Balke, S.T.; Schunk, T.C. J Chromatogr., A 2001, 911, 27.

42. Juran, J.M. In Juran's Quality Handbook 5th ed, Juran, J.M.; Godfrey, A.B.; Hoogstoel, R.E.; Schilling, E.G., Eds.; McGraw-Hill: New York, 1999, Chap. 5.

43. Pareto, V. J Political Economy 1897, 5. 485.

44. Deb, K.; Mitra, K.; Dewri, R.; Majumdar, S. Chem Eng Sci 2004, 59, 4261.

45. Massebeuf, S.; Fonteix, C.; Hoppe, S.; Pla, F. J Appl Polym Sci 2003, 87, 2383.

46. Moshinsky, L.; Figovsky, O.L. Scientific Israel - Technol Adv 1999, 1, 28.

47. Carraher., C.E.. Polymer Chemistry 5th ed; Marcell Dekker: New York, 2000.

48. Möller, A.; Lang, P.; Findenegg, G.H.; Keiderling, U. J Phys Chem B 1998, 102, 8958.

49. Marinov, R.; Panayotova, S.; Dehrzhanski, A. Prog Colloid Polym Sci 2001, 118, 256.

50. Lianos, P.; Lang, J.; Zana, R. J Phys Chem 1982, 86, 4809.

51. Lianos, P.; Lang, J.; Strazielle, C., Zana, R. J Phys Chem 1982, 86, 1019.

52. Sjoeblom, E.; Henriksson, U.; Stenius, P. Finnish Chem Lett 1982, 6-8, 114.

53. Roux-Desgranges, G.; Roux, A.H.; Grolier, J.P.E.; Viallard, A. J Solution Chem 1982, 11, 357.

54. Von Rybinski, W.; Guckenbiehl, B.; Tesmann, H. Colloids Surf., A 1998, 142, 333.

55. Aramaki, K.; Ozawa, K.; Kunieda, H. J Colloid Interface Sci 1997, 196, 74.

56. Kosmas, M.K. J Phys A: Math Gen 1981, 14, 2779.

57. Suzuki, K. Bull Chem Soc Jpn 1947, 20, 19.

58. National Nanotechnology Institute. What is nanotechnology? http://www.nano.gov/html/facts/whatIsNano.html.

59. Gan, H.H.; Eu, B.C. J Chem Phys 1998, 109, 2011.

60. Flory, P.J. Statistical Mechanics of Chain Molecules; Hanser Gardner: New York, 1988.

CHAPTER 4 WAS SUBMITTED TO

COLLOID & POLYMER SCIENCE

4. INSTRUCTIONS FOR AUTHORS

Colloid and Polymer Science

Legal Requirements

The author(s) guarantee(s) that the manuscript will not be published elsewhere in any language without the consent of the copyright owners, that the rights of third parties will not be violated, and that the publisher will not be held legally responsible should there be any claims for compensation.

Authors wishing to include figures or text passages that have already been published elsewhere are required to obtain permission from the copyright owner(s) and to include evidence that such permission has been granted when submitting their papers. Any material received without such evidence will be assumed to originate from the authors.

Manuscripts must be accompanied by the "Copyright Transfer Statement". The form can be obtained from the link below.
Copyright Transfer Statement

Manuscript Submission

Authors should submit their manuscripts to the Editor online to facilitate even quicker and more efficient processing. Electronic submission substantially reduces the editorial processing and reviewing times and shortens overall publication times.
Please log directly onto the site https://mc.manuscriptcentral.com/cps
and upload your manuscript following the on-screen instructions.
If you have any questions please contact the Editorial office (e-mail: cps@pc.rwth-aachen.de; kremer@physik.uni-leipzig.de)

When online access is unavailable, manuscripts should be submitted in print (three copies), together with one set of original illustrations and be accompanied by a disk containing the electronic version (one file including text and figures), preferrably in word or rtf format.
https://mc.manuscriptcentral.com/cps

Manuscript Preparation
Leading contributions should not exceed 20 manuscript pages and 18 figures, all other articles 15 manuscript pages and 8 figures.

Short communications are limited to 8 pages and 4 figures. Short communications will be published with high priority, at least within 3 months after acceptance of the manuscript.

Reviews of books, proceedings and conferences are written by invitation of the editors; suggestions are welcome. Reviews should not exceed four manuscript pages.

To help you prepare your manuscript, Springer offers a template that can be used with Winword 7 (Windows 95), 97, 2000, and Word for Macintosh. For details see point "Electronic submission of final version".

Manuscripts may also be written in LaTeX for which Springer-Verlag offers a macropackage (see Sect. "Electronic submission of final version"). All manuscripts are subject to copy editing.

Title page

- The name(s) of the author(s)
  A concise and informative title
  The affiliation(s) and address(es) of the author(s)
  The e-mail address, telephone and fax numbers of the communicating author

Abstract

Each paper must be preceded by an abstract presenting the most important results and conclusions in no more than 150 words.

Keywords

Up to 5 keywords are to be supplied. They should not simply be taken from the title, but should represent the content of the whole article and be characteristic of the terminology used within the particular field of study. should be supplied after the Abstract for indexing purposes.

Abbreviations

Should be defined at first mention in the abstract and again in the main body of the text and used consistently thereafter.

Chemical formulae and nomenclature

Chemical formulae and nomenclature must be unambiguous and in accordance with the relevant international recommendations.

Units and abbreviations.

- Please adhere to internationally agreed standards such as those adopted by the commission of the International Union of Pure and Applied Physics (IUPAP) or defined by the International

Organization of Standardization (ISO). Metric SI units should be used throughout except where non-SI units are more common [e.g. litre (l) for volume].

Main Text

The Introduction should be clear and brief and should include the relevant references.

In the experimental sections all materials used and the methods by which the results were obtained must be clearly described.

Conclusion should stress the major findings, outlining their significance and indicating any possible future applications.

Acknowledgements of financial support technical assistance etc. may be given at the end of the main body of the paper.

References

The list of References should only include works that are cited in the text and that have been published or accepted for publication. Personal communications should only be mentioned in the text. If available the DOI can be added at the end of the reference in question. Citations in the text should be identified by numbers in square brackets, and the list of references at the end of the paper should be listed in numerical order. References with correct punctuation should be styled as follows.

Here are a few examples for the style of references:

1. Nagata M, Kitazima I (2006) Coll Polym Sci 284: 380. DOI 10.1007/s00396-005-1393-3

2. Britz D (2005) Digital Simulation in Electrochemistry, 3rd edn. Springer, Berlin Heidelberg New York

3. Houston JE (2004) Interfacial Force Microscopy. In: Bushan B, Fuchs H, Hosaka S (eds) Applied Scanning Probe Methods. Springer, Berlin Heidelberg New York, pp. 41-115

The DOI should be added at the end of the reference in question.

Example:

1. Nagata M, Kitazima I (2006) Coll Polym Sci DOI 10.1007/s00396-005-1393-3

Illustrations and Tables

All figures (photographs, graphs or diagrams) and tables should be cited in the text, and each numbered consecutively throughout. Figure parts should be identified by lowercase roman letters. The placement of figures and tables should be indicated in the left margin. For submission of figures in electronic form see below.

Line drawings

Please submit good-quality prints. The inscriptions should be clearly legible.
Half-tone illustrations (black and white and color)

Please submit well-contrasted photographic prints with the top indicated on the back. Magnification should be indicated by scale bars.

Plates

Several figures or figure parts should be grouped in a plate on one page.

Size of figures

The figures should either match the width of the column (8,6 cm) or be 13,1 cm or 17,6 cm wide. The maximum length is 23,6 cm.

Figure legends

Figure legends must be brief, self-sufficient explanations of the illustrations. The legends should be placed at the end of the text.

Tables

Tables should have a title and a legend explaining any abbreviation used in that table. Footnotes to tables should be indicated by superscript lower-case letters (or asterisks for signifi- cance values and other statistical data).

Color illustrations

For color illustrations the authors will be expected to make a contribution (€ 950, US $ 1150, plus 16% VAT) towards the extra costs, irrespective of the number of color figures. Color figures can be included in the electronic version free of charge, these will however appear in black and white in the print edition.

Electronic Submission of Final Version
Please send only the final version of the article, as accepted by the editors.

Preparing your manuscript

Text

A template is available:

Springer.com

Choose your country (or INTERNATIONAL VERSION) press.
– Chemistry
– For Authors
– choose journal's template

via browser: ftp://ftp.springer.de/pub/Word/journals/
File names: readme-cjour.pdf, sv-cjour.dot
The zip file should be sent uuencoded.

Layout guidelines

Use a normal, plain font (e.g., Times Roman) for text.

Other style options:
– for textual emphasis use italic types.
– for special purposes, such as for mathematical vectors, use boldface type.

Use the automatic page numbering function to number the pages.

Do not use field functions.

For indents use tab stops or other commands, not the space bar.

Use the table functions of your word processing program, not spreadsheets, to make tables.

Use the equation editor of your word processing program or MathType for equations.

Place any figure legends or tables at the end of the article.

Submit all figures as separate files and do not integrate them within the text.

Data formats

Save your file in two formats:

1. Text: RTF (Rich Text Format) or Microsoft Word compatible formats Figures: EPS or TIFF.
2. PDF (a single PDF file including text, tables and figures). Make sure that all fonts are embedded

LaTex

The electronic version should include the original source (including all style files and figures) and a PostScript version of the compiled submission. Authors who prepare their papers with LaTeX are encouraged to use Springer's macro package for this journal, available at the journals webpage at springer.com.

Illustrations

The preferred figure formats are EPS for vector graphics exported from a drawing program and TIFF for halftone illustrations. EPS files must always contain a preview in TIFF of the figure. The file name (one file for each figure) should include the figure number. Figure legends should be included in the text and not in the figure file.

Scan resolution

Scanned line drawings should be digitized with a minimum resolution of 800 dpi relative to the final figure size. For digital halftones, 300 dpi is usually sufficient.

Color illustrations

Store color illustrations as RGB (8 bits per channel) in TIFF format.

Vector graphics

Fonts used in the vector graphics must be included. Please do not draw with hairlines. The minimum line width is 0.2 mm (i.e., 0.567 pt) relative to the final size.

Chemical Structures

Chemical Structures should be submitting using ChemDraw or ISISDraw in the original format as well as in eps format

Electronic Supplementary Material
Electronic supplementary material (ESM) for an article in the journal will be published in SpringerLink provided the material is:

submitted to the Editor(s) in electronic form together with the paper and is subject to peer review
accepted by the journals Editor(s)

ESM may consist of

information that cannot be printed: animations, video clips, sound recordings

information that is more convenient in electronic form: sequences, spectral data, etc.

large original data that relate to the paper, e.g. additional tables, illustrations (color and black & white), etc. After acceptance by the journals Editor(s) ESM will be published as received from the author in the online version only. Reference will be given in the printed version.

Proofreading
Authors should make their proof corrections on a printout of the pdf file supplied, checking that the text is complete and that all figures and tables are included. After online publication, further changes can only be made in the form of an Erratum, which will be hyperlinked to the article.

The author is entitled to formal corrections only. Substantial changes in content, e.g. new results, corrected values, title and authorship are not allowed without the approval of the responsible editor. In such a case please contact the Editorial Office or the Editor-in-Chief before returning the proofs to the publisher.

Offprints, Free Copy
25 offprints of each contribution are supplied free of charge. If you wish to order additional offprints you must return the order form with the corrected proofs.

CHAPTER 4

EFFECTS OF THE COSURFACTANT AND MONOMER FEED RATIO ON NANOSIZED POLYMERS SYNTHESIZED BY MICROEMULSION COPOLYMERIZATION OF STYRENE AND ETHYL METHACRYLATE

DANIEL P. OTTO, HERMANUS C.M VOSLOO, WILNA LIEBENBERG, MELGARDT M. DE VILLIERS

Daniel P. Otto, Melgardt M. de Villiers

School of Pharmacy

University of Wisconsin-Madison

777 Highland Avenue

Madison

WI 53705

Correspondence: e-mail: dotto@wisc.edu, tel.: 608-262-9351, fax: 608-262-5345

Hermanus C.M. Vosloo

School of Chemistry

North-West University

Private Bag X6001

Potchefstroom

2520

South Africa

Daniel P. Otto, Wilna Liebenberg

Unit for Drug Research

Faculty of Health Sciences

Nortth-West University

Private Bag X6001

Potchefstroom

2520

South Africa

Abstract

Various random poly(styrene-*co*-ethyl methacrylate) (P(St-*co*-EMA)) copolymers were synthesized by aqueous microemulsion copolymerization. Various levels of the cosurfactant (1-butanol), surfactant (sodium dodecyl sulfate), temperature and monomer feed ratio were investigated as determined by a fractional factorial design. The copolymer molecular weight, radius of gyration and conformation of the isolated copolymer nanoparticles were characterized by size exclusion chromatography coupled to multi angle laser light scattering (GPC-MALLS). Compositional analysis was conducted with attenuated total reflectance Fourier transform infrared spectroscopy (ATR-FTIR). Pareto analysis revealed that an increase in cosurfactant concentration from 1-5% wt. dominated the concurrent decreases in copolymer molecular weight (600-150 $kg.mol^{-1}$) and radius of gyration with (40-12 nm). The copolymers illustrated compact, random coil configurations in THF. The monomer feed ratio was the only significant determinant of copolymer composition, demonstrating virtually perfect templating. It is suggested that micellar clustering induced by 1-butanol could be employed to synthesize nanoparticulate copolymers of various weight and size without affecting chemical composition.

Keywords: microemulsion, copolymerization, cosurfactant, GPC-MALLS, ATR-FTIR

4.1 INTRODUCTION

Microemulsions were first defined as thermodynamically stable and optically clear dispersions of two immiscible liquids created with the aid of a suitable surfactant or more commonly a mixture a surfactant and cosurfactant [1]. These mixtures decrease the interfacial tension between the liquid phases to ultra-low levels, resulting in the spontaneous dispersion of the phases [2]. Although these liquid dispersions are thermodynamically stable, the microemulsion domains continuously undergo spontaneous coalescence and redispersion [3]. Examples of such micellar coalescence were reported for two of the most commonly used surfactants for microemulsions, sodium dodecyl sulfate (SDS) and cetyl trimethyl ammonium bromide (CTAB) in the presence of cosolvents icluding acetophenone and methyl ethyl ketone [4].

Despite their complex phase behavior, microemulsions found several technological applications i.e. crude oil recovery [5], industrial cleaning formulations [6], drug solubilization, i.e diclofenac sodium [7]. In several of these studies 1-butanol (BuOH) proved superior to other alcohols to maximize the microemulsion phase of the dispersion i.e. in the production of pharmaceutical formulations of practically insoluble drugs such as cyclosporin [8] or the synthesis of polymeric nanoparticles [9].

A unique technique for hompolymerization of methyl acrylate using microemulsions was first realized in the 1980's in the presence of either 1-pentanol [10] or 4-pentene-ol [11]. Styrene (St) has subsequently been polymerized in the presence of SDS and short chain alcohol cosurfactants [12], with 1-butanol resulting in the highest level of flocculation of the polymeric product [13]. Copolymerizations in microemulsions were also reported for St as comonomer of acrylic acid [14], acrylonitrile [15] and for butyl acrylate and acrylonitrile [16]. In addition, alcohols were employed as cosurfactants in microemulsion copolymerizations of vinyltoluene with methyl methacrylate (MMA) and St [17]. In many of these studies, the effect of the alcohol chain length [18, 19], functional group number [20-22] and aromaticity [23] were investigated to determine cosurfactant localization in micelles. The results showed that BuOH and 1-pentanol were effective cosurfactants because they selectively resided in the interface[24-26].

In many instances the application of alcoholic cosurfactants in microemulsion reaction mixtures resulted in seemingly inexplicable changes in molecular weight and particle size of polymeric nanoparticles. Some explanations for these observations included macroradical chain transfer by the cosurfactant [27] and film formation [28, 29] around the surface of the micelle, both of which stunt chain propagation.

In an effort to investigate these effects, a copolymer series, poly(styrene-*co*-ethyl methacrylate) (P(ST-*co*-EMA)), was synthesized using various levels of cosurfactant, surfactant, temperature and monomer mixture combinations. This study demonstrated concurrent variations in molecular weight and radius of gyration of the particles as a consequence of the variation of BuOH concentration. It is suggested that BuOH modulated micellar aggregation in the microemulsion due to hydrogen bonding interactions between BuOH molecules and with the alkyl chains of the surfactant. Subsequently the molecular weight and size varied as determined for the redispersed artificial polymer latexes [30, 31] of the isolated products. The copolymers invariantly illustrated compact, random coil configurations in the theta solvent, THF. The composition of the copolymers was virtually perfect templates of the monomer feed ratio.

4.2 EXPERIMENTAL

4.2.1 Materials

Ethyl methacrylate (EMA) was donated by Degussa (Düsseldorf, Germany) and styrene (St) was purchased from Merck (Modderfontein, South Africa). EMA and St were purified prior to polymerization by adsorption of the inhibitors onto dried neutral alumina-packed glass columns. A slightly yellow band was noted for St at the top of the alumina column. BuOH, >99%) was purchased from Merck (Modderfontein, South Africa) and incorporated as cosurfactant. Ultra pure (>99%) SDS and hydroquinone (HQ) were obtained from Sigma-Aldrich (Kempton Park, South Africa). Potassium persulfate (KPS) was employed as reaction initiator and double-deionized water was utilized to produce the dispersion medium.

4.2.2 Synthesis procedure and latex treatment

4.2.2.1 Reaction procedure

A report by Tauer *et al.*[32] on the polymerization of butyl acrylate and was used as a formulation guideline to devise the compositions of the microemulsions (in comparison to the compositions of emulsion, suspension, solution and mini-emulsion polymerizations) by variation of the monomer concentration, surfactant and dispersion media. A 500 mL three-necked flask was charged with the requisite quantities of the reagents according to a fractional 3-level-4-factor factorial design, to comprise a final mixture weight of 100 g (Table 1).

Table 4.1: Copolymerization conditions/mixtures according to the factorial design. Each reaction employed one level per factor.

	Concentration (% wt)		
Factor/Level	Low	Intermediate	High
SDS	2	4	8
BuOH	1	3	5
%St*	60	70	80
Temperature (°C)	60	70	80

*% St in monomer mixture with a total weight of 6 g monomer mixture. This ratio was converted to %mole fraction and denoted f_{ST} in the text.

According to the factorial design water (to 100 g), 500 mg KPS (all experiments), SDS and BuOH were added to a three-necked flask equipped with a condenser and thermometer. The reactor vessel was maintained at the desired reaction temperature (60, 70 or 80 ± 1 °C) to decompose KPS to produce initiator radicals (at least 60 °C is required for decomposition). The reaction proceeds with KPS providing the initiator radicals to form primary monomer radicals that propagate the polymer chains. The mixture was magnetically stirred at 500 r.p.m. whilst continuously purged with filtered nitrogen. After 15 minutes of nitrogen purging at the specified reaction temperature, 6 g of degassed, vortex-mixed monomer reagents (in the desired ratio) were added to the dispersion medium through a syringe fitted with a 0.22 µm Teflon® (Cameo™, Fisher Scientific) filter. After monomer addition, colloidal particle growth was observed from the slightly blue, translucent microemulsions. Figure 4.1 renders a depiction of the colloidal reaction environment in the glass reactor vessel. A reaction time of 2 h was employed for all experiments and after this period, the reaction was quenched with an excess of HQ. The design and procedures were performed in duplicate to render 54 experiments.

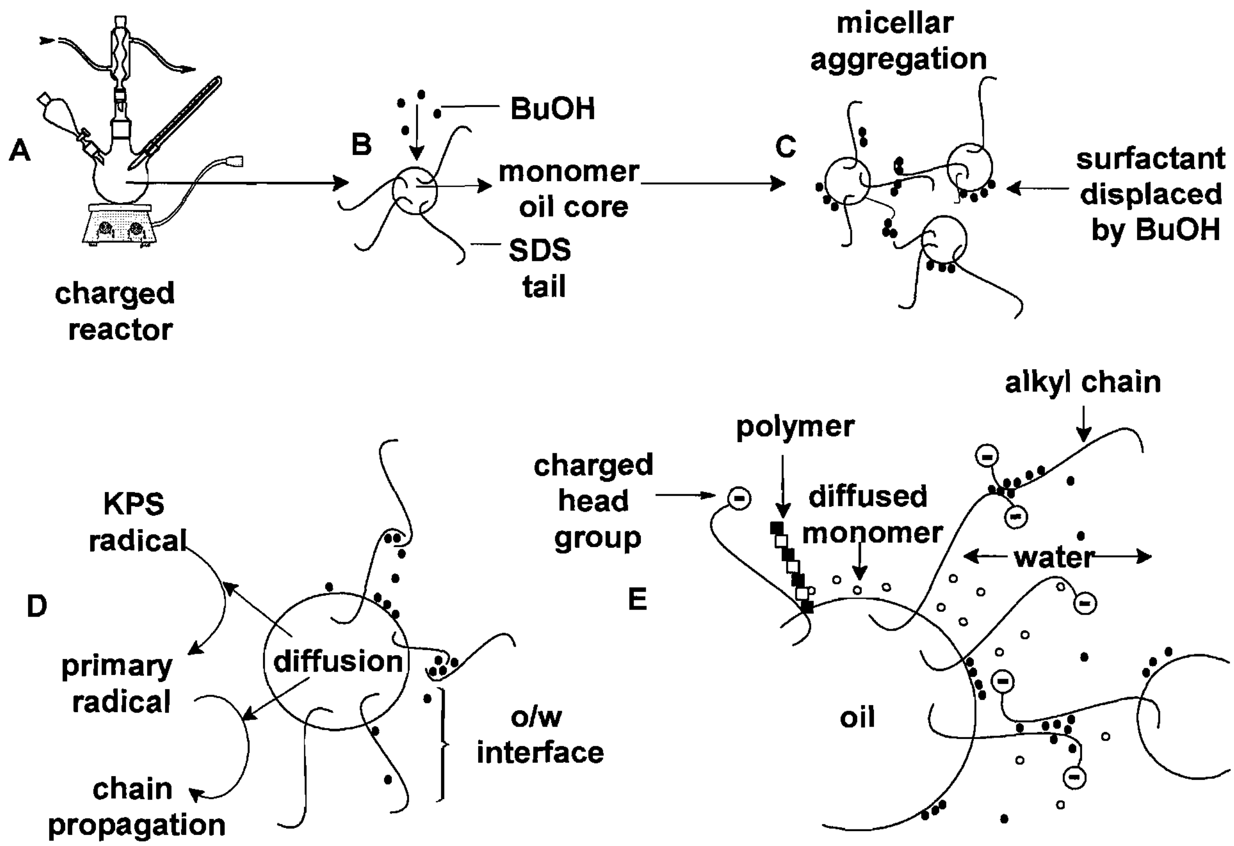

Figure 4.1: (A) The colloidal reaction environment is created in the charged reactor (B) Micelles form as BuOH and SDS interacts with monomer droplets and surrounding aqueous medium. The alkyl chains of SDS show some penetration of monomer core with the charged head groups associating with the water medium (C) Micellar aggregation takes place as BuOH interacts with SDS alkyl tails (D) Monomer molecules diffuse from the micelle core to the o/w interface and are engaged by initiator radicals. Primary radicals are produced and these propagate the copolymer chain (E) The interface comprises of monomer molecules, BuOH molecules, SDS alkyl chains as well a SDS charged head groups, KPS radicals and water. The growing polymer chain remains associated with the interface and eventually extend to some degree to the aqueous medium. The aggregation of SDS alkyl chains is also shown. (Not a scale drawing).

The polymer latex was collected in 50 cm^3 centrifuge tubes in an excess of methanol and allowed to cool to room temperature. The fractions were then centrifuged at 3500 r.p.m. for 10 minutes and redispersed and washed in fresh aliquots of methanol and repeated until the latex could no longer be redispersed. Subsequently, the latex was dried in a fume hood until the material was brittle and this material was then milled to produce a fine, white powder. The powdered product was dried under a vacuum of 13 mbar for 24 hours at a regulated temperature of 40 °C (well below T_g of the copolymers ~90-100 °C). Finally, the dried polymer samples were stored in opaque, airtight containers.

4.2.3 Sample analysis

4.2.3.1 GPC-MALLS

A DAWN® DSP photometer (Wyatt Corp., Santa Barbara, California) was employed for absolute weight measurements utilizing a size exclusion chromatography setup. The multi-angle laser light scattering (MALLS) detector consisted of a 5 mW He-Ne laser that illuminated samples at a wavelength of 632.8 nm. The MALLS detector was carefully calibrated with filtered HPLC grade toluene (BDH, Merck) and its diodes normalized with an isotropic scattering polystyrene standard (□$_w$ 30 000 g.mol^{-1}, polydispersity < 1.05, Pressure Chemical). The MALLS was connected to a refractive index (RI) detector (Agilent® 1100 series) to determine concentration of the eluting species. On-line determination of the specific refractive index (dn/dc) was performed as reported elsewhere [33-35] by addition of a small, accurately known quantity of a low weight polystyrene standard (□$_w$ 2550 g.mol^{-1}, □$_w$/□$_n$ < 1.05, Pressure Chemical) to the polymer sample.

Samples were prepared at a concentration of 3 mg.mL^{-1} by sonication of the appropriate quantities of polymer and dn/dc standard in HPLC-grade THF (BDH, Merck) for 10 minutes. Sample solutions were filtered utilizing Teflon® 0.45 μm (Cameo™, Fischer Scientific) filters. All the sample artificial latexes were prepared and injected in duplicate.

100 μl polymer samples were injected with an HPLC (Agilent® 1100) into the GPC columns using THF as both solvent and mobile phase. The columns comprised of a PLGel® mixed bed type C™ (7.6 × 300 mm, exclusion range 300 – 2 000 000 g.mol^{-1}, particle size of 5 μm) and a Phenogel™ (Phenomenex®, 7.8 × 300 mm, exclusion range > 5000 g.mol^{-1}, particle size of 5 μm). HPLC-grade THF (BDH) was employed as elution liquid at a regulated flow rate of 1 mL.min^{-1} whilst maintaining the system temperature at 30 °C.

ASTRA™ for Windows® version 4.73.04 (Wyatt Corp., Santa Barbara, California) was utilized to record, overlay and analyze the MALLS and RI detector signals. The software calculated the number average molecular weight (□ $_n$), the weight average molecular weight (□ $_w$), the radius of gyration ($<s^2>^{1/2}$) and the conformation of the copolymer in the solvent, THF. All computations were made according to the Zimm formalism.

Conformational analysis was performed by evaluation of the linear segment of the data if plotted as a double-logarithmic plot and fitted to a power law regression equation [36, 37] of the form (1):

$$\left\langle s^2 \right\rangle^{1/2} \propto M_w^q \tag{1}$$

where the z-average root mean square radius of gyration is $<s^2>^{1/2}$ is related to the weight average molecular weight M_w of the copolymer chain. The exponent q is derived by fitting a power law regression on the linear segment of the double-logarithmic plot of $<s^2>^{1/2}$ versus □ $_{w,}$. The slope of this regression curve is equal to q and revealed the bulk chain conformation of the polymer chains. For the theoretical condition of q = 1/3 a spherical, compact conformation of the chain is demonstrated. Under ideal conditions where q = 1/2, the θ condition prevails indicating that a cluster of chains has been separated by solvent and no resultant intra-and intermolecular force exists, however limited chain expansion is evidenced and a more compact conformation is still present. A chain that revealed $0.5 < q \leq 0.6$ indicates that a random coil conformation is assumed and the solvent resulted in some degree of swelling of the species. Values of $q > 3/5$ indicate that the chain assumed a rigid, rod-like conformation possibly with a constant diameter.

Calculation of reliable conformation exponents necessitated eliminating size values and their corresponding weights with a correction factor (2):

$$\left\langle s^2 \right\rangle_{\lim}^{1/2} = \frac{I_s}{20n} \tag{2}$$

Where I_s is representative of the source wavelength. The limit at which a reliable radius of gyration could be determined *in vacuo* is set at $1/20^{th}$ of the I_s. Below this limit, intensity of Rayleigh scattering declines as Debye scattering prevails at this limit [38, 39]. Additionally, scattering becomes isotropic below 10 nm and therefore, angle-independent. However, in reality the refractive index of the solvent, *n*, lowers the limit. The limit for reliable $<s^2>^{1/2}$ in these calculations was therefore determined at approximately 20 nm. In addition, adjustment of the start and endpoints of the light scattering peak made data evaluation possible in the section of low dispersity as well as excluded the minimum radius limit and uncertainties at the high end of the double logarithmic plot of $<s^2>^{1/2}$ versus □$_w$.

STATISTICA 7.1 (Statsoft Inc., Tulsa, Oklahoma, USA) was used to evaluate data for possible linear or non-linear single factor effects as well as for two-way linear by linear interactions between the experimental factors and to determine the significance of factor influences by Pareto density analysis.

4.2.3.2 ATR-FTIR

Attenuated total reflectance Fourier transform infrared (ATR-FTIR) is a popular method for quantitative analysis of copolymer composition.[40-43] The (ATR) procedures were performed in the mid-IR region and spectra were recorded in the region 4000-650 cm^{-1}. An Equinox™ 55 (Bruker, Germany) IR spectrometer was employed for all data collections. The spectrometer employed a He-Ne laser operated at 632.8 nm and was equipped with a micro ATR sampling accessory containing a ZnSe crystal. Spectra were recorded by co-addition of 32 scans with a spectral resolution of 4 cm^{-1}. Opus™ 5.1 software (Bruker, Germany) was employed to collect and process the ATR spectra. Baseline correction was performed on all spectra. The spectrometer was operated under continuous N_2 purge.

Low weight homopolymers of low polydispersity were selected to prepare homopolymer blends varying in composition. Suitable quantities of poly(ethyl methacrylate) (PEMA) (Fluka & Riedel de Haën, USA) and poly(styrene) (PS) (Scientific Polymer Products Inc., USA) were dissolved in THF and then precipitated. The polymer blends were subsequently vacuum-dried for at least 12 hours. Subsequently, the precipitates were ground to produce fine powders. These standards were analyzed directly on the ATR crystal and four spectra were collected per standard. Calibration curves were constructed by plotting the absorbance ratio of two peaks, which could be assigned unambiguously to either the styrene monomer (~699 cm^{-1} for the out of plane deformation of the phenyl ring) and for the methacrylate monomer (saturated alkyl ester carbonyl stretch at ~1725 cm^{-1}), versus the mole fraction ratio (f_{St}/f_{EMA}) of the two homopolymers employed in each set. Four spectra of the experimental samples were acquired by recording two spectra of a copolymer sample followed by analysis of a duplicate sample of the same specimen.

4.3 RESULTS AND DISCUSSION

4.3.1 Statistical analysis

All 54 reactions produced polymeric materials under the conditions shown in Table 4.1 and their molecular weights and radii of gyration were characterized with GPC-MALLS. Compositional content of St and EMA was determined by ATR-FTIR analysis. In Figure 4.2 an example of the chromatograms obtained with GPC-MALLS/RI for two copolymer samples are shown.

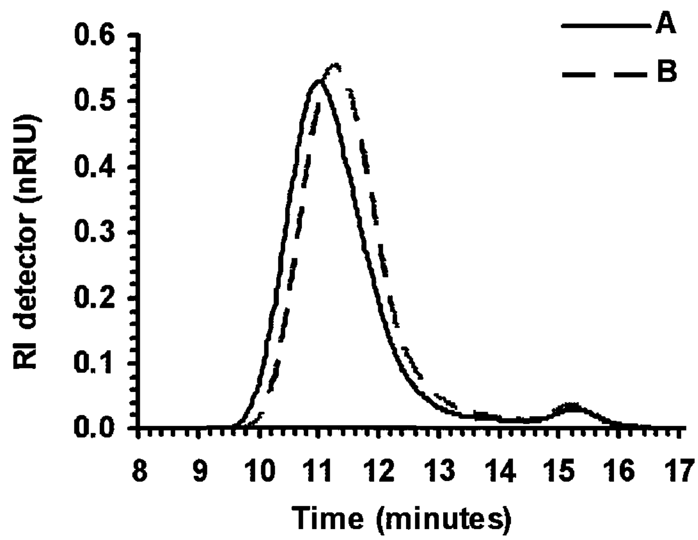

Figure 4.2: Chromatograms of P(St-*co*-EMA) samples synthesized under different conditions (A) 2 %SDS, 1% BuOH, 70 °C and f_{St} of 81.4% and (B) 2% SDS, 1% BuOH, 80 °C and f_{St} of 81.4%. The primary peak represents the synthesized polymer whilst the smaller secondary peak represents the standard that was included to determine dn/dc.

Figure 4.3 illustrates an example of the weight distributions as a function of elution volume calculated from these chromatograms.

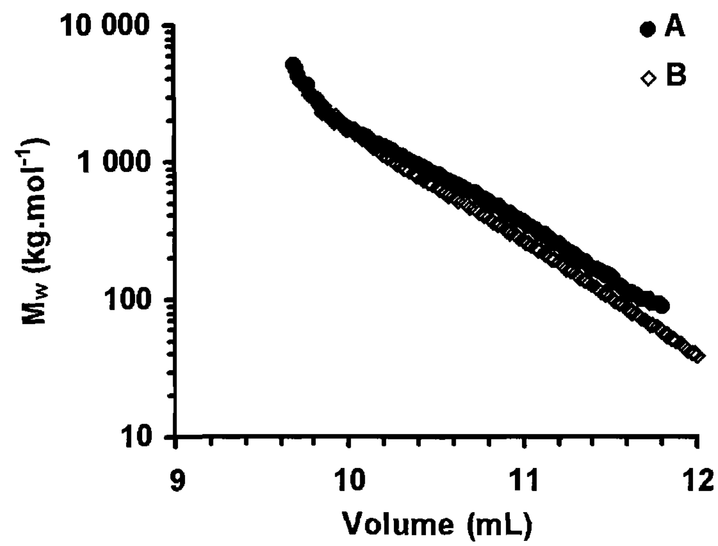

Figure 4.3: The weight distribution of P(St-*co*-EMA) samples synthesized under conditions of (A) 2% SDS, 1% BuOH, 80 °C and f_{St} of 81.4%and B)) 2% SDS, 1% BuOH, 70 °C and f_{St} of 81.4%. Secondary distributions of the dn/dc standard could not be observed at its corresponding elution volume, confirming that it did not interfere with the sample analysis.

A selection of the results that was calculated from the GPC-MALLS raw data and ATR-FTIR is listed in Table 4.2.

Table 4.2: Excerpt of the results for P(ST-co-EMA) as categorized by 2% SDS†.

Reaction conditions			Results						
%BuOH	°C	f_{St} (%)	%St	%EMA	$\square_n$	$\square_w$	$\square_w/\square_n$	$\langle s^2 \rangle^{1/2}$(nm)	q
	60	62	61±7.6	39±7.6	234.2±1.0	414.1±3.0	1.77±0.0	30.3±2.4	0.482±0.01
1	70	82	83±0.1	17±0.1	221.5±45	411.1±85	1.96±0.1	28.1±8.3	0.495±0.01
	80	72	76±1.8	39±2.5	217.2±7.0	375.9±45	1.73±0.0	31.4±6.2	0.475±0.04
	60	82	83±0.9	17±0.9	265.1±36	394.2±13	1.81±0.0	28.3±8.9	0.472±0.03
3	70	72	74±3.0	26±3.0	257.9±24	385.6±88	1.85±0.0	23.7±0.6	0.466±0.04
	80	62	61±8.9	39±8.9	247.2±47	447.3±81	1.89±0.2	29.1±8.3	0.467±0.01
	60	72	75±3.5	25±3.5	141.2±9.0	255.9±21	1.78±0.0	23.5±4.7	0.498±0.01
5	70	62	63±11	37±11	232.6±5.0	375.1±45	1.81±0.0	22.9±3.2	0.489±0.02
	80	82	82±1.7	18±1.7	96.35±17	193.2±18	1.91±0.2	15.5±5.1	0.484±0.01

†All molecular weight values are reported in $kg.mol^{-1}$

The data was collected and the factorial design analyzed with STATISTICA 7.1 (Statsoft, Inc., Tulsa, OK) followed by Pareto analysis with the same software. The Pareto principle had its origins in economical science [44] and has been applied in various recent polymer studies to determine effect probability and optimize polymerization reaction parameters.[45-47] An example of a Pareto graph of standardized factor effects on □ n for P(ST-*co*-EMA) is shown in Figure 4.4

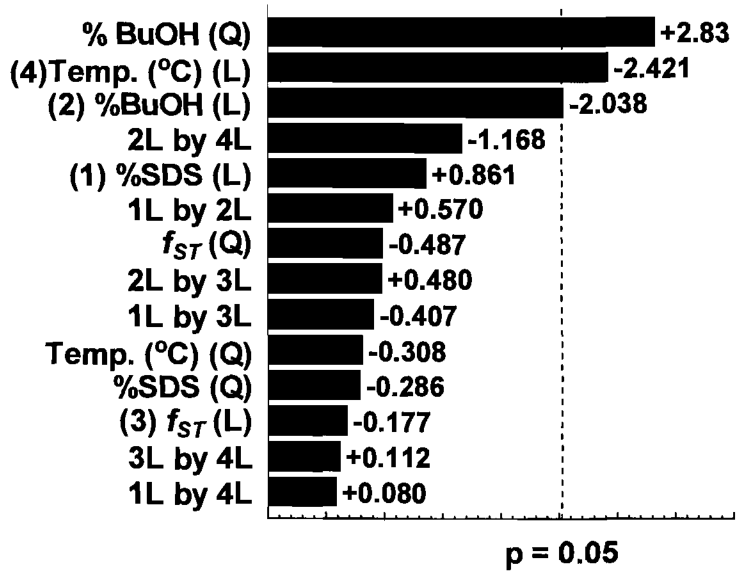

Figure 4.4: Pareto graph of standardized factor effects on □ n for P(ST-*co*-EMA). Linear effects are denoted as 'L' and the non-linear (or quadratic) as 'Q'. Interactions are denoted as, 'by'. Numbers preceding the factors were generated from the spreadsheet column number and are not intended to rank effects.

According to the Pareto analysis a quadratic (Q) effect was seen as BuOH concentration increased with a maximum turning point from the sign of the coefficient (Q, +2.83). In contrast, the effect of temperature proved to be significantly negative (-) linear (L), (L -2.421). Pareto coefficients were calculated for all responses and these are tabulated in Table 3. The Pareto analysis calculated in this experimental design stipulated that a minimum coefficient value of 2.023 should be exceeded for significance at a 95% confidence interval (Figure 4.4, Table 4.3). Additional graphs were constructed to illustrate the significant effects identified by Pareto analysis to further refine the factorial design analysis.

Table 4.3: Pareto coefficients for the full population of P(ST-*co*-MMA). For explanation of the abbreviations used in the Factor/ Interaction column see experimental section and Figure 4.4.

Factor/ Interaction†	P(ST-*co*-EMA)					
	$\square_n$	$\square_w$	$\square_w/\square_n$	$<s^2>^{1/2}$	q	%ST
(1) SDS (L)	+0.861	+0.709	-1.151	-1.012	-0.533	-0.009
SDS (Q)	-0.286	-0.347	+0.832	+0.287	-0.310	-0.629
(2) BuOH (L)	-2.038*	-2.237*	-2.361*	-2.170*	+1.454	-0.132
BuOH (Q)	+2.825*	+2.880	-0.127	+1.282	-1.423	-1.318
(3) f_{ST} (L)	-0.177	-0.326	-0.927	-0.362	+0.166	+8.053*
f_{ST} (Q)	+0.861	-0.062	+2.052*	-0.659	-0.191	+0.067
(4) Temp (L)	-2.422*	-2.269*	+2.086*	-1.871	+0.287	-0.647
Temp (Q)	-0.307	+0.050	+1.004	+0.209	-1.374	-0.191
1L by 2L	+0.570	+0.449	-1.104	+1.378	-0.196	-0.181
1L by 3L	-0.407	-0.258	+0.343	-0.668	-1.225	-1.464
1L by 4L	+0.079	-0.152	-1.904	-0.373	-0.048	-1.173
2L by 3L	+0.480	+0.355	+0.689	-0.253	-0.823	-0.063
2L by 4L	-1.168	-0.688	+1.836	-1.176	+0.866	-1.170
3L by 4L	+0.112	+0.044	-1.473	+0.016	+0.629	+0.252

*Effects are significant ($p < 0.05$) if the Pareto coefficient exceeds as value of 2.023.
†Effects not noted according to rank.

4.3.2 Molecular weight

4.3.2.1 Number average molecular weight

Pareto analysis indicated the dominance of the effect of the cosurfactant in the determination of the □ $_n$ for the set of P(ST-*co*-EMA). A quadratic response was observed for BuOH (Q, + 2.825) and the linear effect of butanol was bordering on significance (L, -2.037). The differences observed for □ $_n$ for the cosurfactant at 1% (series average of 197.5 $kg.mol^{-1}$) to 3% (series average of 228.2 $kg.mol^{-1}$) were marginal (Figure 4.5). However, a more distinct decrease in the value is seen at 5% (series average of 151.1 $kg.mol^{-1}$), resulting in the surface plot to assume a parabolic continuance.

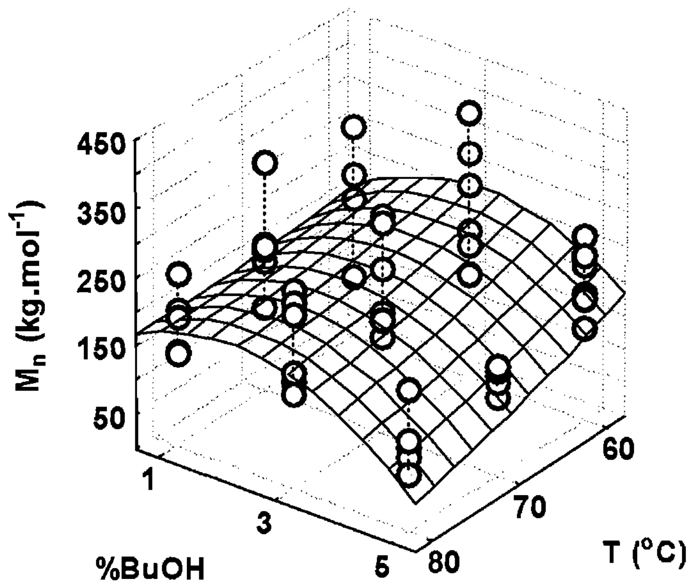

Figure 4.5: Surface plot of the effect of BuOH and temperature on the □ $_n$ of P(ST-*co*-EMA).

This change in direction of the □ $_n$ continuance was surprising, however, it was reported that alcohols could have a significant solubilization effect on the methacrylates. The chain length of the alcohol with higher solubility in the higher length alcohols and the basicity of the methacrylate (increasing as a function of ester alkyl group size) markedly influenced the solubilization of the methacrylate in the alcohol and stability of the system [48, 49]. From this one could conclude that for the low and intermediate levels, the increase in interfacial BuOH concentration would result in an increase in particle weight due to the increase in the local monomer concentration.

However, as the level increased to 5% a more significant diffusion barrier could be posed to the monomer in the interface surrounding the micellar core in addition to aggregation of micelles. This additional interfacial effect of BuOH could retain both monomers to the point where it would possibly not be available for reaction to the same extent as seen at 1% or 3%.

Temperature had a negative linear effect (L, -2.442, Table 5.3) and resulted in a decrease $\square_{n}$ as it progressed from 60 - 80 °C. The series average obtained for 60 °C was 225.6 $kg.mol^{-1}$, 194.0 $kg.mol^{-1}$ at 70 °C and 173.7 $kg.mol^{-1}$ at 80 °C ($r^2 \sim 0.98$), implying that the highest number of effective reactors were present at 80 °C and the least at 60 °C due to clustering of micelles.

A rise in temperature might surmount the clustering of reactors and could explain the decrease in number average weight as a temperature-dependent function. The effect of temperature was also more pronounced at the 5% level than at 1 and 3% indicating the likelihood that once the effect of clustering due to BuOH was overcome, a more pronounced decrease was seen than at the lower cosurfactant levels. The changes in $\square_{n}$ as function of %BuOH were still more significant than that induced by temperature and confirmed the ranking of BuOH as the most dominant factor in the observations made.

4.3.2.2 Weight average molecular weight

The effects of BuOH and temperature were in agreement as found for the trends seen in number weight and we again correlate these observations to the reactor conditions in the microemulsion. A prominent quadratic effect (Q, +2.880) was observed for BuOH, dominating the linear effect (L, – 2.269) of temperature. The average values for $\square_{w}$ were again calculated for each temperature and showed a linear decline of 403.0 $kg.mol^{-1}$ at 60 °C, 360.5 $kg.mol^{-1}$ at 70 °C and a minimum of 314.5 $kg.mol^{-1}$ at 80 °C ($r^2 = 0.9995$) (Figure 4.6).

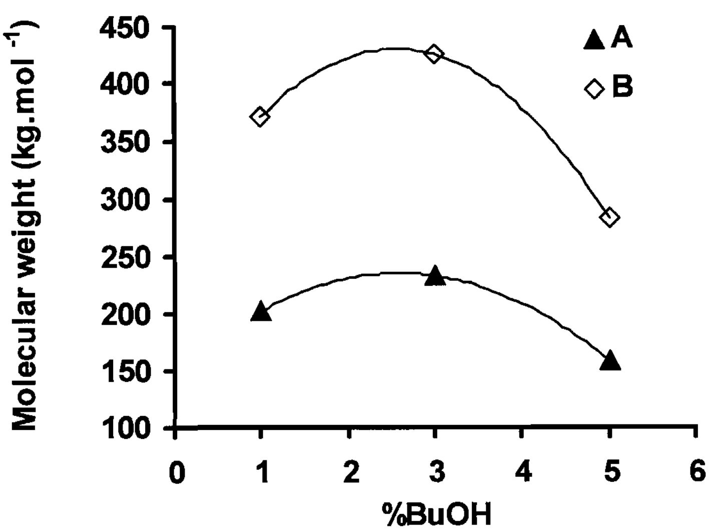

Figure 4.6: Classification of (A) □$_n$ and (B) □$_w$ of P(ST-*co*-EMA) according to cosurfactant concentration.

A higher degree of monomer retention in the cosurfactant layer could decrease the efficiency of monomer polymerization, even at a comparable micellar number (related to □$_n$) as that found at 1% BuOH and therefore the monomer assembly was significantly reduced at the 5% level of BuOH.

4.3.2.3 Polydispersity index

The P(ST-*co*-EMA) systems also demonstrated a broad dispersity index with values ranging 1.5– 2.0 for the 54 evaluated species. The change in □$_w$ closely followed the change in □$_n$ values as shown in Figure 4.6.

The Pareto distribution (Table 4.3) indicated that the ratio of St to EMA (f_{St}) demonstrated a significant non-linear effect (Q, +2.060), however, surpassed yet again by the effect of BuOH (L, -2.361).

The increase in cosurfactant level seemed to counteract the uniqueness of the micellar reactors resulting in higher polydispersity. The most probable cause could again be attributed to an increase in the interfacial concentration of BuOH that solubilized the monomers to a higher extent. Classification of the data according to temperature demonstrated the negatively linear effect of BuOH (L, -2.361) on polydispersity. The 60 °C series proved most sensitive (slope = -0.0353, $r^2 \sim 0.97$) to the increase in %BuOH and 80 °C the least sensitive (slope = -0.0037, $r^2 \sim 0.91$). The 70 °C series showed intermediate sensitivity to the %BuOH (slope = - 0.0183, r^2

= 0.9994). The effect of temperature was observed to be detrimental to polydispersity (Figure 4.7).

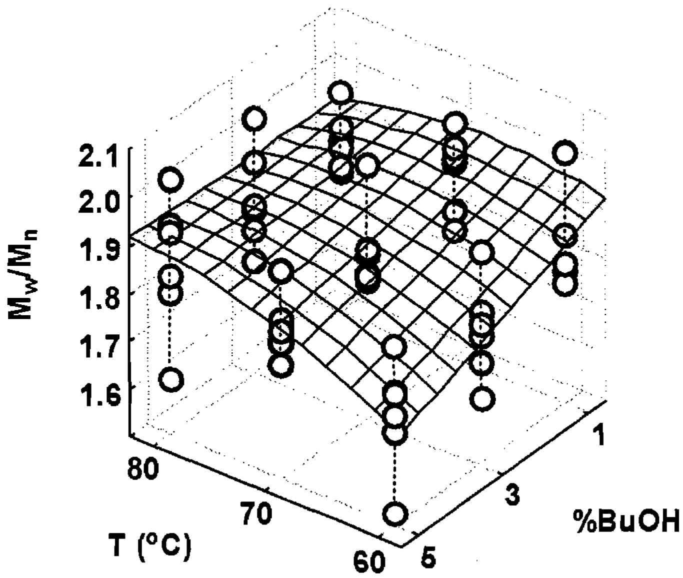

Figure 4.7: Effect of temperature and BuOH on the weight polydispersity of P(ST-*co*-EMA) copolymers.

The increase in temperature levels from 60–80 °C also increased micellar mobility and therefore increased the probability of radicals encountering each other to terminate. The 80 °C series additionally showed that micellar mobility overshadowed the advantageous effect of micellar clustering induced by BuOH as was evident from the 60 °C series. The mobility could result in a higher level of radical termination and increase polydispersity. Polydispersity remained at a high level and were virtually constant over the whole series of BuOH concentration.

The polydispersity for the 80 °C series averaged 1.87, 1.86 and 1.85 at 1, 3 and 5% BuOH respectively and contradicted the more pronounced changes observed for 60 °C. The 60 °C series averaged 1.88, 1.78 and 1.73 at 1, 3 and 5% BuOH respectively. The result at 80 °C was an increase in the amount of unique reactors that could be observed as the concurrent increase in polydispersity.

Since the polydispersity is a reflection of changes in $\square_w$ and $\square_n$ and these both showed linear increases as function of increasing temperature, the effect of temperature will be shortly discussed in this section.

In examples of copolymerizations systems between St and some acrylate derivatives, an increase in the number of radicals as a function of the increase in temperature was found [50-52]. The kinetic parameters such as polymerization rate and activation energy are affected by different temperatures. This would additionally contribute to changes in both □$_n$ and □$_w$, with rates of termination and propagation being influenced. Since these steps occur in competition one could argue from the values of □$_w$ and □$_n$ that the higher number of radicals favored termination steps at high temperatures and favored propagation at lower temperatures. This was illustrated by the Pareto coefficients for the effect of temperature and subsequently reflected in polydispersity. One should note that seen from this perspective, the effect of BuOH in terms of clustering and the effect of radical termination as influenced by temperature are indeed compensating each other to some extent, therefore explain the opposite signs of the Pareto coefficients for the effects of BuOH and temperature respectively (Table 4.3).

As noted, the ratio of the monomers had a significant non-linear effect (Q, +2.060) on polydispersity and the decrease on polydispersity is observed in Figure 4.7. At first glance one might question why an increase in St content would affect the polydispersity. However, it should be realized that the level of EMA also varied with St content in the reaction flask. At the highest level of EMA content, i.e. the lowest ratio value, polydispersity attained a minimum with a series average of 1.79 at a monomer ratio of 1.64. A maximum (1.88) was observed at the intermediate level of 2.56 and a second minimum at the highest St content of 1.84. It was argued that the increase in BuOH would result in an increase in EMA level in the interface. Consequently EMA could also contribute to the total amphiphilic effect observed and therefore result in more particles of unique character due to an increase in the number of micelles. The effect of BuOH and EMA seemed to compliment each other.

It would seem at the highest level of EMA, dispersity reached a minimum possibly also attributed to the effect of self-association due to a comparatively high level of interfacial EMA. At the intermediate level, the amphiphilic effect e.g. the oil in water dispersion effect was probably the dominant effect and resulted in higher reactor variation and number. At the highest monomer ratio, EMA was present in the lowest concentration and had no significant amphiphilic action. The overall polarity of the interface was most probably at a level where some clustering was possible due to self-association although not as pronounced as for a higher level of EMA.

We again emphasize that the effect of cosurfactant dominated the ranking of the observations and again illustrated the powerful analyses provided by the factorial design and Pareto analysis to determine the significance of experimental variables in measured properties.

Additionally, the polydispersity did not suggest chain transfer upon increases in BuOH since the polydispersity index ranged between 1.5 and 2.0 for all samples produced.

4.3.3 Radius of gyration

The immediate observation from the data was that all the synthesis products were in the nanoscale range. The particles ranged from 10-40 nm as far as $\langle s^2 \rangle^{1/2}$ was concerned. The current definition of nanoparticles defines that at least one size dimensional aspect of the material in question should be between 1-100 nm [50] and the particles here fall well within this range if the diameters were extrapolated from $\langle s^2 \rangle^{1/2}$. As seen with the molecular weight results, the increase in cosurfactant concentration from 1-3% resulted in no change in average particle size, however narrowed the distribution range by one category. A more significant decrease in the average radius of gyration, 26 to 20 nm, was seen as the concentration of BuOH increased to 5%. It could also be noted that particle size distribution became even narrower as the cosurfactant level increased from 1-5% wt (Figure 4.8).

Since the change in particle size was also related to the changes seen in the molecular weight, it could be suggested that the micellar aggregation and monomer diffusion arguments could be applied to explain the concurrent movements in particle size distribution and molar weight. The classification of particle size according to the concentration of BuOH, the sole determinant of size, is shown in Figure 4.8.

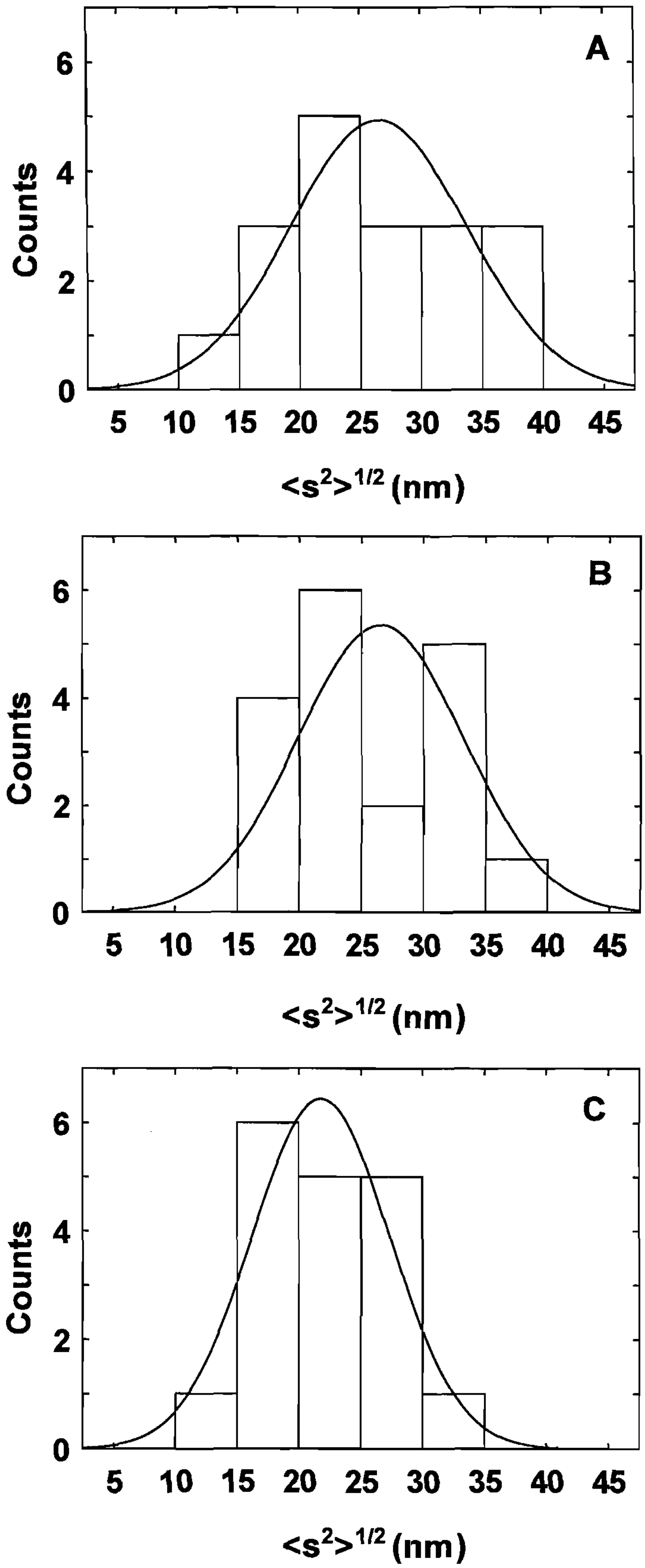

Figure 4.8: Classification of radii of gyration of P(St-*co*-EMA) according to A) 1% BuOH B) 3% BuOH and C) 5% BuOH.

Higher misciblity of nanoparticles were reported compared to their larger microscale counterparts and therefore we might be able to exploit these particles in polymeric blends that tend to phase separate [53].

4.3.4 Conformation

GPC-MALLS allows determination of the bulk chain conformation of the copolymers. The conformation of polymer chains is the result of intra and intermolecular force interactions between polymer-polymer and solvent-polymer associations. Solubility in the solvent could have a significant influence on polymer conformation with different solvent inducing compact through extended conformations of the polymers. Since the copolymers in this study all approached the maximum solubility in THF, they could not show significant extension. This is clearly evident from the values of the q exponents all of which assumed values close to the theoretically ideal value of 0.5 (Table 2 and data not shown).

Pareto analysis of copolymer conformation did not reveal statistically significant effects (Table 4.3), however could still rank the factors and magnitude of the effects. The cosurfactant again prevailed to be the most dominant factor. These observations were probably related to the effect that the interfacial cosurfactant had the most profound impact on the polymer size and weight properties during the synthesis. This is an important fact to consider when working with these materials in THF. One could manipulate film coating applications by depositing a layer of these compact nanoparticles onto a substrate if the diameter could be equated to film thickness preceding drying.

4.3.5 Composition

ATR-FTIR analysis revealed two spectral regions of interest for the analysis of the copolymers. The out-of-plane ring deformation of the phenyl ring in St was clearly observed at ~699 cm^{-1} and the stretching of the saturated ester carbonyl groups of EMA at ~1725 cm^{-1}. Several spectra were recorded and calibration curves constructed. Figure 4.9 compares typical spectra of PS, PEMA and a copolymer.

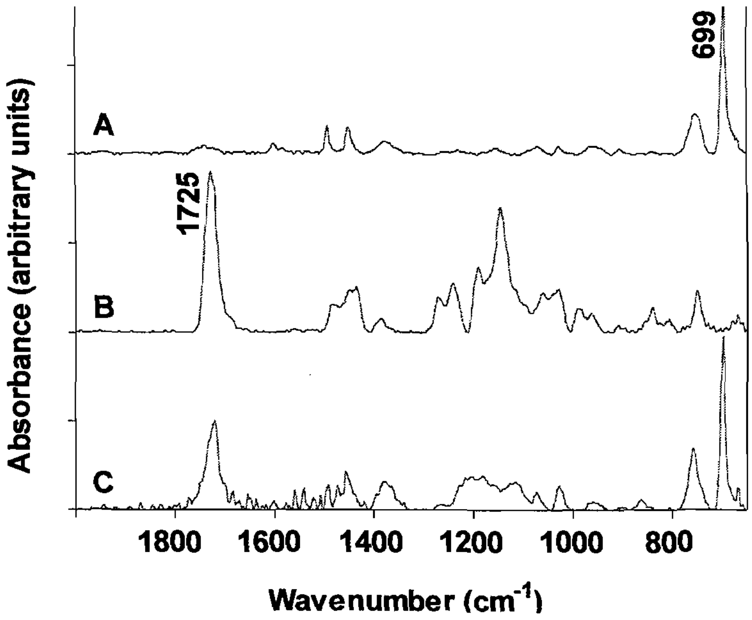

Figure 4.9: Expanded ATR-FTIR spectra of (A) phenyl ring out-of-plane bending of PS (B) saturated alkyl ester carbonyl stretch of PEMA and (C) synthesized P(St-*co*-EMA) comprising of 61% St and 39% EMA.

The standards showed strong linearity plotting absorbance ratio versus (f_{St}/f_{EMA}) with $r^2 > 0.99$ for calibration curves. Pareto analysis revealed that only the monomer feed determined the copolymer composition. The effect of feed ratio was clearly dominating (L, +8.053) and should serve as the only classifier to correlate copolymer composition (Table 4.3). Figure 4.10 illustrates the excellent correlation between the copolymer and feed compositions.

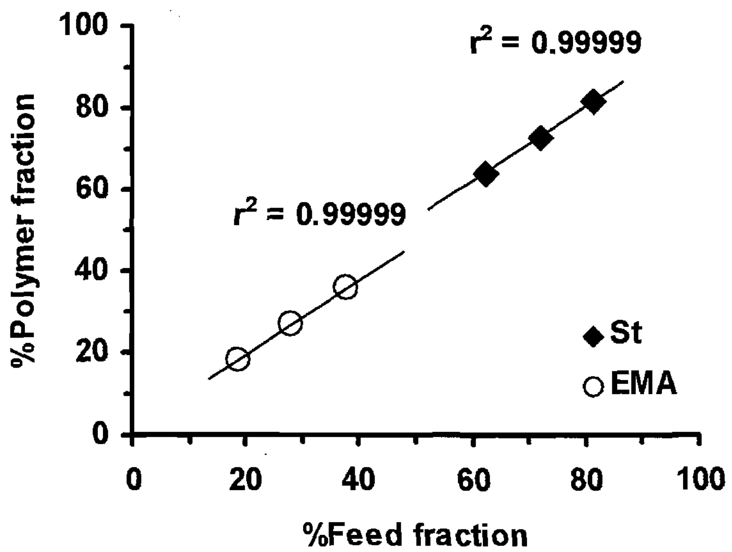

Figure 4.10: Copolymer composition as function of monomer feed composition.

These copolymers were virtually perfect templates of the feed (r^2 = 0.99999). Copolymers containing 64% St were produced from a feed containing 62% St, 73% (copolymer) from feeds of 71% and 81% (copolymer) from feeds of 81% St.

It is known that PMMA and PS are usually immiscible [54] and the copolymer could provide a means of producing composites containing sections of the desired monomers as alternative to blending. The syntheses here allowed excellent templating of the polymer composition for the feed ratio employed here.

4.4 CONCLUSIONS

Only a single study could be found in the literature in which styrene was copolymerized with ethyl methacrylate employing an emulsion polymerization, however in the absence of a cosurfactant [55]. The study showed a dependence of molecular properties on surfactant concentration and temperature. In our study the effect of the cosurfactant was evaluated was exploited in this study to synthesize copolymeric nanoparticles in an aqueous medium.

The cosurfactant, BuOH, dominated the molecular weight properties of P(St-*co*-EMA) resulting in a parabolic continuance for both number average and weight average molecular weights. It could be argued that micellar aggregation was induced by the interfacial presence of the cosurfactant, resulting in changes in the reactor number and the amount of monomer available for chain propagation. The partitioning of the EMA could be stunted by the increase in the BuOH concentration to 5% and prohibit the formation of EMA monomer radicals that would nucleate the micelles. At 1-3% BuOH the partitioning of EMA was still high enough to nucleate micelles to result in higher molecular weight particles in this concentration range.

The copolymers were prepared as nanoparticles and these particles should prove useful in future applications i.e. film coatings. The effect of the cosurfactant prevailed again as the primary determinant of particle size, complimenting the changes in molecular weights as a function of BuOH concentration.

In addition to allowing manipulation of weight and particle size, it was also demonstrated that the microemulsion copolymerizations here lent themselves to excellent compositional templating for the feed ratios employed in this study. The EMA and St probably resided in the micelle cores and therefore resulted in templating of the copolymer composition.

4.5 REFERENCES

1. Danielsson I, Lindman B (1981) Colloids Surf 3:391
2. Klier J, Tucker, CJ, Kalantar, TH, Green, DP (2000) Adv Mater (Weinheim, Ger) 12:1751
3. Zana R, Lang J (1987) Microemulsions: Structure and Dynamics CRC Press, Boca Raton, FL
4. Ganesh T, Balamururgan D, Sabesan R, Krishnan, S (2006) J Mol Lip 123:80
5. Schwuger M, Stickdorn K (1995) Chem Rev 99:10313
6. Schambil F, Schwuger M (1987) J Colloid Polym Sci 265:1009
7. Kantarci G, Karasulu HY, Ozguney I, Guneri T (2002) Acta Pharm Turcica 44:77
8. Sarciaux JM, Acar L, Sado PA (1995) Int J Pharm 120:127
9. Capek I (1991) Adv Colloid Interface Sci 80:85
10. Stoffer JO, Bone, T (1980) J Dispersion Sci Technol 1:393
11. Stoffer JO, Bone, T (1980) J Polym Sci Part A: Polym Chem 18:2641
12. Chern CS, Wu LJ (2001) J Polym Sci Part A: Polym Chem 39:3199
13. Chern CS, Liu CW (2000) Colloid Polym Sci 278:329
14. Puig JE, Corona-Galvan S, Maldonado A, Schulz PC (1990) J Colloid Interface Sci 137:308
15. Mendizabal E, Rodriguez-Ruvalcaba R, Rabelero, V, Puig JE, Velazquez R, Castano, V (1995) Int J Polym Mater 30:167
16. Capek I, Juranicova V (1996) J Polym Sci Part A: Polym Chem 34:575
17. Santhanalakshmi J, Anandhi, K (1996) Colloids Surf A 108:191
18. John AC, Rakshit AK (1995) Colloids Surf A 95:201
19. Khadir A, Roux-Desgranges G, Roux AH (1997) Thermochim Acta 292:59
20. Abuin E, Lissi E, Olivares K (2004) J Colloid Interface Sci 276:208
21. Pokhriyal NK, Devi S (2000) Eur Polym J 36:333

22. Alany RG, Rades T, Agatonivic-Kustrin S, Davies NM, Tucker IG (2000) Int J Pharm 196:141

23. Sarma S, Bora M, Dutta RK (2005) Colloids Surf A 256:105

24. Rubio DAR, Zanette D, Nome F, Bunton CA (1994) Langmuir 10:1151

25. Tomšic M, Bešster-Rogač M, Jamnik A, Kunz W, Touraud D, Bergmann A, Glatter O (2006) J Colloid Interface Sci 294:194

26. Attwood D, Terreros A, Lopez-Cabarcos E, Gallera-Gomez E (2000) J Colloid Interface Sci 225:25

27. Gómez-Cisnernos M, Treviño ME, Peralta RD, Rabelero M, Medizábal E, Puig JE, Cesteros C, López RG (2005) Polymer 46:2900

28. Shi Y, Wu Y, Hao J, Li G (2005) Colloids Surf A 262:191

29. Puig JE, Mendizábal E, Delgado S, Arellano J, López-Serrano, F (2003) CR Chim 6:1267

30. Nguyen CA, Konan-Kouakou YN, Allémann E, Doelker E, Quintanar-Guerrero D, Fessi H, Gurny R (2006) AAPS PharmSciTech 7:Article 3

31. Yan F Texter J (2006) Soft Matter 2:109.

32. Tauer K, Ramírez AG, López RG (2003) CR Chim 6:1245

33. Hofe T, Koenigsmann H (2003) GIT Labor-Fachzeitschrift 47:380

34. Kendrick B, Kerwin BA, Chang BS, Philo JS (2001) Anal Biochem 299:136

35. Mhatre R, Krull IS (1993) Anal Chem 65:283

36. Liu Y, Bo S, Zhu Y, Zhang W (2003) Polymer 44:7209

37. De Gennes PG (1979) Scaling concepts in polymer physics Cornell Univ Press New York 324p

38. Jovin TM, Morris SJ Striker G Schultens HA Digweed M Arndt-Jovin D (1976) J Histochem Cytochem 24:269

39. Clasen C Kulicke WM (2001) Prog Polym Sci 26:1839

40. Masson JF, Pelletier L, Collins P (2001) J Appl Polym Sci 79:1034

41. Prasad A (1998) Polym Eng Sci 38:1716

42. Qin D (2001) Appl Spectrosc 2001 55:871

43. Karami A Balke ST Schunk TC (2001) J Chromatogr A 911:27

44. Pareto V (1897) J Political Economy 5:485

45. Deb K, Mitra K Dewri R, Majumdar S (2004) Chem Eng Sci 59:4261

46. Massebeuf S, Fonteix C, Hoppe S, Pla F (2003) J Appl Polym Sci 87:2383

47. Moshinsky L Figovsky OL (1999) Scientific Israel - Technol Adv 1:28

48. Hofe T, Koenigsmann H (2003) GIT Labor-Fachzeitschrift 47:380

49. Kendrick B, Kerwin BA,Chang BS, Philo JS (2001) Anal Biochem 299:136

50. Ahmad H, Islam AHMT, Hossain MA, Miah MAJ Tauer K (2006) e-Polymers 30:1

51. Sanghvi PG, Pokhriyal NK, Devi S (2002) Polym Int 51:721

52. Sanghvi PG, Pokhriyal NK, Hassan PA, Devi S (2000) Polym Int 49:1417

53. National Nanotechnology Institute. What is nanotechnology? [http://www.nano.gov/html/facts/whatIsNano.html]. Accessed: 06.06.2007

54. Raczkowska J, Montenegro R, Budkowski A, Landfester K, Bernasik A, Rysz J, Czuba P (2007) Langmuir 23:7235

55. Rosa CS, FN Sandra (1995) Bol Soc Chil Quím 40:141

CHAPTER 5 WAS SUBMITTED TO

JOURNAL OF CONTROLLED RELEASE

Official journal of the Controlled Release Society, and of the Japanese Society of Drug Delivery Systems

5. GUIDE FOR AUTHORS

1. Scope of the journal

The journal publishes papers innovative, original research involving the controlled release and delivery of drugs and other biologically active agents. The terms "controlled release" and "delivery" are used in their broadest sense to include mechanisms such as diffusion, chemical and enzymatic reactions, dissolution, osmosis, targeting, as well as the utilization and manipulation of biological processes. A broad spectrum of studies dealing with all aspects of controlled release and delivery, including gene delivery, tissue engineering and diagnostic agents, is encouraged. The use of prodrugs and carriers such as water-soluble polymers, micro and nanoparticles, liposomes and micelles is included in the scope.

Papers that provide no new concepts or mechanistic insights will not be considered. The Letter of Submission should explain in one paragraph the originality and significance of the submitted work. The manuscript will not be processed without this information.

2. Preparation of manuscripts

Manuscript Types

Full length papers are recommended not to exceed a total of 20 double-spaced, font size 12, typewritten pages, excluding references, tables, figure legends, and figures, and should include Title, Abstract, Methods and Materials, Results, Discussion, Conclusions, Acknowledgments and References (see below). It is also recommended that the total number of tables and figures does not exceed 8. Rapid Communications are preliminary reports of research that are of sufficient importance and general interest that accelerated publication is justified. The length is limited to 1000 words. Notes are shorter manuscripts, limited to 1500 words, that describe studies of general interest and significance, but which may be limited in scope.

General procedures

The language of the Journal is English. Manuscripts must be written in the third person and, when possible, in the past tense. The authors should ensure that they have written entirely original works, and if the authors have used the work and/or words of others, this has been appropriately cited or quoted.An author should not in general publish manuscripts describing essentially the same research in more than one journal of primary publication. Plagiarism in all its forms as well as submission of the same manuscript to more than one journal concurrently constitutes unethical publishing behaviour and are unacceptable.Thus, the Letter of Submission should explain in one paragraph the originality and significance of the submitted work. The manuscript will not be processed without this information.

The following format and order of presentation is suggested:

Title, author(s), address(es). The title should be no longer than 100 letters and spaces. The address should include the country mailing or *Zip* code when available, as well as the telephone and fax numbers, and e-mail address. Indicate to whom correspondence and proofs should be sent.

Abstract. The abstract should present a summary of the problem, scientific method, major findings and conclusions, in no more than 200 words and one paragraph. Unsubstantiated speculation should not be included. Footnotes may not be used. References, if cited, must provide complete publication data.

Keywords (5)

Introduction. The purpose of this section is not to review the literature, but to briefly introduce the objective of the research and its significance.

Materials and methods. Procedures should be described in sufficient detail to permit others to repeat and reproduce the results of the work. Sources of commercial products need not be listed unless unique. Published methods need not be restated but must be referenced. Where the reference is to papers under review or in press, copies should be provided to the Editor to facilitate review. Full chemical names of drugs/polymers/exipients, etc. should be given. Trade names should not be used. Appropriate statistical analysis of data should be provided.

The Declarations of Helsinki and Tokyo for humans, and the European Community guidelines as accepted principles for the use of experimental animals, must be adhered to. Therefore, the Journal of Controlled Release will only consider manuscripts that describe experiments that have been carried out under approval of an institutional or local ethics committee. Authors must state in the manuscript that the protocol complies with the particular recommendation and that approval of their protocols was obtained.

Full chemical names of drugs/polymers/exipients, etc. should be given. Trade names should not be used. Appropriate statistical analysis of data should be provided.

Results. Tables and Figures that summarize the results and improve their comprehension are encouraged, but only if the space required is not excessive and less than can be stated in the text. The reproducibility and statistical significance of measurements, material or biological, must be included when relevant.

Discussion. This section should deal with the interpretation of the results and their significance to the field of study. Repetition of information presented in other sections should be avoided, as should general reviews of the literature. In some cases it may be advantageous to combine the Results and Discussion sections.

Conclusion (optional). A short, one paragraph summary of the most important finding(s) of the research.

Acknowledgment (if any). Recognition of financial support, technical assistance and advice.

References. Responsibility for the accuracy of bibliographic citations lies entirely with authors. Number consecutively throughout the text and supply a separate Reference List. Abbreviate according to the 'Bibliographic Guide for Editors and Authors', 1974 (Chemical Abstracts Service, The Ohio State University, Columbus, OH 43210) and the 'List of Serial Title Word Abbreviations', 1985, ISDS, 20 rue Bachaumont, 75002 Paris, France; ISBN 2-904938-02-8. Examples:

Journal:

[1] E. Porges, B. Schade, W. Ropte, Automated flow-through method to determine the dissolution rate of slightly soluble substances, Pharm. Ind. 47(1) (1985) 77-86.

Book:

[2] A.R. Gennaro, Remington's Pharmaceutical Sciences, XXII, Mack Publishing Company, Easton, PA, 1990.

Book Chapter:

[3] S.L. Ali, Nifedipine, in: K. Florey (Ed.), Analytical Profiles of Drug Substances, Vol. 18, Academic Press, New York, 1989, pp. 221-288.

Patent:

[4] J.B. Phipps, D.F. Untereker, Iontophoresis apparatus and methods of producing same, U.S. Patent 4, 744, 787, May 17, 1988.

Report:

[5] N.F. Cardarelli, K.E. Walker, G. Zweig, Development of registration criteria for controlled release pesticide formulations, U.S. Environmental Protection Agency, Washington, DC 20460, EPA-504/9077-916, January 1978.

Articles in Special Issues: Please ensure that the words 'this issue' are added (in the list and text) to any references to other articles in this Special Issue.

Use of Digital Object Identifier (DOI):
The digital object identifier (DOI) may be used to cite and link to electronic documents. The DOI consists of a unique alpha-numeric character string which is assigned to a document by the publisher upon the initial electronic publication. The assigned DOI never changes. Therefore, it is an ideal medium for citing a document particularly "Articles in press" because they have not yet received their full bibliographic information.

The correct format for citing a DOI is shown as follows: doi:10.1016/j.conrel.2004.11.016

Tables. Number consecutively and type on a numbered, separate page. Please use arabic numerals and supply a heading. Column headings should be explanatory and carry units.

Figures. Number consecutively with Arabic numerals. Figures should be used to illustrate experimental results clearly. Authors are requested to submit figures for a one-column width where possible and ensure that symbols, lettering and lines are sufficiently large and clear to be legible. Figure width is approximately 3 inches or 7.5 cm. Legends for each figure should be typed on a separate page.

Colour illustrations should be submitted as original photographs, high-quality computer prints or transparencies, close to the size expected in publication, or as 35 mm slides. Polaroid colour prints are not suitable. If, together with your accepted article, you submit usable colour figures then Elsevier will ensure, at no additional charge, that these figures will appear in colour on the web (e.g., ScienceDirect and other sites) regardless of whether or not these illustrations are reproduced in colour in the printed version. For colour reproduction in print, you will receive information regarding the total cost from Elsevier after receipt of your accepted article. The 2006 price for colour figures is 285 Euro for the first page and 191 Euro for subsequent pages.

For more detailed instructions please visit our artwork instruction pages at http://www.elsevier.com/artworkinstructions.

Please note: Because of technical complications which can arise by converting colour figures to 'grey scale' (for the printed version should you not opt for colour in print) please submit in addition usable black and white prints corresponding to all the colour illustrations.

Units and abbreviation. SI units should be used: English units or other equivalents should be given in parentheses if necessary. On graphs, if values are recorded in non-SI units, then additional scales in SI units should be used. If a large number of symbols are used, it is helpful if authors submit a list of these symbols and their meanings.

3. Submission

Authors should submit their manuscripts electronically by using the Elsevier submission site at http://www.elsevier.com/locate/jconrel

After registration, authors will be asked to upload their manuscript and associated artwork. Full instructions on how to use the online submission tool are available at the web address listed above.

REMARK:

The manuscript was formatted for uniformity of the thesis; however, the reference citation style was preserved.

CHAPTER 5

DEVELOPMENT OF MICROPOROUS DRUG-RELEASING FILMS CAST FROM ARTIFICIAL NANOSIZED LATEXES OF POLY(STYRENE-*CO*-METHYL METHACRYLATE) OR POLY(STYRENE-*CO*-ETHYL METHACRYLATE)

Daniel P. Otto[1,2], Hermanus C.M. Vosloo[3], Wilna Liebenberg[2] and Melgardt M. de Villiers[1]

1 School of Pharmacy, University of Wisconsin – Madison, WI 53705, USA
2 Unit for Drug Research, Faculty of Health Sciences, North-West University, Potchefstroom, 2520, South Africa
3 School of Chemistry, North-West University, Potchefstroom, 2520, South Africa

Corresponding author: Daniel P. Otto, School of Pharmacy, University of Wisconsin-Madison, WI 53705, USA. E-mail: dotto@wisc.edu Telephone: 1-608-262-9351.

Abstract

Two sets of copolymers comprising of styrene and either methyl or ethyl methacrylate as comonomer were conveniently synthesized by microemulsion copolymerization. The purified materials were characterized by GPC-MALLS and were shown to form artificial nanolatexes in THF. ATR-FTIR analysis revealed differences in copolymer composition and based on the copolymer properties, a selection of copolymers was chosen to cast drug-loaded, microporous films that exhibit microencapsulation of drug agglomerates. The contact angles of the copolymers suggested potential applications in medical devices to prevent the formation of bacterial biofilms that commonly result in infections. Additionally, the different copolymeric films showed two phases of drug release characterized by a rapid initial drug release followed by a zero-order phase. Depending on the application, one could select the copolymer films that best suited the application i.e. for short-term drug release applications such as urinary catheters or long-term applications such as artificial implants.

5.1 INTRODUCTION

Several studies have reported the introduction of infections in patients which received polymer-based medical devices i.e. orthopedic surgical implants [1], urinary catheters [2], cardiovascular stents [3] and ventilator-associated pneumonia with use of endotracheal tubes [4]. The procedures associated with the use of these devices are invasive and compromise natural barriers of the body that protect it from infection [5].

In the event of bacterial accumulation, a so-called biofilm is created on a surface i.e. a polymer film or coating. This biofilm is often a very resistant and physically strong structure comprising of several stacked layers of microorganisms [6]. Once the biofilm has been established the onset of an infection could be observed. Therefore, the development of strategies to curb infections associated with the use of polymeric devices is warranted if the devices should actually benefit, not compromise, the health of patients [7,8].

Circumvention of biofilm formation could entail a number of approaches. Some techniques modify the surface chemistry of the polymer film to hinder bacterial attachment by methods such as thioncyanation since thiol groups could be microbiocidal [9]. Other methods employed loading the polymer device with an antimicrobial agents i.e. rifampin, fusidic acid and mupirocin combinations [10], rifampin and minocycline [11], gentamicin [12,13], vancomycin [14] and ciprofloxacin [15] that release low quantities of the drugs over prolonged periods that effectively eradicate the biofilm.

Several tests could be conducted to establish the surface properties and the contact angle of the polymer film could serve as a first, although not absolute, indicator of the potential adhesion properties of bacteria onto film surfaces. Bacteria usually adhere to polymer substrates of similar hydrophobicity or hydrophobicity [16,17].

A convenient way to produce a polymer film is by solvent casting of a pseudolatex or artificial latex [18] produced from a characterized material. The production of a film from a pseudolatex is advantageous since unwanted monomer and other materials or remnants from polymerization reactions could be removed from the material before it is used [19].

At the molecular level, it is very difficult to truly blend polymer materials and one of the classic examples of phase separation occurs in blends of poly(methyl methacrylate) (PMMA) and poly(styrene) (PS) [20,21]. Despite the incompatibility of PS and PMMA, it might be advantageous to incorporate different polymers comprised of methacrylate and styrene units to modify an application.

A method to produce a true blend of different monomers (and therefore avoid phase separation) is by copolymerization of the desired monomers. It was shown that the phase separation observed for blends of PS and PMMA was not observed for a copolymer of styrene and methyl methacrylate [22]. Furthermore, copolymers consisting of monomers corresponding to those found in immiscible homopolymers could act as compatibilizers to augment miscibility [23]. Microemulsion copolymerization lends itself to the production of nanoscale random copolymer latexes which could be purified to produce a final copolymeric material comprising of the desired chemical composition [24].

Several random copolymers are available that incorporate methacrylic monomers. Typical examples of random methacrylic copolymers in the pharmaceutical industry are marketed as Eudragit® that was applied in various film coatings for numerous purposes including. taste-masking and controlled release of drugs [25].

Some applications could be found for poly(styrene-*co*-methyl methacrylate) (P(St-*co*-MMA)) as bone cement i.e. Endurance® cement [26]. However, no pharmaceutical application could be found for poly(styrene-*co*-ethyl methacrylate) (P(St-*co*-EMA)) copolymers. Subsequently, P(St-*co*-EMA) and P(St-*co*-MMA) copolymers were synthesized, characterized and evaluated for potential pharmaceutical applications.

5.2 EXPERIMENTAL SECTION

5.2.1 Materials

Rifampin (RIF) was purchased from Youhan Corp. (Seoul, Korea). The homopolymers used in this study PMMA, poly(ethyl methacrylate) (PEMA) and PS (Scientific Polymer Products, Inc., Ontario, NY). Copolymers comprising of styrene (St) and either methyl (MMA) or ethyl methacrylate (EMA) were synthesized by microemulsion copolymerization. Tetrahydrofuran (THF) (Fisher Scientific, Pittsburgh, PA) was used as solvent for all the polymers and RIF.

5.2.2 Copolymerization procedure

The microemulsion copolymerization was conducted according to a 3-level-4-factor fractional factorial design applying some formulation guidelines provided in literature [27]. Briefly the reactions employed double deionized water (qs 100% wt.) (Milli-Q®, Microsep, Sandton, South Africa) as dispersion medium with ultrapure sodium dodecyl sulfate (SDS) (Sigma-

Aldrich, Kempton Park, South Africa) as surfactant (2-8% wt.). The cosurfactant, 1-butanol (BuOH) (Merck, Modderfontein, South Africa) was incorporated in all reaction mixtures at levels between 1-5% wt. Potassium persulfate (KPS) (Sigma-Aldrich, Kempton Park, South Africa) was used as the reaction initiator at 0.5% wt. for all reactions. A mixture of 60-80% of styrene (St) (Merck, Modderfontein, South Africa) and 20-40% either methyl methacrylate (MMA) or ethyl methacrylate (EMA) (donated by Degussa, Düsseldorf, Germany) were added to the reaction medium. These monomer mixtures constituted 6% wt. of the total reaction mixture and were copolymerized for 2 h. The reactions were performed at a specified temperature between 60-80 °C. All reactions were performed with magnetic stirring at 500 r.p.m. under continuous N_2 purge. An excess of hydroquinone (Sigma-Aldrich, Kempton Park, South Africa) was added to quench the reaction after 2 h.

The copolymer latexes were a translucent blue color, indicating the existence of very fine colloidal particles. The latex was precipitated with copious quantities of methanol (MeOH) (Merck, Modderfontein, South Africa). The mixtures were vortex-shaken (Vortex Genie 2®, Daigger®, A. Daigger & Company, Vernon Hill, IL) and centrifuged in 50 cm^3 tubes at 3500 r.p.m for 10 min. The sediments were subsequently redispersed and washed with MeOH followed by centrifugation until no redispersion could be effected by addition of MeOH.

Susequently, the copolymers were dried in a fume hood until only brittle material remained. These white products were finely pulverized and then dried for an additional 24 h under a vacuum of 13 mbar. The powders were then sealed in opaque, airtight containers until further use.

5.3 COPOLYMER CHARACTERIZATION

5.3.1 GPC-MALLS

GPC-MALLS was utilized to characterize the absolute molecular weight and particle size of the polymer samples. A DAWN® DSP laser photometer (Wyatt Corporation, Santa Barbara, CA) in and a refractive index detector (Agilent® 1100 series) were used as detectors. Briefly, 100 μL of 3 mg/mL polymer samples dissolved in THF were injected into the GPC columns (PLGel® mixed bed type C™, 7.6 × 300 mm, exclusion range 300 – 2 000 000 $g.mol^{-1}$, particle size of 5 μm and a Phenogel™ Phenomenex®, 7.8 × 300 mm, exclusion range > 5 000 $g.mol^{-1}$, particle size of 5 μm, Separations Scientific CC, Honeydew, South Africa) with THF as mobile phase. The weighted molecular weight and radii of gyration averages (Equation 5.1-2) as well as conformation of the copolymer chains were calculated from the scattering data (Equation

5.3) (ASTRA™ 4.73, Wyatt Corp.) according to the Zimm formalism employing all MALLS scattering angles between 17-155° [28]:

$$\frac{R_{\Theta}}{Kc} = MP(\Theta) - 2A_2cM^2P^2(\Theta) + \ldots \tag{5.1}$$

where M is the molecular weight of a slice of the sample chromatogram, R_{Θ} is the excess Rayleigh ratio at the scattering angle Θ. Additionally, the wavelength and scattering angle-dependent particle scattering factor is represented by $P(\Theta)$. Furthermore, the concentration of the particles is denoted as c (determined with the refractive index detector) and A_2 is the second virial coefficient which becomes negligible at low concentrations as employed here). The constant K was derived by employing Equation (2):

$$K = \frac{4\pi^2 n_0^2}{\lambda_0^4 N_A}\left(\frac{dn}{dc}\right)^2 \tag{5.2}$$

where the refractive index of the solvent in vacuum is n_0 at the incident wavelength of the vertically polarized laser radiation, λ_0, the Avogadro number is N_A and the specific refractive increment of the polymer is dn/dc.

Evaluation of the linear segment of the data if plotted as a double-logarithmic plot and fitted to a power law regression according to Equation (3):

$$\left\langle s^2 \right\rangle^{1/2} \propto M_w^q \tag{5.3}$$

where the z-average root mean square $\langle s^2 \rangle^{1/2}$ radius was related to the weight average molecular weight M_w.

5.3.2 ATR-FTIR

The composition of the copolymer particles was determined with attenuated total reflectance Fourier transform infrared spectroscopy (ATR-FTIR). The ATR-FTIR (Bruker, Ettlingen, Germany) comprised of a ZnSe crystal and a microsample accessory. Sufficient quantities of the samples were transferred to the crystal sample accessory and clamped onto the crystal. 32 spectra were collected at a spectral resolution of 4 cm^{-1} for each sample. Wave numbers could be assigned for quantitative analysis i.e. the out-of-plane bending of the phenyl ring in styrene units at ~699 cm^{-1} and the saturated alkyl ester carbonyl of the methacrylates at ~1729 cm^{-1} [29]. Monodiperse, low weight standards of PMMA and PS (Fluka, St. Louis, MO) were prepared to contain various mole fractions of St and either MMA and EMA.

5.3.3 Film casting

Following the synthesis of the copolymers, analysis of the polymers by GPC-MALLS and ATR-FTIR revealed suitable candidates for application in film casting. Pseudolatexes of the homopolymers and copolymers were prepared in THF (5% w/v) by sonication, allowing a 12 h swelling period. RIF was dissolved in THF (5% w/v) before film casting. The requisite quantities of the synthesized copolymer or homopolymer and drug solution were mixed to produce mixtures of 20% drug/80% polymer.

These solutions were cast onto previously cleansed, weighed glass surfaces and left to slowly dry under ambient conditions at 23 °C for 12 h followed by additional drying in a vacuum oven at 40 °C for 12 h (to obtain constant weights). The complete film cast with glass surface was weighed to determine the weight of the film. Strips measuring 6 × 2.5 cm were cut and weighed. The theoretical amount of drug in the strip was calculated. Film strips were stored in a desiccator preceding additional evaluations of the films.

5.4 FILM CHARACTERIZATION

5.4.1 Scanning electron microscopy

Scanning electron microscopy (SEM) studies were performed on film samples taken before and after release studies. These samples were affixed on carbon-taped stubs and thinly coated with Au/Pd in an Argon-filled bell jar under vacuum of ~130 Torr. A Hitachi S570 was used to photograph the samples employing Gatan DigitalMicrograph™ imaging software (Gatan, Inc., Warrendale, PA). All micrographs were recorded with a crystal emission of 10 keV.

Additional SEM micrograph analysis was conducted with automated image analysis routines utilizing ImageJ 1.38x imaging analysis software [30].

5.4.2 Contact angle

Contact angle measurements were made by carefully depositing a drop of 10 μL of deionized water or release medium on various spin-coated films of the (co)polymers or (co)polymer/drug solutions. The droplet was photographed via a remote-controlled digital camera (Canon USA, Inc., Lake Success, NY) that was interfaced with a computer. The obtained images were analyzed with ImageJ 1.38x to measure the contact angle [31,32].

5.4.3 Release studies

Drug release from the films was evaluated in triplicate according to the USP apparatus II basket rotation method utilizing a VanKel VK 7000 dissolution tester (VanKel Technology Group, NJ) adjusting the rotational speed to 50 r.p.m. 500 cm3 phosphate buffer [33] pH 7.40 served as the release medium and was maintained at 37±0.5 °C. Samples (5 cm^3) were collected at predetermined intervals over a 24 h period through 0.45 μm MCE membrane syringe filters (Fisher Scientific, Pittsburgh, PA)) and release vessels were immediately replenished with 5 cm3 fresh buffer. Sample were analyzed by UV spectrophotometry at a wavelength of 333 nm [34, 35] with a Beckman DU® 640 UV/Vis spectrophotometer (Fullerton, CA). Linear calibration curves could be constructed in the range 0.5-40 μg/mL RIF ($r^2 > 0.9999$) using the release medium as solvent and blank. Different release kinetics models were used to investigate the release mechanism of the drug from the films:

The Peppas-model [36,37]:

$$\frac{M_t}{M_\infty} = Kt^n \tag{5.4}$$

where M_t is the amount of drug released at time t, and M_∞ is the amount of drug that is released after infinite time-lapse, therefore approaches the maximum potential release. K is a constant and n is the exponent characterizing the release process. If typical Fickian diffusion was observed, n would assume values of 0.5, 0.45 and 0.43 for thin films, cylinders and spheres respectively. This equation should be used carefully as with all other power law descriptions to model release up to the fraction $M_t/M_\infty < 0.6$

Higuchi-model [38, 39]:

$$M_t = A[D(2C_0 - C_s)C_s]^{1/2} \tag{5.5}$$

where M_t is the amount of drug release until time t, A defines the release area, D is the drug diffusion coefficient, C_0 is the initial concentration of the drug in the delivery system and C_s denotes the solubility of the drug.

A zero-order release kinetics model could also be applied in the secondary release phase [40,41]:

$$C_t = C_0 - k_0 t \tag{5.6}$$

where C_t is the concentration of the drug that is released at time t, C_0 is the initial concentration of the drug incorporated in the delivery device, k_0 is the zero-order release constant that describes the constant release rate for any time point in a zero-order release phase.

5.5 RESULTS AND DISCUSSION

5.5.1 Copolymers

5.5.1.1 Copolymer molecular weight, radius of gyration and conformation

Two replicates of 27 copolymers were synthesized for each monomer pair and analyzed to determine their molecular weight, polydispersity, radius of gyration, conformation and chemical composition. Statistical analysis of the factorial design revealed that the cosurfactant dominated the molecular weight properties as well as determined the size of the polymer chains.

The effect of the cosurfactant on □ $_w$ (Figure 5.1) was clearly not similar for both series of copolymers. A linear increase in polymer weight of P(St-*co*-MMA) was seen with weight ranging from 250-700 kg.mol^{-1} as the concentration of BuOH increased. The P(St-co-EMA) series demonstrated weights ranging 150-600 kg.mol^{-1}.

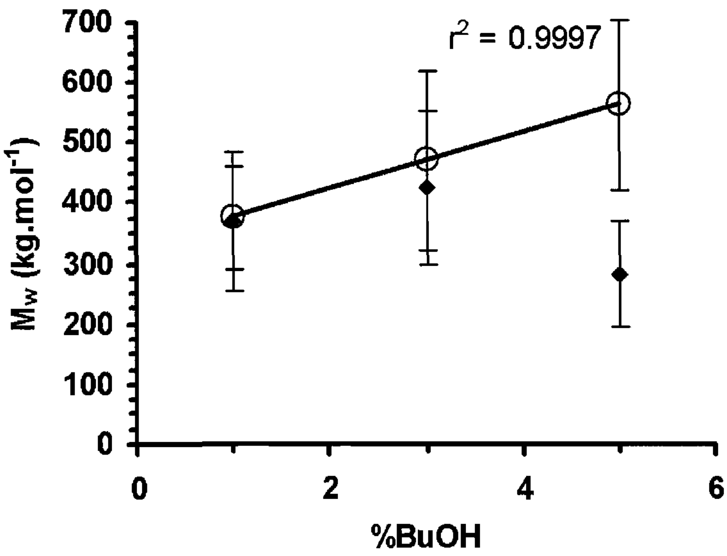

Figure 5.1: The effect of the cosurfactant on $\bar{M}_w$ of (○) P(St-*co*-MMA) and (◆) P(St-*co*-EMA) copolymers.

At the highest concentration of BuOH, P(St-*co*-EMA) copolymers had the lowest weight and this was the only point where significant differences in weight was seen, although the P(St-*co*-EMA) polymers were comparatively lighter than the P(St-*co*-MMA) produced under the same conditions.

The effect of BuOH on $\langle s^2\rangle^{1/2}$ (Figure 5.2) paralleled the effect on $\bar{M}_w$ as can be seen from the linear in crease in $\langle s^2\rangle^{1/2}$ for P(St-*co*-MMA) versus the parabolic continuance for P(St-*co*-EMA). All the copolymer particles illustrated sub 50 nm values for $\langle s^2\rangle^{1/2}$ with P(St-*co*-EMA) ranging between 20-26 nm and P(St-*co*-MMA) between 25-37 nm.

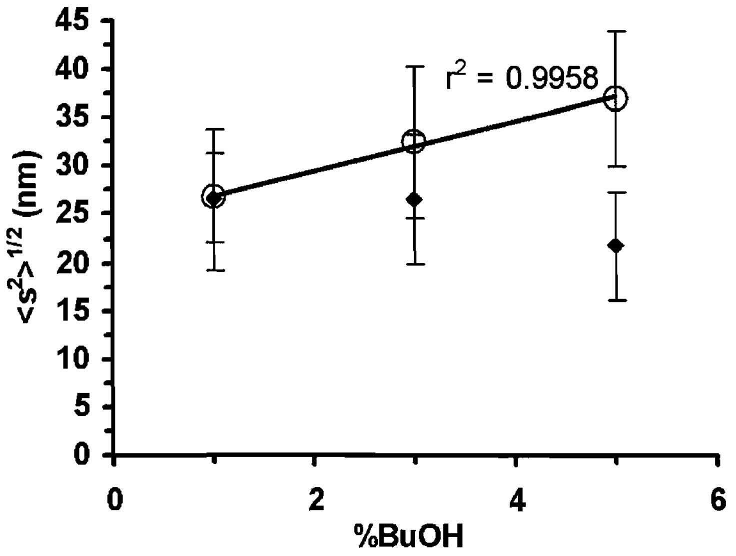

Figure 5.2: The effect of the cosurfactant on $<s^2>^{1/2}$ of (O) P(St-*co*-MMA) and (♦) P(St-*co*-EMA) copolymers.

Based on the HLB value of 7.0 for BuOH [42] one could envision that micelles clustered together during the polymerization since BuOH would reside in the surfactant alkyl tail in the interface of the micellar reactors. The local concentration of the monomers would therefore increase as BuOH concentration increased and P(St-*co*-MMA) molecular weights increased. At the highest concentration of BuOH, the partitioning of EMA (more hydrophilic than St) to the interface is limited. Subsequently, a decrease in monomer oligomer radicals formed in the interface, reducing radical entry into the monomer swollen micelles (reaction locus) that could nucleate the micelles [43].

The conformational analysis (Figure 5.3) was performed to determine the suitability of the solvent, THF, to disperse the polymer chains. The conformation was determined with consideration of the limitation of MALLS detection of small particles below ~20 nm [44-46]. The polymers predominantly illustrated conformation values of $q \approx 0.4$ -0.5. The samples indicating a q value of ~0.5 were selected, since these illustrated the ideal θ conformation.

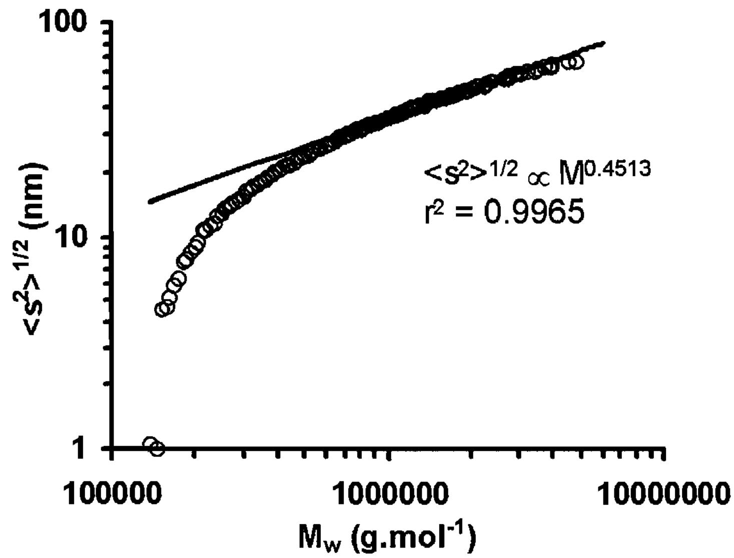

Figure 5.3: Conformation plot of P(St-*co*-MMA) comprising of 37% MMA and 86% St. The power law regression was performed by negating the uncertainties for particles under 20 nm.

The θ condition for a polymer chain dispersed in a solvent is found at a specific temperature (in this case ambient temperature) and could be compared to the state at which a sample would start to melt [47]. This indicated that both the intra- and intermolecular attractive forces were in equilibrium and that polymer chains could interpenetrate each other freely with no nett interaction [48].

Therefore optimal copolymer dispersion would occur in THF if copolymers were chosen that illustrated conformations close to the θ condition, facilitating the mixture with a drug solution in THF. Not surprisingly, these copolymers were found in the lower weight range of both sets.

Studies found that melting of RIF resulted in decomposition of the drug [34,35,49]. Furthermore, the copolymers melt at temperatures higher than the melting point of RIF, precluding the melting method for producing films. Subsequently THF solutions of the selected copolymers and RIF could be utilized for solvent casting of films. Additionally, THF is a volatile, pharmaceutically acceptable class III solvent [50].

5.5.1.2 Copolymer composition

The statistical analysis revealed that copolymer composition was determined solely by the monomer feed composition (Figure 5.4).

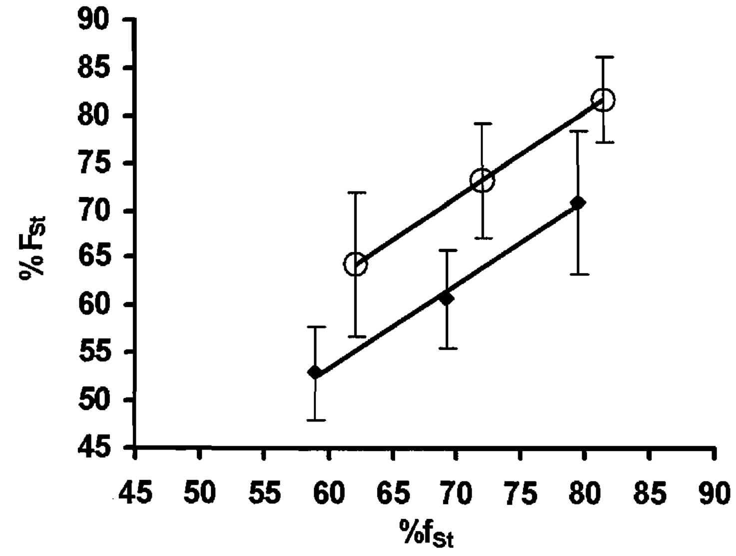

Figure 5.4: The effect of the feed fraction of St on the polymer fraction of St for (○) P(St-*co*-MMA) and (◆) P(St-*co*-EMA) copolymers.

It was argued that the clustering of micelles, induced by BuOH would ultimately determine the number of radicals that could nucleate the micelles and therefore determine the molecular weight of the copolymer particle. However, MMA is slightly more hydrophilic than EMA and therefore MMA partitioned to a higher extent to the interface where primary radicals were formed that could re-enter and nucleate the micelles. This also reflected in the composition, since higher fractions of MMA was found in the corresponding copolymer. Subsequently higher fractions of St was found in the P(St-*co*-EMA), indicating that both monomers resided to a larger extent in the micelle compared to the uneven partitioning of MMA systems.

Table 5.1 lists the properties of the copolymers that were selected for development of a pharmaceutical application.

Table 5.1: Properties of the copolymers synthesized by microemulsion copolymerization.

P(St-*co*-MMA)

Polymer	$\bar{M}_w$ (kg.mol^{-1})	$\bar{M}_w/\bar{M}_n$	$\langle s^2\rangle^{1/2}$ (nm)	q	%MMA	%St
1	474.2	1.8	32	0.492	19	81
2	309.1	1.8	23	0.502	37	63
3	183.1	1.8	18	0.459	52	48

P(St-*co*-EMA)

Polymer	$\bar{M}_w$ (kg.mol^{-1})	$\bar{M}_w/\bar{M}_n$	$\langle s^2\rangle^{1/2}$ (nm)	q	%EMA	%St
1	244.0	2.0	22	0.500	14	86
2	217.5	1.8	18	0.458	24	76
3	314.6	1.8	18	0.527	34	66

These copolymers (Table 5.1) were subsequently dissolved in THF and solvent cast to produce films that are characterized next.

5.5.2 Films

5.5.2.1 Morphology

The cavities of the honeycomb structures of P(St-*co*-MMA) films had Feret-diameters ranging from 12-17 μm, circumferences ranging 40-73 μm, and projected areas of 89-98 μm^2 resulting from an increase in MMA content from 18-52%. P(St-*co*-EMA) films had cavity Feret diameters of 4.6-5.9 μm, perimeters of 14-19 μm with projected areas of 15-20 μm^2 as EMA content increased from 14-34%. Figure 5.5A & B shows that the surface cavities of P(St-*co*-MMA) was approximately double the size of those found for P(St-*co*-EMA). In addition all these cavities exhibit circularities of 0.9-1.0, indicating that an oblong to circular type of shape could describe the cavities. The P(St-*co*-EMA) films therefore seemed more porous and the P(St-*co*-MMA) films more dense.

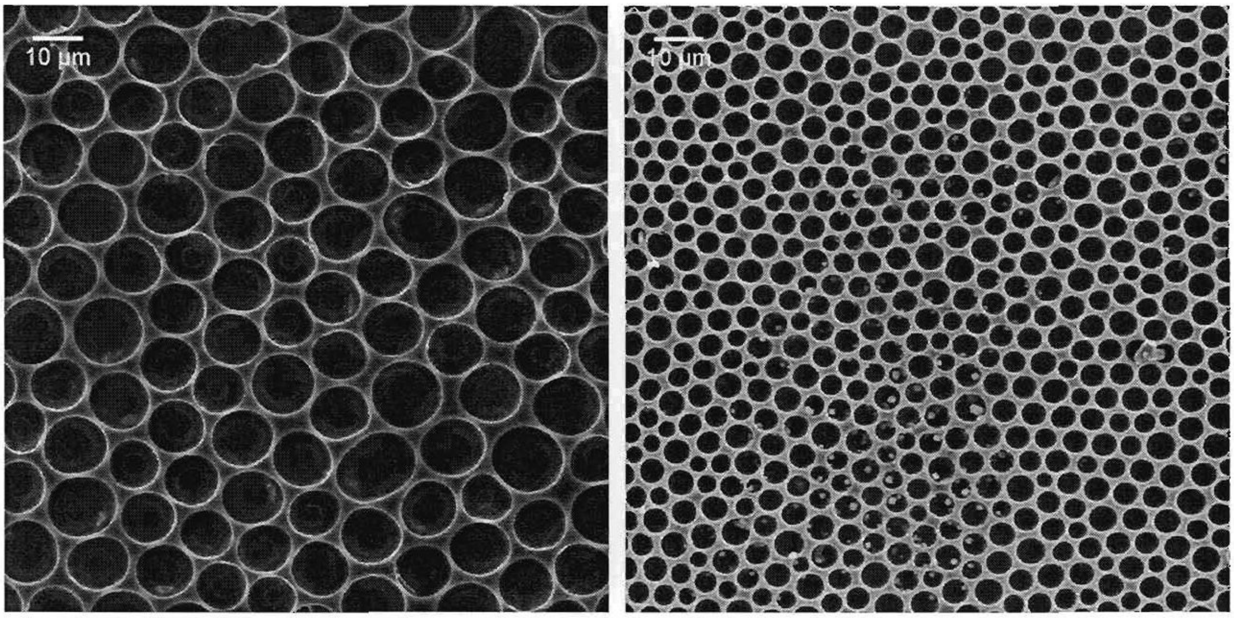

(A) (B)

Figure 5.5: Top surface cavities of blank films of (A) P(St-*co*-MMA) (52% MMA) and (B) P(St-*co*-EMA) (14% EMA).

The honeycomb structure of the copolymer films evolved due to a complex set of events. Figure 5.6 shows various SEM micrographs of different films that were loaded with RIF.

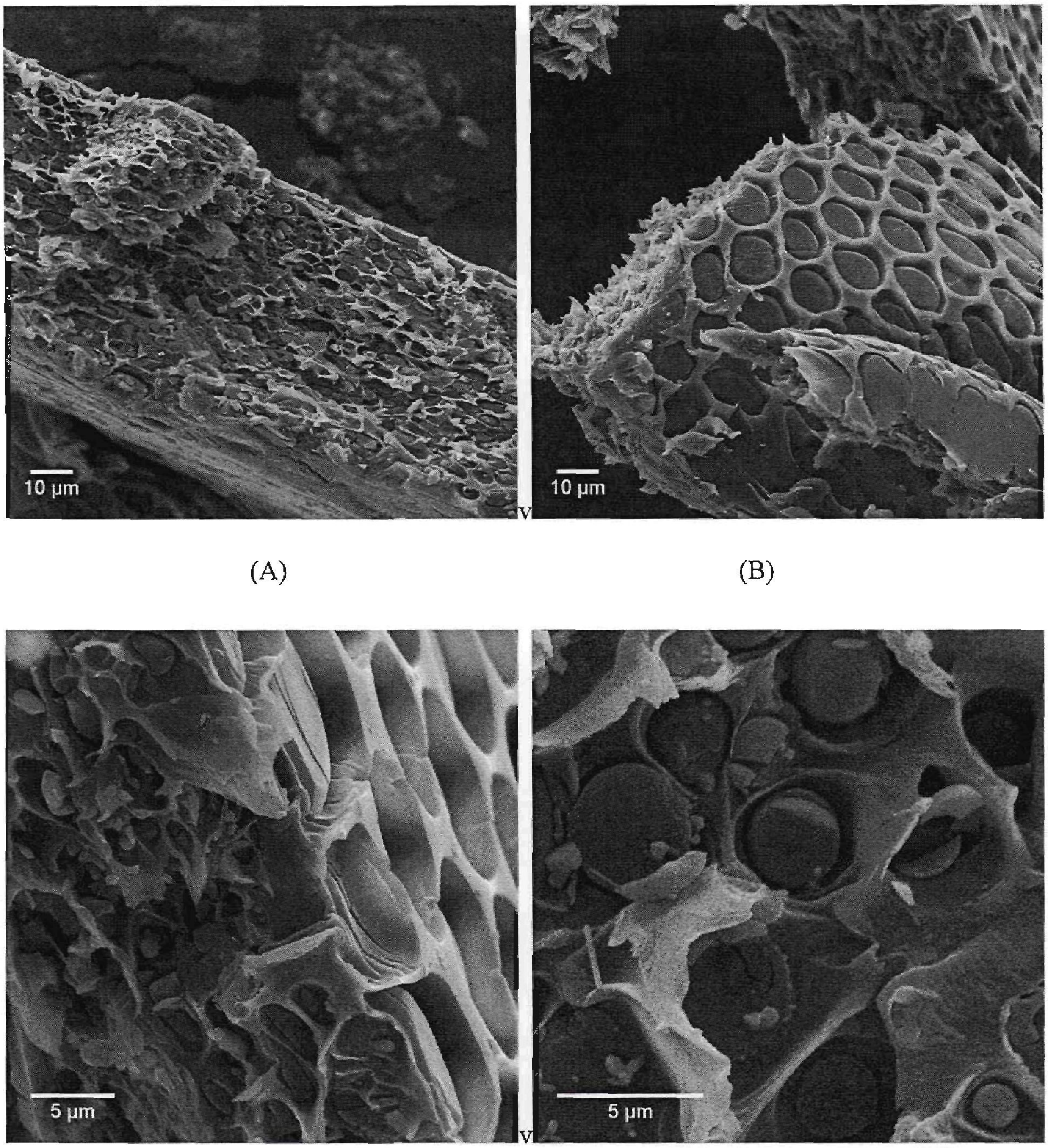

(A) (B)

(C) (D)

Figure 5.6: Cross section of RIF-loaded P(St-*co*-MMA) films (37% MMA) (A) honeycomb structure before release, (B) tilted view of the film after release and (C) magnified cross sectional view of the film after release. (D) Cross-section of P(St-*co*-EMA) (14% EMA) showing that RIF was still present in the micropockets after a release period of 24 h.

The solubility parameters (δ in $J^{1/3}/cm^{3/2}$) based on the Hansen and Hildebrandt methods was found for THF (δ=18.6-19.47) [51,52], RIF (δ=20.76) [53], PS (δ=18.19) [51], PMMA (δ=19.65) [51], PEMA (δ=20.46) ([52]) and the corresponding copolymers (δ=18.85) [51]. These values indicated that these materials would all be miscible in a THF solution since the values of Δδ was small - a prerequisite for miscibility [54].

The free energy of mixing theory [47] was applied to explain the morphology of the drug-loaded films:

$$\Delta G_m = \Delta H_m - T\Delta S_m \tag{5.7}$$

where ΔG_m is the free energy of mixing and should be negative to favor mixing, ΔH_m is the exothermic mixing enthalpy (therefore if spontaneous, it should be negative), T is the Kelvin temperature and ΔS_m is the mixing entropy (which should be positive to show and increase in the disorder, therefore mixing in the system).

According to the Flory-Huggins theory [47], the heat of mixing is determined by the volume fraction of each component that should be mixed as well as the solubility parameter of each component. Furthermore, the interaction energy between the polymer and solvent is described by the interaction parameter. Equation 5.8 was derived [47] to describe the free energy of mixing in a polymer-solvent system:

$$\Delta G_m = RT\left(n_1 \ln \phi_1 + n_2 \ln \phi_2 + \chi n_1 \phi_2\right) \tag{5.8}$$

where ΔG_m is the free energy of mixing, R and T are the universal gas constant and absolute temperature respectively, n_1 and n_2 are the molar quantities of the solute and solvent respectively, ϕ_1 and ϕ_2 and χ is the interaction parameter of the solute and the solvent.

In Equation 5.8 the first two terms represent the enthalpy of mixing and the third term the entropy of mixing. For the following argument, RIF should be seen as a small oligomer that is monodisperse (RIF has a molecular weight of 822.94 $g.mol^{-1}$) and in combination with the copolymer, formed the polydisperse component 1 (Equation 5.8). Additionally, the molecular weight of this oligomer is much lower than any of the copolymer fractions (the □ $_w$ of the copolymers were ~10^3 kg.mol^{-1}, Figure 5.3), therefore not overlapping with any copolymer weight fraction. Finally, due to the weight polydispersity of component 1, χ should be summed as an index of the different weight fractions [47].

When casting the film, the solvent starts to evaporate and subsequently the interaction between the solute component and solvent becomes weaker and the interactions between the solute components increase (θ condition dissipates). Additionally, the volume fraction of the solvent decreased as evaporation proceeded. Ultimately, ΔG_m becomes less negative, mixing becomes improbable and therefore phase separation occurs [55].

Phase separation also occurs as a series of steps with the higher weight copolymer fractions showing the highest propensity to precipitate, followed by lower weight fractions. During this process of precipitation, the polymer latex extrudes some of the THF, producing two liquid phases. The one phase is rich in the polymer fraction that is about to precipitate, the other is richer in solvent and species less prone to precipitate i.e. the oligomer [55]. This coacervation phase finally results in numerous liquid-filled pockets in the film. Since the oligomer was still encapsulated in these pockets, the oligomer finally precipitated in these pockets once the solvent evaporated. Consequently, a film with polymer-encapsulated drug micropockets assembled into a honeycomb structure.

5.5.2.2 ATR-FTIR characterization

ATR-FTIR spectra were recorded for the copolymer films before and after loading with RIF (Figure 5.7).

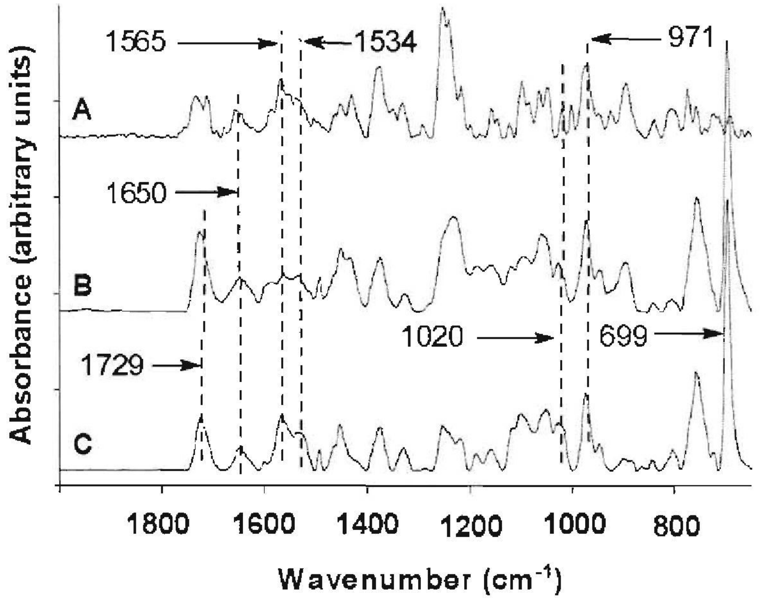

Figure 5.7: Expanded ATR-FTIR spectra of (A) RIF Form II and RIF-loaded copolymer films of (B) P(St-*co*-MMA) (19% MMA) and (C) P(St-*co*-EMA) (14% EMA).

The characteristic peaks of RIF was identified as the symmetric (C-O-C acetyl) ~1020 cm^{-1} vibration, the amide II vibration at ~1534 cm^{-1}, the (C=C) vibration at ~1565 cm^{-1}, the amide I vibration at 1650 cm^{-1} and 971 cm^{-1} [34,35,56]. The characteristic phenyl ring out-of-plane bending for St was observed at 699 cm^{-1} and the characteristic saturated alkyl ester carbonyl stretch for the methacrylate was observed at 1729 cm^{-1}. RIF showed its characteristic carbonyl stretch in the same spectral region as the methacrylate ester carbonyl and therefore the spectra was significantly overlapped in this region, although these peaks did not shift. Note that Form II of RIF showed 2 peaks in the carbonyl region at 1712 cm^{-1} and 1730 cm^{-1} whereas the amorphous form showed only 1 peak at 1725 cm^{-1}.

This suggested that no interactions could be detected between RIF and the copolymers. Additionally, the SEM micrographs in Figure 5.6, illustrated that drug molecules were present in the micropockets as seen from the agglomerate spheres. This confirmed findings that RIF did not interact with methacrylate-based non-ionic Eudragit® copolymers [57,58].

5.5.2.3 Contact angles

The contact angles of all the homopolymers were fairly high at around 80°, indicating a hydrophobic character. The contact angle of rifampin that was spin-coated from a THF solution also indicated a poor wetting ability from an angle of 70°. From these findings one would expect that the copolymers should possess the same hydrophobicity. One would also expect that the inclusion of RIF would not affect the contact angle significantly. However, Figure 5.8 depicted that the contact angles that were obtained, contradicted these expectations.

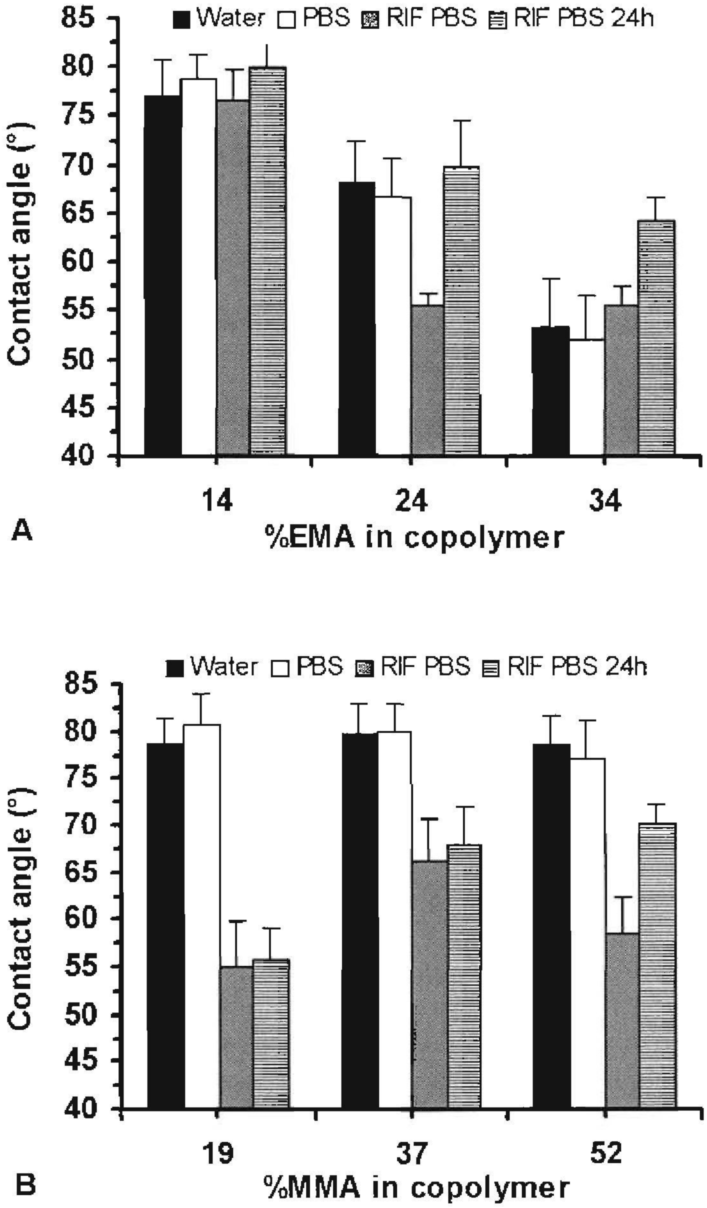

Figure 5.8: Contact angles of (A) P(St-*co*-EMA) and (B) P(St-*co*-MMA) copolymers that were spin-coated onto glass surfaces. RIF indicates the films loaded with rifampin and the films after 24 h release is indicated as RIF PBS 24 h. PBS is phosphate buffer solution at pH 7.4 (release medium). Error bars indicate standard deviations.

Of note was that the inclusion of RIF resulted in a decrease in the contact angle of the film relative to the blank polymer film. This could indicate a potential application of the drug solely for decreasing the contact angle, thus minimizing the accumulation of bacteria. The decrease in contact angle with the incorporation of RIF was observed for both the P(St-*co*-EMA) and P(St-*co*-MMA) copolymer films. Additionally, the contact angles for the blank P(St-*co*-EMA) films showed a linear decrease as the content of EMA was increased producing angles from 80-55°. However, blank P(St-*co*-MMA) films produced consistent contact angles despite the variation in MMA content.

Seen from the perspective of the contact angles, the application of the copolymers would pose an advantage compared to homopolymer films with regards to limiting bacterial biofilm formation of certain bacterial strains. It is known that hydrophobic bacteria i.e. *Pseudomonas aeruginosa* would preferentially adhere to a hydrophobic substrate compared to hydrophilic *Staphylococcus liquefaciens* that prefers hydrophilic surfaces [17].

5.5.3 Release studies

5.5.3.1 Homopolymer films

The films demonstrated that they possessed favorable properties regarding contact angles and the possible application to limit biofilm formation. The question, however arose whether the contact angle would affect the drug release pattern as well.

An attempt was made to load PS, PMMA and PEMA with 20% RIF followed by monitoring the release of RIF over a 24 h period. The release studies revealed that the loading of the poly(methacrylate)s were more successful than that seen for the PS film as observed from the initial release of drug from the films. Figure 5.9 shows the release patterns of RIF from the homopolymer films.

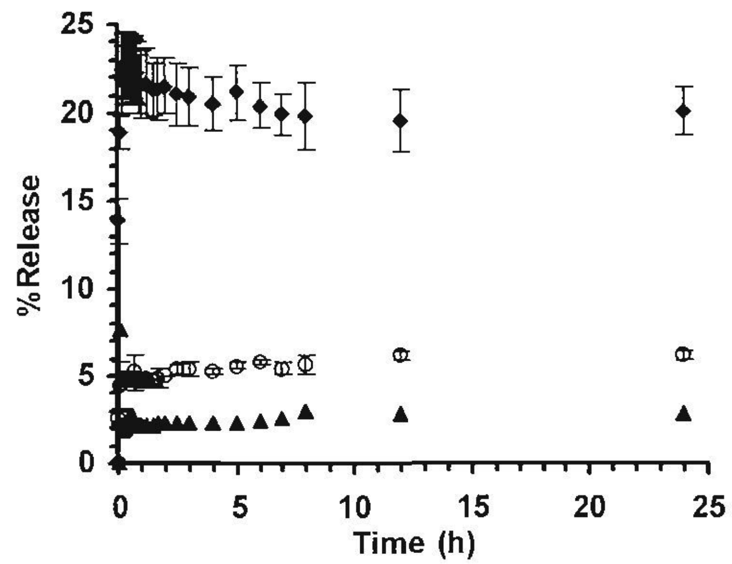

Figure 5.9: Release profiles of RIF from ▲ PEMA, ○ PMMA and ◆ PS films. Error bars indicate standard deviations.

The PS films released approximately 20% of the drug in the first hour of the 24 h period followed by a seemingly negative release or in fact no release in the remainder of the study. It was therefore predicted that fairly quick release would be seen if high styrene content was found in the copolymers. The PEMA and PMMA films released approximately 3 and 6% respectively in the first hour followed by no obvious release or more erratic release as seen from the fluctuation in release values for the remainder of the 24 h period (Figure 5.9). No time-correlated release patterns could be observed for these homopolymer films since zero-order and Higuchi kinetics demonstrated poor fits of the release curves with $r^2 < 0.5$.

It would however seem that the incorporation of a methacrylate monomer in the copolymer would be beneficial in curbing the extent of the unwanted quick initial release. Additionally one could conclude that the solubility of the drug was higher in the methacrylate polymers compared to PS and that the methacrylate units would favor the efficiency of drug loading.

5.5.3.2 Copolymer films

5.5.3.2.1 Initial phase

The Peppas model was fitted to the release profiles and could not describe the initial release as a typical Fickian diffusion-controlled process during the initial release phase of the drug. These regressions produced exponent values of much lower than the expected exponents of n =

0.5. One could most probably state that a combination of diffusion and dissolution of surface molecules was possible for drug that was not incorporated in the polymer film.

However, the $\Delta\delta$ value between the copolymer and the solvent/oligomer could reach a maximum value as the methacrylate content increased. This would result in a larger extrusion of solvent/oligomer during coacervation, finally depositing drug on the surface. The higher prevalence of pores in P(St-*co*-EMA) could enhance this extrusion compared to P(St-*co*-MMA) up to certain critical composition. Furthermore, it was illustrated that polar solvent flux through copolymers of styrene and a more hydrophilic monomer could facilitate solvent pervaporation, therefore an increase in methacrylate levels could facilitate solvent and drug flux to surface of the film [59].

The initial release phases showed an approximate proportionality to an increase in the methacrylate content in both sets of the copolymers (Table 5.2). Additionally, no obvious relationship could be found to correlate the initial release phase with the contact angles of the copolymer films.

Table 5.2: The release of drug in the initial and secondary release phases.

P(St-*co*-EMA) (onset of secondary phase at ~6h)					
%EMA	Initial (mg)[a]	$R_{initial}$ (%)[b]	Secondary (mg)[c]	%Load[d]	%wt/wt[e]
14	17.4	37.8	10.8	62.2	12.4
24	17.5	43.5	9.9	56.5	11.3
34	17.2	68.5	5.4	31.5	6.3
P(St-*co*-MMA) (onset of secondary phase at ~3h)					
%MMA	Initial (mg)	$R_{initial}$ (%)	Secondary (mg)	%Load	%wt/wt
19	17.4	15.3	14.8	84.7	16.9
37	17.3	19.5	13.9	80.5	16.1
52	17.2	75.5	4.22	24.5	4.9

[a]The average amount of drug per film strip (n=3).
[b]The average %release of the initial dose.
[c]Amount of drug captured in micropockets at onset of secondary release phase.
[d]Percent of drug available for controlled release.
[e]Concentration of drug in film at onset of zero-order release.

In contradiction to the homopolymer films, the copolymers resulted in drug release patterns that could be correlated to time at least for some part of the release profile. Figure 5.10 displays the release patterns of RIF from P(St-*co*-EMA) and P(St-*co*-MMA) films respectively. The most obvious observation was that both sets of polymer films released the drug in an initial phase at a high rate and then at a significantly slower rate for the remainder of the monitored period.

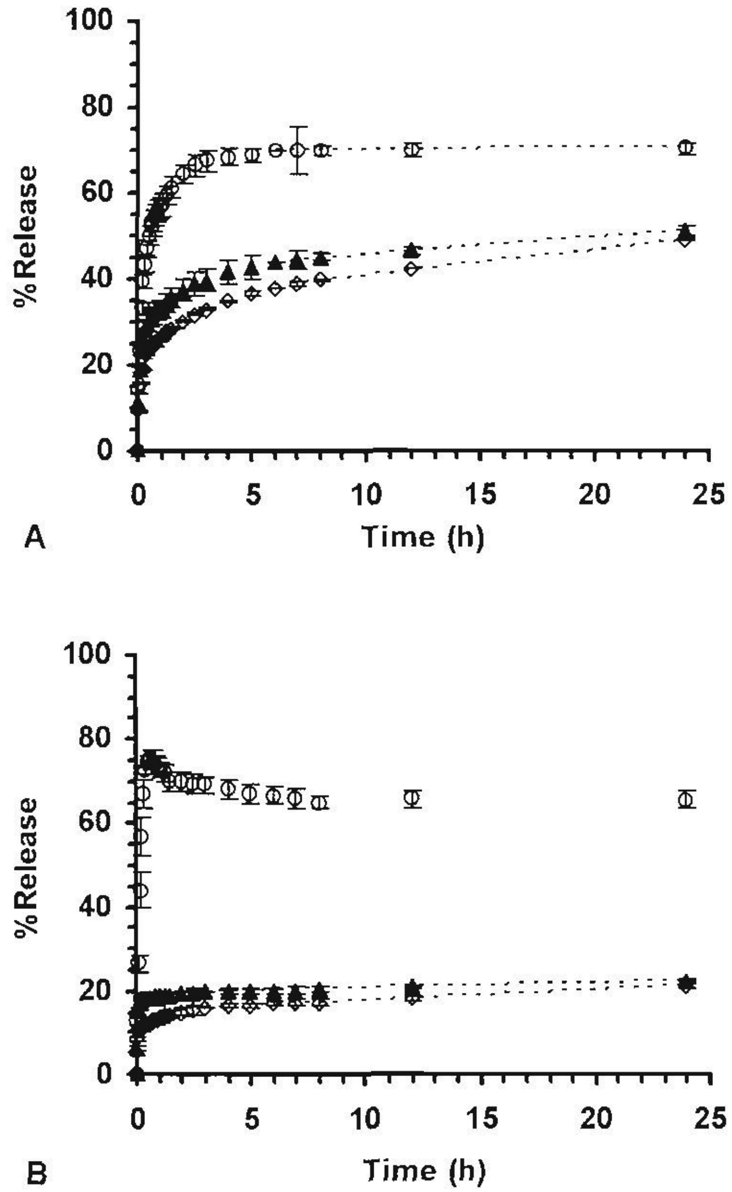

Figure 5.10: Release profiles of RIF from films of (A) P(St-*co*-EMA) comprising of ◇ 14%, ▲ 24% or ○ 34% EMA and (B) P(St-*co*-MMA) comprising of ◇ 19%, ▲ 37% or ○ 52% MMA.

In both sets, two of the polymers released a high quantity of drug (~60% for EMA and ~70% for MMA copolymers) within the first hour and this corresponded to the highest content of the methacrylate in the copolymer i.e. 34% EMA and 52% MMA respectively. It was suggested that a large fraction of RIF was deposited in the surface cavities of the 52% MMA film (Figure 5.11 A & B) and a large fraction of the drug in cavities on the film surface for the 34% EMA composition (Figure 5.11C). This indicated a limit in the methacrylate content if the release of a substantial quantity of drug should be controlled over an extended period (Table 5.2).

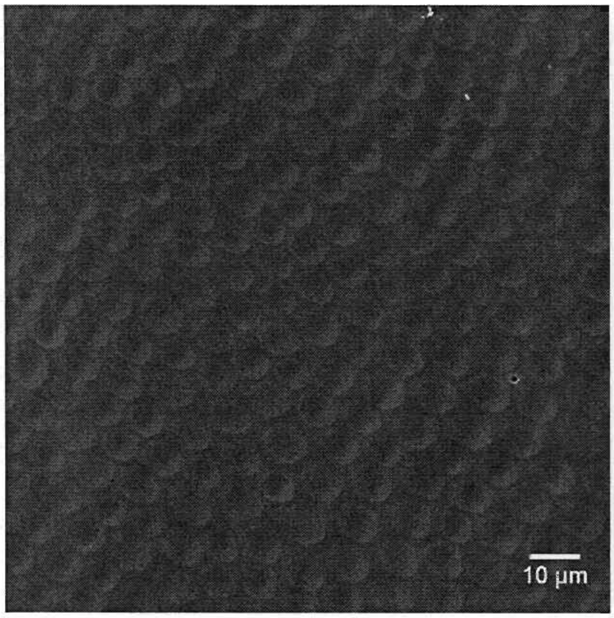

(A)

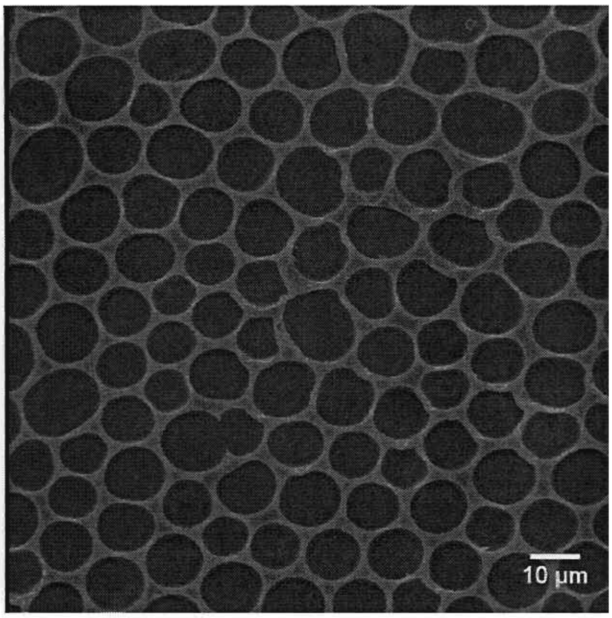

(B)

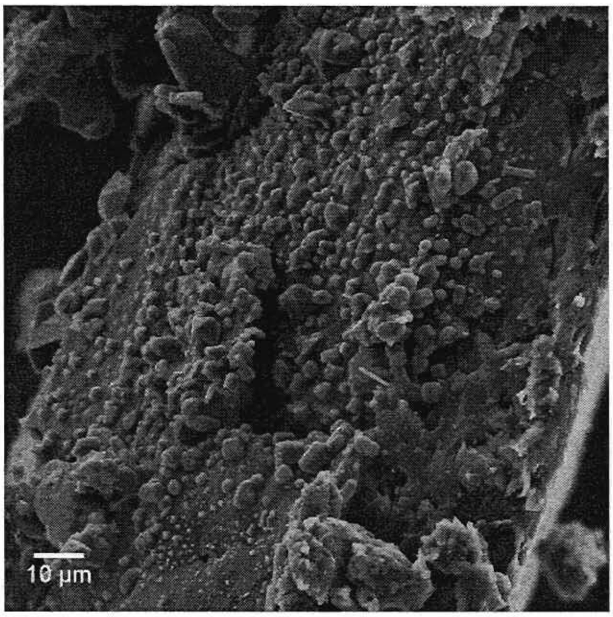

(C)

Figure 5.11: Surface of RIF-loaded P(St-*co*-MMA) films (52% MMA) (A) before release and (B) after release. (C) Surface deposition of a RIF-loaded P(St-*co*-EMA) (34% film) before the release study was performed.

Indeed the amount of initial release was lower for the copolymers that contained the low and intermediate content of the methacrylates i.e. 14% EMA and 24% EMA for P(St-*co*-EMA), 19% MMA and 37% MMA for P(St-*co*-MMA).

The release profiles of the 14% and 24% EMA content P(St-*co*-EMA) films indicated approximately 40% release within the first 6 h or release before a zero-order rate of release was observed. On the contrary, approximately 20% initial release was measured for the 19% and 37% MMA content P(St-*co*-MMA) films, before a stable release tempo could be obtained after 3 h. The morphology of the films could play some role in this release phase since the P(St-*co*-EMA) films illustrated a more porous material compared to the MMA copolymer films.

It was concluded that P(St-*co*-EMA) films should not exceed a composition of more than 24% EMA and P(St-*co*-MMA) should not incorporate more than 37% MMA in order to curb a high, unwanted initial release phase. The different sets of copolymers could however be employed to provide a different quantity of initial drug release, followed by prolonged release. The second phase of release will now be discussed to determine the usefulness of the copolymer films as sustained drug delivery systems.

5.5.3.2.2 Secondary phase

For the discussion here, the assumption was made that the initial phase considered the drug molecules that were released primarily without being controlled by the polymer film matrix. Therefore, the secondary phase considered the release of the drug molecules that was successfully loaded into the polymer film.

Despite the larger initial release of drug from the copolymers compared to the homopolymers, they could still provide the advantage of drug release during the second phase of release. More importantly, these copolymers show potential to control the release of drug at a predictable rate. Inspection of Figure 5.10 revealed a strong tendency towards zero-order release for P(St-*co*-EMA) and P(St-*co*-MMA) films respectively (indicated by the dotted lines).

At the initial point of zero-order release one could find an approximate loading of the drug in the polymer matrix. At this point one could state that all the drug molecules that were not incorporated in the matrix have now been released and that the remaining drug molecules will now be released by the matrix according to the properties of the matrix. Table 5.2 lists the release values obtained for the secondary release phase of the various films.

The percentage of drug that was effectively captured in the matrix could be calculated and this is often described as the drug load. Table 5.2 reported the percentage of RIF that was successfully captured in the copolymer film micropockets. The percentage load of the drug corresponded closely to the copolymer composition with a decrease in the drug load as methacrylate concentration increased (or St content decreased). This illustrated one advantage for the copolymer films over the homopolymer films in that the homopolymer could incorporate a larger quantity of drug in the matrix, however with no apparent extended release pattern. Table 5.3 lists the values that were calculated for the secondary phase release kinetics of RIF that was successfully captured in the micropockets of the film.

Table 5.3: Kinetic parameters calculated for the secondary phase of RIF release from the various copolymer films.

P(St-*co*-EMA)

	Zero-order				Higuchi	
%EMA	r^2	k_0 (%/day)*	$t_{1/2}$ (days)	t_{max} (days)	r^2	k ($\mu g/cm^2/h^{1/2}$)
14	0.9964	14.27 (0.49)	3.5	7.0	0.9901	34.42
24	0.9949	9.463 (0.38)	5.3	10.6	0.9919	31.06
34	0.9797	0.631 (0.06)	79	158.4	0.9562	1.290

P(St-*co*-MMA)

	Zero-order				Higuchi	
%MMA	r^2	k_0 (%/day)	$t_{1/2}$ (days)	t_{max} (days)†	r^2	k ($\mu g/cm^2/h^{1/2}$)
19	0.9939	5.801 (1.21)	8.6	17.2	0.9916	8.748
37	0.9944	2.868 (0.10)	17.4	34.9	0.9906	3.966
52				obscured		

*All k_0 values in the table are statistically different from each other ($p < 0.05$)
†t_{max} is the calculated time required for complete release of the matrix-captured drug via zero-order kinetics.

Clearly, the zero-order release rate also decreased as the RIF captured in the film micropockets in the different copolymer films decreased. This suggested a diffusion-type release pattern. Subsequently the release data was converted to illustrate the flux of drug from a fixed surface of 30 cm^2 versus the square root of time. These Higuchi plots for P(St-*co*-EMA) and P(St-*co*-

MMA) films (Figure 5.12A & B) illustrated a good fit with $r^2 > 0.95$ for all curves. Higuchi kinetics describes the diffusion of molecules through a polymer matrix to the surface of the matrix with the diffusion distance increasing an infinitesimal amount per unit time towards the core of the matrix.

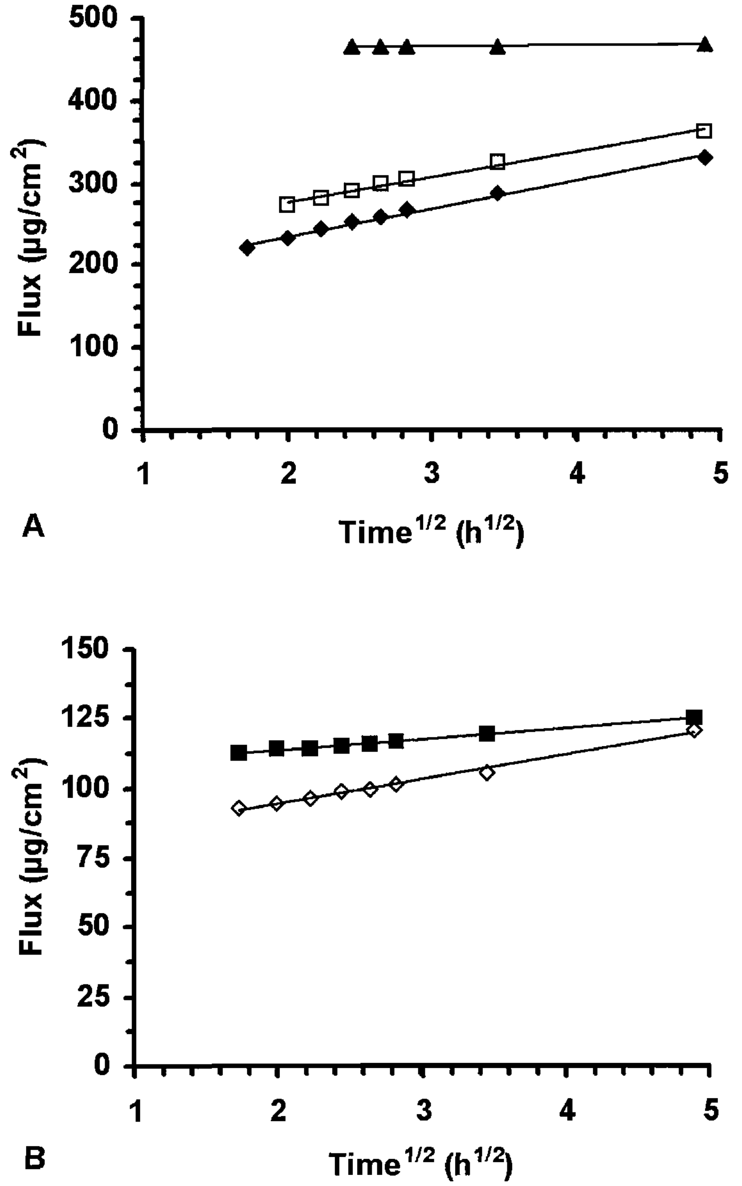

Figure 5.12: Higuchi release plots of RIF after initial release from (A) P(St-*co*-EMA) comprising of ◆ 14%, □ 24% or ▲ 34% EMA and (B) P(St-*co*-MMA) comprising of ◇ 19 or ■ 37% MMA. Error bars are too small to display on this scale.

The thickness of the films measured 40±2 µm for all films and remained constant since the films did not degrade in the release medium. Thus, the assumption was made that the diffusion distance to the film surface did not vary significantly. The fact that zero-order release kinetics showed slightly better fits of the data ($r^2 > 0.97$), one could conclude that the diffusion of dissolved drug molecules to the release medium was regulated by the polymer barrier, therefore resulting in zero-order release.

Closer analysis of the second, controlled-release phase also revealed correspondence to copolymer composition. An inverse relationship was seen between the zero-order release rates and the concentration of the methacrylate in the P(St-*co*-EMA) films (Figure 5.13).

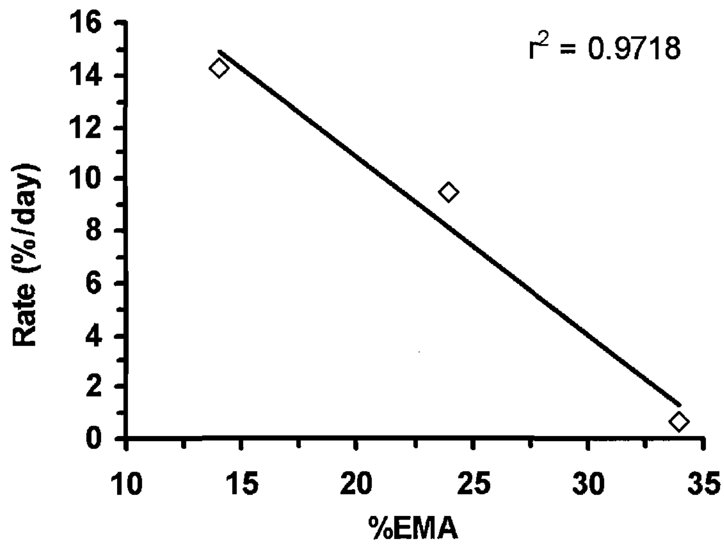

Figure 5.13: The linear dependence of zero-order release on copolymer composition of P(St-*co*-EMA).

The conclusion was made that the methacrylate did indeed decelerate the zero-order release rate, a fact that was suggested by the drug release from PMMA and PEMA. Since the drug loads decreased as a function of methacrylate content in the copolymer, it is suggestive that diffusion rate was determined by the load, again indicating a diffusion-controlled release mechanism maintained by copolymer properties.

It could be predicted from the zero-order release rates that 35% EMA would be the maximum concentration in the copolymer if any zero-order phase release was expected for RIF. Additionally it would seem that the content of MMA in copolymers could be higher than that of the EMA in order to still obtain zero-order release.

The P(St-*co*-MMA) films illustrated lower release rates (~0.5 fold) compared to the P(St-*co*-EMA) films with higher quantities of the drug captures in the P(St-*co*-MMA) films. These systems could probably be suited for longer-term use i.e. coating of prosthetic implants or medicated devices as seen from the calculated $t_{0.5}$ values of 8.6 and 17.4 days for the 19% and 37% MMA films respectively.

The P(St-*co*-EMA) films could release a higher quantity of drug over a shorter period of time. This could indicate shorter term applications such as application in temporary urinary catheters predicting a maximum usage period of 7-10 days for the 14% EMA and 24% EMA P(St-*co*-EMA) films respectively. Figure 5.14 shows the predicted release periods that were calculated from the zero-order rate constants for RIF from the P(St-*co*-EMA) films.

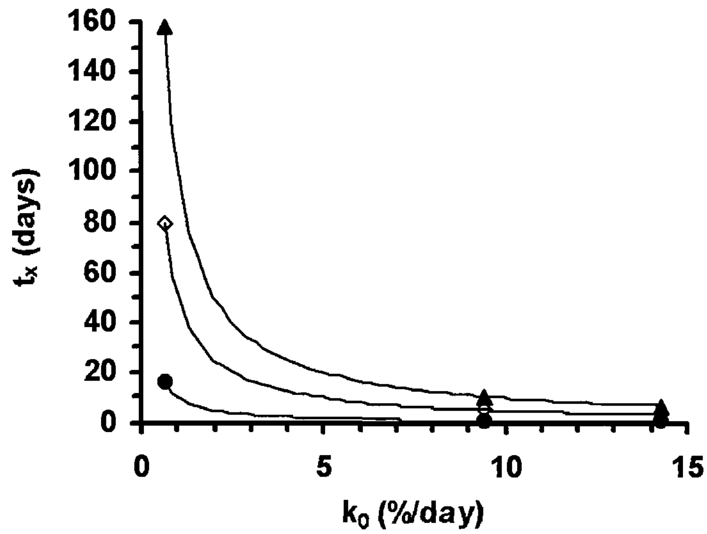

Figure 5.14: Predicted release periods for RIF from P(St-*co*-EMA) for ● 10, ◇ 50 or ▲ 100% of RIF loaded in the film at the onset of zero-order release.

5.6 CONCLUSION

A series of nanosized styrene-methacrylate copolymers with molecular weights in the 10^2 $kg.mol^{-1}$ range were synthesized by microemulsion copolymerization. The cosurfactant dominated the size and weight properties of these copolymers due to induction of micellar coagulation during the reaction. Additionally, copolymer composition was primarily determined by the monomer feed ratio, however with some deviation from the feed. All these copolymers resulted in the formation of pseudolatexes if dissolved in THF as was indicated by the prevalence of the θ conformation of the copolymer chains as determined by GPC-MALLS.

The $\Delta\delta$ values, suggested that all components were miscible in THF. However, casting of the nanoscale drug-loaded pseudolatexes resulted in coacervation, phase separation of the drug and copolymer species and finally microencapsulation of the drug. Additionally, the copolymeric microcapsule walls interpenetrated resulting in a film that bridged yet another size hierarchy into the macroscale region.

No interaction between the drug and copolymers could be illustrated. The copolymer composition determined the magnitude of the initial release phase, subsequently also that of the second release phase. The second phase seemed to be a diffusion-controlled zero-order release phase. Predictions of release patterns showed that the copolymers could be useful in delivering drugs at zero-order release rate for a few days up to a few months.

As a compromise to their lower loading capacity, P(St-*co*-EMA) demonstrated a decrease in the contact angle upon incorporation of the drug or an increase in the EMA content. The use of these copolymers therefore seems promising despite their comparatively shorter controlled release phase. Different applications may be realized for these copolymers i.e. short-term use as catheter coatings or long-term employment in implants.

5.7 REFERENCES

[1] C.R. Arciola, Y.H. An, D. Campoccia, M.E. Donati, L. Montanaro, Etiology of implant orthopedic infections: a survey on 1027 clinical isolates, Int. J. Artif. Organs 28 (2005) 1091-1100.

[2] G. Reid, H.J. Busscher, S. Sharma, M.W. Mittelman, S. McIntyre, Surface properties of catheters, stents and bacteria associated with urinary tract infections, Surf. Sci. Rep. 21 (1995) 251-273.

[3] D.S. Jones, J.G. McGovern, A.D. Woolfson, C.G. Adair, S.P. Gorman, Physicochemical characterization of hexetidine-impregnated endotracheal tube poly(vinyl chloride) and resistance to adherence of respiratory bacterial pathogens, Pharm. Res. 19 (2002) 818-824.

[4] A. Jegatheeswaran, B. Jagdish, Pathology of infectious and inflammatory diseases in prosthetic heart valves, Cardiovasc. Pathol. 15 (2006) 252-255.

[5] J.M. Schierholz, C. Morsczeck, N. Brenner, D.P. Konig, N Yucel, M. Korenkov, E. Neugebauer, A.F.E. Rump, G. Waalenkamp, J. Beuth, G. Pulverer, S Arens, Special aspects of implant-associated infection in orthopedic surgery. From the pathophysiology to custom-tailored prevention strategies, Der Orthopade 33 (2004) 397-404.

[6] M., Henriques, N. Cerca, J. Azeredo, R. Oliveira, Influence of sub-inhibitory concentrations of antimicrobial agents on biofilm formation in indwelling medical devices, Int. J. Artif. Organs 28 (2005) 1181-1185.

[7] C.R. Arciola, Why focus on implant infections? Int. J. Artif. Organs 28 (2005) 1061.

[8] L.D. Christensen, C. Moser, P.Ø. Jensen, T.B. Rasmussen, L. Chirstophersen, S. Kjelleberg, N. Kumar, N. Høiby, M. Givskov, T. Bjarnsholt, Impact of *Pseudomonas aeruginosa* quorum sensing biofilm persistence in an in vivo intraperitoneal foreign-body infection model, Microbiology 153 (2007) 2312-2320.

[9] N.R. James, A. Jayakrishnan, Surface thiocyanation of plasticized poly(vinyl chloride) and its effect on bacterial adhesion, Biomaterials 24 (2003) 2205-2212.

[10] J.M. Schierholz, G. Pulverer, Investigation of a rifampin, fusidic-acid and mupirocin releasing silicone catheter, Biomaterials 19 (1998) 2065-2074.

[11] I. Raad, R. Darouiche, R. Hachem, M. Mansouri, G.P. Bodey, The broad-spectrum activity and efficacy of catheters coated with minocycline and rifampin, J. Inf. Dis. 173 (1996) 418-423.

[12] C.V. Ragel, M. Vallet-Regí, In vitro bioactivity of and gentamicin release from glass-polymer-antibiotic composites, J. Biomed. Mater. Res. 51 (2000) 424-429.

[13] L.C. Li, J. Deng, D. Stephens, Polyanhydride implant for antibiotic delivery – from the bench to the clinic, Adv. Drug Delivery Rev. 54 (2004) 963-986.

[14] D.M. Chilukuri, J.C. Shah, Local delivery of vancomycin for the prophylaxis of prosthetic device-related infections, Pharm. Res. 22 (2005) 563-572.

[15] C.S. Kwok, T.A. Horbett, B.D. Ratner, Design of infection-resistant antibiotic-releasing polymers II. Controlled release of antibiotics through a plasma-deposited thin film barrier, J. Controlled Release 62 (1999) 301-311.

[16] S. Bayoudh, A. Othmane, F. Bettaieb, A. Bakhrouf, H.B. Ouada, L. Ponsonnet, Quantification of the adhesion free energy between bacteria and hydrophobic and hydrophilic substrata, Mater. Sci. Eng., C 26 (2006) 300-305.

[17] G.M. Bruinsma, H.C. van der Mei, H.J Busscher, Bacterial adhesion to surface hydrophilic and hydrophobic contact lenses, Biomaterials 22 (2001) 3217-3224.

[18] C.A. Nguyen, Y.N. Konan-Kouakou, E. Alléman, E. Doelker, D. Quintanar-Guerrero, H. Fessi, R. Gurny, Preparation of surfactant-free nanoparticles of methacrylic acid copolymers used for film coatings, AAPS PharmSciTech 7 (2006): article 63.

[19] P. Couvreur, C. Dubernet, F. Puisieux, Controlled drug delivery with nanoparticles: current possibilities and future trends, Eur. J. Pharm. Biopharm. 41 (1995) 2-13.

[20] S.D. Hong, C.M. Burns, Compatibility of polystyrene and poly(methyl methacrylate) in benzene. Effects of molecular weight and temperature, J. Appl. Polym. Sci. 15 (1971) 1995-2006.

[21] K.L. Foster, R.P. Wool, Strength of polystyrene-poly(methyl methacrylate) interfaces, Macromolecules 24 (1991) 1397-1403.

[22] W.C. Johnson, J. Wang, Z. Chen, Structures and properties of polystyrene/poly(methyl methacrylate) blends and copolymers, J. Phys. Chem., B 109 (2005) 6280-6286.

[23] R.L. Oréfice, A.P.C. Barbosa, M.M.N. Noguiera, Controlling the phase stability of polymer blends through the introduction of impenetrable surfaces, J. Appl. Polym. Sci. 187 (2003) 1619-1627.

[24] Y. Zhang, T. Guo, G. Hao, M. Song, B. Zhang, Nanosize polymer latexes made by microemulsion copolymerization: preparation and characterization, J. Appl. Polym. Sci. 90 (2003) 3625-3630.

[25] M. Dittgen, M. Durrani, K. Lehmann, Acrylic polymers. A review of pharmaceutical applications, S.T.P. Pharma Sci. 7 (1997) 403-437.

[26] M. Baleani, C. Persson, L. Guandalini, E. Piazza, P. Erani, S. Squarzoni, M. Viceconti, The effect of gentamicin sulphate on the fracture properties of manually mixed bone cement, Fat. Fract. Eng. Mater. Struct. 30 (2007) 479-488.

[27] K. Tauer, A.G. Ramírez, R.G. López, Effect of the surfactant concentration on the kinetics of oil in water microemulsion copolymerization: a case study with butyl acrylate, C.R. Chim. 6 (2003) 6:1245-1266.

[28] P.J. Wyatt, Light scattering and the absolute characterization of macromolecules, Anal. Chim. Acta 272 (1993) 1-40.

[29] A. Karami, S.T. Balke, T.C. Schunk, Quantitative interpretation of Fourier-transform infrared spectroscopic data from a size-exclusion chromatography solvent-evaporation interface, J Chromatogr., A 911 (2001) 27-37.

[30] W.S. Rasband, ImageJ 1.38x, U.S. National Institutes of Health, Bethesda, Maryland, USA, http://rsb.info.nih.gov/ij/, 1997-2007.

[31] T. Wu, Y. Sun, N. Li, M.M. de Villiers, Y. Lian, Inhibiting surface crystallization of amorphous indomethacin by nanocoating, Langmuir 23 (2007) 5148-5153.

[32] G. Zografi, S.S. Tam, Wettability of pharmaceutical solids: estimates of solid surface polarity, J. Pharm. Sci. 65 (1976) 1145-1149.

[33] The United States Pharmacopeia XXIX, 2006. The United State Pharmacopeial Convention, Inc., Rockville, MD.

[34] S.Q. Henwood, W. Liebenberg, L. Tiedt, A.P. Lötter, M.M. de Villiers, Characterization of the solubility and dissolution properties of several new rifampicin polymorphs, solvates, and hydrates, Drug Dev. Ind. Pharm. 27 (2001) 1017-1030.

[35] S.Q. Henwood, M.M. de Villiers, W. Liebenberg, A.P. Lötter, Solubility and dissolution properties of generic rifampicin raw materials, Drug Dev. Ind. Pharm. 26 (2001) 403-408.

[36] P.L. Ritger, N.A. Peppas, A simple equation for description of solute release. I. Fickian and non-Fickian release from non-swellable devices in the form of slabs, spheres, cylinders or disks, J. Controlled Release 5 (1987a) 23-36.

[37] P.L. Ritger, N.A. Peppas, A simple equation for description of a solute release. II. Fickian and anomalous release from swellable devices, J. Controlled Release 5 (1987b) 37-42.

[38] T. Higuchi, Rate of release of medicaments from ointment bases containing drugs in suspension, J. Pharm. Sci. 50 (1961) 874-875.

[39] T. Higuchi, Physical chemical analysis of percutaneous absorption process from creams and ointments, J. Soc. Cosmet. Chem. 11 (1960) 85-97.

[40] J.R. Robinson, S.P. Eriksen, Theoretical formulation of sustained-release dosage forms, J. Pharm. Sci. 55 (1966) 1254-1263.

[41] G. Di Colo, Controlled drug release from implantable matrices based on hydrophobic polymers, Biomaterials 13 (1992) 850-856.

[42] R. Marinov, S. Panayotova, A. Derzhanski, The phase behavior of the Triton X-114 - water system and the hydrophile - lipophile balance theory, Prog. Colloid Polym. Sci. 118 (2001) 256-259.

[43] I.A. Maxwell, B.R. Morrison, D.H. Napper, R.G. Gilbert, Entry of free radicals into latex particles in emulsion polymerization, Macromolecules 24 (1991) 1629-1640.

[44] C. Clasen, W.-M. Kulicke, Determination of viscoelastic and rheo-optical material functions of water-soluble cellulose derivatives, Prog. Polym. Sci. 26 (2001) 1839-1919.

[45] Y. Liu, S. Bo, Y. Zhu, W. Zhang, Determination of molecular weight and molecular sizes of polymers by high temperature gel permeation chromatography with a static and dynamic laser light scattering detector, Polymer 44 (2003) 7209-7220.

[46] S. Grcev, P. Schoenmakers, P. Iedema, Determination of molecular weight and size distribution and branching characteristics of PVAc by means of size exclusion chromatography/multi-angle laser light scattering (SEC/MALLS), Polymer 45 (2004) 39-48.

[47] P.J. Flory, Principles of polymer chemistry, Cornell University Press:Ithica, NY, 672 p.

[48] X.J. Xu, F. Chen, Preparation of nanoparticles of poly(methyl methacrylate) latexes at θ condition, Langmuir 20 (2004) 528-531.

[49] N.S. Fernandes, M.A. da Silva Carvalho Filho, R.A. Mendes, M. Ionashiro, Thermal decomposition of some chemotherapeutic substances, J. Braz. Chem. Soc. 10 (1999) 459-462.

[50] L.S. Wigman, X. Zhang, D.O. Fisher, S.W. Walinsky, ICH guideline: harmonization of residual solvents in pharmaceuticals, Pharm. Technol. 20 (1996) 102, 104, 106, 108.

[51] J.A. Gonzalez-Leon, A.M. Mayes, Phase behavior of ternary polymer mixtures, Macromolecules, 36 (2003) 2508-2515.

[52] D.L. Ho, C.J. Glinka, New insights into Hansen's solubility parameters, J. Polym. Sci., Part B: Polym. Phys. 42 (2004) 4337-4343.

[53] J.M. Schierholz, Physico-chemical properties of a rifampicin-releasing polydimethylsiloxane shunt, Biomaterials 18 (1997) 635-641.

[54] D.J. Greenhalgh, A.C. Williams, P. Timmins, P. York, Solubility parameters as predictors of miscibility in solid dispersions, J. Pharm. Sci. 88 (1999) 1182-1190.

[55] A.R. Shultz, P.J. Flory, Phase equilibria in polymer-solvent systems, J. Am. Chem. Soc. 74 (1952) 4760-4767.

[56] S.M. Safwat, S.S. Tous, S.S., I.A. Hassan Preformulation of antituberculous drugs in polymeric based blends, Bull. Pharm. Sci. Assiut University 17 (1994) 127-138.

[57] B.B. Barik, B.K. Gupta, M. Pal, Preparation and in vitro dissolution of Eudragit RS micropellets containing rifampicin, S.T.P. Pharma Sci. 3 (1993) 472-476.

[58] H.O. Ammar, R.M. Khalil, Preparation and evaluation of sustained-release solid dispersions of drugs with Eudragit polymers, Drug Dev. Ind. Pharm. 23 (1997) 1043-1054.

[59] S. Ray, S.K. Ray, Effect of copolymer type and composition on separation characteristics of pervaporation membranes – A case study with separation of acetone-water systems, J. Membr. Sci. 270 (2006) 73-87.

CHAPTER 6

CONCLUSION

6.1 THE APPLICATION OF NANOTECHNOLOGY

The development of nanotechnology predominantly arose from improvements in the characterization techniques and technology available to study materials. The sub 100 nm benchmark was realized for the production of materials including polymeric materials with the advent of microemulsion polymerization in the 1980's. Since then the application of the technique was expanded to copolymerization in the 1990's and applications of this technique in various other scientific disciplines began to appear in the early 21st century. Pharmaceutical industry is currently beginning to reap the benefits of this multidisciplinary effort to improve or develop specialized drug delivery systems.

6.2 CONTEXT OF THIS PROJECT

In this study several copolymers were synthesized employing microemulsion copolymerization of styrene and selected methacrylate monomers. Some applications could be found for styrene copolymers applied as bone cements i.e. Endurance® bone cement and some pharmaceutical applications were found for methacrylate-based copolymers i.e. Eudragit®. However, the search for new materials and applications thereof is continuous. In this study the synthesized styrene-methacrylate copolymers were employed to cast drug-containing films, an application that has not been employed in pharmaceutical industry to a wide extent. Before the application could be realized, some development of the materials were required to make appropriate copolymer selections.

6.3 SYNTHESIS OF NANOMATERIALS

6.3.1 Experimental design

The microemulsions of the monomers were prepared according to a guideline found in the literature and subsequently all these reaction dispersions could be polymerized. The concentration of the surfactant (sodium dodecyl sulfate), cosurfactant (1-butanol), monomer feed ratio and temperature level were investigated as reaction parameters. These reaction variables were interplayed as determined by a factorial design that simultaneously varied the four factors at three levels. Although several experiments were devised, the factorial design provided a method to still minimize the number of experiments whilst covering a statistical range of variables for maximum data evaluation. This exploration was performed to investigate which of the variables would affect the final polymer properties the most. Pareto-analysis served as a refinement of the global trends observed in response-surface curves devised by the factorial design. The Pareto analysis determined if the effects of the variables on the response-surface was linear, non-linear and if linear-by-linear interactions of the different variables contributed significantly to the observations.

6.3.2 Key experimental findings

6.3.2.1 Copolymer properties

The molecular weight and size properties of the copolymers synthesized in this project were dominated by the cosurfactant. Variation in the concentration of the cosurfactant, 1-butanol, resulted in different extents of coagulation of the monomer swollen micelles in the microemulsion that were produced here.

The copolymerization depended on the nucleation of the micelles by primary monomer radicals that in turn was formed by reaction of monomer molecules with initiator radicals. Potassium persulfate was utilized as a water-soluble initiator that could engage monomer molecules that diffused into the interface between the monomer rich micellar core phase and the aqueous dispersion phase. The interface was established by a palisade of sodium dodecyl sulfate molecules of which the hydrophobic alkyl tales associated with the monomer core and the polar head groups with the surrounding aqueous medium. Due to the HLB balance of 1-butanol (HLB 7.0), it would preferentially reside in the micellar interface and induce coagulation of micelles due to association of surfactant alkyl chains by hydrogen bonding.

Due to this aggregation of micelles, the number of effective particles could be reduced, resulting in larger cluster reactors. Since fewer reactors were found the competitive nature of propagation and termination steps in the copolymerization could be adjusted to favor propagation in the P(St-*co*-MMA) copolymer series. Subsequently the molecular weight and radius of gyration values increased for P(St-*co*-MMA) as the concentration of 1-butanol increased.

The P(St-*co*-EMA) did not demonstrate the butanol-dependent increases in molecular weight as well as radius of gyration as was seen for P(St-*co*-MMA). It was argued that the partitioning of the EMA monomer was stunted to a larger extent than the more hydrophilic MMA monomer due to the cosurfactant-induced aggregation of the micelles. Subsequently a decrease in molecular weight and radius of gyration was observed as the concentration of 1-butanol increased.

This suggested that the methacrylate monomers were more prone to initiate the polymerization reaction since they would partition to a larger extent to the interface than styrene. This observation was also confirmed by compositional analysis of the copolymers. It was observed that P(St-co-MMA) contained larger fractions of methacrylate in the final polymer, whereas P(St-co-EMA) polymers showed closer agreement to the monomer feed ratio.

Additionally, conformational evaluation of these copolymers illustrated that THF could be a useful solvent for these materials. The copolymers predominantly exhibited conformation between 0.4-0.5, with 0.5 indicating the ideal *6* conformation. At this conformation state the intra- and intermolecular forces between the polymer chain and solvent is effectively neutralized and polymer chains could interpenetrate without any resultant interaction force. This could be helpful in the selection of both polymers and solvents that could be utilized for polymer dispersion.

To conclude, several nanoscale copolymer particles were conveniently synthesized by microemulsion copolymerization. The copolymer molecular weight ranged between 150-700 kg.mol^{-1} whilst radius of gyration was in the region 20-45 nm. The cosurfactant 1-butanol could be employed to control these properties whereas the monomer feed ratio could independently vary the chemical composition of the copolymer species.

6.3.2.2 Pharmaceutical application

The analyses of the synthesized copolymers revealed the invaluable role of GPC-MALLS in determining the effect of reaction variables on the polymerization reaction, however, also provided the basis for the selection of the materials for the chosen pharmaceutical application. Copolymer nanoparticles could have several advantages over other materials of which one property is the limitation of phase separation between immiscible polymers. In addition, the small size of nanoparticles could facilitate the mixture with other substances.

In this study, artificial latexes were reconstituted from selected copolymer samples that presented conformations close to the ideal *6* conformation. A drug, rifampin, was selected as model drug since its application in films was already proven in some polymeric medical devices, i.e. orthopedic implants and catheter coatings. The drug was also soluble in THF and this ensured thorough mixing with the copolymer latex.

Films of the drug-copolymer solutions were cast and through a mechanism of coacervation and finally encapsulation, a film could be produced with drug captured in micropockets of the produced honeycomb structure.